The origin and evolution of the signaling pathway of the plant hormone cytokinin

Dissertation

Zur Erlangung des akademischen Grades des Doktors in den Naturwissenschaften (Dr. rer. nat.)

eingereicht im Fachbereich für Biologie, Chemie und Pharmazie der Freien Universität Berlin

vorgelegt von

Nijuscha Gruhn

Berlin, den 18. März 2014

Diese Arbeit wurde von Juni 2008 bis Februar 2014 am Lehrstuhl für “Molekulare Entwicklungsbiologie der Pflanzen” des Instituts für Biologie / Angewandte Genetik der Freien Universität Berlin unter der Leitung von PD Dr. Alexander Heyl angefertigt.

1. Gutachter: PD Dr. Alexander Heyl
2. Gutachter: Prof. Dr. Thomas Schmülling

Disputation am: ___06.Juni 2014_____

Index of contents

1. Introduction

Cytokinins are important growth regulators. This can be inferred from the so-called cytokinin deficiency syndrome (Werner *et al.,* 2001; Werner *et al.,* 2003; Werner *et al.,* 2008), which is caused by a lack of cytokinin or by cytokinin signal transduction deficiency and results in plants with slow-growing, stunted shoots that bear small leaves while the root system is enhanced (Werner *et al.,* 2001; Higuchi *et al.,* 2004; Nishimura *et al.,* 2004; Riefler *et al.,* 2006). This study addresses two aspects of cytokinin biology that will contribute to the understanding of the evolution of cytokinin signaling. Firstly, three hybrid histidine kinase genes from the moss *P. patens* which resemble in their domain architecture (the sequential arrangement of domains from the N- to the C-terminus of a protein (Vogel *et al.,* 2004a)) will be characterized. Secondly, the question of how the cytokinin signaling system evolved in the land plant lineage will be discussed. The evolution of two-component systems will be outlined; a short introduction on the general evolution of land plants and a more detailed introduction to the evolution of *P. patens* will be given. Finally in this introduction, the current state of research on cytokinins in *P. patens* will be remarked upon.

Since the bulk of the research that revealed the function of the cytokinin signaling system was carried out in *A. thaliana*, the introduction focuses on what is known about the cytokinin signaling system in this context.

1.1. The phytohormone cytokinin

Cytokinins are plant hormones which play an important role in many physiological and developmental processes (Mok and Mok 2001; Heyl and Schmülling 2003; Hwang *et al.,* 2012) such as germination (Miller 1958), regulation of the meristematic region in shoot and root growth (Mok and Mok 2001; Werner *et al.,* 2001; Werner *et al.,* 2003; Lohar *et al.,* 2004), leaf senescence (Richmond and Lang 1957; Gan and Amasino 1995), plastid development (Lerbs *et al.,* 1984; Cortleven *et al.,* 2009; Cortleven *et al.,* 2011), stress response (Werner and Schmülling 2009) and pathogen resistance (Choi *et al.,* 2011). Even though most research is carried out in *A. thaliana*, other plants have contributed to the understanding of the response to cytokinin (Hellmann *et al.,* 2010). Chemically, cytokinins are N^6-substituted adenine derivates and the structure and conformation of the N^6-substituted side chain influences their biological activity (Auer 1997). The side chain may be isoprenoid or aromatic, thus dividing cytokinins into two groups (Figure 1). The isoprenoid-type cytokinin can further be divided into isopentenyl-type cytokinins, which have isopentenyl side chains, and zeatin-type cytokinins, which have a hydroxylated isopentenyl side chain. The zeatins are either *cis*- or *trans*-hydroxylated. This conformational difference has also been shown to have an effect in terms of cytokinin activity in different plants (Spichal *et al.,* 2004; Yonekura-Sakakibara *et*

al., 2004; Romanov *et al.,* 2006; Choi *et al.,* 2012). In *A. thaliana*, *trans*-zeatin and isopentenyladenine are the prevalent cytokinins found in a concentration of about 0,7-2,5 nM (Takei *et al.,* 2004; Riefler *et al.,* 2006); while *trans*-zeatin is primarily synthesized in the root, isopentenyladenine seems prevalent in the upper plant body (Hirose *et al.,* 2008).

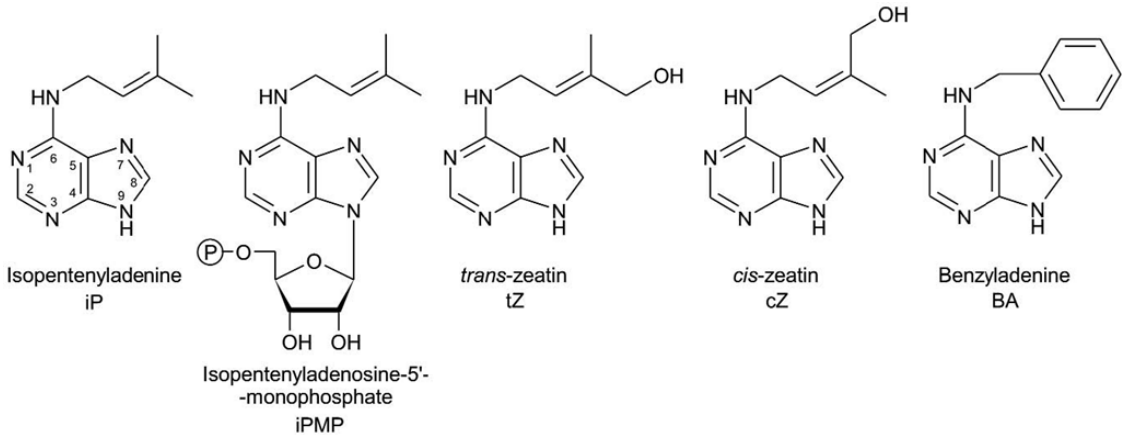

Figure 1: Chemical structures of some naturally occurring cytokinins carrying an isoprenoid or aromatic side chain. Figure modified from (Heyl *et al.,* 2006).

1.1.1. Cytokinin metabolism

Cytokinins are formed from adenosine mono- or di- or tri-phosphates and dimethylallylpyrophosphate (DMAPP), where adenylate isopentenyl diphosphate transferases (adenylate IPTs) catalyze the rate-limiting transfer of the isopentenyl group of DMAPP to the N^6-position of the adenosine phosphate to form the respective isopentenyl nucleotides (Kakimoto 2001; Takei *et al.,* 2001; Miyawaki *et al.,* 2006). Conversion of the isopentenyl nucleotide to *trans*-zeatin nucleotides is carried out by cytochrome P450 monooxygenases (CYP735As). Isopentenyl and *trans*-zeatin nucleotides are dephosphorylated by phosphatases and the mono-phosphate form can either be dephosphorylated to the biologically active cytokinin-riboside, or directly converted to the active free cytokinin base by a cytokinin riboside 5´-monophosphate phosphoribohydrolase (Lonely guy, LOG) (Kurakawa *et al.,* 2007; Kuroha *et al.,* 2009) (Figure 2). Alternatively the *cis*-zeatin type cytokinins are produced by tRNA-IPTs (Kakimoto 2001; Takei *et al.,* 2001) that modify the adenosine at position 37 of tRNAs recognizing the UNN codon (Persson *et al.,* 1994) and are released upon tRNA breakdown (Koenig *et al.,* 2002). *IPT* genes have been found in organisms as diverse as *Dictyostelium discoideum* (Taya *et al.,* 1978), *Agrobacterium tumefaciens* (Akiyoshi *et al.,* 1984; Barry *et al.,* 1984) and the model plant *Arabidopsis thaliana* (Kakimoto 2001; Takei *et al.,* 2001).

Naturally occurring cytokinins can be modified by *in vivo* glycosylation. N-glycosylation at the N^7- and N^9- positions of cytokinin is believed to be one inactivation pathway for cytokinins

(Mok and Mok 2001). Recently, one N-glucosyltransferase, UGT76C2, was shown to be involved in the homeostatic regulation of cytokinin, also influencing expression levels of known cytokinin signaling genes (Wang *et al.,* 2011). O-glycosylation occurs at the N^6- side chain and renders cytokinin resistant to degradation (Jameson 1994). Since this state is reversible by β-glucosidases, it is believed to be a storage form for cytokinins (Brzobohaty *et al.,* 1993).

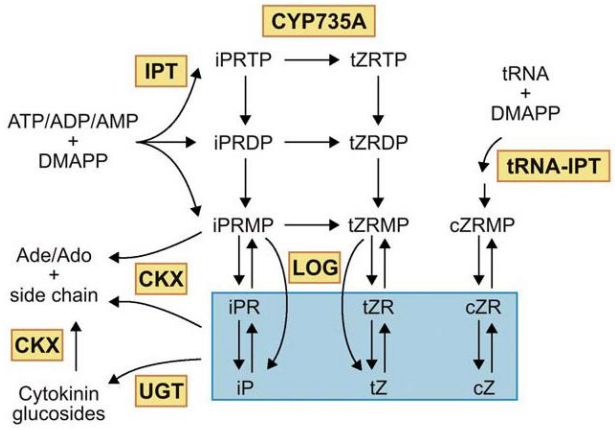

Figure 2: Metabolism of cytokinin and its interconversion. Cytokinins are synthesized either by adenylate isopentenyl transferases (IPTs) or by tRNA isopentenyl transferases (tRNA-IPTs). IPTs catalyze the formation of isopentenyladenine riboside mono-/di- or tri-phosphates (iPRTP/iPRDP/iPRMP) from the respective adenosine phosphate and dimethylallyldiphosphate (DMAPP). Substrates for tRNA-IPTs are tRNAs and DMAPP which will be set free upon tRNA degradation as *cis*-zeatinribosidemonophophate (*c*ZRMP). cZRMP and iPRTP/iPRDP/iPRMP can be converted to *cis*-zeatinriboside (*c*ZR) and *cis*-zeatin (*c*Z) and *t*ZRTP/*t*ZRDP/*t*ZRMP respectively via CYP735A, a P450 monooxygenase. Further Lonely guy (LOG) leads to the conversion of iPRMP and tZRMP to the respective cytokinin riboside or the free cytokinin. Active cytokinins (highlighted in blue) of the *trans*-zeatin (*t*Z) and isopentenyladenine (iP) type are degraded by cytokinin oxidases/dehydrogenases (CKXs), as well as iPRMP and cytokinin glucosides by cleavage of the side chain, releasing adenine/adenosine (Ade/Ado) and the side chain. Cytokininglucosides are synthesized by the glucosyltransferase (UGT). Modified figure from (Werner and Schmülling 2009).

Cytokinin oxidases/dehydrogenases (CKX) are the key enzymes in cytokinin degradation which selectively cleave the unsaturated N^6-isoprenoid side-chain of cytokinins (Mok and Mok 2001). In *A. thaliana* there are seven partially redundant genes for CKX. They are expressed in different tissues and different compartments of the cell (Werner *et al.,* 2001; Werner *et al.,* 2003). The overexpression of *CKX* genes from *Arabidopsis* in tobacco lead to a clear cytokinin deficiency phenotype, including retarded growth in shoots and an enhanced growth in roots (Werner *et al.,* 2001).

Lately, the identification of cyanobacterial *IPT* and *CKX* genes (Frebort *et al.,* 2011) has reinforced the idea that cytokinin metabolism is of bacterial origin and has entered the plant genome via primary endosymbiosis (Frebort *et al.,* 2011; Spichal 2012).

1.2. The two-component cytokinin signal transduction system

Cytokinins are perceived and the signal is transduced by a multistep two-component system (TCS). Basic TCSs comprise of a histidine kinase and a response regulator (RR) protein

(Figure 3, A), known from bacteria (West and Stock 2001). The first identified TCS component in plants was the ethylene receptor ETR1 in *A. thaliana* (Chang *et al.,* 1993). Furthermore bacteria use a modified TCS that is also found in plants (Figure 3, B), where the histidine kinase is fused with a RR domain, hence is called hybrid histidine kinase (HK) (Stock *et al.,* 2000; West and Stock 2001). After an intra-molecular phosphate transfer from the histidine of the HK to the aspartate of the RR domain, the phosphoryl group is transferred to a histidine phosphotransfer protein (HPT). These proteins are not present in basic TCSs. The extended TCS is also referred to as phosphorelay (West and Stock 2001). Further on, the signal cascade employs a RR protein that contains a phosphoryl-accepting Asp in the RR domain and also includes an output domain, such as a DNA-binding domain. Upon phosphorylation the regulatory characteristics of these RR proteins change into an activated state and subsequent dephosphorylation resets the pathway. Conserved residues in this signaling cascade are His and asp, and this is why this TCS is also called the His-to-Asp phosphorelay. In the following these residues will be called canonical residues.

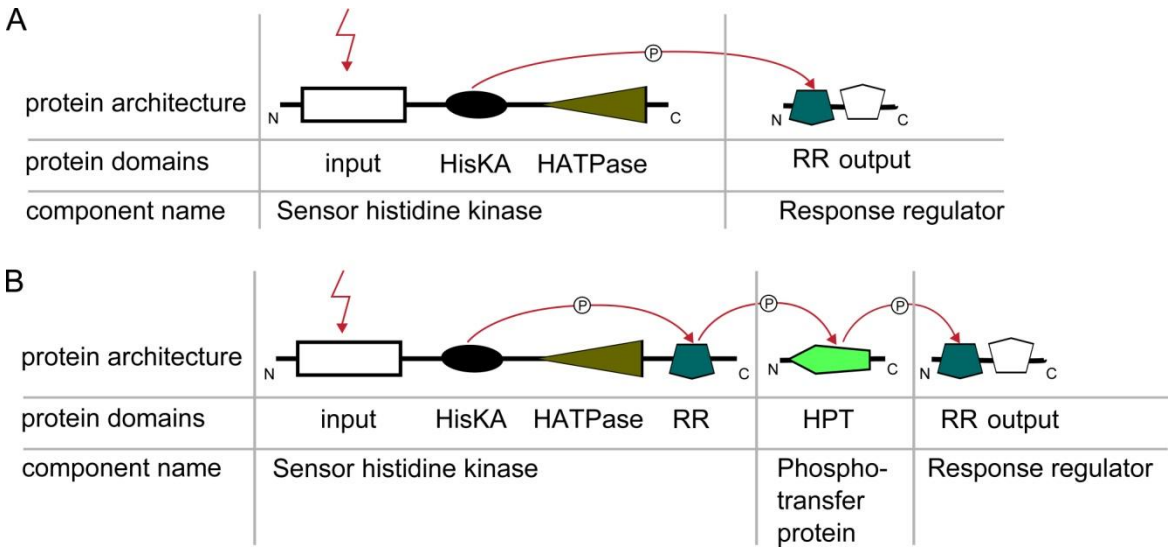

Figure 3: The basic and the phosphorelay two component system. (A) Scheme of the basic two component system that involves a sensory histidine kinase and a response regulator protein. **(B)** Scheme of the phosphorelay two component system that involves a hybrid histidine kinase, a histidine phosphotransfer protein and a response regulator protein. **Protein domains:** Input domain, a variety of input domains are used, depending on the signal; HisKA domain, PF00512, comprises the canonical His residue; HATPase domain, PF02518, transfers the phosphoryl group from an ATP to the canonical His; RR domain, PF00027, response regulator receiver domain contains the canonical Asp; HPT domain, PF01627, Histidine phosphotransfer domain contains a canonical His residue; red flash, signal; red arrow, transfer of the phosphoryl group (P); N, N-terminus of the protein; C, C-terminus of the protein.

1.2.1. TCS in plants

The TCS in plants is thought to have integrated into the plant genome during primary endosymbiosis (Koretke *et al.,* 2000; Duplessis *et al.,* 2007; Spichal 2012). TCS components have been found encoded in algae chloroplasts (Duplessis *et al.,* 2007), but not in the chloroplast genomes of land plants. Despite the lack of TCS components encoded in the

plastids of land plants, detailed analyses indicate the action of TCSs in their chloroplasts (Puthiyaveetil and Allen 2009), and only recently Lysenko and colleagues suggested that nuclear-encoded HKs function in plastid-based TCSs in land plants (Lysenko *et al.,* 2012). Lysenko and colleagues identified two HKs, based on their similarity to proteins encoded in algae plastids, and also suggested that a splicing variant from the ethylene receptor of maize might work as a HK in plastids. This ethylene receptor based plastid HK would then lack the RR domain, and thus could only work in a basic TCS (Lysenko *et al.,* 2012). Not only have HKs contributed to the understanding of TCSs and their evolution, RRs have also been found to be encoded in the chloroplast genome of *Chlorokybus atmosphericus* (Duplessis *et al.,* 2007). These RRs work in conjunction with the σ-subunit of a eukaryotic RNA polymerase (encoded in the nucleus). This cooperation may have given the ancestral eukaryotic cell a simple and efficient method to regulate protein production of integrated chimeric gene sets encoded in the nuclear and in the plastid genome (Duplessis *et al.,* 2007). However, Lysenko and colleagues doubt the existence of TCS components in the plastomes of charophyte algae (Lysenko *et al.,* 2012). Besides these new data about TCS components in plastids, TCS components encoded in the nucleus of plants have long been known. Cytokinin receptors, ethylene receptors, CKI1 and CKI2 receptors, AHK1 osmosensors and phytochromes have all been shown to derive from TCS ancestors (Yeh and Lagarias 1998; Hutchison and Kieber 2002; Lohrmann and Harter 2002; Schaller *et al.,* 2002; Mizuno 2005; Tran *et al.,* 2007; Schaller *et al.,* 2011). Interestingly, response regulators working directly in conjunction with non-cytokinin TCS receptor proteins are not identified and only the cytokinin signaling system is assigned a full signaling cascade via the TCS. One of the reasons might be that the receptors fulfill different signaling functions (such as phytochromes that work as Ser/Thr kinase (Yeh and Lagarias 1998)), while others feed into the cytokinin signaling system (Phytochromes → RRA (Sweere *et al.,* 2001), CHK1 → (receptors, HPTs, RRBs, RRAs) (Hwang and Sheen 2001; Lohrmann and Harter 2002; Mähönen *et al.,* 2006b; Hejatko *et al.,* 2009; Deng *et al.,* 2010); ethylene receptor → RRB (Hass *et al.,* 2004)). Why the cytokinin signaling system remains the only system where cognate TCS partners are clearly assigned is still unknown.

The cytokinin signaling system will now be introduced by each individual signaling component.

1.2.2. Cytokinin receptors

In plants, a multistep phosphorelay system comprised of three signaling steps is used to sense cytokinin and transduce the signal. Experiments have shown that in *A. thaliana* the cytokinin signal is perceived by three hybrid histidine kinase receptors (AHK2, AHK3, AHK4) and transduced via a His-to-Asp phosphorelay system (Mähönen *et al.,* 2000; Hwang and

Sheen 2001; Inoue *et al.,* 2001; Suzuki *et al.,* 2001a; Yamada *et al.,* 2001). Like other hybrid histidine kinases, the cytokinin receptors consist of a ligand binding domain, a histidine kinase domain, a HATPase domain and a response regulator domain (Figure 4). The cytokinin molecule is bound by the ligand-binding domain of the receptor, the cyclase/histidine kinase associated sensory extracellular (CHASE) domain (Anantharaman and Aravind 2001; Mougel and Zhulin 2001) with an affinity in the lower nanomolar range (Yamada *et al.,* 2001; Spichal *et al.,* 2004; Romanov *et al.,* 2006). Interestingly, the ligand specificity profiles of AHK4 (Yamada *et al.,* 2001; Romanov *et al.,* 2005; Romanov *et al.,* 2006) and the AHK2 CHASE domain overlap (Stolz *et al.,* 2011) significantly, showing a preference for biologically active cytokinins. Isopentenyladenine and *trans*-zeatin are the prevalent cytokinins in *A. thaliana*. The cytokinin receptor AHK3 accepts a broader spectrum of cytokinin molecules as a ligand than AHK2 and AHK4 (Spichal *et al.,* 2004) and recognizes isopentenyladenine about 10-fold less than *trans*-zeatin (Romanov *et al.,* 2006). The ligand binding is thought to lead to a conformational change of the receptor hybrid histidine kinase and triggers an autophosphorylation at a conserved histidine residue (Miwa *et al.,* 2007; Hothorn *et al.,* 2011), which is then intra-molecularly transferred to the aspartate of the response regulator domain. Activity of the cytokinin receptor AHK4 and AHK3 to function in a TCS was also shown in the yeast *Saccharomyces cerevisiae*, who's sole and essential hybrid histidine kinase SLN1 was replaced with AHK4 or AHK3 and was able to grow in the presence of cytokinin (Inoue *et al.,* 2001; Ueguchi *et al.,* 2001a; Ueguchi *et al.,* 2001b). Other TCSs from the bacterium *Escherichia coli* and the fission yeast *Schizosaccharamyces cerevisiae* were also activated when the intrinsic receptor molecules were absent and the cytokinin receptor AHK4 together with cytokinin complemented for this deficiency (Suzuki *et al.,* 2001a). However, the cytokinin receptors AHK2 and AHK3, were not able to complement *E. coli* and *S. cerevisiae* deficiencies (Suzuki *et al.,* 2001a). Despite the lacking complementation effect of AHK2 in *E. coli* (Suzuki *et al.,* 2001a), experiments with protoplasts generated from *A. thaliana* proved the ability of all *A. thaliana* cytokinin receptors to activate the *ARR6* promoter in response to cytokinin (Hwang and Sheen 2001).

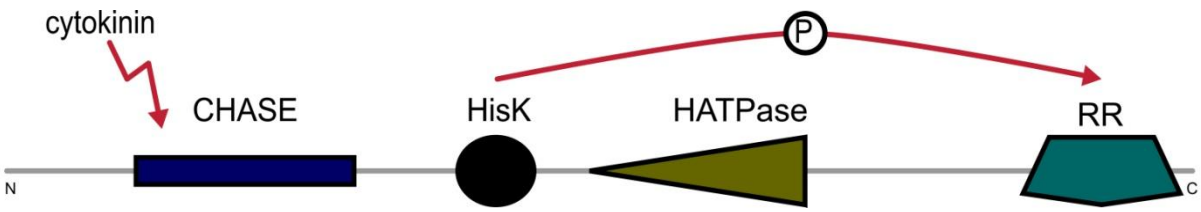

Figure 4: Domain structure of the cytokinin receptors of *Arabidopsis thaliana*. The cytokinin ligand binds to the cyclase/histidine kinase associated sensory extracellular (CHASE) domain, The dimerization and phosphoacceptor domain (HisK) is phosphorylated, upon which an intra-molecular phosphotransfer takes place and positions the phosphate at the canonical aspartate residue of the response regulator (RR) domain for subsequent signal transfer to histidine phosphotransfer proteins. Protein domains: Abbreviation of the domains are according to the Pfam-database (http://pfam.sanger.ac.uk): CHASE, PF03924; HisKA, PF00512; HATPase, PF02518; RR, PF00027. N. N-terminus; C, C-terminus Figure from (Gruhn *et al.,* 2014).

On the subcellular level, cytokinin receptors were found to primarily localize to the Endoplasmatic reticulum (ER) (Caesar *et al.,* 2011; Wulfetange *et al.,* 2011a) and, in the case of AHK3, also to the plasma membrane (Kim *et al.,* 2006; Wulfetange *et al.,* 2011a). Homo- and heterodimerization was shown in yeast two-hybrid assays (Dortay 2006) and for AHK3 and AHK4 *in planta* (Wulfetange 2010; Wulfetange *et al.,* 2011a).

Furthermore, the investigation of the expression domain of the three receptors and knockout mutants contributed to the understanding of the receptors functionalities. In the following, the expression domain of the respective receptor gene is described.
The expression of the *AHK4* gene has been primarily found in the root (Ueguchi *et al.,* 2001a), but can also be localized in the shoot, leaves and flowers (Higuchi *et al.,* 2004; Nishimura *et al.,* 2004). Moreover, the *AHK4* transcript has also been shown in the embryo of *A. thaliana* and was shown to be important in primary root formation (Mähönen *et al.,* 2000). Promoter fusion constructs of *pAHK4::GUS* have also indicated a function of the receptor in the shoot apical meristem, but *ahk4* mutant plants did not show a phenotype related to this expression domain (Mähönen *et al.,* 2000; Gordon *et al.,* 2009).
The expression of *AHK3* and *pAHK3::GUS* has been found mostly in the upper plant body, where it was primarily in rosette leaves but also in the flowers, while the expression in the root was moderate (Higuchi *et al.,* 2004). Even though the expression of *AHK3* was prevalent in the rosette leaves, a function of AHK3 involved in the differentiation of the transition zone in the root meristem was found (Dello Ioio *et al.,* 2008).
The *AHK2* transcript and the *pAHK2::GUS* reporter activity has been found in root and shoot tissues alike (Higuchi *et al.,* 2004). A distinct function of this receptor was not identified. Altogether, all three *AHKs* were expressed in the vasculature and in cells with meristematic activity.

Furthermore, each single mutant, the double mutants and the triple mutant have contributed to our understanding of the receptors functionalities.
Mutant *A. thaliana* plants deficient for *AHK4* (found in different mutant screens) were found to be retarded in cytokinin-dependent cell proliferation and cytokinin-induced shoot development of calli and cytokinins root inhibition effect was diminished (Inoue *et al.,* 2001). The *AHK4* allelic mutation *Wooden leg* (*WOL)* (Mähönen *et al.,* 2000) showed disordered root vascular tissue that resulted in root growth inhibition and was shown to have a dominant negative effect on the cytokinin signaling system (Mähönen *et al.,* 2006b). The mutants from *AHK2* and *AHK3* did not show a phenotype (Nishimura *et al.,* 2004).
The analysis of single, double and triple receptor mutants of *Arabidopsis* demonstrated that the three receptors have at least a partial overlap in their positive regulatory function in the cytokinin signaling system (Nishimura *et al.,* 2004). Single mutants, as well as the double mutants *ahk2 ahk4* and *ahk3 ahk4*, did not show a significant phenotype, while the *ahk2 ahk3*

mutant was reduced in leaf and stem size (Higuchi *et al.,* 2004). Also a synergistic effect of AHK2 and AHK3 action was found in leaf senescence (Kim *et al.,* 2006; Riefler *et al.,* 2006). The detailed analysis of the cytokinin responsive *ARR5* promoter in double mutants was activated in domains of the intact AHK2 or AHK3 and overlapped in the shoot apex and the root cap region, while the intact AHK4 activated the *pARR5*::*GUS* reporter gene also in the root vasculature. However, the *pARR5*::*GUS* reporter gene was also activated in the root vasculature in plants with AHK2 or AHK3, after the addition of exogenous cytokinin (Stolz *et al.,* 2011).

The mutation of all three receptors caused insensitivity to cytokinin and a strong inhibition in plant growth (Higuchi *et al.,* 2004; Nishimura *et al.,* 2004; Riefler *et al.,* 2006). Nevertheless, these plants were able to grow, although they resulted in a small plant compromised in its fertility (Higuchi *et al.,* 2004; Nishimura *et al.,* 2004; Riefler *et al.,* 2006). These results confirm that cytokinins are an important class of plant hormones, but the fact that a plant body was formed in the absence of cytokinin responsiveness raises the question of whether cytokinins are necessary to establish a basic body plan. It has been proposed that basic activity levels of cytokinin signaling are maintained by other two-component signaling proteins that cross-feed into the cytokinin response system, as shown for the hybrid histidine kinase CKI1. CKI1 activates *ARR6* transcription (Hwang and Sheen 2001) and phosphorylates HPTs (Mähönen *et al.,* 2006b). Another possibility is that there exists a form of cytokinin signaling which ensures basic cytokinin-dependent cellular functions even if the TCS is knocked out (Higuchi *et al.,* 2004; Nishimura *et al.,* 2004).

In a phylogenetic tree of the histidine kinase domains, the *Arabidopsis* cytokinin receptors are more closely related to their respective maize orthologs than to any of the other *Arabidopsis* His-kinases, indicating that the founding member of the gene family evolved before the separation of the mono- and dicots (Yonekura-Sakakibara *et al.,* 2004; Pils and Heyl 2009). While the TCSs of higher plants seem quite comparable, not much is known about this signaling pathway in lower plants (Pils and Heyl 2009).

1.2.3. Histidine phosphotransfer proteins

Histidine phosphotransfer proteins (HPTs) share the Hpt domain (PF01627 of the Pfam database http://pfam.sanger.ac.uk), which includes the canonical histidine residue for the function in the His-to-Asp relay. In *A. thaliana*, the HPT family consists of six members (AHPs) that are single-domain proteins. Five of these HPTs possess the canonical His in the conserved amino acid (aa) sequence stretch XHQXKGSSXS, hence clearly function in the TCS (Hwang *et al.,* 2002). All canonical AHPs have been shown to localize to the nucleus and the cytoplasm, as well as interact with AHKs and RRBs (Imamura *et al.,* 1998; Imamura *et al.,* 1999; Suzuki *et al.,* 2001b; Tanaka *et al.,* 2004; Dortay *et al.,* 2006; Dortay *et al.,*

2008). Punwani and colleagues suggested a continuous shuttling between the nucleus and the cytoplasm (Punwani *et al.,* 2010). In a functional complementation assay in yeast, AHP1, AHP2 and AHP3 were shown to complement the deficiency of intrinsic HPT proteins (Suzuki *et al.,* 1998). The knockout of single and double *HPT* genes did not show a significant phenotype in *A. thaliana*; only mutants lacking three of the five canonical AHPs were insensitive towards exogenous cytokinin in root and in hypocotyl elongation assays (Hutchison *et al.,* 2006). The most severe phenotype was shown in the quintuple knockout that arrested its primary root growth, resulting in a short root (Hutchison *et al.,* 2006). The cytokinin-dependent activation of RRAs was also reduced significantly and the residual activation might be due to a leaky knockout of the *AHP2* gene (Deng *et al.,* 2010). Other experiments showing the phosphate transfer from the yeast osmosensor SLN1 to AHP1, AHP2 and AHP5 also tested another AHP protein (AHP6). This protein does not possess the canonical His and hence was not able to accept the radioactive labeled phosphate (Mähönen *et al.,* 2006a). Moreover the simultaneous expression of the non-canonical *AHP6* with canonical *AHP1* and *ARR1* interfered with the phosphotransfer from AHP1 to ARR1. The description of AHP6 as a negative regulator in the cytokinin signaling system was further corroborated by an *ahp6* knockout mutant that reacted hypersensitively with respect to vasculature development to cytokinin in the *AHP6* expression domain, the developing protoxylem and in the heart-shaped embryo (Mähönen *et al.,* 2006a).

1.2.4. Response regulators

The *A. thaliana* response regulators (ARRs) are grouped into four different subgroups (type-A, -B, -C and pseudo RRs) by their domain structure. All RRs possess the response regulator receiver domain that includes the canonical Asp residue.

The first group that is activated in the cytokinin signaling cascade is the group of type-B RRs (RRBs). They consist of a family of eleven members in *A. thaliana* and share the domain architecture comprising of the response regulator receiver domain and a MYB-related DNA binding domain (Mason *et al.,* 2004). These proteins activate the transcription of their target genes in response to the cytokinin stimulus. Primary target genes include the type-A RRs (RRAs) and some of the cytokinin response factors (CRFs) (Hwang and Sheen 2001; Sakai *et al.,* 2001; Rashotte *et al.,* 2003; Mason *et al.,* 2005; Rashotte *et al.,* 2006; Taniguchi *et al.,* 2007; Yokoyama *et al.,* 2007). While the expression of RRBs has been shown to be not regulated by cytokinin (Lohrmann *et al.,* 1999; Brenner *et al.,* 2005), the protein degradation of only one member of the RRBs, namely ARR2, was found to be dependent on cytokinin-induced phosphorylation and the target site for ubiquitination modulated by the 26S proteasome (Kim *et al.,* 2012). A high redundancy between members of RRBs has been shown by the analysis of multiple knockout mutants (Mason *et al.,* 2005; Argyros *et al.,* 2008;

Ishida *et al.,* 2008). Only recently, it was shown in complementation studies that complementation of *arr1 arr12* is independent from different RRB subgroups (Hill *et al.,* 2013).

Primary target genes of the RRBs are the type-A RRs (RRAs). These proteins are single-domain proteins that are rapidly, transcriptionally induced after exogenous cytokinin application (D'Agostino *et al.,* 2000; Rashotte *et al.,* 2003; Brenner *et al.,* 2005). The RRAs are involved in a feedback loop, regulating the activity of cytokinin signaling and linking the cytokinin signaling pathway with other cellular signaling pathways (Hwang and Sheen 2001; Sweere *et al.,* 2001; To *et al.,* 2004; Dortay *et al.,* 2006; Heyl *et al.,* 2006). The negative regulation of the RRAs was experimentally shown by the expression of RRAs together with the *pARR6::LUC* or *pARR6::GUS* (a RRA promoter fused to a reporter gene) that showed a reduction of reporter gene activity in *A. thaliana* protoplasts after cytokinin treatment (Hwang and Sheen 2001). The activity of the RRAs is dependent on their phosphorylation status, as shown by the phosphorylation insensitive mutant $ARR5^{D87A}$, which lost its ability to complement the quadruple knockout mutant *arr3 arr4 arr5 arr6* while the phosphomimic, constitutively active $ARR7^{D87E}$ altered shoot development by arresting the meristem growth, blocked of organ formation and abolished cytokinin-dependent root elongation inhibition (Leibfried *et al.,* 2005; To *et al.,* 2007; Lee *et al.,* 2008). The phosphorylation status of the protein has also been shown to influence protein degradation in the way that not phosphorylated (inactive) proteins will be degraded faster (To *et al.,* 2007). Similarly the degradation via the related-to-ubiquitin (RUB)/26S proteasome pathway of ARR5, a RRA, was shown to be dependent on Auxin resistant 1 (AXR1) (Li *et al.,* 2013). These alterations in protein stability are at least partially influenced by AHK and AHP proteins (To *et al.,* 2007).

Another group of RRs are the type-C RRs (RRCs), which resemble the RRAs in their domain architecture – they are single-domain proteins – but expression of the RRCs is not induced after cytokinin treatment (Kiba *et al.,* 2004). Phosphotransfer studies showed that the transfer takes place between ARR22 and AHP5 *in vitro* (Kiba *et al.,* 2004) and ARR22 and AHP2, AHP3 and AHP5 in tobacco cells (Horák *et al.,* 2008), and that ARR22 plays a role as negative regulator in cytokinin signaling because *ARR22* overexpresser (*ARR22ox*) mutants exhibited a dwarf phenotype that has previously been associated with cytokinin deficiency (Kiba *et al.,* 2004). While the overexpression of *ARR22* (Gattolin *et al.,* 2006) and the expression of the genomic sequence *gARR22* under the native promoter also showed the dwarf phenotype (Horák *et al.,* 2008), the *arr22* (Gattolin *et al.,* 2006; Horák *et al.,* 2008), the *arr24* and the *arr22 arr24* double knockout mutant were without phenotype (Gattolin *et al.,* 2006).

The class of pseudo-response regulators (PRRs) takes a special position. Even though they share the response regulator receiver domain with the other RRs, the canonical Asp in this group has diverged and is substituted by a glutamate (Mizuno 2004). This renders them inactive in the His-to-Asp phosphorelay system. Additionally to the RR domain, these proteins may incorporate a CCT (CONSTANS, CO-like, and TOC1) or WD40 DNA binding domain (Mizuno 2004). A role of the PRRs has been suggested in circadian rhythm (Mizuno 2004; Mizuno and Nakamichi 2005).

1.2.5. Cytokinin response factors

To elucidate cytokinin action outside of the cytokinin signaling system, experiments were undertaken to identify genes regulated by cytokinin other than the RRAs (Rashotte *et al.,* 2003; Brenner *et al.,* 2005). A subset of *Ethylene Responsive element-binding Factors* (ERFs), showed transcriptional up-regulation upon cytokinin treatment (Rashotte *et al.,* 2003). This subset was accordingly named *Cytokinin Response Factors* (CRFs) and further analyzed in different experiments which proved them to be a part of the cytokinin signal transduction pathway, thereby offering an alternative route of targeted gene regulation besides the RRB → RRA route (Rashotte *et al.,* 2006; Rashotte and Goertzen 2010; Cutcliffe *et al.,* 2011).

The above sections (section 1.2.2 to section 1.2.5) describe the different components that together form the cytokinin signaling system. A schematic overview of the interplay of the components is found in Figure 5.

1.1. Evolution of two-component signal transduction systems

The origin of the complexity in signaling pathways is not fully understood. Signaling pathways in general consist of numerous components, different interaction possibilities and compartmentalization. Furthermore, they can form networks and their components and reactions are not unique, but can be carried out by redundant components (Weng *et al.,* 1999). It is not clear why nature evolves towards such complex networks, since the resulting complexity outnumbers what is required for function. It has been shown that simpler pathways consisting of oscillators and switches can result in the same biological response as complex signaling networks (Furusawa and Kaneko 2000). Work by Soyer and Bonhoeffer (2006) with computational systems, containing three proteins, a selective force and random mutations of the proteins, showed that mutations increasing the pathway size had only a slight effect on fitness, whereas size decreasing mutations were almost certain to turn pathways inviable. As pathways grow, the deleterious effect of size decreasing mutations weakens, allowing pathways to survive both types of mutations with equal chance, and the average pathway size of the population reaches an equilibrium (Soyer and Bonhoeffer 2006).

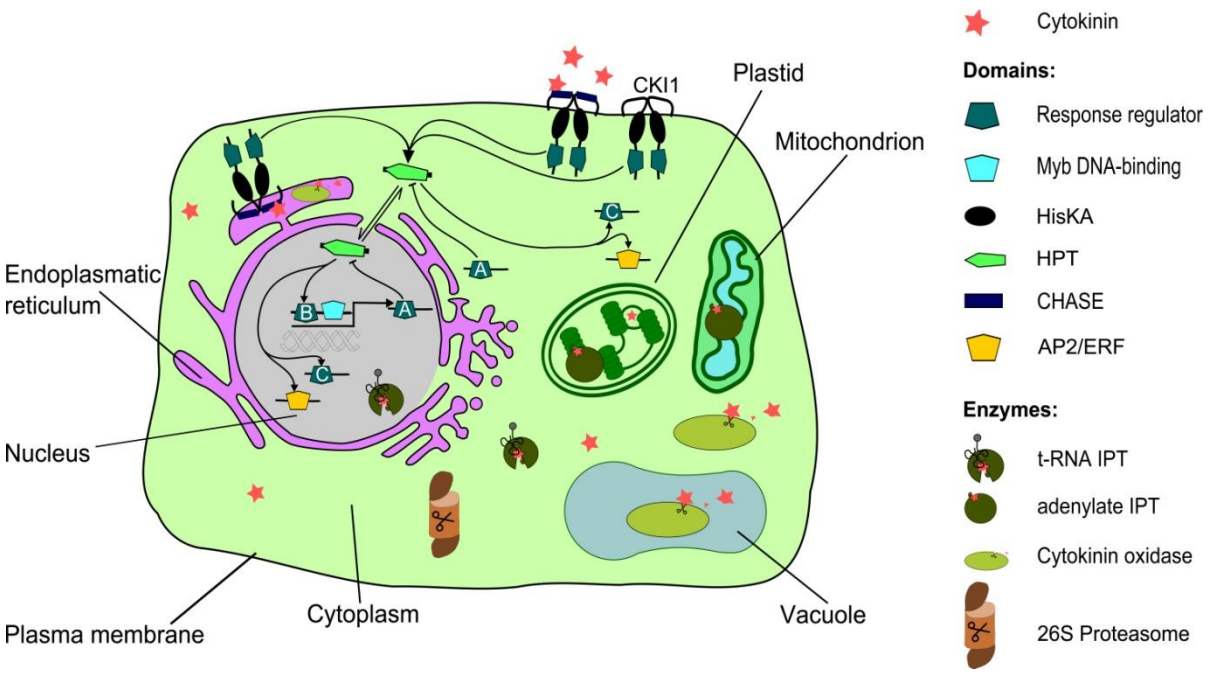

Figure 5: Model for the cytokinin signal transduction via the two-component system and the occurrence of cytokinin metabolism enzymes in *A. thaliana*. Cytokinin ligand binding takes place at the cytokinin receptors (AHK2, AHK3 and AHK4) that are characterized by their ligand binding Cyclase/Histidine kinase Associated Sensory Extracellular (CHASE) domain and the binding induces autophosphorylation of the receptor. Subsequently the phosphoryl group is transferred via a His-to-Asp-phosphorelay from the receptor to the histidinetransfer proteins (HPTs) in the cytoplasm and then further to type-B response regulators (RRBs) in the nucleus. RRBs transcribe target genes, among them type-A response regulators (RRAs). RRAs in turn, down-regulate the primary cytokinin signal response via a negative feedback loop acting on phosphorylation of the RRBs. Another feedback loop is established via the AHPs and the type-C response regulators (RRCs) that drain the activating phosphorylgroup from the cytokinin signaling system. Simultaneously cytokinin insensitive 1 (CKI1) feeds a phosphorylation signal, via the HPTs, into the phosphorelay. HPTs then phosphorylate RRBs and activate cytokinin response factors (CRFs) that contain an AP2/ERF domain. Cytokinins are produced in the plastid and the mitochondrion by adenylate- isopentenyltransferases (IPTs) and in the nucleus and the cytoplasm by tRNA-IPTs. Cytokinin degradation via the cytokinin oxidase/dehydrogenase (CKX) is found in the ER, the cytoplasm and the vacuole. Figure modified from (Gruhn and Heyl 2013).

TCSs, the most widely used signal transduction systems in bacteria (West and Stock 2001), exist not only singularly but multiple times in one organism, and one pathway could interfere with proper signal transduction in the other. Hence the insulation of two or more TCSs to each other is an important objective in the establishment of a new TCS (Capra and Laub 2012). This insulation is achieved e.g. by incompatibility of the components from one pathway with the other. Together, diversity and robustness enabled the evolution of a responsive TCS (Soyer *et al.,* 2006). The expansion of TCS components was also correlated with more diverse environmental challenges faced by the respective organism (Koretke *et al.,* 2000; Galperin *et al.,* 2001; Alm *et al.,* 2006).

The generation of new TCSs was shown to be dependent on gene duplication or lateral gene transfer, while duplication was the primary source of new TCSs (Alm *et al.,* 2006). Immediately after duplication, a new TCS does not fulfill any new function, and duplication

can be regarded as the raw material for new pathway generation (Capra and Laub 2012). To establish the new function of the duplicated TCS, three steps remain to be taken. First, the input signal needs alteration, and the sensory domain of the HK is to be changed. Second, the output should change. Third, the new interactions/transactions are to be insulated against cross-talk from the other TCSs (Capra and Laub 2012). This would then yield a new functional TCS that responds to a different signal and generates a different output from the progenitor pathway. In some cases the full execution of all steps might not be necessary, for instance when the amplification of the signal input is desired to generate the same output, or vice versa the same input signal is desired to generate a more diverse output, the first or the second step might be abandoned (Capra and Laub 2012). Furthermore, despite diverging, the duplicated pathway needs to retain its activity. An experimental example shows that the duplicate moves along a series of single substitutions towards the altered specificity while functionality is maintained throughout (Capra *et al.,* 2010). Not only does duplication and subsequent diversification elaborate upon the TCS-controlled responses but duplication is also the key to the invention of "phosphorelays". Phosphorelays are a variant of the basic TCS elaborated by HPT proteins, thereby adding an internode for multiplication of signal transduction possibilities (Stephenson and Hoch 2002) and increased accessibility because of their mobility in the cell (Shenoy 2000). Another fact highlights the importance of HPTs: His-to-Asp signaling is not found in metazoans, and it has been speculated that the instability of the aspartyl-phosphate moiety is the reason for this (Capra and Laub 2012). It is thought that the disadvantage of the instable aspartyl-phosphate moiety could be remedied by the incorporation of the more stable histidyl-phosphate moiety, which is applied for the signal transfer from the signal input location to the signal output location (Cui *et al.,* 2009). The complexity of phosphorelays increases as its components are multiplied. Interestingly, it has been found that components of a signaling network evolve faster depending on their localization. Molecules at the extracellular space evolve fast and the evolutionary rate decreases in the direction of the signal flow, from the outside of the cell to the nucleus (Kim *et al.,* 2007; Waterhouse *et al.,* 2007; Cui *et al.,* 2009).

While the signal transduction domains seem highly conserved in HKs, those domains involved in ligand sensing are highly variable. The comparison of active sites from TCSs of *Bacillus spp*. shows a high degree of conservation on the interaction sites of signal transduction proteins (Hoch and Varughese 2001). HKs have also been described as intrinsically modular, meaning that the sensory domain in a HK can be exchanged to generate a chimeric HK with a different input function (Utsumi *et al.,* 1989; Stolz *et al.,* 2011), a result reflected in the fact that the ligand sensing and transmembrane domains show a high degree of variation needed to adapt the system to the different ligands (Stephenson and Hoch 2002). Besides the extracellular, ligand sensing domains of histidine kinases, the

overall domain structure and its evolutionary development has been examined. Correlations between domain structure and course of evolution were found in bacteria (Alm *et al.,* 2006). More general investigations confirm this finding, stating that the domain architecture relates to the descent of the protein, in the way that proteins with the same domain architecture evolved from a common ancestor protein (Vogel *et al.,* 2004a). Lineage specific expansion of the HK receptors was accompanied by rearrangements in domain structure, and horizontal gene transfer resulted in histidine kinase domains with preserved domain structure (Alm *et al.,* 2006). The comparison of the evolution of HKs and their cognate RR in bacteria revealed both components remain unchanged over a relatively long period of time (Capra and Laub 2012) or regularly co-evolve (Wuchty *et al.,* 2006; Waterhouse *et al.,* 2007; Burger and van Nimwegen 2008; Skerker *et al.,* 2008; Capra *et al.,* 2010). Most co-evolving sites are located at the protein-protein interaction sites of the protein (Casino *et al.,* 2009; Cui *et al.,* 2009). Dimerization of HKs and also RRs are another possibility to generate specificity in the system. While TCS receptors from *A. thaliana* have been shown to also form heterodimers in yeast (Dortay 2006) and *in planta* (Wulfetange *et al.,* 2011a), almost no indication was found for physiologically relevant heterodimerization in bacteria (Capra and Laub 2012).

1.2. The evolution of plants

The formation of embryophytes (land plants) represents a hallmark in the development of the modern ecosystem because colonialization substantially changed the terrestrial environment. To understand the colonialization of land by plants, the evolutionary history of this event is a prerequisite. There have been a number of discussions over how to group basal land plants and what features have to be considered (Karol *et al.,* 2001; Waters 2003; Lewis and McCourt 2004; Qiu *et al.,* 2006; Simon *et al.,* 2006). Green algae, which are one of the three evolutionary lineages (glaucophytes, red and green algae) derived from primary endosymbiosis of a cyanobacterium and an α proteobacterium (Keeling 2010), led to the founding member of the early plant lineage. The lineage of green algae such as *Chlorophyceae* and *Charophyceae* are considered a sister lineage to the land plant lineage (Wodniok *et al.,* 2011). Despite the arguments about the evolutionary base of higher plants, it is generally accepted that the closest algae relatives to land plants are the *Charophyceae* (Waters 2003). Evolution of the land plant lineage lead to distinct groups within the land plants such as for example bryophytes, lycophytes, monilophytes, gymnosperms and angiosperms (Hedges *et al.,* 2004; Nishiyama 2007; Finet *et al.,* 2010; Wodniok *et al.,* 2011; Timme *et al.,* 2012). It is the subject of current research as to what order *Charophycean* and *Bryophytes* (mosses, liverworts, and hornworts) internally evolved (Karol *et al.,* 2001; Waters 2003; Qiu *et al.,* 2006; Finet *et al.,* 2010; Wodniok *et al.,* 2011). The divergence of seed plants and mosses (bryophytes) are estimated to have happened in the range from 496

million years ago (MYA) based on molecular clock analyses (Zimmer *et al.,* 2007), and different parameters such as intron occurrence and UTR structure suggest a divergence of *P. patens* after *Chlamydomonas* (a chlorophyte algae) and before *A. thaliana* from the land plant lineage (Zimmer *et al.,* 2013). Despite the long divergence of algae and seed plants, it has been shown that *A. thaliana* encodes approximately 18% of the nuclear genome of cyanobacterial origin (Martin *et al.,* 2002). While this analysis was conducted on a limited set of proteins, these numbers can only be regarded as an estimate of the true number, which may be even higher (Martin *et al.,* 2002). Unique characteristics of plants compared to charophycean algae are the multicellular gametophyte and sporophyte, as well as the ability to form an apical meristem and differentiated tissues. This is especially of interest because mosses morphologically resemble the first plants that occupied the land (Kenrick and Crane 1997; Ligrone *et al.,* 2012). These characteristics were established when plants first moved from water to land and had to cope with new challenges like high UV radiation, desiccation and gravity. While the lifecycle of mosses is dominated by a haploid gametophytic phase (Richardt *et al.,* 2007) and they retain general genes enabling them to survive conditions inviable to vascular plants (such as permafrost or total desiccation) (Rensing *et al.,* 2007), vascular plants evolved to bear the sporophyte as the dominant stage (Taylor *et al.,* 2005). The need to preserve genes (due to the predominant haploid life style) is also reflected in the genome of *P. patens* that consists of n = 27 chromosomes (Reski *et al.,* 1994) and an average chromosome size of 17 mega base pairs (Mbp), whereas *A. thaliana* has a genome with n = 5 chromosomes that are on average 24 Mbp in size (Liang *et al.,* 2004; Yogeeswaran *et al.,* 2005). Taken together the new environment required means, like the regulation of growth, to respond to the changing surroundings.

Characteristics of plants that enabled the colonialization of land, like the multicellular gametophyte and sporophyte (Nishiyama 2007), as well as the ability to form an apical meristem and differentiated tissues (Bonhomme *et al.,* 2013), are found in *P. patens*. Regarding the apical meristem, it was postulated that more complex forms such as those in vascular plants derive from simple meristems that are found, for example, in *P. patens* (Graham *et al.,* 2000). Furthermore the comparability of moss morphology with the first plants that moved to the terrestrial habitat (Kenrick and Crane 1997; Ligrone *et al.,* 2012) make mosses interesting organisms to study.

1.2.1. The genome of *P. patens*

The total size of the *P. patens* genome is 510 Mbp (Lang *et al.,* 2008). It is thought that *P. patens* underwent polyploidization in the Eocene (56-33,9 MYA), but subsequently became haploid again, while keeping the duplicated chromosomes. In accordance with that, the investigation of 2907 *P. patens* paralogs led to the conclusion that there was an ancient

large-scale or even genome-wide duplication event, about 45 MYA (Rensing *et al.,* 2007). The duplication of the *P. patens* genome seems to have released the haploid plant from having to preserve its crucial single copy genes under all circumstances, and enhanced opportunities to develop new functions (Rensing *et al.,* 2007). Large scale genome duplications in angiosperms are followed by the retention of genes for transcription and signaling, while in the *P. patens* genome metabolism-associated genes are maintained – a fact reflected in the relative enrichment of these genes (70-80% in *P. patens* in contrast to 10-44% in seed plants) (Rensing *et al.,* 2007). Moreover, the latest re-annotation of the *P. patens* genome counts 32.275 protein coding genes of which 52% have no annotated PFAM domain (Zimmer *et al.,* 2013). In total, 22% of the protein coding genes could not be associated with a homolog from other species. However, these proteins seem not to be pseudogenes in at least 13% of the protein coding genes as they are supported by ESTs (Zimmer *et al.,* 2013). A general expansion of the HK family has also been found in *P. patens*, though it is not known what could have had caused this drastic increase (Rensing *et al.,* 2008).

1.3. Morphology and development of the moss *P. patens*

The first large innovation in evolution of land plants, the multicellular sporophyte, is generally considered to have evolved from a delay in meiosis (Graham *et al.,* 2000; Graham and Wilcox 2000). Even though *P. patens* mainly exists in the gametophyte stage, it forms a three dimensional plant body, the gametophore and the stem-leaf structure is similar to that of higher plants (Liang *et al.,* 2004). The lifecycle of *P. patens* starts with a haploid spore that forms protonema cells (a long branching filament; Figure 6, A). The formation of protonema is limited to aquatic environments and needs to be fully surrounded by liquid (Lienard *et al.,* 2008). The protonema expands by tip growth. Chloronema, the first cell type that is developed, are the photosynthetic cells of protonema that contain more than 100 chloroplasts, a characteristic of these cells is the perpendicular cell wall (Figure 6, C) (Finka *et al.,* 2008). Subsequently the tip cell changes to give rise to caulonema-type protonema. Caulonemata are adventitious cells involved in nutrient absorption and rapid colonization, their regeneration capacity in explants and the ability to form buds decreases, and brown pigment content as well as the potential for poiploidy rises, with individual cell age (Knoop 1978). Caulonema cells contain a few small chloroplasts and have characteristic oblique cell walls (Figure 6, E) and persistently divide in darkness (Finka *et al.,* 2008). For branching of the caulonema, a single-celled initial forms on the second sub apical cell of the caulonema filament. This initial cell can continue to grow by tip growth to form a new lateral filament or takes on the morphology associated with the assembly of a bud (Figure 6, F). The bud may be regarded as a primitive meristem, initializing meristematic gametophore growth (Finka *et al.,* 2008). Further growth of the gametophore is directed by continuous division of the apical

meristematic cell that then forms a new stem cell and a basal primodia for subsequent differentiation into a stem internode and a leaf (Harrison *et al.,* 2009). In contrast to vascular plants, *P. patens* develops leaves consisting of one layer of cells and these leaves do not contain a vasculature. In adult leaves a single midrib is formed (Sakakibara *et al.,* 2003). Unlike homoiohydric plants, that control their water potential trough turgor, *P. patens* lacks water potential regulation; its water content varies with the environment and its developmental stage (Lienard *et al.,* 2008), and water uptake is dependent on capillary action (Proctor and Tuba 2002).

After the formation of the leafy shoot, rhizoids arise from epidermal cells at the base of the gametophore. The development of rhizoid is believed to depend on two factors: auxin (Ashton *et al.,* 1979b; Sakakibara *et al.,* 2003) and another unknown factor. They function in gametophore attachment to the substrate and nutrition uptake (Sakakibara *et al.,* 2003). The mature gametophore later forms gametangia and, following fertilization from anteridium to archegonium, a single diploid capsule – the sporophyte – forms. Recently it was shown that the switch from gametophytic to sporophytic growth is facilitated by a shift of about 12% of the analyzed genes and involves a substantial fraction of transcription factors (O`Donoghue *et al.,* 2013). Ultimately, meiosis occurs within the capsule to produce haploid spores.

The presence of phytohormones, intracellular messaging (e.g. via Ca^{2+} ions) and the responses to environmental stimuli (e.g. light, gravity, cold, salt, and drought) is comparable to vascular plants (Liang *et al.,* 2004), but the molecular mechanisms underlying tissue development started to unfold only recently (Spinner *et al.,* 2010; Wu *et al.,* 2011).

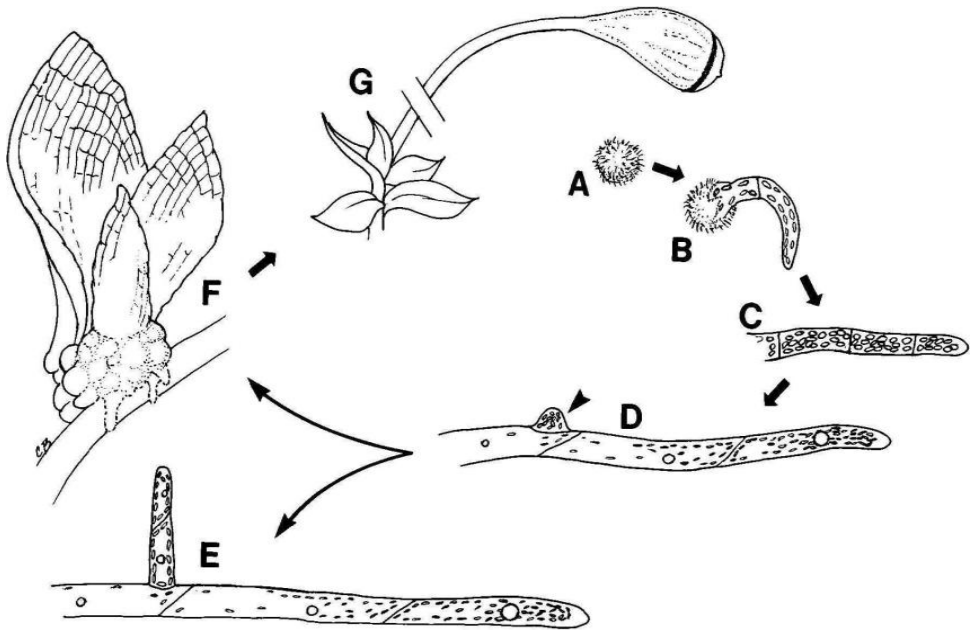

Figure 6: Stages of moss development. Haploid spores (A), chloronema cells (B and C) subsequently the tip cell changes to give rise to caulonema cells (D). A single-celled initial (D, arrowhead) forms on the second sub apical cell of the caulonema filament. This initial cell can continue to grow by tip growth to form a new lateral filament (E)

or takes on the morphology associated with the assembly of a bud to form the leafy shoot (F and G). Following fertilization, a diploid capsule (G) forms on the leafy shoot. Ultimately, meiosis occurs within the capsule to produce haploid spores. Picture modified after (Schumaker and Dietrich 1998).

Altogether, *P. patens* representing a "primitive" land plant (Rensing *et al.,* 2002), seems an ideal candidate for evolutionary studies (Schaefer 2002; Cove *et al.,* 2006). While some of the features in *P. patens* are comparable to "higher" plants, *P. patens* does possess a number of features that make it peculiar (for details see Table 1).

Table 1: Features of *P. patens*.

Feature	*P. patens*
Morphology	
Sporophyte	Develops sporophyte only during a short period
Gametophyte	Dominates lifecycle
Meristematic growth	During gametophore development
Protonema growth	Yes
Roots	No
Growth conditions	
High salt	Normal growth up to 350 mM (Frank *et al.,* 2005)
High sorbitol	Normal growth up to 500 mM (Frank *et al.,* 2005)
Extreme temperatures	Yes (Rensing *et al.,* 2008)
Phytohormones	
ABA	Yes
Regulation via ABI1 related type 2C protein phosphatases	Yes (Komatsu *et al.,* 2009)
Regulation via ABI1 related type three transcription factors	Yes (Marella *et al.,* 2006)
Auxin	Yes
Polar auxin transport	No (Fujita *et al.,* 2008)
PINs	Yes, but no function known (Krecek *et al.,* 2009)
STY controls auxin biosynthesis	Yes (Eklund *et al.,* 2010)
Cytokinin	Yes
Cytokinin receptor with histidine kinase activity	Yes (Ishida *et al.,* 2010)
Ethylene	Yes (Yasumura *et al.,* 2012)
Ethylene receptor	Yes (Ishida *et al.,* 2010)

Feature	*P. patens*
Gibberellin	No (Hirano *et al.,* 2007; Yasumura *et al.,* 2007; Rensing *et al.,* 2008)
Gibberellin precursor diterpene	Yes, functions in chloronema/caulonema transition (Anterola *et al.,* 2009; Hayashi *et al.,* 2010)
Brassinosteroids	No (Rensing *et al.,* 2008; Depuydt and Hardtke 2011); Yes (Prigge and Bezanilla 2010)
Jasmonates	No (Rensing *et al.,* 2008); Yes (Prigge and Bezanilla 2010)
Strigolactones	Yes (Proust *et al.,* 2011)

1.4. Cytokinin in the moss *P. patens*

Cytokinin biology in mosses began only shortly after the isolation of kinetin from yeast (Miller *et al.,* 1956), when Gorton and colleagues tested kinetin's effect on the formation of buds in the moss *Tortella caespitosa* (Gorton and Eakin 1957; Gorton *et al.,* 1957). This predates the isolation of zeatin from maize (Letham 1963), which was followed by the isolation of a kinetin-like substance, present in moss, that was later discovered to be isopentenyladenine (Beutelmann 1973). Owing to cytokinin's obvious effect, the bud formation, many experiments describing this phenomenon were carried out (Brandes and Kende 1968; Ashton *et al.,* 1979a; Ashton *et al.,* 1979b; Abel *et al.,* 1989; Christianson and Hornbuckle 1999; Schulz *et al.,* 2000). It is known that isopentenyladenine is the major cytokinin in moss (Wang *et al.,* 1981a; Wang *et al.,* 1981b) and that other types of cytokinins such as *cis*-zeatin are also present in *Physcomitrella* (von Schwartzenberg 2006). Overall, a multitude of cytokinins that belong to the isopentenyladenine-, *trans*-zeatin- and *cis*-zeatin-, and DHZ-type (at least 20 different cytokinins, containing cytokinin-bases, ribosides and nucleotides as well as O-glucosides of *trans*- and *cis*-zeatin) have been isolated from *Physcomitrella* (von Schwartzenberg *et al.,* 2007). Evidence that the cytokinins in the culture medium modulate the differentiation of *P. patens* protonema was found when cytokinins were depleted from the medium (Klein 1967; Brandes and Kende 1968). This is also reflected by the fact that approximately 80% of total cytokinins are secreted to the medium (Schween *et al.,* 2003). Whole-culture extracts have shown isopentenyladenine to be the predominant cytokinin in *P. patens* culture (56% isopentenyladenine; 32% *cis*-zeatin; 11% *trans*-zeatin of total cytokinin content) (Schulz *et al.,* 2000; Yevdakova *et al.,* 2008), while *cis*-zeatin is the major cytokinin in protonema tissue (von Schwartzenberg *et al.,* 2007). In general, mosses share these *cis*-zeatin and isopentenyladenine-type cytokinins with evolutionarily earlier-diverging species such as cyanobacteria and algae (Stirk *et al.,* 1999; Stirk *et al.,* 2003). *Trans*-zeatin,

the major cytokinin of seed plants, has been detected in moss only at low levels (Wang *et al.,* 1981b; von Schwartzenberg *et al.,* 2003).

1.4.1. Cytokinin biosynthesis in *P. patens*

Six tRNA-IPT enzymes have been predicted in *P. patens* (Frebort *et al.,* 2011; Patil and Nicander 2013) and *PpIPT1* has been shown to be expressed in protonema and functional in cytokinin biosynthesis (Yevdakova and von Schwartzenberg 2007). Lately, other two *tRNA-IPT* genes were shown to complement a UNN recognizing tRNA-deficient yeast mutant and to produce isopentenyladenine (Patil and Nicander 2013).

Other evidence of cytokinin production comes from *ove* mutants belonging to the cytokinin over-producing mutants (*ove*). This was first hypothesized because they cross-feed a substance to the WT that triggers bud and gametophore formation in the WT (cross-feeding experiments were carried out by culturing the *ove* mutant separated by permeable membrane from the WT) (Ashton *et al.,* 1979a). The hypothesis that this substance is cytokinin has been confirmed by measuring the cytokinin content in the extracellular space (Schulz *et al.,* 2000). Another effect observed in the *ove* mutants accompanied by the overproduction of cytokinin is the development of more caulonemal filaments in the dark than in the WT under the same conditions (Ashton *et al.,* 1979a). However, the molecular basis in the *ove* mutants has not been shown so far.

1.4.2. Cytokinin catabolism in *P. patens*

Cytokinin degradation has been characterized in *Funaria hygrometica,* a moss closely related to *P. patens*, *in vivo* and *in vitro*. Protonema extracts from *Funaria hygrometica* grown in the presence of radioisotope tagged kinetin and benzyladenine indicate a degradation of kinetin within 30 hours and a long presence of benzyladenine (Gerhäuser and Bopp 1990a). The *in vitro* assay suggested a substrate cleavage in the case of radioisotope-tagged kinetin and isopentenyladenine, while benzyladenine was not degraded (Gerhäuser and Bopp 1990b). In *P. patens* six *PpCKX* genes are known (Gu *et al.,* 2010; Frebort *et al.,* 2011) and, with the exception of PpCKX2 (no prediction), all are predicted to the secretory pathway (Gu *et al.,* 2010), although no PpCKX enzyme has been characterized. Overexpression of the *A. thaliana* CKX2 enzyme in *P. patens* resulted in the decrease of inactivated *trans*-zeatin compounds (2-fold decrease of *tZ*ROG and *tZ*OG) in tissue extracts (von Schwartzenberg *et al.,* 2007). In contrast to the moderate change inside the tissue, isopentenyladenine was completely degraded in the culture medium (von Schwartzenberg *et al.,* 2007). It should be noted that *AtCKX2* is targeted to the secretory pathway (Schmülling *et al.,* 2003) consistent with the available forecast localization of the *PpCKXs*. Von Schwartzenberg and colleagues also report the activity of PpCKX in crude extracts to be seven times more efficient on *cis*-

zeatin than *trans*-zeatin and isopentenyladenine (von Schwartzenberg *et al.,* 2007). The only molecular data about PpCKX enzymes are EST data of cytokinin-treated *P. patens* gametophores that were enriched in *PpCKXs* (Nishiyama *et al.,* 2003).

1.4.3. Cytokinin effects in *P. patens*

The effect of cytokinin seems to be different in the extracellular space than in the intracellular space (Reutter *et al.,* 1998). To date, no data about the prevalent site of cytokinin action in *P. patens* are available, although the extracellular space has been suggested as the site of major cytokinin action (von Schwartzenberg *et al.,* 2007). This is in accordance with the finding that most cytokinin can be found in the culture medium (Schween *et al.,* 2003) and that cytokinin degradation is also predicted to be located in the extracellular space (Gu *et al.,* 2010), meaning that the regulation of cytokinin content is predominant in the extracellular space.

Cytokinin affects protonema development. The exogenous application of cytokinins arrests protonema cells in the G1 Phase and favors the event of polyploidy creation in caulonema (Schween *et al.,* 2003). This then has an effect on the regeneration capacity of these cells (Knoop 1978). The depletion of cytokinin from the culture medium by the expression of *AtCKX2* causes altered protonema morphology (von Schwartzenberg *et al.,* 2007), indicating that fundamental growth regulation is dependent on cytokinin. The morphologic changes exhibit a range of swollen protonema cells of the chloronemal and caulonema type in plants expressing the transgene at a lower rate (*AtCKX2-7*), and were comprised of pure chloronemal protonema in the mutant (*AtCKX2-16*) being more active in cytokinin degradation (von Schwartzenberg *et al.,* 2007).

Increased extracellular cytokinin triggers bud formation (Brandes and Kende 1968; Ashton *et al.,* 1979a; Ashton *et al.,* 1979b; Abel *et al.,* 1989; Christianson and Hornbuckle 1999; Schulz *et al.,* 2000) and depletion of cytokinin from the culture medium reduces budding rates (Brandes and Kende 1968; von Schwartzenberg *et al.,* 2007). Moreover, it has been shown that cytokinin does not induce bud formation in the absence of auxin (Cove 1984; Cove *et al.,* 2006). A detailed analysis of the biological activation capacity of different cytokinins in the budding assay showed isopentenyladenine, *trans*-zeatin, and benzyladenine to have strong bud-inducing capacities in *P. patens* (von Schwartzenberg *et al.,* 2007). Furthermore time-dependent cytokinin concentration maxima were found in WT *P. patens*. Plants were investigated for their production of cytokinin and a cytokinin maximum was found to be present at nine days after subculture; this triggered the subsequent bud formation at day 13 (Schulz *et al.,* 2000). The mutant PC22 (that is characterized by a macro-chloroplast, which reenters division after cytokinin application) (Abel *et al.,* 1989) was defective for this mechanism and, despite two cytokinin peaks at day 9 and day 21, no bud formation was observed (Schulz *et al.,* 2000). *P. patens* overexpressing the *IPT* gene from *Agrobacterium* in

turn had high levels of cytokinin (34-fold to 372-fold of WT) that resulted in the formation of callus like buds from the first day onwards (Schulz *et al.,* 2000).
Description of bud formation in more detail revealed that calcium plays a role in the formation of the initial cell. The initial cell formation can be triggered by the application of exogenous cytokinin and further bud formation also requires cytokinin (Saunders and Hepler 1983). While the formation of the initial cell has been described as the first cytokinin-dependent step in bud formation, further progression to the manifested bud was described as the second cytokinin-dependent step in bud formation (Michael and Christianson 2000). ABA has been shown to be an inhibitor of the second cytokinin-dependent step in bud formation (Christianson 2000).

A basic growth regulation effect of cytokinin has only recently been identified in the development of gametophore leaves. Exogenous application of cytokinin enhanced cell division, while cell expansion was inhibited (Barker and Ashton 2013). Furthermore cytokinin-deficient *P. patens* plants do not develop gametangia or sporophytes (von Schwartzenberg *et al.,* 2007).

1.4.4. Cytokinin signaling in *P. patens*

In contrast to the cytokinin metabolism and growth regulation by cytokinin, there is almost nothing known about cytokinin signaling in *Physcomitrella*.

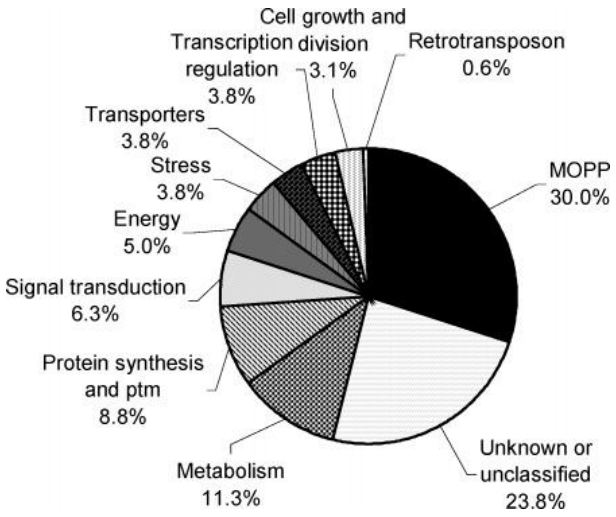

Figure 1: Distribution of *P. patens* phosphorylated proteins by putative similar function. Abbreviation: MOPP, Moss phosphorylated proteins; ptm, post transcriptional modification. Modified from (Heintz *et al.,* 2006)

The first attempt to elucidate how *Physcomitrella* perceives and transduces the cytokinin signal was by investigating phosphorylated proteins from a cytokinin-treated *Physcomitrella* whole cell lysate (Heintz *et al.,* 2006). This study showed that cytokinin signal propagation mediated through phosphorylation involves proteins from various functional categories (shown in Figure 7). However, due to experimental conditions, phosphate groups residing to histidine or aspartate amino groups were lost during the procedure. Hence the information gained from these experiments is limited and reveals nothing about the classical, TCS based cytokinin signaling pathway, in which a phosphorelay between

histidine and aspartate plays a key role (Heintz *et al.,* 2006). In 2009 Pils and Heyl conducted a comprehensive bioinformatic analysis of algae and land plants to uncover cytokinin signaling components. They identified three possible cytokinin receptors which share a common domain architecture with *A. thaliana* cytokinin receptors, two HPT proteins, five RRBs, seven RRAs and two RRCs (Pils and Heyl 2009). Apart from this study, Ishida and colleagues published that PpCHK2 (called PpHK4b in the respective publication) is capable of complementing a deletion in the *E. coli* TCS upon application of *trans*-zeatin (Ishida *et al.,* 2010). Nothing more has been published about the molecular basis of the cytokinin signal transduction in the moss *Physcomitrella*

1.5. Aim of the project

Two central questions guided the process of this work. First, how does *P. patens* perceive the cytokinin signal? Second, where did the cytokinin signaling system found land plants originate from?

How does *P. patens* perceive cytokinin?

Cytokinin research in moss has a long history (Gorton and Eakin 1957; Gorton*, et al.* 1957), but the molecular mechanisms underlying the well studied physiological response of *P. patens* to cytokinin, the formation of buds (von Schwartzenberg 2009) has not been elucidated. To unravel the molecular basis of cytokinin action in *P. patens*, this project aimed to investigate the first step in cytokinin signaling, the perception of the cytokinin signal. Three cytokinin receptors were annotated in *P. patens* (Pils and Heyl 2009); *PpCHK1*, *PpCHK2* and *PpCHK3.* The investigation of their signal perception, signal transduction and their biological role was subject to the first part of the project.

Where did the cytokinin signaling system found in land plants originate from?

To gain insights about how and when the cytokinin signaling system was established, a comprehensive phylogenetic analysis that included amongst others, data from charophyte algae, which diverged early from the land plant lineage, and of chlorophyte algae, which are not part of the land plant lineage was carried out. The domains of proteins involved in cytokinin signaling and cytokinin metabolism were investigated to identify potential components in cytokinin signaling and metabolism. The phylogenetic relation of these protein domains was analyzed to conclude on the evolution of the respective protein domains and the proteins they are part of.

2. Materials and Methods

All solutions are prepared with bi-distilled, deionisized water (ddH_2O) unless otherwise indicated. Consumables involved in the handling of nucleic acids, bacteria or plants were sterilized beforehand by autoclaving, which was generally carried out at 121°C and 2,1 bar for 15 minutes.

2.1. Materials

Glass and plastic ware and appropriate working environments (S1 laboratory) were provided by the Institute of Applied Genetics, Freie Universität Berlin, Germany.

2.1.1. Organisms

2.1.1.1. Bacteria

Bacterial strains used during this study are listed in Table 2.

Table 2: Overview of bacteria used

Strain	Reference	Genotype	Application /Description
E. coli DB3.1	(Hanahan 1983; Bernard and Couturier 1992)	F$^-$ *gyr*A462 *end*A1 delta(*sr*1-*rec*A) *mcr*B *mrr hsd*S20($r_B^-m_B^-$) *sup*E44 *ara*14 *gal*K2 *lac*Y1 *pro*A2 *rps*L20(Smr) *xyl*5 delta *leu mtl*1	Cloning
E. coli DH5alpha	(Hanahan 1983; Raleigh *et al.,* 1989)	F$^-$ *rec*A1 *end*A1 *mrr hsd*R17 ($r_K^-m_K^+$) lamda$^-$ *thi*-1 *sup*E44 *gyr*A96 *rel*A1	Cloning
E. coli DH10B	(Calvin and Hanawalt 1988; Raleigh *et al.,* 1988)	F- *mcr*A Δ(*mrr-hsd*RMS-*mcr*BC) Φ80*lac*ZΔM15 Δ*lac*X74 *rec*A1 *end*A1 *ara*D139 Δ(*ara*, *leu*)7697 *gal*U *gal*K λ- *rps*L *nup*G	Cloning
E. coli KMI002	(Mizuno and Yamashino 2010)	*ΔrcsC*::Km^r,ara thi *Δ (pro-lac) Δ(wza-wca), wza*::*lacZ, Δ cps* operon	Protein expression
E. coli BL21 (DE) pLysS	(Grunberg-Manago 1999; Lopez *et al.,* 1999)	F- *omp*T *hsd*SB (rB-mB-) *gal dcm rne*131 (DE3) pLysS (CamR)	Protein expression

Strain	Reference	Genotype	Application /Description
Agrobacterium tumefaciens GV3101::pM90	(Schnell 1978; Koncz *et al.,* 1987)	Rif^R, Gm^R	Transformation of *A. thaliana* and transient expression in *N. benthamiana*

2.1.1.2. Plants

Experiments employing *P. patens* were carried out using *Physcomitrella patens* (Hedw) B.S.G collected from Grandsden Wood, Huntingdonshire, UK (1968), provided by D. Cove (University of Leeds, UK); deletion mutants of *Ppchk1 Ppchk2* were provided by K. von Schwartzenberg, Universität Hamburg, Hamburg (von Schwartzenberg *et al.,* in preparation).

Experiments with *A. thaliana* were carried out using wild type plants of *Arabidopsis thaliana* (Col-0) obtained from NASC – The European *Arabidopsis* Stock Centre (Nottingham, UK) and *ahk2 ahk3* knockout plants (*ahk2-5 ahk3-7*, (Riefler *et al.,* 2006) and *ahk2-2 ahk3-3* , (Higuchi *et al.,* 2004)).

Transient protein expression was carried out in *Nicotiana benthamiana*.

2.1.2. Chemicals

2.1.2.1. Essential chemicals

During this work all chemicals were supplied by the institutional stock. If special care was to be taken, the supplier is mentioned in the respective protocol. In general the chemicals were ordered from:
Fluka (Buchs, Switzerland), Merck (Darmstadt), Roth (Karlsruhe), Serva (Heidelberg), Peqlab (Erlangen), Sigma (Deisenhofen).

2.1.2.2. Reaction kits

Routine nucleic acid purification was carried out with commercial reaction kits (see Table 3).

Table 3: Reaction kits used during this project

DNA isolation kit	Supplier	Application
Invisorb™ Spin Plasmid Mini Kit	Invitek, Berlin	Plasmid preparation, small scale
Nucleobond Xtra Maxi kit	Macherey-Nagel, Düren	Plasmid preparation, large scale
QiaQuick Gel extraction kit	Qiagen, Hilden	DNA extraction from agarose gels
QiaQuick PCR purification kit	Qiagen, Hilden	DNA purification after enzymatic reactions

DNA isolation kit	Supplier	Application
Qiagen RNAeasy Kit	Qiagen, Hilden	Purification of RNA

2.1.2.3. Antibiotics

All antibiotics were dissolved in the respective solvent and filter sterilized (Table 4). Aliquots were then stored at -20°C until use.

Table 4: Antibiotics used during the course of the project

Antibiotic	Concentration in Stock solution	Concentration in medium	Solvent
Ampicillin	50 mg/mL	50 µg/mL	H_2O
Carbencillin	50 mg/mL	50 µg/mL	H_2O
Kanamycin	100 mg/mL	100 µg/mL	H_2O
Tetracycline	10 mg/mL	10 µg/mL	EtOH
Zeocin	50 mg/mL	50 µg/mL	H_2O
Chloramphenicole	25 mg/mL	25 µg/mL	EtOH
Spectinomycin	30 mg/mL	30 µg/mL	H_2O
Geneticin (G418)	25 mg/mL	25 µg/mL	H_2O
Hygromycin	50 mg/mL	50 µg/mL	H_2O
Rifampicin	50 mg/mL	50 µg/mL	DMSO

2.1.2.4. Enzymes

Restriction enzymes

All restriction enzymes were obtained from Fermentas (St. Leon-Rot) or New England Biolabs (Frankfurt).

DNA/RNA modifying enzymes

The respective enzyme (see Table 5) was chosen dependent on the application stated in the description text.

Table 5: Enzymes used during the course of the project

Enzyme	Supplier	Application
BP- and LR-clonase	Invitrogen, Karlsruhe	Recombination via Gateway™ technology
Taq polymerase	In-house preparation	PCR reaction
Pfu polymerase	In-house preparation	PCR reaction
High fidelity *Pfu*-Polymerase	Agilent, Böblingen	PCR reaction

Enzyme	Supplier	Application
Immolase	Bioline, Luckenwalde	Quantitative real time PCR
Superscript III reverse transcriptase	Invitrogen, Karlsruhe	Reverse transcription of RNA
T4-DNA ligase	Fermentas, St. Leon-Rot	Ligation, classical cloning

Enzymes for the generation of protoplasts

Protoplast generation is described in the following text. Enzymes used to digest the cell wall are found in Table 6.

Table 6: Enzymes used for protoplast generation

Enzyme	Supplier	Purpose
Cellulase R-10	Serva, Heidelberg	Generation of protoplasts from *A. thaliana*
Macerozyme	Serva, Heidelberg	Generation of protoplasts from *A. thaliana*
Driselase	Sigma, Deisenhofen	Generation of protoplasts from *P. patens*

2.1.3. Media

2.1.3.1. Media for bacteria

In the course of this work, bacteria were cultivated with Luria Bertani (LB) medium made either from components (see Table 7) or from premixed media according to the manufacturer's instruction. M9 medium (see Table 7) is a mineral medium that provides the essentials for bacteria to grow. This medium was used for the weak expression of receptor proteins. Any other requirements beyond carbon and nitrogen are not served in this medium (Sambrook and Russell 2001). Cultures of *A. tumefaciens* were grown in the nutrient rich YEB medium (see Table 7) (Vervliet *et al.,* 1975).
Media were supplemented with antibiotics (see Table 4) according to the use of the medium.

Table 7: Media for bacteria

Media	Components	Concentration
LB		
	Tryptone	10 g/L
	Yeast extract	5 g/L
	$NaCl_2$	5 g/L
	Autoclaved at 121°C, 2,1 bar For solid LB 15 g agar were added prior to autoclaving.	
M9		
	KH_2PO_4	22 mM
	$NaHPO_4$ water free	50,8 mM
	NaCl	8,6 mM

Media	Components	Concentration
	NH_4Cl	18,8 mM
	$MgSO_4$	2 M
	$CaCl_2$	100 mM
	Glucose	0,4 %
	Autoclaved at 121°C, 2,1 bar, add the following components after medium has cooled to RT.	
	Casamino acids (Difco, Detroit USA)	0,1% %
	IPTG	0,025 mM
YEB		
	Bacto peptone	5 g/L
	Yeast extract	1 g/L
	Beef extract	5 g/L
	Saccharose	5 g/L
	Autoclaved at 121°C, 2,1 bar	
	For solid LB 15 g agar were added prior to autoclaving.	
	$MgCl_2$	0,5 g/L

2.1.3.2. Media for plants

P. patens was cultured in BCD medium (see Table 8). If necessary, antibiotics were supplemented. BCD was either produced as a liquid medium or as agar plate. For protoplast generation a standard liquid culture (described in section 2.5.4.1) was inoculated six weeks prior to protoplast generation and BCD medium was supplemented by ammonium tartrate.
A. thaliana was grown on soil in the green house or on MS-medium agar plates in the growth chamber (see Table 8). If necessary, antibiotics were supplemented.

Table 8: Growth media for plants

Media	Components	Final concentration
BCD		
	$MgSO_4$ x $7H_2O$	1 mM
	KH_2PO_4	2 mM
	KNO3	10 mM
	$FeSO_4$ $7H_2O$	0,045 mM
	$CuSO_4$ x 5 H_2O	0,22 µM
	H_3BO_3	10 µM
	CoCl x 6 H_2O	0,23 µM
	$NaMoO_4$ x 2 H_2O	0,1 µM
	$ZnSO_4$ x $7H_2O$	0,19 µM
	$MnCl_2$ x 4 H_2O	2 µM

Media	Components	Final concentration
	KI	0,17 µM
	Agar (if required)	1,1 %
	Glucose Autoclaved at 121°C, 2,1 bar, let cool to 60°C	10 mM
	If required ammonium tartrate	5 mM
	$CaCL_2$	2 mM
MS		
	MS-Salt	2,1 g/L
	MES	1,25 g/L
	Saccharose	15 g/L
	Thiamine	20 mg/L
	Nicotinic acid	1 mg/L
	Pyridoxine	1 mg/L
	Biotin	1 mg/L
	Agar	9 g/L

2.1.4. Oligonucleotides

Oligonucleotides, also called primers, used during the course of this project were obtained from Invitrogen, Karlsruhe, dissolved at a concentration of 100 µM in bidestilled, deionisized water and stored at -20°C. Primers used during this study are listed in Table 9.

Table 9: Oligonucleotides (primers) used during the course of the project

Name	Application	Sequence (5´→ 3´)
qRT-PCR in *A. thaliana*		
ARR16_qRT r	qRT-PCR primer for *AtARR16* At2g40670	AACCCAAATACTCCAATGC
ARR16_qRT f	qRT-PCR primer for *AtARR16* At2g40670	TCAGGAGGTTCTTGTTCGTCTT
ARR7_qRT_r	qRT-PCR primer for *AtARR7* At1g19050	ATCATCGACGGCAAGAAC
ARR7_qRT_f	qRT-PCR primer for *AtARR7* At1g19050	CTTGGAACCAATCTGCTCTC
UBC10 qPCR rv	ubiquitin-protein ligase UBC10 (At5g53300) used as internal reference gene in qRT-PCR analyses with *A. thaliana* samples	TTCATTTGGTCCTGTCTTCAG
UBC10 qPCR fw	ubiquitin-protein ligase UBC10 (At5g53300) used as internal reference gene in qRT-PCR analyses with *A. thaliana* samples	CCATGGGCTAAATGGAAA
qRT-PCR in *P. patens*		
C45-tg2F	Primer for the 60s ribosomal protein L21 (Pp1s107_181V6.1) used as internal reference gene in qRT-PCR analyses with *P. patens* samples	ACGCACCGGCATCGT
C45-tg2R	Primer for the 60s ribosomal protein L21 (Pp1s107_181V6.1) used as internal reference gene in qRT-PCR analyses with *P. patens* samples	TGCTTGTTCATCACGACACCAA
PpCRE1_left_qPCR	qRT-PCR primer for *PpCHK1*	CAGTTCTTGGCAACTGTGTC
PpCRE1_right_qPCR	qRT-PCR primer for *PpCHK1*	TTAGCCTGATCAAGGACCTC
PpCRE2_left_qPCR_A	qRT-PCR primer for *PpCHK2*	GATGCATTACCTCCTTGGAC
PpCRE2_right_qPCR_A	qRT-PCR primer for *PpCHK2*	GTCGCCAGAAACTGAGACTT
PpCRE3_left_qPCR	qRT-PCR primer for *PpCHK3*	GCGTGTACTCGTAGTGGATG
PpCRE3_right_qPCR	qRT-PCR primer for *PpCHK3*	CCCCATGCATCCTTATCTAC

Name	Application	Sequence (5´→ 3´)
PpCRE4_qPCR_fwd	qRT-PCR primer for *PpCHK4*	CTTTTTTCTCAAGCCGACAGCAACAG
PpCRE4_qPCR_rev	qRT-PCR primer for *PpCHK4*	GAAGTTGCGGCTTACTCCCTCCA
PpRR11_left_qPCR	qRT-PCR primer for *PpRR11*	TCCTCGGACTTTCAGATAGC
PpRR11_right_qPCR	qRT-PCR primer for *PpRR11*	TCTGAAGACATGACCACGAC
Gateway™-cloning		
attB12-GW-3´a	Gateway™ adapter PCR	GGGGACCACTTTGTACAAGAAAGCTGGGT
attB1-GW-5´s	Gateway™ adapter PCR	GGGGACAAGTTTGTACAAAAAAGCAGGCT
PpCRE1_gb_anno_spec_rev	Amplification of *PpCHK1* gene	GCGGTTGCCAAGCATTTCTTCGACGTGAACTAA
PpCRE1_gb_anno_spec_fwd	Amplification of *PpCHK1* gene	ATGCACAGGGCTACTGGCTCTGGACG
PpCRE1_gb_GW1_fwd	Amplification of *PpCHK1* gene with Gateway™ attachment sites	AAAAAGCAGGCTTGATGCACAGGGCTACTGGC
PpCRE1_gb_GW1_rev	Amplification of *PpCHK1* gene with Gateway™ attachment sites	AGAAAGCTGGGTCCGGTTAAGTTATTACAAG
PpCRE1_gb_wo_stop_rev	Amplification of *PpCHK1* gene without STOP codon, with Gateway™ attachment sites	AGAAAGCTGGGTCGTTCACGTCGAAGAAATG
PpCRE2_fwd_gene	Amplification of *PpCHK2* gene	ATGCACAGGACAACAGGACC
PpCRE2_rev_gene	Amplification of *PpCHK2* gene	TCAGTTTGGCCCGAAGAAG
PpCRE2_gene_GW fwd	Amplification of *PpCHK2* gene with Gateway™ attachment sites	AAAAAGCAGGCTTGATGCACAGGACAACAGGA
PpCRE2_gene_GW rev	Amplification of *PpCHK2* gene with Gateway™ attachment sites	AGAAAGCTGGGTCTCAGTTTGGCCCGAAGAA
PpCRE2_wo_stop_rev	Amplification of *PpCHK2* gene without STOP codon, with Gateway™ attachment sites	AGAAAGCTGGGTCGTTTGGCCCGAAGAAGTG
PpCRE3_fwd_gene	Amplification of *PpCHK3* gene	ATGAGACAAAGAAAACAGTTGATCAATC
PpCRE3_rev_gene	Amplification of *PpCHK3* gene	TTAATTCGCCTGGAAGAAATGC
PpCRE3_gene_GW fwd	Amplification of *PpCHK3* gene with Gateway™ attachment sites	AAAAAGCAGGCTTGATGAGACAAAGAAAACAG
PpCRE3_gene_GW rev	Amplification of *PpCHK3* gene with Gateway™ attachment sites	AGAAAGCTGGGTCTTAATTCGCCTGGAAGAA

2.1.5. Plasmids

Plasmids used during the course of the project are shown in Table 10.

Table 10: Plasmids used in this project

Name	Reference / Supplier	Application	Selection marker bacteria /plants
pB2GW7	(Karimi *et al.,* 2002)	Binary gateway™ plasmid for overexpression of the gene of interest under the 35S promoter in plants	Spectinomycin / Basta
pB7m34GW	(Karimi *et al.,* 2005)	Binary gateway™ plasmid for the fusion of a promoter and a gene of interest	Spectinomycin / Basta
pDEST15	Gateway™ destination-vector, Invitrogen Karlsruhe	Creates a N-terminal GST fusion for protein expression	Cabencillin
pDONR201	Gateway™ entry-vector, Invitrogen Karlsruhe	Cloning	Kanamycin
pDONR221	Gateway™ entry-vector, Invitrogen Karlsruhe	Cloning	Kanamycin
pDONR222	Gateway™ entry-vector, Invitrogen Karlsruhe	Cloning	Kanamycin
pK7FWG2	(Karimi *et al.,* 2002)	Binary gateway™ plasmid for C-terminal fusion to GFP for expression in plants	Spectinomycin / Kanamycin
pK7WGF2	(Karimi *et al.,* 2002)	Binary gateway™ plasmid for N-terminal fusion to GFP for expression in plants	Spectinomycin / Kanamycin
pROK219_NAN	(Kirby and Kavanagh 2002)	PTA reference	Kanamycin

2.2. DNA/RNA modification

2.2.1. DNA/RNA quantification

DNA quantification was performed using a NanoDrop (Thermo Scientific/Peqlab, Erlangen) photometer at 260 nm. Absorption of one unit equals 50 µg/mL DNA, and sample DNA concentration was calculated accordingly. The absorption ratio of 260 nm for DNA, relative to the absorption at 280 nm for proteins was calculated to evaluate the purity of the sample. Samples were positively evaluated when the DNA/protein ratio was in the range of 1,8 to 2,0.

2.2.2. Polymerase chain reaction

In vitro amplification of DNA was conducted using polymerase chain reaction (PCR) (Mullis and Faloona, 1987). Amplified DNA was subsequently used for identification of positive transformants in plants and *E. coli*, or for cloning. Details about the quantitative real time PCR are described in the following section 2.2.1. The annealing temperature in the PCR program (Table 11) was set to 5°C below the lowest calculated annealing temperature of the forward and reverse primer (see Table 9) and elongation time was chosen dependent on the length of the amplicon. When amplification was carried out with *Taq* polymerase, elongation temperature was 72°C and the time was adjusted to 1 min/kb in the first and 2 min/kb in the first and second elongation steps, respectively.

Table 11: Standard PCR reaction mix and program

Standard PCR reaction mix		Standard PCR program			
x µL	Template DNA (1-100 ng)	1. Denaturation	3 min	95°C	
2 µL	10-times *Pfu* buffer	2. Denaturation	45 sec	94°C	
0,8 µL	dNTPs (5 mM each nucleotide)	3. Hybridization	45 sec	Annealing temperature	25-30 cycles
1 µL	Primer 1	4. Elongation	2 min/kb	68°C	
1 µL	Primer 2	5. Elongation	4 min/kb	68°C	
0,2 µL	*Pfu*-polymerase	6. Pause	∞	16°C	
Add ddH_2O until 20 µL					

2.2.3. Quantitative real time polymerase chain reaction

For sensitive quantification of transcript levels, quantitative real time PCR (qRT-PCR) was used. RNA was isolated according to section 2.5.1 and transcribed into cDNA using SuperScript III Reverse Transcriptase (Invitrogen, Karlsruhe), according to the manufacturer's instructions, without the use of RNAseOUT enzyme and with an amount of 500 ng RNA (see section 2.2.1). For the subsequent analysis a master mix for one full analysis run (96-wells per plate) was prepared Table 12).

Table 12: Standard qRT-PCR reaction mix

Standard reaction mix for 96 wells	
320 µL	10-times reaction buffer
128 µL	50 mM MgCl2
64 µL	dNTPs (5 mM of each nucleotide)
32 µL	SYBR™ green (Sigma, Munich)
844,8 µL	ddH_2O
6,4 µL	25 µM Rox (Sigma, Munich)
6,4 µL	Immolase (Bioline, Luckenwalde) [5 units/µL]

This master mix was then divided into aliquots of 170 µL (sufficient for 12 wells) and 0,48 µL of each primer (Table 9) was added. Aliquots of 10 µL were pipetted into each well and supplemented with 10 µL of cDNA (100 ng/µL). Additionally to the samples, a negative control including ddH_2O instead of cDNA was also prepared. These reaction mixes were then analyzed in a 7500 Fast Real time PCR System (Applied Biosystems, Foster City, USA) according to the manufacturer's description (Table 13).

Table 13: Standard qRT-PCR program

Standard qRT-PCR program				
1.	Denaturation	15 min	95°C	
2.	Denaturation	10 sec	94°C	
3.	Hybridization	15 Sec	55°C	x 45 cycles
4.	Elongation	10 sec	72°C	
5.	Pause	∞	16°C	

The machine readout was inspected for errors and quality of the negative controls. After positive evaluation, the transcript levels relative to the housekeeping gene (see Table 9) were calculated according to the manufacturer's instruction using the relative quantification method (Software Version 2.3; Applied Biosystems, Foster City, USA).

2.2.4. DNA and RNA size separation by electrophoresis

Size separation of DNA molecules was carried out in horizontal gel chambers in a TAE buffer according to Sambrook and Russel (2001). Pore size of the gel was adjusted by the percentage of agarose depending on the expected length of the DNA fragment (routinely between 0,8 and 2%) and DNA detection was facilitated by the addition of ethidium bromide to the gel. DNA size standards were chosen according to the fragment of interest and loaded to a separate slot. For the readout of the separated DNA bands, Gene Genius apparatus and Gene Snap software (Syngene, Cambridge, UK) were used. The separation of RNA was carried out analogously to the above description for DNA.

2.2.5. PCR product purification

PCR products were directly purified by QiaQuick PCR Purification kit (Qiagen, Hilden) or after agarose gel separation manually excised under UV illumination and then purified with QiaQuick Gel Extraction kit (Qiagen, Hilden).

2.2.6. Gateway™ cloning

The efficient cloning of a gene of interest from an entry vector into a wide array of destination vectors is provided by the λ phage recombination-based (Landy, 1989) Gateway™ system (Invitrogen, Karlsruhe). Standard procedure was carried out according to the manufacturer's instructions, with minor changes: enzyme (BP- and LR-clonase™) concentration was decreased to 0,5 µL per reaction and incubation was prolonged to o/n at 25°C. However, if this approach was not successful the full protocol (4 µL of enzyme) was carried out.

2.3. Biochemical methods

2.3.1. Subcellular fractionation

To investigate the subcellular distribution of the protein of interest, transiently transformed, deep frozen tobacco leaves were ground to powder with mortar and pestle and 1 g of the material was further analyzed. The tissue powder was dissolved in 3 mL extraction buffer (Table 14), filtered with two layers of miracloth (Merck, Hilden), and first centrifuged for five minutes at 2.500 xg, 4°C. The supernatant was then again centrifuged for 45 minutes at 100.000 xg, 4°C, and the membrane-enriched pellet fraction was resuspended in 350 µL extraction buffer (Harford and Bonifacino 2009). Equal amounts of the cytosolic (supernatant) fraction and of the membrane fraction were further analyzed for protein occurrence with SDS-PAGE (section 2.3.2), protein blot and immunodetection according to section 2.3.3.

Table 14: Extraction buffer for subcellular fractionation

Extraction buffer		
50	mM	Tris -HCl, pH 7,5
20	%	Glycerol
150	mM	NaCl
1	mM	DTT
1	mM	PMSF

Protease inhibitor (complete mini, Roche, Mannheim) according to the supplier's instructions.

2.3.2. SDS-polyacrylamide gel electrophoresis (SDS-PAGE)

Isolated whole-mount proteins were separated by denaturing SDS-PAGE (Laemmli 1970) routinely in 8% SDS gels. SDS-PAGE separation gel (Table 15) was cast and overlaid by isopropanol until full polymerization, isopropanol was removed and the stacking gel (Table 15) was cast on top.

Table 15: SDS-PAGE gel (8%) preparation

10 mL SDS-PAGE separation gels		
	ddH_2O	4,8 mL
40%	Acryl-BisAcrylamide	2,5 mL
1,5 M	Tris pH 8,8	2,5 mL
10%	SDS	0,1 mL
10%	Ammonium persulfate (APS)	0,1 mL
	N,N,N',N'-Tetramethylethylenediamine (TEMED)	0,004 mL

5 mL SDS-PAGE stacking gel		
	ddH_2O	3,6 mL
40%	Acryl-BisAcrylamide	0,625 mL
1,5 M	Tris pH 6,8	0,63 mL
10%	SDS	0,05 mL
10%	APS	0,05 mL
	TEMED	0,005 mL

Samples were boiled at 95°C for five minutes with 5-times SDS sample buffer (0,225 M Tris-HCl, pH 6,8; 50% Glycerol; 10% SDS; 0,05% Bromphenolblue; 0,25 M DTT), and applied to the SDS gel. Protein separation (~25 mA pro Gel) was conducted in a running buffer (0,025 M Tris; 0,192% Glycin; 0,1% SDS). Gels were subsequently used for protein blot analysis.

2.3.3. Protein blot and immunodetection

Proteins separated by SDS-PAGE were transferred overnight at 4°C (30 V, 90 mA) to a PVDF membrane (Bio-Rad, Munich) by tank blotting (Gultekin and Heermann 1988) in a standard Twobin-buffer (0,25 M Tris; 1,92 M Glycin) (Towbin *et al.,* 1979).

Membranes with blotted proteins were washed in Tris-buffered saline with Tween (TBS-T; 50 mM Tris; 150 mM NaCl; 0,05% Tween 20; pH 7,5 with HCl) for 3 times each wash for five minutes and once for five minutes with TBS. The washed membrane was subsequently blocked for 1 hour with 5% skim milk powder dissolved in the TBS buffer, washed, incubated with the primary antibody mouse Anti-GFP (Roche, Mannheim) or mouse Anti-GST (Santa Cruz Biotechnology, Santa Cruz, USA), and diluted in a blocking buffer for 3 hours at RT. The membrane was then washed and subjected to incubation with the secondary antibody coupled to horse radish peroxidase (HRP), anti mouse-HRP (Santa Cruz Biotechnology, Santa Cruz, USA), for 1 hour at RT. Detection was carried out using an Enhanced Chemo Luminescence (ECL) reagent kit (Pierce/Fisher Scientific, Schwerte) according to the

manufacturer's instructions (Schrimpf 2002). The appropriate number of washing steps and dilution of the antibodies were tested empirically before sample processing.

2.4. Methods and handling of bacteria

2.4.1. Generation and transformation of electro-competent *E. coli* cells

An overnight culture of the respective *E. coli* strain was inoculated and grown at 37°C and 140 rpm. When the optical density at 600 nm (OD_{600}) reached 0,5 the culture was transferred to 4°C and all subsequent steps were carried out at 4°C. The culture was pelleted at 4000 xg and the pellet was washed with chilled ddH_2O and again pelleted at 4000 xg. The washing was repeated another two times before the pellet was resuspended in 1 mL cold glycerin. A 50 µL aliquot of the resulting bacteria suspension was either directly used for transformation or stored at -80°C until it was used (Calvin and Hanawalt 1988). Electro-competent *E. coli* cells were thawed on ice and DNA solution was added. After gentle mixing the cells were incubated for an additional 20 minutes on ice and then transferred to an electroporation-cuvette and pulsed at 1,7 kV (Micropulser™ by Biorad, Munich), resulting in a 5 ms current on average. Transformed cells were recovered from the cuvette by adding 1 mL LB medium, transferred to a new reaction vial and incubated for one hour at 37°C on a shaker (1400 rpm). Dilutions of the *E. coli* suspension were plated on solid LB medium with antibiotics according to the transformed DNA, and grown overnight at 37°C (Calvin and Hanawalt 1988) and grown over night at 37°C (Calvin and Hanawalt 1988).

2.4.2. Generation and transformation of heat shock competent *E. coli* cells

An overnight culture of the respective *E. coli* strain was inoculated and grown at 37°C and 140 rpm. When the optical density at 600 nm (OD_{600}) reached 0,5, the culture was transferred to 4°C (all subsequent steps were carried out at 4°C). The culture was subsequently pelleted at 4000 xg and the pellet was then resuspended in 2 mL TSS solution (Table 16), after which 200 µL 87% Glycerol was added. A 100 µL aliquot of the resulting bacteria suspension was directly used for transformation, or stored at -80°C until it was used (Chung *et al.,* 1989). Heat shock competent *E. coli* cells were thawed on ice and DNA solution was added. After gentle mixing, the cells were incubated for an additional 20 minutes on ice followed by a 60 seconds heat shock at 42°C, which was stopped by adding 1 mL of LB medium. Transformed cells were cultured for one hour at 37°C on a shaker at 1400 rpm and then dilutions of the *E. coli* suspension were plated on solid LB medium with antibiotic selection according to the transformed DNA and grown overnight at 37°C (Chung *et al.,* 1989).

Table 16: TSS solution for generation of heat shock competent cells

TSS solution	
85 %	LB
10 g	PEG6000
5 %	DMSO
50 mM	$MgCl_2$

2.4.3. Plasmid isolation from *E. coli* liquid culture

2.4.3.1. Plasmid isolation via alkaline lysis

For small-scale plasmid, isolation via alkaline lysis was used – a detailed protocol has been described by Sambrook and Russel (Sambrook and Russell 2001). The air-dried DNA pellet was resuspended in an appropriate amount of bidestilled water (sterile if desired) and analyzed for the DNA concentration by photometric means (NanoDrop 2000) (description see section 2.2.1).

2.4.3.2. Plasmid isolation via a DNA binding column

Plasmid isolation via DNA binding columns was conducted with a commercially available plasmid isolation kit (Invitek, Berlin; for details see Table 3), according to the manufacturer's instructions. Large scale plasmid isolation via DNA binding columns was conducted with commercially available plasmid isolation kit (for details see Table 3), according to the manufacturer's instructions.

2.4.4. Generation and transformation of electro-competent *A. tumefaciens* cells

An overnight preculture was started by inoculation with *A. tumefaciens* and grown at 28°C. Main cultures were generated in two times 100 mL YEB with 1 mL of the preculture and again incubated overnight at 28°C at 140 rpm (Vervliet *et al.,* 1975). When the optical density at 600 nm (OD_{600}) reached 0,5 the culture was transferred to 4°C and all following steps were carried out according to the preparation in section 2.4.1 ('generation of electro-competent *E. coli* cells') and (Sambrook and Russell 2001). Electro-competent *A. tumefaciens* cells were thawed on ice and DNA solution was added. After gentle mixing the cells were incubated for an additional 20 minutes on ice and then transferred to an electorporation-cuvette and pulsed at 3,6 kV (Micropulser™ by Biorad, Munich). Transformed cells were recovered from the cuvette by adding 1 mL LB medium, transferred to a new reaction vial and incubated on a shaker for three hours at 28°C. Dilutions of the *A. tumefaciens* suspension were plated on solid LB medium, with antibiotic selection for the host strain according to the transformed DNA, and grown overnight at 28°C.

2.4.5. Plasmid isolation from *A. tumefaciens*

Plasmid isolation via alkaline lysis (Sambrook and Russell 2001) was executed following the modified protocol described in this section. An overnight culture of transformed *A. tumefaciens* was pelleted at 13.000 xg and the pellet was resuspended in 150 µL buffer 1 (Table 17). Cell lysis was achieved by adding 20 µL Lysozyme (20 mg/mL) solution and subsequent incubation at 37°C for 20 minutes. Then 200 µL buffer 2 (Table 17) were added and the reaction vial was inverted five to ten times. For neutralization and precipitation of proteins, 150 µL buffer 3 (Table 17) were added and incubated for five minutes on ice. After centrifugation at maximal speed, equal volumes (400 µL) of supernatant and phenol-chlorophorm-isoamylalcohol (25:25:1) were mixed in a new reaction vial. After incubation for another five minutes, DNA was precipitated from the upper phase in a new reaction vial by addition of 300 µL isopropanol. For the efficient precipitation and recovery of the DNA this mixture was incubated 10 minutes on ice. The DNA pellet obtained after centrifugation at maximum speed, for 15 minutes at 4°C was washed with 70% ethanol, again pelleted, air dried and dissolved in an appropriate amount of bidestilled water (sterile if desired) and analyzed for the DNA concentration by photometric means (NanoDrop 2000; see section 2.2.1).

Table 17: Buffers for plasmid isolation from *A. tumefaciens*

Buffer 1	Buffer 2	Buffer 3
50 mM Glucose	0,2 N NaOH	3 M potassium acetate
25 mM Tris-HCl (pH 8,0)	1% SDS	pH 4,8 (adjusted with glacial acid)
10 mM EDTA		

2.4.6. Protein expression in *E. coli*

Protein expression was carried out in *E. coli* strains BL21 (DE) pLysS, KMI001 and KMI002 (see Table 2). Precultures in M9 medium (see Table 7) were inoculated from solid LB medium and grown o/n until growth reached the stationary phase. A fresh culture in M9 medium was inoculated from the preculture, isopropyl-1-thio-β-D-galactopyranoside (IPTG) was added to a final concentration of 0,025 mM, and bacteria were incubated for two days at 21°C, 140 rpm in the dark.

2.4.7. *In vivo* cytokinin binding assay

Cytokinin receptors were expressed according to section 2.4.6 and binding of cytokinin to the respective receptor was analyzed using *trans*-[^{3}H]-zeatin. Experimental procedure for the analysis of PpCHK1, PpCHK2 and PpCHK3 are found in Romanov and Loomin (2009), which

use *E. coli* strain BL21 (DE) pLysS for protein expression. The experimental procedures for the analysis of PpCHK4 and MpCHK1 are found in Mizuno and Yamashino (2010), who express the receptor protein in the *E. coli* strain KMI002. Tritium-labeled *trans*-[^{3}H]zeatin (592 GBq/mmol) was obtained from the Isotope Laboratory of the Institute of Experimental Botany (Prague, Czech Republic).

2.4.8. *E. coli* complementation assay

Cytokinin receptors were expressed in *E. coli* KMI002 (see Table 2) according to section 2.4.6 and cytokinin-triggered activation of the TCS coupled reporter gene was analyzed according to the description of Mizuno and Yamashino (2010).

2.5. Methods and handling of plants

2.5.1. DNA and RNA preparation from plants

RNA and DNA were extracted from the same sample of *A. thaliana* or *P. patens* tissues. First, RNA extraction was conducted as described before (Chomczynski and Sacchi 1987) with modifications. Tissue samples up to 100 mg were frozen in liquid nitrogen, disrupted with two steel balls (diameter 1 mm) in a mixer mill (MM300, Retsch, Haan) at 30 Hz for 2 minutes or manually with mortar and pestle, and supplemented with 1 mL of TRIzol (Table 18). The reaction vial was vigorously mixed until all frozen parts were thawed, then 500 µL chlorophorm was added to the reaction mix and the whole amount was transferred into phase lock reaction vials (5 prime, Hamburg). Phase separation was allowed for 10 minutes on ice and phase lock gel was positioned at phase barrier by spinning the sample at 16.000 xg and 4°C for five minutes. The upper (RNA containing) phase was transferred to a new phase lock reaction vial and phase separation using chlorophorm was carried out as described above; the upper phase (water phase) was transferred to another, new reaction vial and complete RNA was precipitated by the addition of 300 µL isopropanol and subsequent storage at -20°C, o/n. For simultaneous extraction of DNA (Triant and Whitehead 2009), the first organic phase of the RNA isolation was kept and supplemented with 1 mL back-extraction buffer in the same vial (Triant and Whitehead 2009) (Table 18) by breaking the phase lock barrier. DNA reaction mix was incubated on ice for 10 minutes and then phases were separated at maximum speed (16.000 xg) and 4°C. The separated upper phase was transferred to a new reaction vial, an equal volume of isopropanol was added and precipitation of DNA was carried out o/n at -20°C. Both precipitates were recovered the next day by centrifugation at 16.000 xg for 20 minutes. RNA and DNA pellets were first washed in 1 mL of 75% and 70% ethanol, respectively, then in 200 µL 75% and 70% ethanol, respectively. The pellet from each washing step was recovered by discarding the supernatant, then dried and dissolved in bidestilled water. For the estimation of nucleic acid

concentration, photometrical analysis was used (described in section 2.2.1). If an appropriate amount of RNA was quantified, RNA was further purified, and residual DNA was digested with DNAse I using the Quiaquick RNA extraction kit (Quiagen, Hilden), according to the manufacturer's instructions.

Table 18: Solutions for the simultaneous extraction of RNA and DNA

TRIzol			Back-extraction buffer		
38 %	phenol	v/v	4 M	guanidinium thiocyanate	
20 %	4M guanidinium thiocyanate	v/v	50 mM	sodium citrate	
10 %	4 M ammonium thiocyanate	v/v	1 M	Tris pH adjusted to pH 8,0 with HCl	
6,7 %	glycerol	v/v			
3,3 %	3 M lithium acetate	v/v			

2.5.2. *Arabidopsis thaliana*

2.5.2.1. Transformation of *A. thaliana*

A. thaliana plants were transformed according to the floral dip method (Clough and Bent 1998). Liquid cultures of 200 mL *A. tumefaciens* were grown at 28°C and 150 rpm, pelleted at 3.800 xg for 10 minutes and resuspended in 300 mL fresh infiltration medium (Table 19). Flowers of five week old *A. thaliana* plants were dipped into the medium and dried under cover at 21°C, o/n. Plants were then transferred back to the green house.

Table 19: Infiltration medium for *A. thaliana* transformation

Infiltration medium		
2,15	g/L	MS-salts
50	g/L	Saccharose
0,1	g/L	BAP
0,015	%	silvet

2.5.2.2. Seed sterilization

Seeds were sterilized according to Salinas and Sanchez-Serrano (2006) with slight modifications (Salinas and Sanchez-Serrano 2006). Approximately 50 mg seeds were incubated in 70% ethanol, 0,01% Triton X-100 at 1400 rpm at 21°C for 9 minutes. Seeds were then washed with 70% ethanol, dried and resuspended in 0,1% sterile agarose medium. Single seeds were distributed on solid medium plates. All work was carried out under sterile conditions.

2.5.2.3. Protoplast transactivation assay

The protoplast transactivation assay (PTA), in its simple form, comprises two components. Firstly, an effector is expressed in the protoplast via transformation with a universal promoter and, secondly, a reporter gene is activated by the effector. In the version of the assay applied here, the cytokinin-inducible transcription factor *ARR2* was used as effector and transformed into protoplast. The 350bp fragment of the *ARR6* promoter (*p350ARR6*) fused to the β-glucuronidase (*GUS*) gene was co-transformed to be activated by the ARR2 protein. The ARR2 protein activates the *ARR6* promoter in accordance with its phosphorylation status – that is, activated when phosphorylated and vice versa. When cytokinin is sensed by a cytokinin receptor, phosphorylation is fed to the signaling chain, which results in activated ARR2. To test the cytokinin sensing capacity of potential cytokinin receptors, the respective receptor was co-transformed with *p350ARR6::GUS* and *ARR2*. Activation of the reporter protein was measured by enzyme activity. To limit internal activation by endogenous receptors, the *Arabidopsis* plants with a double knockout of cytokinin receptor (*ahk2 ahk3*) were used. For a detailed description of the assay please refer to Hwang and Sheen (2001), who use the PTA to show receptor activity by relying on the *A. thaliana* TCS activation capacity of the reporter gene; Choi and colleagues (2010), who describe the use of the PTA with effector and reporter to test cytokinin receptors; and Ramireddy and colleagues (2013), who use the exact same combination of effector and reporter gene (Hwang and Sheen 2001; Choi *et al.,* 2010; Ramireddy *et al.,* 2013).

Arabidopsis plants were grown under low light conditions (75 to 100 µE) for five to six weeks in a growth chamber (Percival AR-66L, CLF Plat Climatics, Wertlingen). For quantification of the transformation efficiency, a plasmid encoding a constitutively expressed neuraminidase (*NAN*) was co-transformed and its enzyme activity was used as internal reference (Kirby and Kavanagh 2002). The specific emission of the sample at 460 nm was analyzed in a plate reader (Synergy 2, Biotek, Bad Friedrichshall) after excitation at 360 nm. The relative *trans*-activation capacity was expressed as the ratio between GUS/NAN values of the same sample, similar to the description by Ehlert and colleagues (Ehlert *et al.,* 2006).

2.5.2.4. Complementation analysis in *A. thaliana*

A. thaliana plants were grown in the greenhouse under normal conditions. Complementation analyses were carried out with 50 plants in single pots for each line. qRT-PCR material was harvested from an additional 15 plants, grown on soil in one large pot per line at 16 days after germination (DAG), and harvested plants were pooled and RNA extracted according to section 2.5.1. Transcriptional regulation of the introduced receptor and the cytokinin response genes (*ARR7* and *ARR16*) was analyzed according to section 2.2.1 using the respective primer pair (see Table 9). Rosette diameters were measured at 16, 27 and 32 DAG. The

number of rosette leaves was counted when bolting had just started. Height and branch number were measured when flowering came to an end and siliques began to dry.

2.5.3. *Nicotiana benthamiana*

2.5.3.1. *Agrobacterium* mediated transformation of tobacco leafs

Tobacco plants were grown in the greenhouse for five to six weeks. Transformation according to a protocol based on (Sparkes *et al.,* 2006) was performed when plants had six to seven full leaves. An overnight culture of *A. tumefaciens* transformed with the desired expression plasmid was grown in YEB medium containing the appropriate selection. The culture was pelleted at 4000 xg and washed twice with 10 mL freshly prepared infiltration buffer (Table 20). The resulting pellet was resuspended in 2 mL infiltration buffer, and a 1:10 dilution was measured for its OD_{600} and diluted to an end-concentration of OD_{600}= 0,1. A second *A. tumefaciens* culture containing the plasmid p19, which encodes the p19 protein that has been shown to suppress posttranscriptional gene-silencing (Lakatos *et al.,* 2004), was treated similarly. The OD_{600} of the p19 bacteria suspension was set to a ration of 0,7/1 (expression plasmid/p19) in the mixed suspension of both cultures. For adjustment of the bacteria to the changed conditions, the mixture was incubated at RT for two hours. The mixture was applied to the bottom side of the leaves by pressing it into the leaf with a syringe without needle. Transformed plants were analyzed in a confocal microscope for fluorescence after two days and then each subsequent day to find optimal expression of the fluorescing product.

Table 20: Infiltration buffer for *Agrobacterium* mediated transformation of tobacco leaf cells

Infiltration buffer	
10 mM	MES-NaOH; pH 5,7
10 mM	$MgCl_2$
150 µM	Acetosyringon

2.5.3.2. Subcellular localization in *N. benthamiana*

Subcellular localization in *N. benthamiana* was carried out in tobacco mesophyll epidermis cells of transiently transformed tobacco leaves (see section 2.5.3.1) that expressed a GFP fusion protein. Small tissue sections were cut from the transformed leaves and positioned on a microscope slide. GFP was exited at 488 nm with an argon laser of a confocal microscope (Leica TCS SP5, Leica, Solms) and emission was measured at 509 nm. The plasma membrane was stained with FM4-64 (Bolte *et al.,* 2004) for 10 minutes and fluorescence was analyzed at 625-665 nm. Tissue sections were incubated in 4´-6-diamino-2-phenylindole (DAPI)-buffer for 10 minutes and nuclear DNA staining was recorded under UV-light.

Table 21: DAPI-buffer for subcellular infiltration Abbreviation: DAPI, 4´-6-diamino-2-phenylindole

DAPI buffer		
85	mM	NaCl
5	mM	MgCl2
100	mM	Tris
0,1	%	Triton-X 100
0,1	mg/L	DAPI-solution

2.5.4. *Physcomitrella patens*

2.5.4.1. Cultivation of *P. patens*

Agar plates with BCD medium (see section 2.1.3.2) were used for *P. patens* culture on plates. Solid medium was inoculated with *P. patens* by pushing a piece of tissue with forceps into the agar, or by adding protonema in liquid medium on top of the agar. These plates were maintained for up to three months for long-term culture.

For standardized culture, *P. patens* were cultivated in liquid BCD medium (see section 2.1.3.2). To initiate a culture, plant material was harvested from BCD agar plates and homogenized in 150 mL liquid BCD medium using an Ultra-Turax (T18 basic Ultra-Turax, IKA, Staufen, Germany). The plant material was then separated from the medium by filtration (pore size 100 µm) and transferred to new medium every seventh day. Every second week the biomass was analyzed and 500 mg fresh weight *P. patens* was transferred to 150 mL medium. Standardization of the culture with a homogenization every week results in protonemal growth. After six weeks a culture was synchronized to the protonemal growth phase and ready to be used in any assay.

2.5.4.2. Generation of protoplasts from *P. patens*

Protoplasts were generated from standardized cultures (see section 2.5.4.1) grown in the presence of ammonium tartrate. Ammonium tartrate is known to arrest protonema cells in the chloronemal state of which protoplasts are generated most efficiently. Plant material (up to 10 g wet weight) was separated from the medium by filtration (pore size 100 µm), transferred to a new reaction vial and incubated with 12 mL 0,5 M mannitol and driselase (1% w/v) solution (Table 6) in the dark and under continuous shaking (approximately 50 rpm) for 2 hours. Resulting protoplasts were isolated by size separation, first with a 100 µm pore sieve, then a 60 µm pore sieve, and subsequently pelleted for 10 minutes at 300 xg in a Haereus Multifuge 3SR+ centrifuge (Thermo Scientific, Langenselbold). The resulting pellet was washed cautiously in 5 M mannitol solution and protoplast density was inferred by cell counting in a 20 µL aliquot on a Fuchs-Rosenthal chamber.

2.5.4.3. Transformation of *P. patens*

Transformation of isolated *P. patens* protoplasts was conducted according to Strepp and colleagues (Strepp *et al.,* 1998). In short, 30 µg of sterile, linearized plasmid DNA was incubated with 1,2 x 10^6 protoplasts and PEG-solution. Subsequent dilution of PEG was achieved by the addition of increasing amounts of 3M medium and ultimately replaced by regeneration medium (for detailed description of the solutions please refer to the original publication (Strepp *et al.,* 1998)). Protoplasts were allowed to recover for 24 hours in the dark, transferred for 10 days to solid medium, and then to 14 days of antibiotic selection according to the transformed construct. This round of selection was followed by 14 days release (since extrachomosomal replicated DNA is lost during this time (Ashton *et al.,* 2000)) and another round of selection for 14 days to select *P. patens* plants that stably integrated the T-DNA region of the transformed plasmid (Table 10) into their genome. The presence of the T-DNA in the genome was analyzed by PCR (section 2.2.2) on isolated genomic DNA (2.5.1).

2.5.4.4. Subcellular localization in *P. patens*

Subcellular localization of GFP fluorescence in *P. patens* was carried out according to section 2.5.3.2 with stably transformed plants that expressed a GFP fusion protein under the control of the 35S promoter (the respective plant generation is described in section 2.5.4.3).

2.5.4.5. Area growth assay

P. patens grown on agar plates (for a detailed description see section 2.5.4.1) were harvested and cut with a razor blade into pieces of approximately 2 mm length, these pieces were filtered through a mesh with a pore size of 2 mm, and 30 mg plant material were used to inoculate a fresh 15 mL BCD medium culture. This culture was grown for five days, washed thoroughly with autoclaved water, resuspended in 0,1% agarose solution and drops of 200 µL were inoculated on agar plates. For a detailed analysis of growth influencing factors, BCD medium was supplemented with additives listed in Table 22.

Table 22: Additives for *P. patens* growth assay. BCD medium was prepared (see Table 8) and the respective additive was added.

Additive	Concentration in the medium	Dissolved in
DMSO	0,2 %	ddH_2O
NAA	10 µM	DMSO
Kinetin	1 µM	DMSO
Kinetin	10 µM	DMSO

Additive	Concentration in the medium	Dissolved in
BA	10 µM	DMSO
isopentenyladenine	10 µM	DMSO
ABA	10 µM	DMSO
NaCl	200 mM	ddH_2O
Sorbitol	200 mM	ddH_2O
Ampicillin	100 µM	ddH_2O
Glucose	2 %	ddH_2O
Ammonium tartrate	2 mM	ddH_2O
No Ca^{2+}	No $CaCl_2$ added to BCD	
No Phosphate	according to (Wang *et al.,* 2008)	

Pictures were taken of the respective colony at the 3rd, 14th and 30th day. Colonized area was manually inspected on all pictures, marked and calculated using the Image J program (Schneider *et al.,* 2012). The standard deviation from triplicates was calculated and data relative to WT were plotted on a semi log scale. The progression of these curves was approximated with an e-function using Excel (Microsoft Excel (2007), Microsoft, Redmond, USA). Since curve progression was exponential, the formula (Formula 1) applying to the exponential growth of bacteria (Monod 1949) and other organisms was used to approximate the specific growth rate µ. Area growth was compared using the specific growth rate of each line relative to its mutant background.

$N = N_0 \, e \, \mu^t$

Formula 1: Growth equation of exponential growth. N, number of cells; N_0, number of cells at t_0; e, Euler number; µ, specific growth rate; t, time.

2.6. Bioinformatic analysis

2.6.1. Assembly of the dataset

A dataset was assembled that comprised of in the proteomes and/or EST data of 11 bacteria, 13 unicellular eukaryotes, 12 chlorophyte algae, three charophyte algae and 8 land plant species (see Table 23 and section 9.1). Available nucleotide sequences (EST) were translated into all six frames using Virtual Ribosome (Version 1.1) (Wernersson 2006).

Table 23: Collection of organism data included in the Dataset

Species	Source	Data type	
		EST	Proteome
Agrobacterium tumefaciens	GB		x
Amphidinium operculatum	TbestDB	x	
Aquilegia coerula	Phytozome		x

Species	Source	Data type	
		EST	Proteome
Arabidopsis thaliana	TAIR		x
Bacillus subtilis	GB		x
Chlamydomonas reinhardtii	JGI DOE		x
Chlorella variabilis sp. NC64A	GB		x
Coccomyxa C169	JGI DOE		x
Coleochaete orbicularis	GB	x	
Corynebacterium glutamicum	GB		x
Cyanophora paradoxa	GB	x	
Dictyostelium discoideum	Dictybase		x
Dunaliella salina	GB	x	
Escherichia coli K12	GB		x
Glaucocystis nostochinearum	GB	x	
Gloeobacter violaceus	GB		x
Helicosporidium sp. ex Simulium jonesi	GB	x	
Heterocapsa triquetra	GB	x	
Isochrysis galbana	GB	x	
Lotharella amoeboformis	TbestDB	x	
Marchantia polymorpha Blast results	JGI DOE		
Marchantia polymorpha	GB	x	
Mesostigma viride	GB	x	
Micromonas pusilla CCMP1545	JgI DOE		x
Micromonas pusilla RCC299	JGI DOE		x
Mycobacterium tuberculosis	GB		x
Neisseria meningitidis	GB		x
Nostoc PCC7120	GB		x
Oryza sativa	Phytozome		x
Ostreococcus tauri	JGI DOE		x
Otreococcus lucimarinus	JGI DOE		x
Pavlova lutheri	GB	x	
Physarum polycephalum	GB	x	
Physcomitrella patens	cosmoss.org		x
Polytomella parva	GB	x	
Populus trichocarpa	Phytozome		x
Porphyra haitanensis	GB	x	
Porphyra yezoensis	GB	x	
Prototheca wickerhamii	GB	x	

Species	Source	Data type EST	Proteome
Reclinomonas americana	GB	x	
Selaginella moellendorffii	GB	x	
Spirogyra pratensis	GB	x	
Spruce V4.0/ Picea abies	TIGR		x
Streptococcus pyogenes	GB		x
Synechocystis PCC6803	GB		x
Tetrahymena thermophila	GB	x	
Trimastix pyriformis	TbestDB	x	
Volvox carteri	JGI DOE		x

2.6.2. Domain identification, sequence alignment and generation of a phylogenetic tree

Domain profiles of characteristic proteins involved in the cytokinin network were obtained from the public database Pfam (Finn *et al.,* 2010) (Table 24). The respective proteomes were analyzed for the existence of the relevant domain by HMM search of the HMMER3 Package (HMMER 3.0) (Finn *et al.,* 2011) using the PFAM-A model (version 24) available on the Pfam website applying the 'gathering cutoff' option. Subsequently an HMM search was undertaken on the protein sequences that were previously identified as containing the respective domain using HMMER2 (HMMER 2.4i). The HMMER2 domain models were based on the seed alignments initially used to generate the HMMER3 models and calibrated using hmmcalibrate (HMMER2 package). Domains were extracted according to the HMM2 result from the protein sequence and aligned. For multiple sequence alignments (MSA) the MAFFT package (MAFFT v6.846b;(Katoh *et al.,* 2009)), using the local pair-wise alignment option, was applied. For tree construction and bootstrapping, the RAxML package (RAxML v7.0.4; (Stamatakis 2006)) was employed running under the fast optimization method and searching for the best-scoring maximum likelihood (ML) tree using the 'Whelan and Goldman' amino acid substitution matrix, with the GAMMA model for rate of heterogeneity. Each tree was calculated with 100 bootstraps and automatic eliminations of redundant sequences were accepted.

Table 24: HMMer profiles used during the course of the analysis

Domain in the Analysis	Occurrence in cytokinin signaling and metabolism proteins	Domain-Identifier	HMMer 3 model version
CHASE	Cytokinin receptors	PF03924.6	3.0b2|June 2009
CKX	Cytokinin oxidases/decarboxylases	PF09265.3	3.0b2|June 2009
HATPase c	Cytokinin receptors	PF02518.19	3.0b2|June 2009

Domain in the Analysis	Occurrence in cytokinin signaling and metabolism proteins	Domain-Identifier	HMMer 3 model version
HisKA	Cytokinin receptors	PF00512.18	3.0b2|June 2009
HPT	Histidine phosphotransfer Proteins	PF01627.16	3.0b2|June 2009
IPPT	Isopentenyltransferase	PF01715.10	3.0b2|June 2009
RR	Cytokinin receptor and Response regulator proteins	PF00072.17	3.0b2|June 2009
Lysine decarboxylase domains	LOG	PF03641	3.0b2|June 2009

2.6.3. Identification of conservation of critical residues

Amino acid residues, critical for the function of the investigated proteins, were compared. The characteristic amino acid of the protein in the tree-founding alignment was compared to published, characterized residues in known proteins. Since *Arabidopsis thaliana* is the best studied organism in relation to cytokinin signaling, *Arabidopsis* proteins were used as template proteins (CHASE Domain (Heyl *et al.,* 2007; Hothorn *et al.,* 2011); HisK domain (Ueguchi *et al.,* 2001b); HPT domain (Heyl and Schmülling 2003) and DDK motif of the RR domain (Ueguchi *et al.,* 2001b)).

2.6.4. Graphical representation of bioinformatic results

A functional clade is defined as a clade to which members of the clade have been assigned the respective function in experiments. For coloring the functional clades, the least internal node of a colored clade was defined by: the node where known plant proteins derived from (without the incorporation of bacterial proteins), or where two functional annotations met. The graphical presentation of the domain structure of the proteins represented in a phylogenetic tree was drawn using a Perl script (van Dam *et al.,* 2009).

3. Results

3.1. Characterization of the *Physcomitrella patens* cytokinin receptors PpCHK1, PpCHK2 and PpCHK3

The molecular characterization of cytokinin action in *Physcomitrella patens* was facilitated by the disclosure of three potential cytokinin receptors in the genome of *P. patens* (Rensing *et al.,* 2008; Pils and Heyl 2009), all three of which shared the domain architecture with *bona fide* cytokinin receptors known from *A. thaliana*. A closer look at the annotation of these genes revealed discrepancies with regard to intron-exon borders in the different databases (Joint Genome Institute[1], The *P. patens* resource[2], GeneBank[3]). For each *P. patens* receptor the most likely annotation was inferred from expressed sequence tag (EST) evidence and investigation of conservation by a multiple sequence alignment (MSA). The cDNAs of *PpCHK1* and *PpCHK2* were obtained from the "Laboratoire de Biologie Cellulaire", INRA, France. A reliable annotation of the PpCHK3 receptor was not found because existing annotations lacked EST evidence, and so PpCHK3 was investigated only after the full length cDNA was verified from *P. patens* (von Schwartzenberg *et al.,* in preparation). The biologically confirmed DNA sequence was synthesized (GenScript USA Inc., Piscataway, USA). For detailed information about the analyzed DNA sequences please refer to Appendix section 9.2.

3.1.1. Analysis of cytokinin binding

The three *P. patens* genes share the domain architecture that characterizes cytokinin receptors in *A. thaliana* (Figure 4), making them candidates to fulfill the same function in *P. patens*. The characterization of a protein as cytokinin receptor depends, firstly, on the binding of cytokinin to the respective protein and, secondly, on the output of the signal into the appropriate signaling system. It has been shown that cytokinin as a ligand can bind to the CHASE domain of cytokinin receptors in *A. thaliana* (Inoue *et al.,* 2001; Heyl *et al.,* 2007; Romanov and Lomin 2009; Hothorn *et al.,* 2011; Wulfetange *et al.,* 2011a).

3.1.2. *P. patens* cytokinin receptors PpCHK1 and PpCHK2 bind to cytokinin

To show that the *P. patens* cytokinin receptor genes function in cytokinin sensing, I first analyzed the binding of cytokinin to each receptor in turn. This has been done effectively using a bacterial *in vivo* binding assay (Romanov and Lomin 2009). Following the assay procedure, the *P. patens* cytokinin receptors were expressed in *E. coli* BL21 cells (see section 2.4.6), incubated with radioactively labeled cytokinin, washed and then analyzed for

[1] http://www.jgi.doe.gov
[2] www.cosmoss.org
[3] http://www.ncbi.nlm.nih.gov/nuccore

specifically bound cytokinin (see section 2.4.7). The cytokinin *trans*-zeatin bound specifically to GST:PpCHK1 and GST:PpCHK2 and the control protein GST:AHK4. No binding was detected when GST:PpCHK3 was used (Figure 8, A). For verification that the analyzed receptors were expressed in their full length, protein blot analysis (see section 2.3.3) was performed on the same bacterial culture analyzed in the binding assay. In every sample, detection with anti-GST antibody revealed a band of the expected size (GST:AHK, 148 kDa; GST:PpCHK1, 143 kDa; GST:PpCHK2, 140 kDa; GST:PpCHK3 147 kDa; GST, 26 kDa). However, bands with potentially degraded products, as well as free GST, were also detected (see Figure 8, B). It is well known that overexpression of a protein may cause rapid degradation (Wagner *et al.,* 2007).

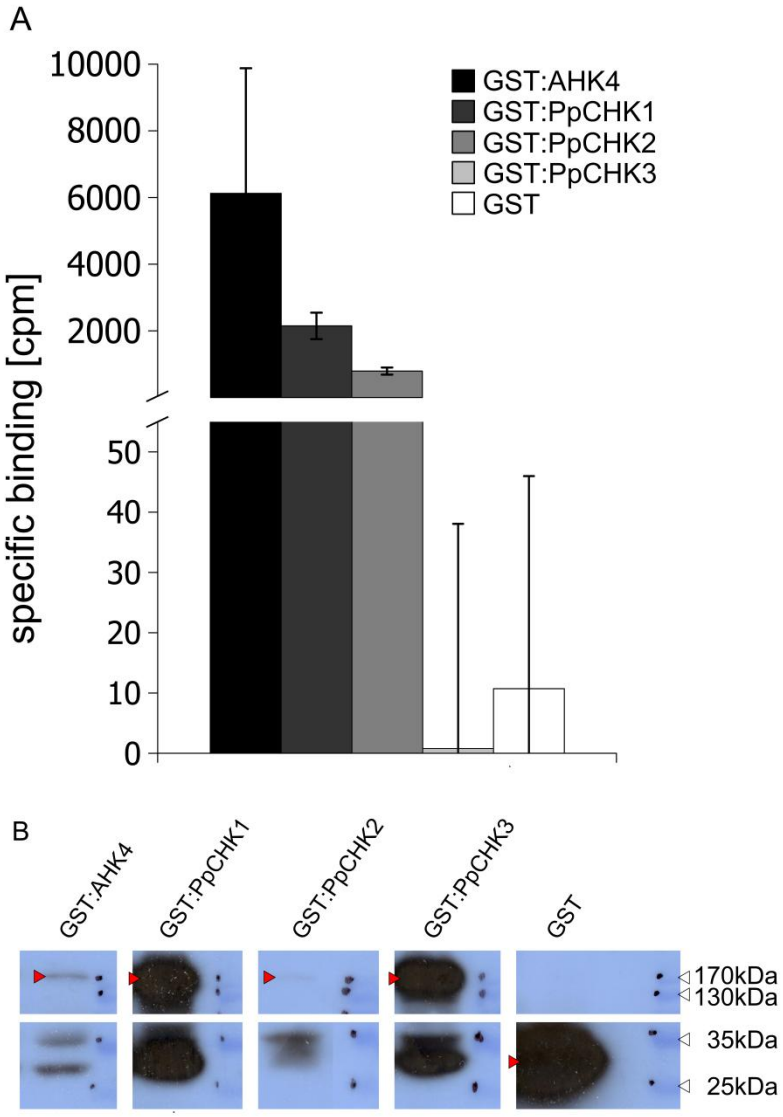

Figure 8: *trans*-[2-^{3}H]zeatin binds to *P. patens* cytokinin receptors GST:PpCHK1 and GST:PpCHK2. A: *In vivo* binding assay. All receptors were expressed as GST-fusion proteins in *E. coli*. The specific binding to *trans*-[2-^{3}H]zeatin was analyzed according to (Romanov and Lomin 2009). Shown are the average of three biological replicates and their standard deviation (whiskers). **B:** Expression control of the fusion proteins analyzed in A. Immunoblot detection was carried out using the pellet of 1 mL bacterial culture that was separated by SDS-PAGE and blotted to a PVDF membrane. GST-containing bands were detected using a GST-specific antibody (Santa

Cruz Biotechnology, Heidelberg). White arrowheads mark the position of the protein marker (PageRuler™ Prestained Protein Ladder (Fermentas, St. Leon-Rot) and black dots mark position of the marker on the developed film; red arrowheads mark the protein band corresponding to the size of fusion protein expressed.

3.1.3. *P. patens* cytokinin receptor PpCHK3 activates TCS components *in vivo*

To further characterize whether the *P. patens* cytokinin receptors could also act in the cytokinin signaling chain, their signal transduction capacity was analyzed in the *E. coli* based complementation assay (Mizuno and Yamashino 2010). *E. coli* strain KMI002 lacks the native hybrid histidine kinase (RcsC) and the reporter gene is transcribed only after phosphorylation of the HPT protein by the transformed receptor. After *PpCHK3* was transformed into *E. coli*, a cytokinin (*trans*-zeatin) concentration-dependent increase of the reporter gene activity was detectable. *E. coli* transformed with *PpCHK1* or *PpCHK2* did not lead to activation of the reporter gene (Figure 9). Both controls verified correct assay execution. *E. coli* transformed with the empty vector did not show high reporter gene activity while *E. coli* transformed with *A. thaliana AHK4* receptor did.

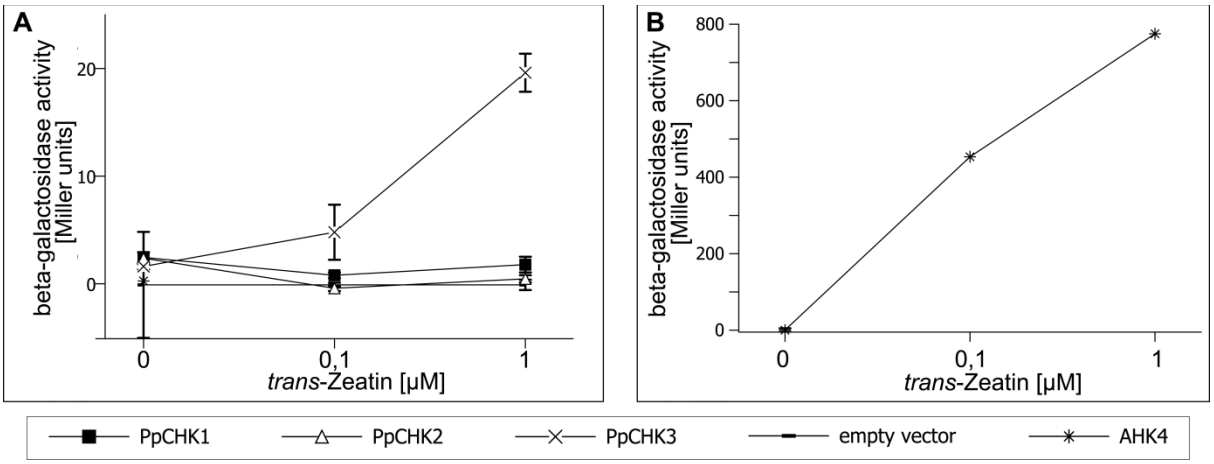

Figure 9: *E. coli* TCS reporter gene activation mediated by PpCHK3 is dependent on cytokinin concentration. *E. coli* strain KMI002 (*ΔrcsC*) was transformed with the respective cytokinin receptor and was grown in medium containing different cytokinin concentrations. **A)** The *P. patens* cytokinin receptor PpCHK3 complemented the lack of *RcsC* and induced the reporter gene dependent on the available cytokinin. **B)** The positive control, *A. thaliana* AHK4 induced the reporter gene to a high extent. Depicted results are mean values of three biological replicates (n = 3) and whiskers represent standard deviation.

3.1.4. PpCHK1 and PpCHK2 activate the cytokinin signaling cascade *in planta*

Cytokinin binds to PpCHK1 and PpCHK2 (section 3.1.1) and PpCHK3 activates downstream components in a TCS (section 3.1.3). These results implied a function of PpCHK1, PpCHK2 and PpCHK3 in the cytokinin signaling pathway. The next step was to investigate whether or not the *P. patens* cytokinin receptors could activate the cytokinin signaling chain *in planta*.

The protoplast *trans*-activation assay (PTA) has been shown to be a powerful tool (Hwang and Sheen 2001; Choi *et al.,* 2012) in demonstrating a receptor's capability to function in the

cytokinin signaling system. The *P. patens* cytokinin receptors were co-expressed with a strong effector, a type-B RR (*ARR2*) and a reporter gene (*β-glucuronidase*) fused to the ARR2-responsive type-A RR promoter (350bp of the *ARR6* promoter) in *A. thaliana ahk2-5 ahk3-7* mesophyll protoplasts. These plants lack two of three endogenous cytokinin receptors, and protoplasts expressing the PpCHK1 or PpCHK2 protein showed an increased activation of the output after *trans*-zeatin treatment of the same level as the positive control AHK4 (Figure 10). The expression of *PpCHK3* did not yield activation upon *trans*-zeatin addition (Figure 10). This inactivity of PpCHK3 was surprising given that PpCHK3 had been previously shown to activate the downstream TCS components in *E. coli* (Figure 9).

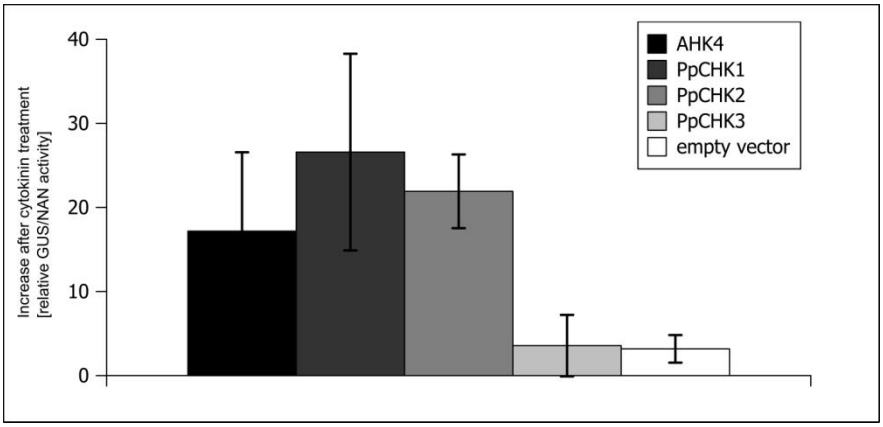

Figure 10: *P. patens* cytokinin receptors PpCHK1 and PpCHK2 activate the cytokinin-dependent TCS in *ahk2-5 ahk3-7* knockout mutants of *A. thaliana*. Cytokinin perception-deficient protoplasts (*ahk2-5 ahk3-7*) (Riefler *et al.,* 2006) were co-transformed with the cytokinin-responsive *ARR2* (effector), the *ARR6* promoter fused to *β*-glucuronidase (reporter), *35S::NAN* (internal reference) and the indicated cytokinin receptor (activator) under the 35S promoter. Protoplasts were incubated overnight with and without *trans*-zeatin; subsequently *ARR6* promoter *trans*-activation was measured. Results were normalized by the internal reference and the specific activity upon cytokinin treatment was calculated (normalized reporter activity with cytokinin minus normalized reporter activity without cytokinin). Depicted results are mean values of three biological replicates (n = 3) and whiskers represent standard deviation.

3.1.5. Subcellular localization of the *P. patens* cytokinin receptors

For further analysis, for example subcellular localization, constructs were generated encoding fusions of the receptors to green fluorescent protein (GFP) driven by the 35S promoter (plasmids pK7WGF; pK7FWG; Table 10). Each fusion protein was also analyzed for its effect on the cytokinin dependent *trans*-activation of the *ARR6* promoter, in order to test its function. N-terminally fused GFP:receptor constructs recapitulated the untagged results (Figure 10), even though activation levels were lower. The fusion proteins GFP:AHK4, GFP:PpCHK1 and GFP:PpCHK2 activated, whereas GFP:PpCHK3 did not activate the cytokinin signaling cascade (data depicted in Figure 11). Next, C-terminal fusion proteins were analyzed in the PTA.

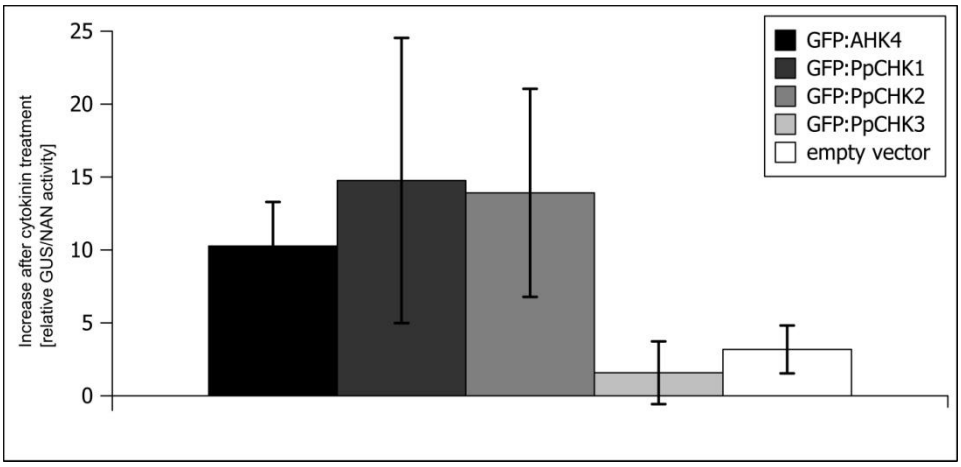

Figure 11: *P. patens* cytokinin receptors PpCHK1 and PpCHK2 N-terminally fused to GFP activate the cytokinin-dependent TCS in *ahk2-5 ahk3-7* knockout mutants of *A. thaliana*. Cytokinin perception-deficient protoplasts (*ahk2-5 ahk3-7*) (Riefler *et al.,* 2006) were co-transformed with the cytokinin-responsive *ARR2* (effector), the *ARR6* promoter fused to *β*-glucuronidase (reporter), *35S::NAN* (internal reference) and the indicated cytokinin receptor (activator) under the 35S promoter. Protoplasts were incubated overnight either with or without *trans*-zeatin; subsequently *ARR6* promoter *trans*-activation was measured. Results were normalized by the internal reference and specific activity upon cytokinin treatment was calculated (normalized reporter activity with cytokinin minus normalized reporter activity without cytokinin). Depicted results are mean values of three biological replicates (n = 3) and whiskers represent standard deviation.

Surprisingly, the C-terminal receptor fusions of GFP to AHK4 and PpCHK1 did not show activity in the PTA, but the C-terminal receptor fusion of GFP to PpCHK2 was active in the PTA (data depicted in Figure 12). Taking the three experiments together, they show firstly that highest activation of the cytokinin signaling system is achieved when the receptors are expressed as untagged proteins, and secondly that GFP fusion to the receptors decreases activation.

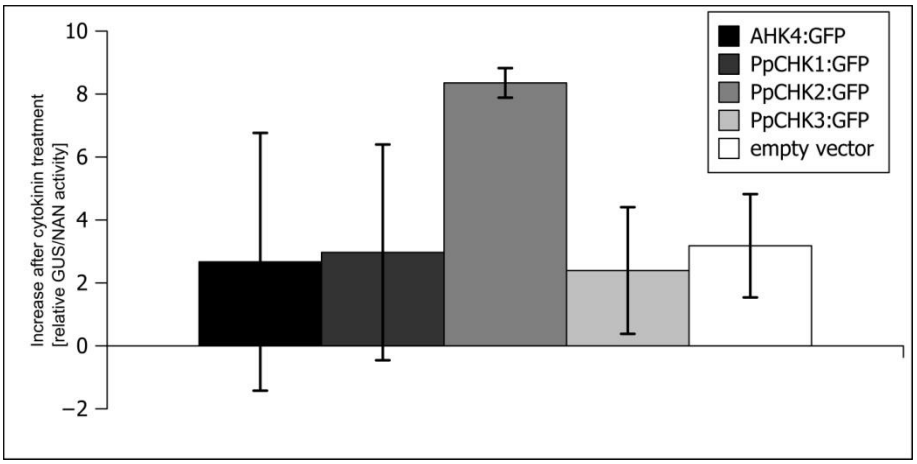

Figure 12: PpCHK2 C-terminal fusion to GFP activates the TCS in *ahk2-5 ahk3-7* knockout mutants of *A. thaliana* cytokinin-dependent. Cytokinin perception-deficient protoplasts (*ahk2-5 ahk3-7*) (Riefler *et al.,* 2006) were co-transformed with the cytokinin-responsive ARR2 (effector), the *ARR6* promoter fused to *β-glucuronidase* (reporter), *35S::NAN* (internal reference) and the indicated cytokinin receptor (activator) under the 35S promoter. Protoplasts were incubated overnight either with or without *trans*-zeatin; subsequently *ARR6* promoter *trans*-activation was measured. Results were normalized by the internal reference and the specific activity upon cytokinin treatment was calculated (normalized reporter activity with cytokinin minus normalized reporter activity without cytokinin). Depicted results are mean values of three biological replicates (n = 3) and whiskers represent standard deviation.

The localization pattern of a protein on the subcellular level has important implications for its possible function. Subcellular distributions should be congruent with protein interaction partners and cellular compartments that are associated with the function. The cytokinin receptors from *A. thaliana,* AHK2, AHK3 and AHK4, are primarily located in the ER (Caesar *et al.,* 2011; Wulfetange *et al.,* 2011a).

To investigate the subcellular localization, the P. patens cytokinin receptors were transiently expressed as C- or N-terminal fusion proteins with GFP in Nicotiana benthamiana leaves. A signal for GFP was detected five days after infiltration. Shorter incubation times after infiltration did not lead to a detection of any GFP fluorescence, whereas longer incubation times resulted in yellowing and subsequent wilting of the infiltrated leaves and by a loss of GFP signal. The sole expression of GFP localizes to the cytosol and the nucleus (Figure 13, J). The GFP protein (27 kDa) is able to enter the nucleus because of its small size (size exclusion of the nuclear pore ~45 kDa, (Slootweg *et al.,* 2010)).

The fluorescent signal of the N-terminally fused PpCHK1 protein to GFP localized to the outside of the nucleus (see Figure 13, A1 and A3). Additional fluorescent speckles, distributed throughout the cell, were found to be concentrated fluorescent spots indicating a weakly labeled network (Figure 13, A1 inset). Other cytokinin receptors like the *A. thaliana* AHKs also localized to the perinuclear region and show a strong staining of the ER when fused to a fluorophore. Only AHK3 showed partial co-localization to the plasma membrane (Wulfetange *et al.,* 2011a), while, in accordance with the subcellular localization of GFP fusion proteins of AHK2 and AHK4, 35S::GFP:PpCHK1 did not co-localize with the plasma membrane staining FM4-64 (Figure 13, A3). A similar fluorescent pattern was observed analyzing the C-terminal fusion protein of PpCHK1 to GFP. Fluorescence signals were clearly detectable around the nucleus (Figure 13, B1 and B4; C1), but did not overlap with the FM4-64-stained plasma membrane or the internal nucleus staining of the DNA by DAPI (see Figure 13, B4 and C3). The formation of fluorescent speckles which are distributed throughout the cell were also found, and were associated with a weakly labeled network structure. Such network structures are characteristic of ER localization and support the result of the ER-localized PpCHK1 GFP fusion indicated by the perinuclear-concentrated fluorescent signal. Co-localization experiments of the GFP-tagged PpCHK1 protein together with an ER marker were carried out (data not shown), but conclusions could not be drawn from these experiments due to unclear localization of the marker in co-expressing cells (ER-rk CD3-959, mCherry; (Nelson *et al.,* 2007)).

A1
A2
A3
A4
B1
B2
B3
B4
B5
C1
C2
C3
C4
D1
D2
D3
D4
D5
E1
E2
E3
E4
E5
F1

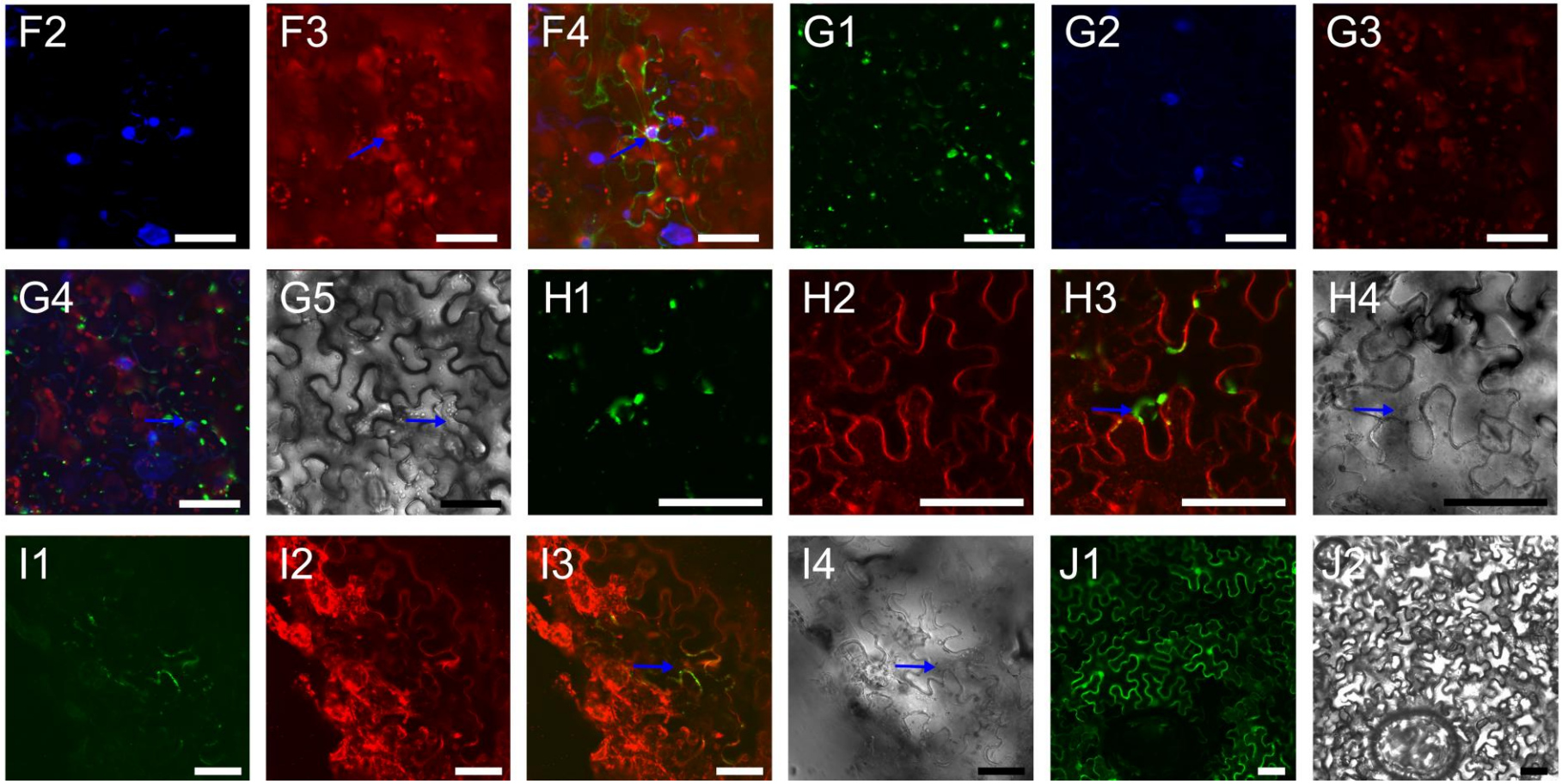

Figure 13: Subcellular localization of the PpCHK1, PpCHK2 or PpCHK3 protein fused to GFP, transiently expressed in *N. benthamiana* leaves. A1-4, GFP:PpCHK1; **B1-5** and **C1-4**, PpCHK1:GFP; **D1-4**, GFP:PpCHK2; **E1-5** and **F1-4**, PpCHK2:GFP; **G1-5** and **H1-4** GFP:PpCHK3; **I1-4**, PpCHK3:GFP;**J1-2**, GFP. All receptor GFP fusions indicated a localization to the perinuclear space. While PpCHK1 and PpCHK2 also show network-like structures (possibly associated with the ER), these are missing from PpCHK3. All constructs are driven by the 35S CaMV promoter and were transformed into *A. tumefaciens* and infiltrated into *N. benthamiana* leaves. Fluorescence was analyzed five days after infiltration in prepared leaf epidermal cells. First photograph shows GFP fluorescence exited at 488 nm, emission detected at 509 nm ; A2,C2, D2, E2, H2, and I2 show fluorescence at 625-665 nm of FM4-64 dye staining the plasma membrane; B2, D3, G2, F2, show DAPI staining indicating the nucleus, exited at 405 nm, emission detected at 460 nm; B3 and F3 show auto-fluorescence of chloroplasts at 650 nm; A3, B4, C3, D4, E4, F4, H3 and I3 show overlay from fluorescent channels; A4, B5, C4, D5, E5, G5, H4, I4, J4, show bright field image. Blue arrows indicate the perinuclear space in overlay and bright field images. Scale bars correspond to 50 µm.

Subcellular localization of the PpCHK2 receptor protein tagged either at the N- or C-terminus of the protein revealed a localization pattern in accordance with the ER localization indicated for fluorophore-tagged AHK2, AHK3 and AHK4 proteins (Caesar *et al.,* 2011; Wulfetange *et al.,* 2011a). Both PpCHK2 receptor fusion orientations revealed a strong fluorescent signal surrounding the nucleus and a cell-spanning network characteristic of ER localization. Co-localization with an ER marker (ER-rk CD3-959, mCherry; (Nelson *et al.,* 2007)) was inconclusive due to the unclear localization of the marker in co-expressing cells (data not shown). No overlap with the FM4-64-labeled plasma membrane was observed when PpCHK2 was fused N-terminally to GFP (see Figure 13, D4), whereas a closer look on the PpCHK2:GFP fluorescent signal seems to indicate a partial co-localization with FM4-64 (depicted in Figure 13, E4). Neither GFP fusion proteins showed an overlap with the DAPI-stained DNA inside the nucleus (depicted in Figure 13, D4 and E4). and, again due to unclear localization of the marker (ER-rk CD3-959, mCherry; (Nelson *et al.,* 2007)), conclusions were not drawn from these experiments (data not shown).

The localization of the PpCHK3 GFP fusion proteins in N- and C-terminal orientation indicated a diverged subcellular localization as compared to the *P. patens* cytokinin receptors PpCHK1 and PpCHK2 (depicted in Figure 13). The ER localization characterized by the network-like structures that was found for PpCHK1 and PpCHK2 was not evident in any PpCHK3 GFP fusion analysis. Nevertheless, the N-terminal fusion of PpCHK3 to GFP still showed the perinuclear localization (depicted in Figure 13, H1). Moreover, fluorescing spots distributed in the cell were observed (see depicted in Figure 13, G1). Such structures were also associated with the PpCHK1 GFP fusion (see depicted in Figure 13, A1 and B1), but could not be linked to the ER-network in the case of PpCHK3 since no network-like structures were found. In comparison with the N-terminal fusion protein, the C-terminal fusion protein showed weaker GFP signal (see Figure 13, I1), which was restricted to small spots in proximity to the FM4-64 labeled plasma membrane (see Figure 13, I3). For both fusion proteins a partial co-localization to the FM4-64-labeled plasma membrane was detected (see Figure 13, H3 and I3 respectively).

3.1.6. *P. patens* cytokinin receptors are membrane associated

The subcellular localization of the *P. patens* cytokinin receptors was shown by the use of fusion proteins with GFP (section 3.1.1). The localization of all receptors was found to be at the perinuclear region, and it is known that the perinuclear ER is situated there as well (Sparkes *et al.,* 2009). To verify the localization to the membranous ER, the membrane fraction of transformed *N. benthamiana* cells was isolated. The immunodetection of the GFP after size separation in an SDS-PAGE indicated bands of the right size for all fusion proteins in the membrane-enriched fraction (see Figure 14). No fusion protein was detected in the

cytosolic fraction. However, free GFP was evident in the membrane-enriched and cytosolic fractions. Misinterpretation of the localization results of the receptors due to the free GFP are unlikely, since GFP localizes to the cytosol (Figure 13, J) and no such localization was found for the receptors. The presence of free GFP in the membrane fraction might also be caused by the high overexpression (compare to Figure 13, J) of the sole GFP protein and an incomplete separation of the cytosolic fraction from the membrane-enriched fraction. In the same experiment fusion proteins of the *A. thaliana* cytokinin receptor AHK3 and GFP were analyzed to serve as a control. The fusion proteins of the *P. patens* cytokinin receptors showed the same distribution as the AHK3 fusion proteins. It should be noted that, according to the immunoblot, the expression of *AHK3:GFP* resulted in a high amount of fusion protein, and it seems likely that band blurring in the case of AHK3:GFP is due to this fact. For comparison of the receptor fusion proteins, the SDS-PAGE was loaded with equal amounts of cell extract.

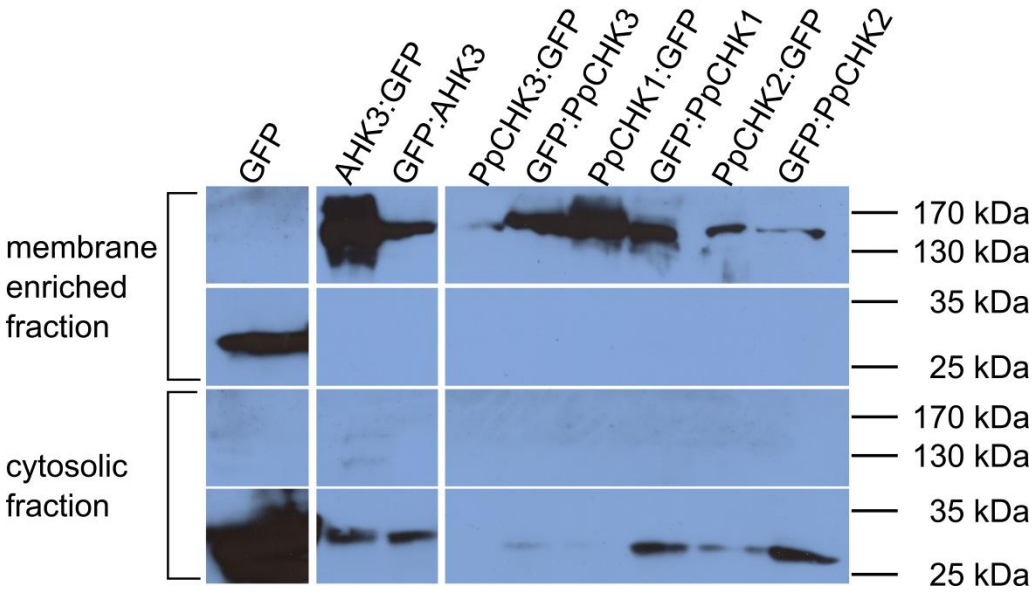

Figure 14: Cell fractionation and immunodetection of *P. patens* cytokinin receptors fused to GFP. *N. benthamiana* leaves transiently expressing the relevant fusion protein were harvested five days after infiltration and cell extracts were separated into a membrane-enriched and a cytosolic fraction (see section 2.3.1). Equal amounts of cell extract were loaded to SDS-PAGE and subsequent immunodetection of the fusion protein was carried out using anti-GFP Antibody (Roche Applied Science, Mannheim). Protein bands for all the receptor fusion proteins could be detected in the membrane-enriched fraction. Fusion protein sizes: GFP:AHK3, 143 kDa; GFP:PpCHK1, 144 kDa; GFP:PpCHK2, 141 kDa; GFP:PpCHK3 148 kDa; GFP, 27 kDa. Free GFP was analyzed as a positive control for expression.

Summarizing the results of this section, PpCHK1 and PpCHK2 GFP fusion proteins share the full scope of subcellular distribution with the *A. thaliana* cytokinin receptors. They are found in the perinuclear region and a network-like structure is weakly labeled by the GFP furthermore they are found in the membranous fraction. In comparison, network-like structures were not found for the PpCHK3 fusion protein, though perinuclear localization was evident. Furthermore, PpCHK3 fusion proteins were found exclusively in the membrane-enriched fraction of the cells, suggesting that ER localization is very likely.

3.1.7. *P. patens* cytokinin receptor PpCHK1 and PpCHK2 complements the cytokinin signaling-deficient *A. thaliana ahk2 ahk3* mutant

In this section it was investigated whether the *P. patens* cytokinin receptors can also complement the lack of two of the three native cytokinin receptors in *A. thaliana*. *A. thaliana* plants (*ahk2-5 ahk3-7*) were transformed using the floral dip method (section 2.5.2.1) with constructs that would lead to the expression of *P. patens* cytokinin receptors PpCHK1 and PpCHK2 as N- and C-terminal fusion proteins, with GFP under the 35S CaMV promoter. The complementation experiment of *ahk2 ahk3* mutants with PpCHK3 was not performed, because the PpCHK3 clone was not available at the time the experiment was conducted. Homozygote lines were selected and each construct's transcriptional overexpression was analyzed by qRT-PCR 16 days after germination (DAG), in *A. thaliana* seedlings of two independent lines for each construct. For the analysis of the transcriptional regulation in the mutants under investigation, the commonly suggested threshold of a minimum of 2,5-fold difference between compared samples, depending on the intra assay variation of about 2-fold, will be used. The lines overexpressing the *PpCHK1* in N-terminal fusion (lines A and B) and C-terminal fusion (lines C and D) showed high (above 500-fold) transcript levels (Figure 15, A). These lines were further analyzed in complementation experiments. High transcript levels were also be found in the *PpCHK2* lines, ranging from 75-fold to 15.000-fold. Higher deviations were detected when comparing the transcript levels of N-terminally fused receptor (lines GFP_PpCHK2_A and GFP_PpCHK2_B) with the C-terminally fused (PpCHK2_GFP_C and PpCHK2_GFP_D) lines (Figure 15, B). These lines were further analyzed in the complementation assay.

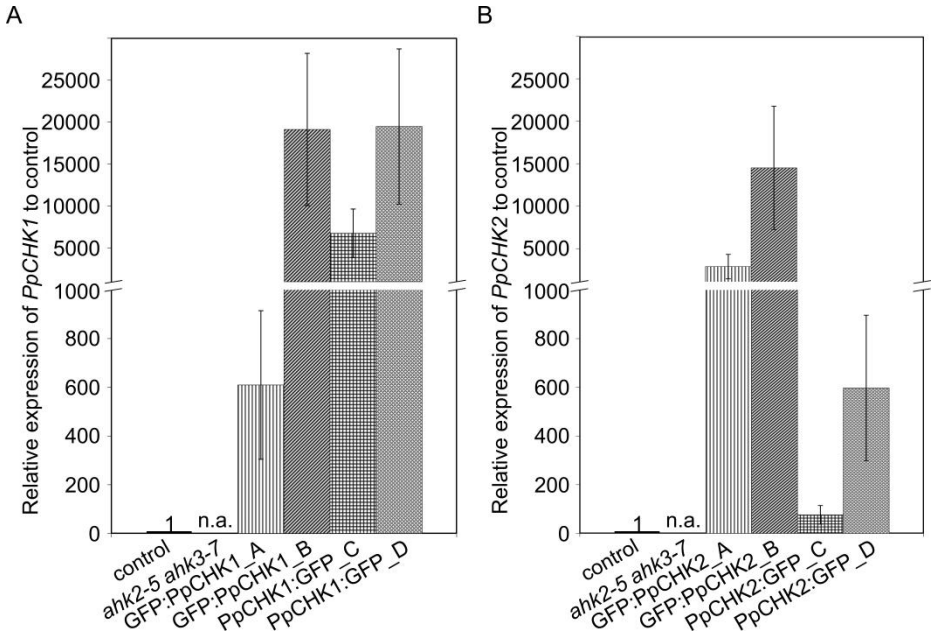

Figure 15: Overexpression of *PpCHK1* and *PpCHK2* in *A. thaliana.* A) Transcript levels of GFP fusions with *PpCHK1* **B)** Transcript levels of GFP fusions with *PpCHK2*. *A. thaliana* seedlings were harvested 16 DAG, RNA

was isolated and transcribed to cDNA and transcript levels were analyzed by qRT-PCR. Control *A. thaliana* cDNA was isolated from wild type and analyzed with the respective *PpCHK1* or *PpCHK2* primers. A maximum of 45 cycles was used as Ct for relative expression calculation. Shown are mean values of three biological replicates and whiskers represent standard deviation. Abbreviation: n.a., not analyzed.

In the complementation assay, two independent lines for each construct (N- and C-terminal fusions of one receptor with GFP) were analyzed for their complementing effect on five parameters (four phenotypic and one molecular) which show significant alterations when the two cytokinin receptors *AHK2* and *AHK3* are knocked out. These are: i) The rosette diameter; ii) the number of leaves that formed the rosette; iii) the total stem height; iv) the number of first-order branches (Riefler *et al.,* 2006); and v) two type-A RRs (RRAs) that are transcriptionally down-regulated in the *ahk2 ahk3* knockout mutant (Brenner *et al.,* 2012; Kang *et al.,* 2012; Brenner pers. communication).

Analysis of the ubiquitinously expressed *P. patens* cytokinin receptor PpCHK1, fused to GFP in the *ahk2-5 ahk3-7* double knockout, showed partial complementation and dependence on the fusion orientation. For the rosette diameter, all diameter measurement results obtained were significantly different to both the WT (100%; corresponding to on average 10,8 cm on 34 DAG) and the mutant background (50%), with less than 0,1% probability of overlap. From the beginning, the *PpCHK1* expressing lines had intermediate diameters compared to the WT and the mutant (data shown in Figure 16, A). Exemplified rosette diameters 27 DAG are depicted in Figure 16, B. It should be noted that both lines of the C-terminal fusions of PpCHK1 performed better than the N-terminal fusions to GFP. The total complementation capacity of the rosette diameter was derived from 34 DAG. The C-terminally fused line

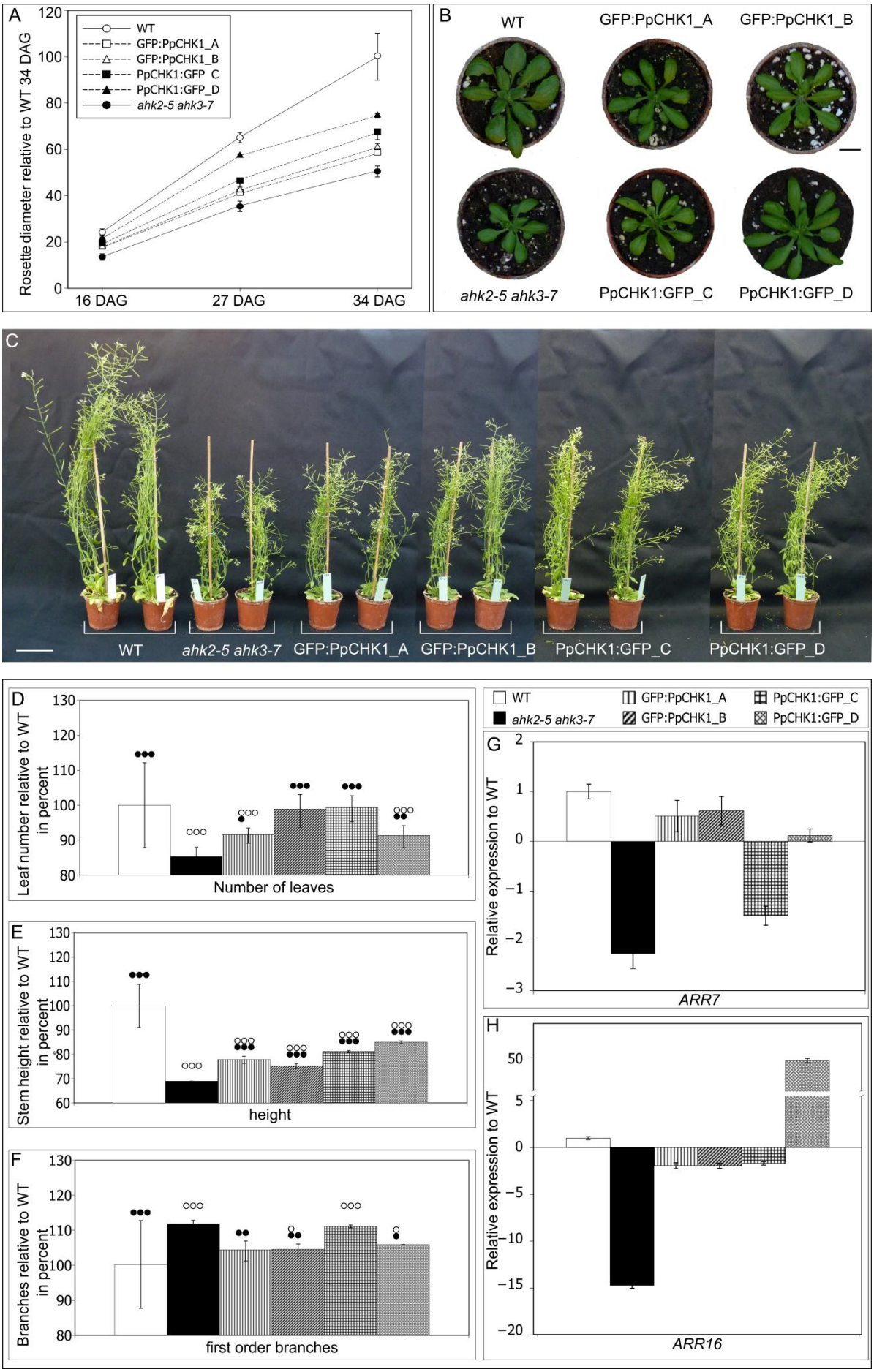
A
Rosette diameter relative to WT 34 DAG
WT
GFP:PpCHK1_A
GFP:PpCHK1_B
PpCHK1:GFP_C
PpCHK1:GFP_D
ahk2-5 ahk3-7
16 DAG
27 DAG
34 DAG
B
WT
GFP:PpCHK1_A
GFP:PpCHK1_B
ahk2-5 ahk3-7
PpCHK1:GFP_C
PpCHK1:GFP_D
C
WT
ahk2-5 ahk3-7
GFP:PpCHK1_A
GFP:PpCHK1_B
PpCHK1:GFP_C
PpCHK1:GFP_D
D
Leaf number relative to WT in percent
Number of leaves
E
Stem height relative to WT in percent
height
F
Branches relative to WT in percent
first order branches
G
Relative expression to WT
ARR7
H
Relative expression to WT
ARR16

Figure 16: Complementation of the *ahk2 ahk3* double knockout by the *P. patens* cytokinin receptor PpCHK1 fused to GFP. All values are given relative to the WT. **A:** Rosette growth from 16 DAG until 34 DAG. For a better comparison all sizes were calculated in percent of the mature (34 DAG) wild type. All values were significantly different from WT and mutant background. **B:** Examples of rosette diameter of 27 DAG. First row: WT and N-terminal fusions of GFP with PpCHK1. Second row: mutant background (*ahk2-5 ahk3-7*) and C-terminal fusions of GFP to PpCHK1 **C:** Phenotypic comparison of mature plants. From left to right: WT, mutant background (*ahk2-5 ahk3-7*), N-terminal fusions of GFP with PpCHK1, C-terminal fusions of GFP to PpCHK1. **D:** Number of leaves of all analyzed genotypes relative to WT. **E:** Stem height of all analyzed genotypes relative to WT. **F:** Branch number of all analyzed genotypes relative to WT. **G:** Relative expression of *ARR7* of all analyzed genotypes. **H:** Relative expression of *ARR16* of all analyzed genotypes. A to F: Each line was analyzed with n = 50 plants. Scale bar in B corresponds to 1 cm. Scale bar in C corresponds to 5 cm. D, E, F: Open circles depict significance to WT values; closed circles depict significance to mutant background values. ooo ≤ 0,1% probability of overlap; oo = 0,1% ≥ 1% probability of overlap; o = 1% ≥ 5% probability of overlap. G, H: WT expression level was set to 1, given is the fold-change of the respective lines. Shown are mean values of three biological replicates (n = 3).

35S::PpCHK1:GFP_D showed the maximal effect on the rosette diameter by reaching 74% of the WT measurement. Line 35S::PpCHK1:GFP_C, also C-terminally fused to GFP, reached 67% of WT diameter, and the N-terminally fused lines 35S::GFP:PpCHK1_A and 35S::GFP:PpCHK1_B showed a diameter size of 58% and 61% of WT respectively. All lines showed a significantly increased rosette diameter as compared to the mutant background which reached 50% of WT diameter.

The second parameter, the total number of leaves when bolting just started, is reduced to 85% of WT in the *ahk2-3/ahk3-7* mutant background (100% WT corresponds to an average number of 12,2 leaves per rosette). Leaf count was partially or fully restored in the N-terminally fused 35S::GFP:PpCHK1_A (91% of WT leaf count) and 35S::GFP:PpCHK1_B (98% of WT leaves) lines. Similarly, 35S::PpCHK1:GFP_C showed a complementation effect back to WT levels (99% of WT), while line 35S::PpCHK1:GFP_D also showed a (partial) increase on the mutant background (91% of WT; data depicted in Figure 16, D). In summary an increased leaf number could be seen in all *PpCHK1*-expressing lines compared to the mutant background, and full complementation to WT levels was achieved in two lines.

Focusing on the third parameter, namely the stem height at the end of flowering, all lines showed significantly different size as compared both to the mutant background (which reached 68% of WT height) and also compared to the WT (100% of WT corresponds to an average stem height of 34,2 cm). While all lines were shorter than the WT, the N-terminally fused PpCHK1 lines showed an improvement on the mutant with 77% and 75% for lines 35S::GFP:PpCHK1_A and 35S::GFP:PpCHK1_B, respectively, and this complementing effect was even more pronounced in the N-terminal fusion lines 35S::PpCHK1:GFP_C and 35S::PpCHK1:GFP_D, reaching 81% and 85% respectively (data shown in Figure 16, E and examples of plants in Figure 16, C).

The final phenotypic parameter under investigation was the number of first-order branches, which are known to be elevated in the *ahk2-5 ahk3-7* mutant background (Riefler et al.,

2006). In this experiment the number of first-order branches rose to 111% of the WT (Figure 16, F; 100% first-order branches in the WT correspond to an average of 7,3 branches per plant). Three of the investigated lines overexpressing *PpCHK1* in the mutant background showed a reduction of branch number (35S::GFP:PpCHK1_A and 35S::GFP:PpCHK1_B had 104% of WT branches; 35S::PpCHK1:GFP_D, 105% of WT branches). The remaining line, 35S::PpCHK1:GFP_C, retained more branches (110% of WT branches) and seemed not to be complemented with regard to branch number.

Altogether, the phenotypic analysis suggests that the ubiquitous expression of *PpCHK1* fused to GFP partially complements the mutant phenotype of *ahk2-5 ahk3-7*, although it cannot fully restore the WT phenotype.

To further analyze whether this partial complementation is also based on transcriptional regulation of the downstream targets in the cytokinin signaling cascade, I analyzed the primary response genes *ARR7* and *ARR16* (Figure 16, G and H). Both target genes were previously shown to be transcriptionally down-regulated in the *ahk2-5 ahk3-7* mutant background without cytokinin treatment (Tran *et al.,* 2007; Brenner *et al.,* 2012; Kang *et al.,* 2012; Brenner pers. communication). The analysis of the transcript abundance of *ARR7* revealed a reversion to almost WT levels in all lines except one, 35S::PpCHK1:GFP_C, which still exhibited mutant background levels of about two-fold transcript reduction compared with WT (Figure 16, G). It should be noted that the oscillation of about 2,5-fold of all *ARR7* mRNA levels is within the range of biological deviations. Nevertheless, these results are in accordance with the result from the analysis of parameter (iv), first-order branching, which was unaltered in the transgenic line 35S::PpCHK1:GFP_C. The second transcriptional response marker gene *ARR16* was more heavily affected in the mutant (*ahk2 ahk3*) background, exhibiting a down-regulation of 15-fold. This reduction was counteracted in all lines expressing the *PpCHK1*, peaking with the line 35S::PpCHK1:GFP_D, which showed a 50-fold up-regulation compared to WT levels (Figure 16, H).

Analysis of the ubiquitously expressed *P. patens* cytokinin receptor PpCHK2 fused to GFP in the *ahk2-5 ahk3-7* double knockout shows partial complementation of the *ahk2-5 ahk3-7* phenotype. Four phenotypical and one molecular parameter were analyzed as above to assess the complementation capacity of PpCHK2 by reverting the alterations caused by the lack of AHK2 and AHK3 in the *ahk2-5 ahk3-7* mutant. The first parameter analyzed was rosette diameter. All diameter measurement results obtained were significantly different to both the WT and the mutant background with less than 0,1% probability of overlap. From the beginning (16 DAG), the *PpCHK2* expressing lines had a slightly larger diameter size than the mutant (ranging from 5% to 10% of WT diameter at 34 DAG; data shown in Figure 17, A). This effect was maintained until 34 DAG, when the *ahk2-5 ahk3-7* mutant had 50%; 35S::GFP:PpCHK2_A reached 54%; 35S::GFP:PpCHK2_B reached 60%,

35S::PpCHK2:GFP_C had 59% and 35S::PpCHK2:GFP_D had 53% of WT diameter size. Exemplified rosette diameter 27 DAG are depicted in Figure 17, B.

In terms of the second parameter, the number of leaves, three lines were compensated to almost WT levels (96%, 99% and 96% of WT leaf number in the transgenic lines B, C and D respectively), and were significantly different only from the mutant background. 35S::GFP:PpCHK2_A was not complemented (88% of WT leaf number compared to the knockout mutant *ahk2-5 ahk3-7*'s 85%) and showed a significant difference only to the WT (data depicted in Figure 17, D).

Analysis of the third phenotypical parameter, the total stem height, showed similar behavior to the rosette diameter. Three lines are slightly, but significantly elevated in stem height (73%, 74% and 72% of WT stem height for transgenic lines A, B and D respectively), while one line 35S::PpCHK2:GFP_C was not significantly different to the mutant background (71% of WT stem height as compared to 68% of WT stem height in the knockout mutant *ahk2-5 ahk3-7*; data shown in Figure 17, E and examples of plants in Figure 17, C).

The last phenotypic parameter under investigation was the number of first-order branches, well known to be affected by cytokinin deficiency (Werner *et al.,* 2001; Riefler *et al.,* 2006). None of the *PpCHK2* overexpressing lines could rescue this phenotype in a significant manner. Moreover, line 35S::PpCHK2:GFP_C showed a higher number of branches (124% of WT number of first-order branches) than the mutant background (111% of WT number of first-order branches).

For further clues on cytokinin signal transduction, two primary response genes were analyzed for their regulation in the *P. patens* cytokinin receptor *PpCHK2* overexpressing lines. These response regulators are down-regulated in the *ahk2-5 ahk3-7* mutant background

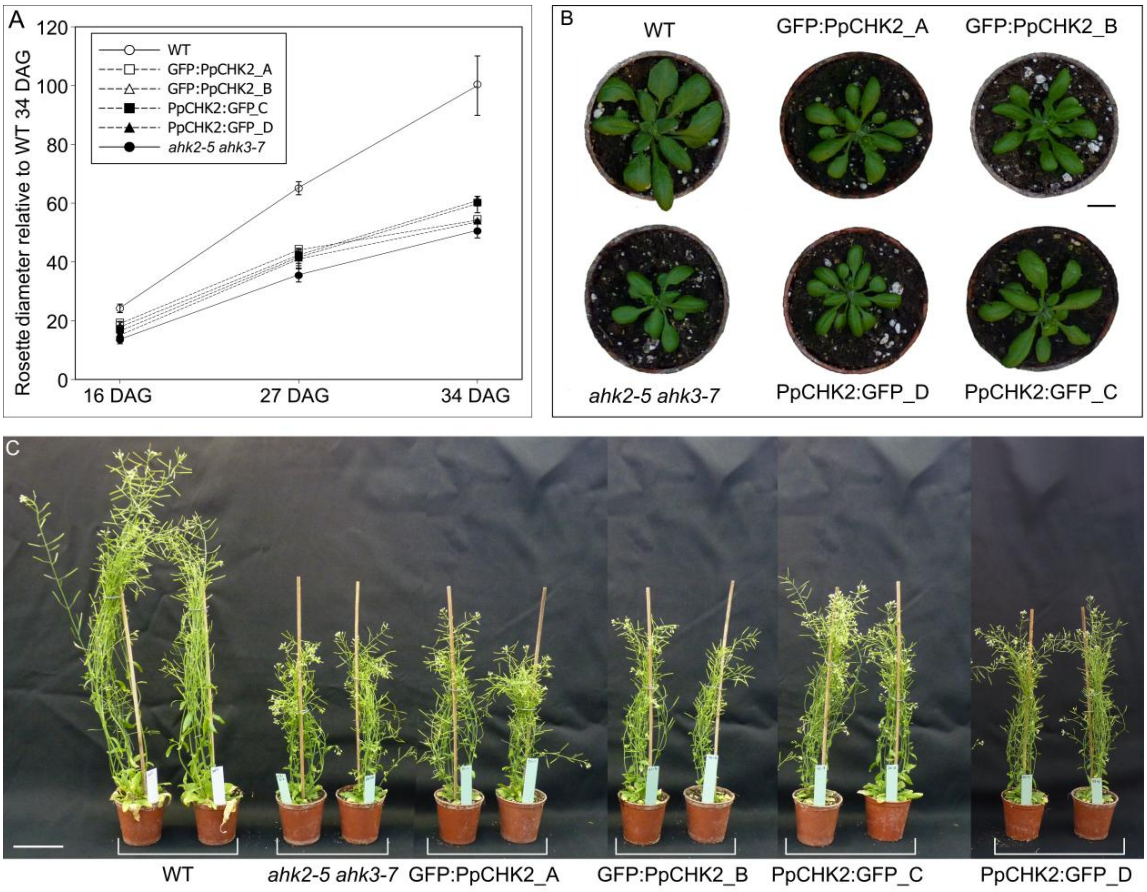
A
Rosette diameter relative to WT 34 DAG
WT
GFP:PpCHK2_A
GFP:PpCHK2_B
PpCHK2:GFP_C
PpCHK2:GFP_D
ahk2-5 ahk3-7
16 DAG
27 DAG
34 DAG
B
WT
GFP:PpCHK2_A
GFP:PpCHK2_B
ahk2-5 ahk3-7
PpCHK2:GFP_D
PpCHK2:GFP_C
C
WT
ahk2-5 ahk3-7
GFP:PpCHK2_A
GFP:PpCHK2_B
PpCHK2:GFP_C
PpCHK2:GFP_D

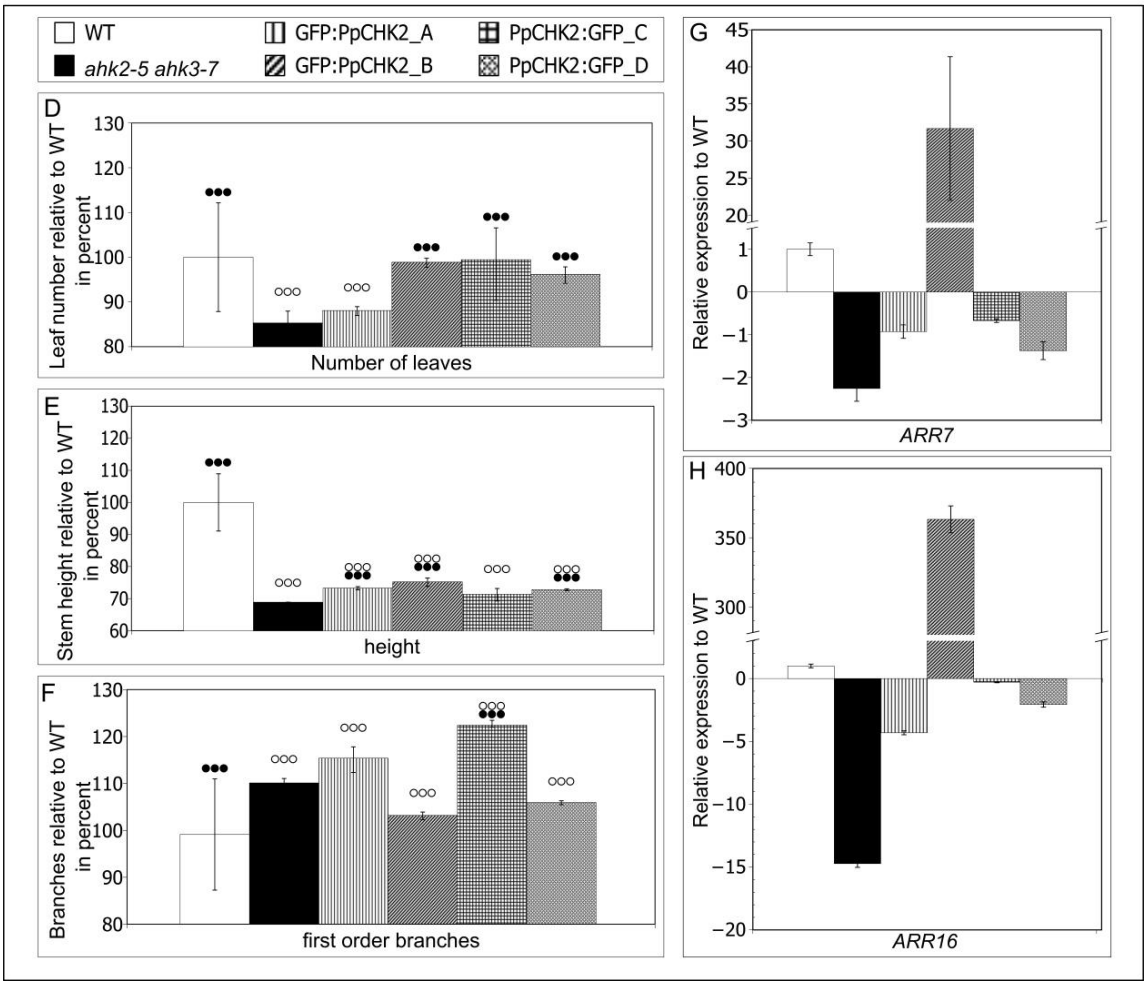
WT
ahk2-5 ahk3-7
GFP:PpCHK2_A
GFP:PpCHK2_B
PpCHK2:GFP_C
PpCHK2:GFP_D
D
Leaf number relative to WT in percent
Number of leaves
E
Stem height relative to WT in percent
height
F
Branches relative to WT in percent
first order branches
G
Relative expression to WT
ARR7
H
Relative expression to WT
ARR16

Figure 17: Complementation of the *ahk2 ahk3* double knockout by the *P. patens* cytokinin receptor PpCHK2 fused to GFP. All values are given relative to the WT. **A:** Rosette growth from 16 DAG until 34 DAG. For a better comparison all sizes were calculated in percent of the fully grown (34 DAG) wild type. All values were significantly different from WT and mutant background. **B:** Examples of rosette diameter of 27 DAG. First row: WT and N-terminal fusions of GFP with PpCHK2. Second row: mutant background (*ahk2-5 ahk3-7*) and C-terminal fusions of GFP to PpCHK2 **C:** Phenotypic comparison of mature plants. From left to right: WT, mutant background (*ahk2-5 ahk3-7*), N-terminal fusions of GFP with PpCHK2, C-terminal fusions of GFP to PpCHK2. **D:** Number of leaves of all analyzed genotypes relative to WT. **E:** Stem height of all analyzed genotypes relative to WT. **F:** Branch number of all analyzed genotypes relative to WT. **G:** Relative expression of *ARR7* of all analyzed genotypes. **H:** Relative expression of *ARR16* of all analyzed genotypes. A to F: Each line was analyzed with n = 50 plants. Scale bar in B corresponds to 1 cm. Scale bar in C corresponds to 5 cm. D, E, F: Open circles depict significance to WT values; closed circles depict significance to mutant background values. ooo ≤ 0,1% probability of overlap; oo = 0,1% ≥ 1% probability of overlap; o = 1% ≥ 5% probability of overlap.
G,H: WT expression level was set to 1, given is the fold-change of the respective lines. Shown are mean values of three biological replicates (n = 3).

(Kang et al., 2012 ; Brenner pers. communication). The transcript of *ARR7* behaved as anticipated in the mutant background, while the three lines 35S::GFP:PpCHK2_A, 35S::PpCHK2:GFP_C and 35S::PpCHK2:GFP_D showed a slight reversion of the down-regulation. Line 35S::GFP:PpCHK2_B was truly over compensated, reaching transcript levels 32-fold higher than the WT (Figure 17, G). The drastic over compensation in line 35S::GFP:PpCHK2_B was even more pronounced when analyzing the transcript abundance of *ARR16*, where it reached 370-fold of WT transcript levels. The other lines did show a reversion of the down-regulation in the mutant background, but did not reach WT levels (Figure 17, H).
Summing up, PpCHK2 and PpCHK1 fused to GFP only partially complement the analyzed parameters of the *ahk2-5 ahk3-7* mutant phenotype.

P. patens cytokinin receptor PpCHK2 complements the cytokinin signaling deficient A. thaliana ahk2 ahk3 mutant under the AHK2 promoter

The above-presented data show that PpCHK1 or PpCHK2 fused to GFP have a complementing effect on the cytokinin signaling-deficient mutant *ahk2-5 ahk3-7*, but cannot fully restore the WT phenotype. This might be due to the fusion of the receptor protein to GFP, which is also implicated by the PTA experiments presented in section 3.1.4, to, but could also be due to the ectopic expression of the receptors under the 35S CaMV promoter or because of incompatibilities in the signaling chain. To delineate these two effects, the *P. patens* cytokinin receptors *PpCHK1* and *PpCHK2* were fused to the native promoter of *AHK2* or *AHK3* from *A. thaliana*, with fusion to the small Myc-tag and transformed into *ahk2-2 ahk3-3* double mutant *A. thaliana* plants. AHK4 can complement the double knockout phenotype when it's expression is limited to the native expression domain of *AHK2*, but not in the *AHK3* domain (Stolz *et al.,* 2011). For this reason, the *P. patens* cytokinin receptor *PpCHK1* was expressed under the promoter of *AHK2* or *AHK3* and *PpCHK2* was expressed under the control of the *AHK2* promoter (the lack of the fusion with the *AHK3* promoter was

due to technical reasons). When *PpCHK1* was expressed driven by either one of the two *A. thaliana* promoters, it was not possible to generate homozygote lines. While it was possible to establish heterozygote *A. thaliana* plants transformed with *PpCHK1* under the promoter of *AHK2* and further selection showed a 3:1 segregation, potentially homozygote plants died at 20 DAG at the latest (see Figure 18). Heterozygote plants were not analyzed for practical reasons only. *A. thaliana* plants transformed with the construct expressing *PpCHK1* under the promoter of *AHK3* never survived the first selection. In conclusion, expression of *PpCHK1* in the native expression domain of *AHK2* or *AHK3* seems to have drastic effects on plant growth.

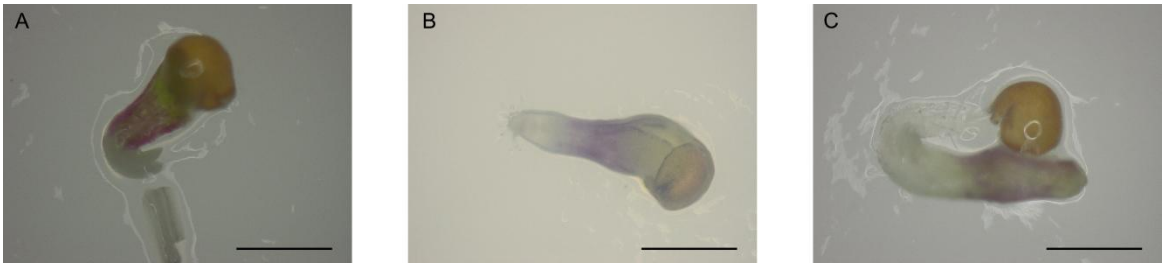

Figure 18: *pAHK2::PpCHK1* [*ahk2-2 ahk3-3*] *A. thaliana* plants. A, B and C show examples of the possibly homozygote *pAHK2::PpCHK1* plants 10 DAG. All plants died latest 20 DAG. Scale bar corresponds to 1 mm.

Stable lines expressing *PpCHK2* under the control of *pAHK3* in the mutant background of *ahk2 ahk3* were analyzed for the efficient transcription of *PpCHK2*. *A. thaliana* seedlings were harvested 16 DAG and subjected to qRT-PCR analysis. Two independent lines that showed significant amounts of transcript (see Figure 19) were further analyzed regarding the previously mentioned five parameters (see above) of phenotypic and molecular complementation of the *ahk2-2 ahk3-3* (Higuchi *et al.,* 2004) phenotype.

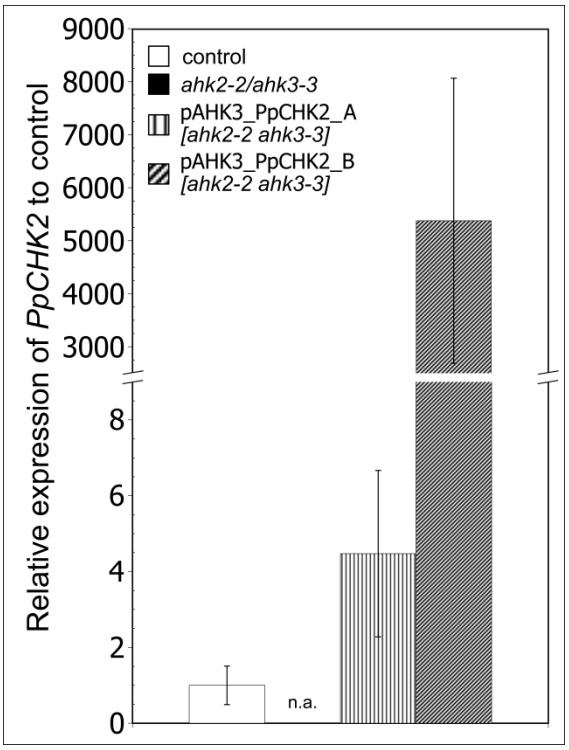

Figure 19: Expression of *pAHK3::PpCHK2* in *A. thaliana plants.* *A. thaliana* seedlings were harvested 16 DAG, RNA was isolated and transcribed to cDNA and transcript levels were analyzed by qRT-PCR. Control *A. thaliana* cDNA was isolated from wild type and analyzed with the respective *PpCHK2* primers. A maximum of 45 cycles was used as Ct for relative expression calculation. Shown are mean values of three biological replicates and whiskers represent standard deviation. Abbreviation: n.a., not analyzed.

The first parameter under investigation was the rosette diameter. All diameter measurement results obtained were significantly different to both the WT and the mutant background, indicating a reversion to 80% and 83% of WT diameter in transgenic lines A and B, respectively, when *pAHK3:PpCHK2* was expressed in the mutant background (Figure 20, A and B). The *ahk2-2 ahk3-3* mutant only reached 48% of WT diameter.

For the second parameter, the number of rosette leaves, the *ahk2-2 ahk3-3* mutant did not show any significant change compared to the WT. Surprisingly, the transgenic line pAHK3_PpCHK2_A exhibited a higher number of rosette leaves (124% of WT leaf number) than all other plants under investigation (data depicted in Figure 20, D). In the third parameter, stem height, the expression of *pAHK3::PpCHK2* showed a compensatory effect of 83% (pAHK3_PpCHK2_A) to 91% (pAHK3_PpCHK2_B) of the total stem height of the WT, while the *ahk2-2 ahk3-3* mutant only reached 70% of the WT (data depicted in Figure 20, E). The last phenotypic parameter, the number of first-order branches, is an indicator of cytokinin involvement: branch number tends to fall in the presence of either cytokinin or cytokinin sensing (Werner *et al.,* 2001; Riefler *et al.,* 2006). Accordingly, the mutant *ahk2-2 ahk3-3* is affected, but *pAHK3::PpCHK2* has significantly more first-order branches (about 120% of WT branching) than the WT (see Figure 20, F).

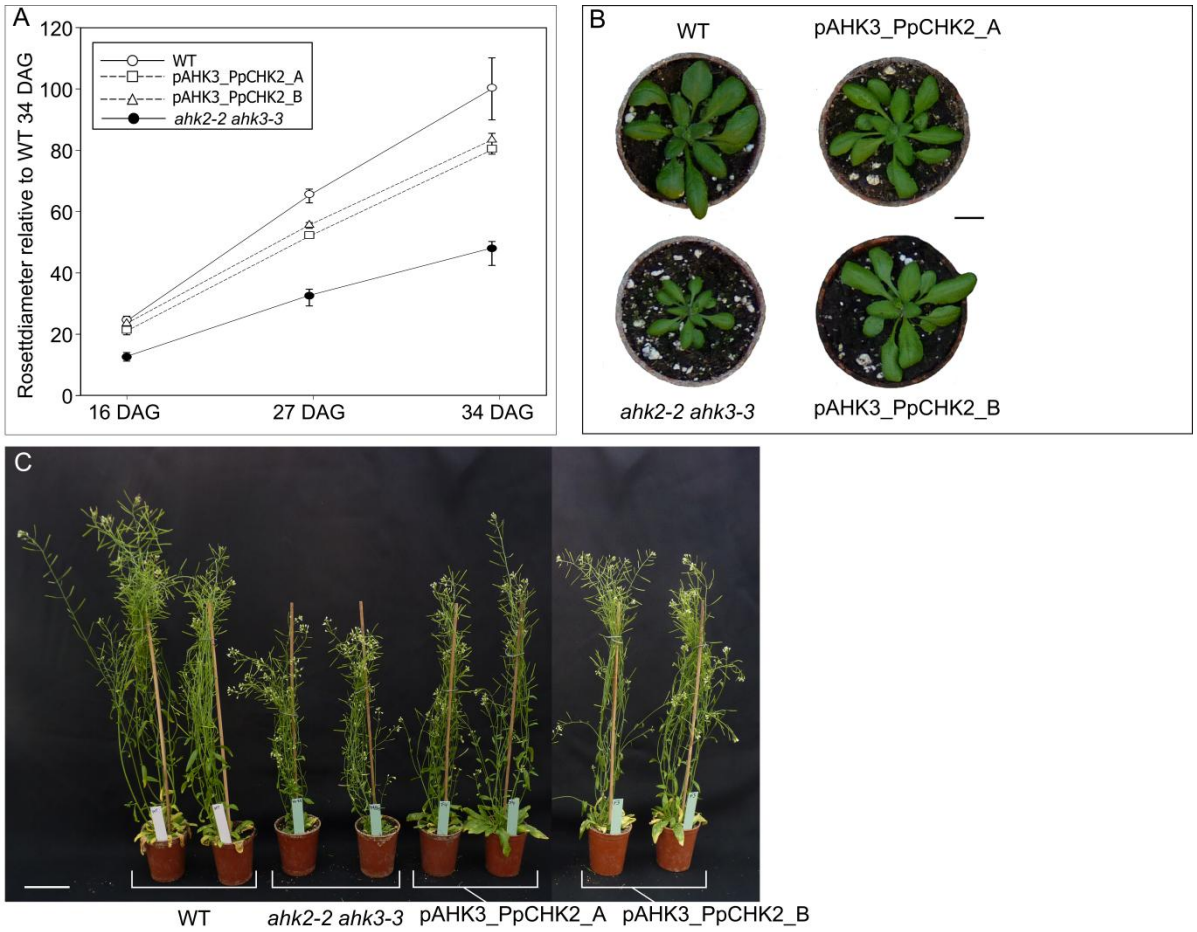
A
Rosettdiameter relative to WT 34 DAG
WT
pAHK3_PpCHK2_A
pAHK3_PpCHK2_B
ahk2-2 ahk3-3
16 DAG
27 DAG
34 DAG
B
WT
pAHK3_PpCHK2_A
ahk2-2 ahk3-3
pAHK3_PpCHK2_B
C
WT
ahk2-2 ahk3-3
pAHK3_PpCHK2_A
pAHK3_PpCHK2_B

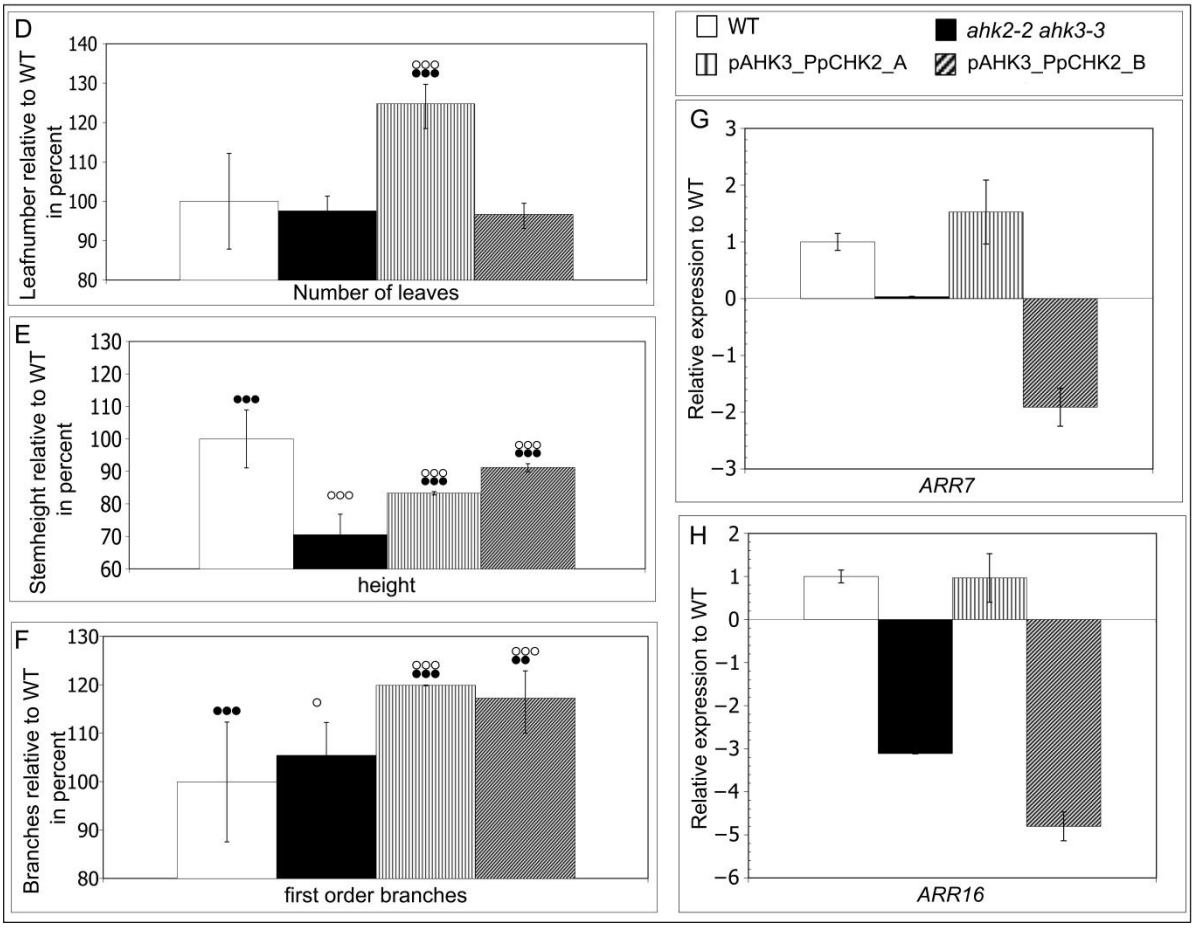
D
Leafnumber relative to WT in percent
Number of leaves
E
Stemheight relative to WT in percent
height
F
Branches relative to WT in percent
first order branches
WT
ahk2-2 ahk3-3
pAHK3_PpCHK2_A
pAHK3_PpCHK2_B
G
Relative expression to WT
ARR7
H
Relative expression to WT
ARR16

Figure 20: Complementation of the *ahk2-2 ahk3-3* double knockout in *A. thaliana* by *P. patens* cytokinin receptor PpCHK2. All values are given relative to the WT. A: Rosette growth from 16 DAG until 34 DAG. For a better comparison all sizes were calculated as percent of the fully grown (34 DAG) wild type. All values were significantly different from WT and mutant background. B: Examples of rosette diameter of 27 DAG. First row: WT and *AHK3* promoter fusion with *PpCHK2*, line A. Second row: mutant background (*ahk2-2 ahk3-3*) (Alonso *et al.,* 2003) and *AHK3* promoter fusion with *PpCHK2*, line B. C: Phenotypic comparison of mature plants (shown) are two examples per line. From left to right: WT, mutant background (*ahk2-2 ahk3-3*), *AHK3* promoter fusion with *PpCHK2* line A and line B. D: Number of leaves of all analyzed genotypes relative to WT. E: Stem height of all analyzed genotypes relative to WT. F: Branch number of all analyzed genotypes relative to WT. G: Relative expression of *ARR7* of all analyzed genotypes. H: Relative expression of *ARR16* of all analyzed genotypes. A to F: Each line was analyzed with n = 50 plants. Scale bar in B corresponds to 1 cm. Scale bar in C corresponds to 5 cm. D, E, F: Open circles depict significance to WT values; closed circles depict significance to mutant background values. ooo ≤ 0,1% probability of overlap; oo = 0,1% ≥ 1% probability of overlap; o = 1% ≥ 5% probability of overlap. G,H: WT expression level was set to 1, given is the fold-change of the respective lines. Shown are mean values of three biological replicates (n = 3).

The final parameter to be investigated was the two primary target genes *ARR7* (data shown in Figure 20, G) and *ARR16* (data shown in Figure 20, H) involved in cytokinin signaling. The RR *ARR7* did not show significant alterations in transcript levels in any plant under investigation. The RR *ARR16*, in contrast, indicated a complementation to almost WT levels (0,96-fold of WT levels) in the transgenic line pAHK3_PpCHK2_A, while transgenic line pAHK3_PpCHK2_B was significantly down-regulated as compared to WT (4,8-fold lower transcript level than the WT) and showed even lower levels of the *ARR16* transcript than the *ahk2-2 ahk3-3* mutant (3,1-fold lower than the WT). This finding supports the lack of complementation found in the analysis of leaf number and first-order branching in transgenic line pAHK3_PpCHK2_B. It does not, however, explain the cytokinin-deficient phenotype of transgenic line pAHK3_PpCHK2_A with regard to first-order branching. Despite the fact that the expression of *PpCHK2* under the *AHK3* promoter had an effect on every parameter, the direction of those effects varied. Whether or not it had an overall promoting or inhibiting effect on phenotype remediation remains ambiguous.

Summarizing, the expression of *PpCHK2* in the expression domain of *AHK3* in the cytokinin signaling-deficient *ahk2-2 ahk3-3* mutant of *A. thaliana* has complementing effects. These effects differ with regard to the parameter analyzed. The expression of *PpCHK1* in the cytokinin receptor expression domain of *AHK2* or *AHK3* results in lethality of the plant.

In the above experiments, it was evident that PpCHK1 and PpCHK2 share certain functions that enable complementation in *A. thaliana*, albeit to different extents. The aim of the next section is to investigate how far exactly these functions overlap.

3.1.8. Characterization of transgenic lines ectopically expressing *PpCHK1* or *PpCHK2* in *P. patens*

PpCHK1 and PpCHK2 have so far been characterized in various different ways, each way showing a specific detail to the receptors' function. It has been shown that PpCHK1 or PpCHK2 are bound by cytokinin (see section 3.1.1), that they activate cytokinin-specific signaling in *A. thaliana* (see section 3.1.4) and that they have a complementing effect in the *A. thaliana* mutant *ahk2 ahk3*, which lacks two native cytokinin receptors (see section 3.1.3). However, for a function in these heterologous model systems, chances are higher that components are incompatible or missing which would be required for full function in the signal transduction system. Additionally, autologous protein folding mechanisms and post translational modifications may be necessary for the full function of the protein. To overcome these pitfalls, vector constructs for the expression of the *PpCHK1* or *PpCHK2 GFP* fusion under the control of the 35S CaMV promoter were introduced into *P. patens*, and stable lines were further analyzed. The generation of knockout lines was also considered, but due to a collaboration with the group of K. v. Schwartzenberg (von Schwartzenberg *et al.,* in preparation), who had already established some of these knockouts, that plan was not followed up. It should be noted that the transcriptional activation of the 35S promoter in *P. patens* is lower than in *A. thaliana* (Horstmann *et al.,* 2004). The expression of *PpCHK1* or *PpCHK2*, fused either N- or C-terminally to *GFP*, was analyzed in stable lines generated from the wild type strain, or the double receptor knockout line *Ppchk1 Ppchk2* (von Schwartzenberg *et al.,* in preparation). To assess phenotypical changes caused by the effect of the transgene, up to three independent lines were analyzed if available.

The expression of the receptors *PpCHK1* and *PpCHK2* in the stable lines was driven by the 35S CaMV promoter. This promoter is almost ubiquitously expressed in plants (Benfey and Chua 1990). To estimate where the cytokinin receptors of *P. patens* are natively expressed, transcript abundance in protonema and gametophore tissue was analyzed (Figure 21; (von Schwartzenberg *et al.,* in preparation). Plant material and RNA-isolation for the transcriptional profile of the *PpCHK1*, *PpCHK2* and *PpCHK3* receptors was carried out by A. C. Lindner (group of K. von Schwartzenberg, Universität Hamburg). The expression of the transgene under the 35S promoter seemed appropriate, since this promoter would enhance transcript abundance in both tissue types (protonema and gametophore), and hence in a similar expression domain as that observed for the native expression domain.

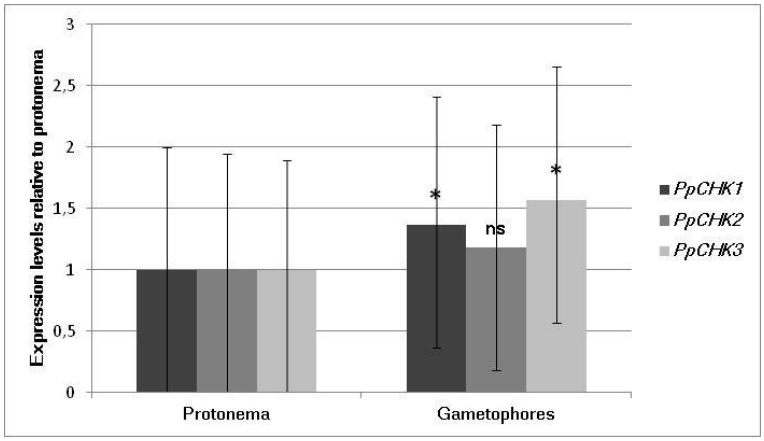

Figure 21: The three cytokinin receptors *PpCHK1*, *PpCHK2* and *PpCHK3* are expressed at similar levels in protonema and in the gametophore. RNA was isolated from protonema- or gametophore-producing tissue. Transcript levels were analyzed by qRT-PCR analysis. Shown are mean values of three biological replicates (n = 3) and standard deviation (whiskers). *= 1% ≥ 5% probability of overlap; ns = not significant.

Phenotypical description of P. patens ectopically expressing PpCHK1

The outline for the remainder of this section is as follows: first, the generated stable transgenic lines expressing *GFP* fusions of *PpCHK1* or *PpCHK2* under the control of the 35S promoter are described. Following a phenotypical description, the transcriptional regulation of some potentially cytokinin signaling-related genes are analyzed, and the macroscopic description of the transgenic lines on media with different phytohormones is investigated. For these descriptions, the *PpCHK1* and *PpCHK2*-related transgenic lines in the WT background are described in turn, followed by an area growth assay of the respective transgenic lines. This process is then repeated for the double knockout *Ppchk1 Ppchk2* background.

Firstly, stable lines (generated according to section 2.5.4.3) were analyzed for the presence of the introduced *PpCHK1* cDNA. All selected lines were positive for the integration of the construct (see Appendix Figure 3, B). While the generation of lines with the construct of GFP fused to the C-terminus of the receptor protein yielded various stable lines (shown here: three selected lines), the construct consisting of N-terminally fused GFP to the receptor generated only one line (35S::GFP:PpCHK1 #27N20) for the following analysis. Secondly, all transgenic lines were phenotypically judged regarding the formation of gametophores (Figure 22 A, upper left quadrant) and the distribution of chloronemal and caulonemal protonema (Figure 22 A, upper right quadrant). For reference, both the WT and the double knockout *Ppchk1 Ppchk2* were included. After 14 days growing on standard BCD medium, both control strains developed gametophore initials (buds), but did not have gametophores. This was also true for the C-terminal fusion line 35S::PpCHK1:GFP #1N4 and the N-terminal fusion line 35S::GFP:PpCHK1 #27N20. In contrast, the C-terminal fusion lines 35S::PpCHK1:GFP #1N32 and 35S::PpCHK1:GFP #1N76 already had fully developed gametophores with

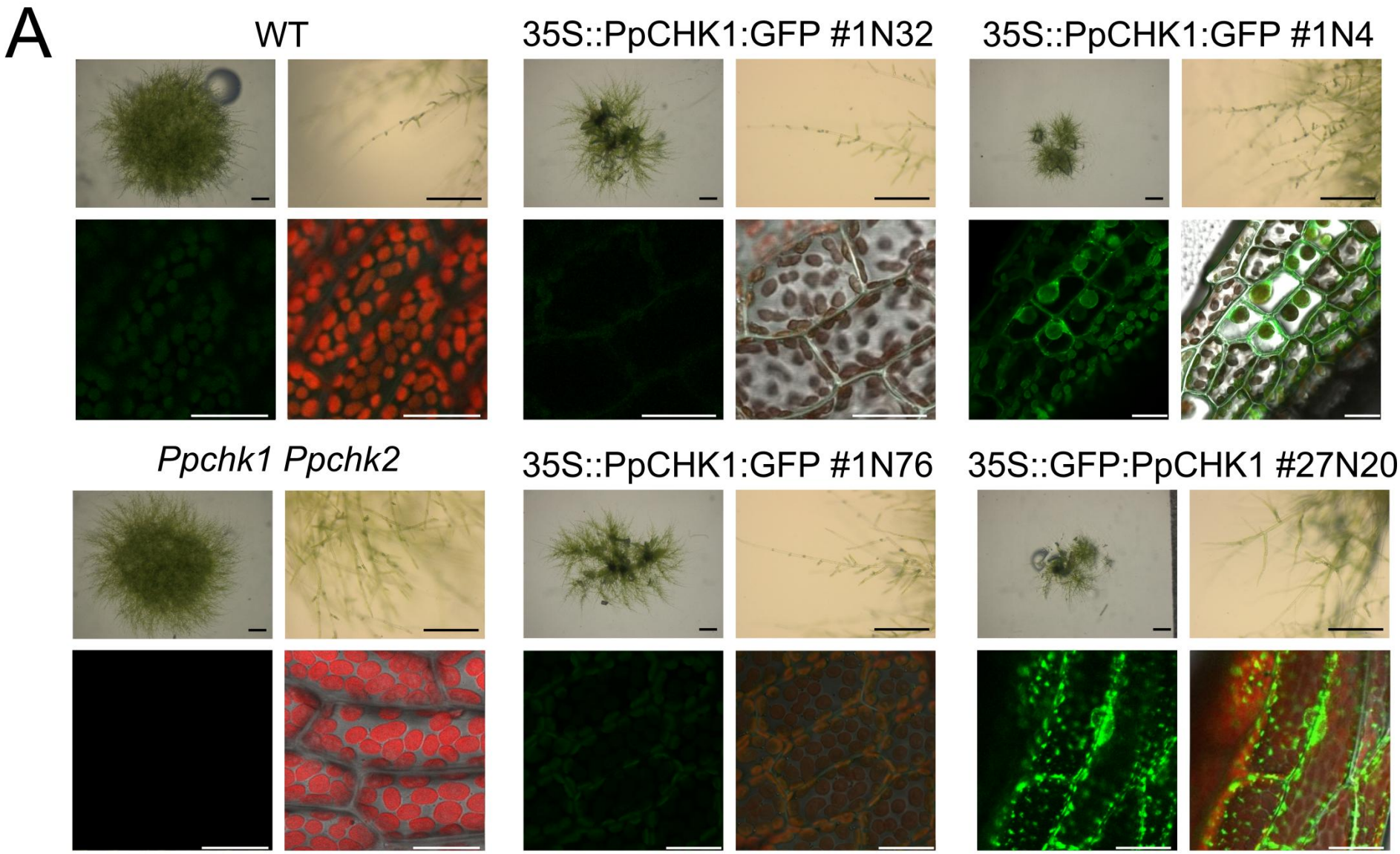
A
WT
35S::PpCHK1:GFP #1N32
35S::PpCHK1:GFP #1N4
Ppchk1 Ppchk2
35S::PpCHK1:GFP #1N76
35S::GFP:PpCHK1 #27N20

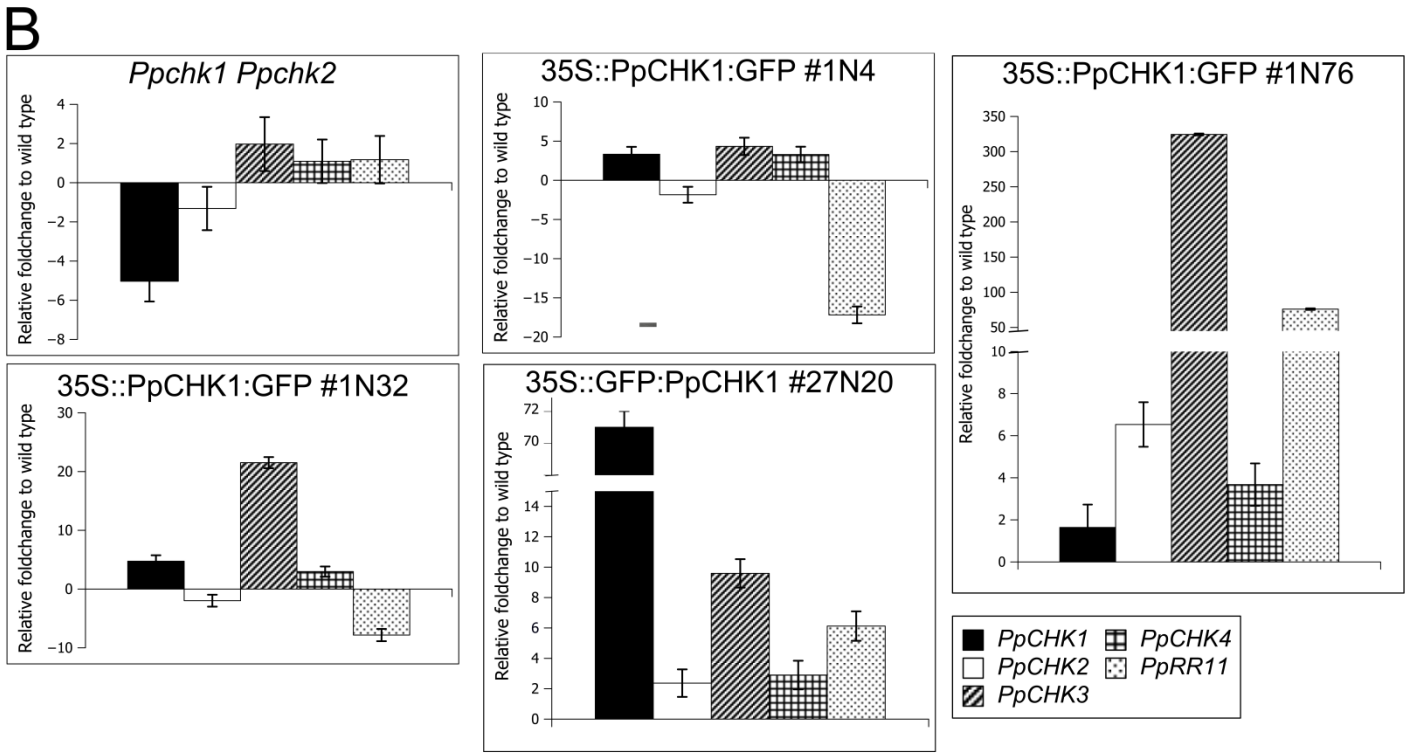

Figure 22: ***PpCHK1*** **ectopically expressed in** ***P. patens***. **A)** Phenotypical description of the analyzed lines. Upper pictures show growth on BCD medium after 14 days. Lower pictures are taken from plants in long-term culture on BCD plates. Scale bars: upper left quadrant, 1mm; upper right quadrant, 0,5 mm; lower quadrants, 25 µm. Lower pictures indicate GFP signal (left) and the overlay of GFP, autofluorescence of the chloroplasts and the bright field image (right). **B)** qRT-PCR analysis of genes associated with cytokinin signaling in the respective transgenic line. Protonema and gametophore tissue was harvested from continuous cultures, RNA was isolated and qRT-PCR was carried out as described in section 2.5.1 and 2.2.1 respectively. WT levels were set to 1 and results are given as fold change compared to WT.

several leaves. When taking a closer look at the protonema, the double knockout strain seemed to have an excess of chloronemal filament compared to WT, although this effect was not quantified. The transgenic lines 35S::PpCHK1:GFP #1N32 and 35S::PpCHK1:GFP #1N76 developed typical features: a caulonemal filament with chloronemal filament branches. The transgenic line 35S::PpCHK1:GFP #1N4 seemed to also have both filamental cell types (chloronema with perpendicular cell walls and more than 100 chloroplasts; caulonema cells with oblique cell walls and less chloroplasts), but also had agglomerates of chloroplasts in the cells making it difficult to decide their identity. The analysis of protonema in the N-terminal fusion line 35S::GFP:PpCHK1 #27N20 revealed both cell types, but did not show the normal distribution. The filaments were shaped irregularly and consisted of either one cell type or the other.

Thirdly, the composition of a single cell of fully developed gametophores was analyzed (Figure 22 A, lower quadrants). While WT and knockout strains had equally distributed, round shaped chloroplasts, this pattern was only found in the transgenic line 35S::PpCHK1:GFP #1N76, where no GFP fluorescence was detected (Figure 22 A, lower quadrants). The other C-terminally fused lines (35S::PpCHK1:GFP #1N32 and 35S::PpCHK1:GFP #1N4) were found to be altered in chloroplast shape (Figure 22 A, lower quadrants). While 35S::PpCHK1:GFP #1N32 had drop shaped chloroplasts and did not show GFP fluorescence, 35S::PpCHK1:GFP #1N4 showed clear GFP fluorescence and in some cells only one, two or three giant chloroplasts. Other cells, however, contained chloroplasts that resembled the WT. The subcellular localization of the GFP signal in these cells was not further analyzed, but seems to be primarily located to the outside of the chloroplasts and to a structure that connects the chloroplasts with the plasma membrane. The N-terminally fused transgenic line 35S::GFP:PpCHK1 #27N20 also showed a clear GFP signal (Figure 22 A, lower quadrants). Except for line 35S::PpCHK1:GFP #1N4 the signal was distributed in small speckles over the whole cell, while also clearly marking the perinuclear area (Figure 22 A, lower quadrants). These observations were not verified by additional markers and should therefore be treated preliminarily.

In summary, three of four transgenic lines expressing *PpCHK1* fused to *GFP* showed a detectable GFP signal and all transgenic lines with C-terminal fusions of GFP to PpCHK1 had altered chloroplast shapes and/or distribution.

On the transcriptional level, one feature was connected to the constructs in use, namely the relatively low overexpression of *PpCHK1* in the C-terminally fused transgenic lines 35S::PpCHK1:GFP #1N32, 35S::PpCHK1:GFP #1N4 and 35S::PpCHK1:GFP #1N76, with fold changes of 4-fold, 3-fold and 2-fold respectively (see Figure 22, B). Although the

transcript of the transgene was largely unaffected, other components potentially related to the signaling cascade of cytokinin were significantly changed. The gene of the putative cytokinin receptor *PpCHK4* was identified as part of a clade of eight *P. patens* CHASE domain-containing hybrid histidine kinase in a phylogenetic tree of the CHASE domains (Figure 30) in this project, and may be a part of the cytokinin signaling system in *P. patens*. Whether or not PpCHK4 is part of the cytokinin signaling system is a question addressed later (in section 3.2). All generated overexpresser mutants were analyzed for the transcriptional regulation of the three previously identified (*bona fide*) cytokinin receptors (*PpCHK1*, *PpCHK2* and *PpCHK3*) and of *PpCHK4* as a representative of the newly identified, putative cytokinin receptors in *P. patens*, since it is plausible that alterations on the transcript level of one receptor might be compensated by the other receptors. Also included was a type-A RR (RRA) from *P. patens* (*PpRR11*, naming according to (Pils and Heyl 2009)). RRAs are primary target genes of the cytokinin signaling system in *A. thaliana* (Hwang *et al.,* 2002; Heyl and Schmülling 2003; Kakimoto 2003; Ferreira and Kieber 2005). Our analysis also included the double knockout *Ppchk1 Ppchk2*, which displays a relatively small down-regulation of the deficient genes. This effect is more due to a technical issue, as both genes were disrupted only about 500 bp downstream of the start codon by the recombination of a selection marker gene into the respective receptor. The annealing sites of the analysis primers were designed to detect the full cDNA, and are hence located as far as possible towards the 5´-end of the gene. The amplicon of ~200 bp detected the remaining transcript of the respective disrupted receptor gene. A detailed analysis of the *Ppchk1 Ppchk2* mutant is described by von Schwartzenberg and colleagues (von Schwartzenberg *et al.,* in preparation). The other transcripts, namely *PpCHK3*, *PpCHK4* and *PpRR11* were unchanged compared to the WT. This is in accordance with the lack of any obvious phenotypic changes in the *Ppchk1 Ppchk2* mutant (von Schwartzenberg *et al.,* in preparation). The transgenic line 35S::PpCHK1:GFP #1N32 expressed *PpCHK1* 4-fold more that the WT, while *PpCHK2* and *PpCHK4* did not change significantly. *PpCHK3* was up-regulated the most, to 21-fold of WT levels, while *PpRR11*, in contrast, was down-regulated to about 8-fold less than WT levels. A related pattern was observed in the mutant 35S::PpCHK1:GFP #1N4, where *PpCHK1* was slightly up-regulated to 3,3-fold, *PpCHK2* was not significantly changed, and *PpCHK4* was also only slightly above threshold limits. Similarly to the 35S::PpCHK1:GFP #1N32 mutant, *PpCHK3* was also up-regulated to 4,3-fold, while *PpRR11* was down-regulated by 17-fold. These mostly moderate regulation patterns were not found in the transgenic line 35S::PpCHK1:GFP #1N76. Even though *PpCHK1* was transcribed at almost WT levels (1,6-fold), all other transcripts under investigation were up-regulated (*PpCHK2*, 6,5-fold; *PpCHK3*, 324-fold; *PpCHK4*, 3,6-fold and *PpRR11*, 76-fold). The transcript of *PpRR11* was highly up-regulated. This up-regulation was exceeded by the transcript of *PpCHK3*, to over

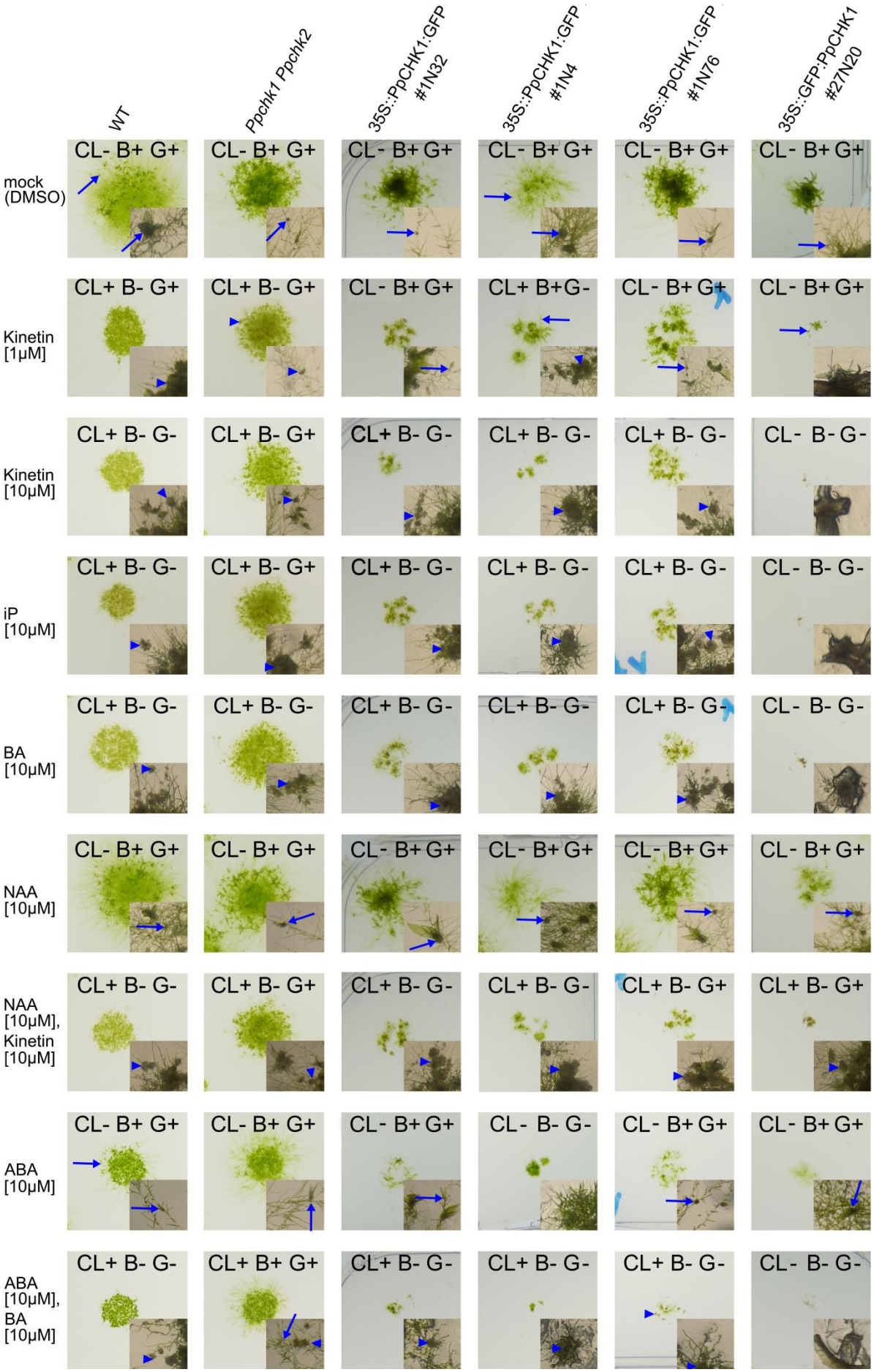
WT
Ppchk1 Ppchk2
35S::PpCHK1:GFP #1N32
35S::PpCHK1:GFP #1N4
35S::PpCHK1:GFP #1N76
35S::GFP:PpCHK1 #27N20
mock (DMSO)
Kinetin [1µM]
Kinetin [10µM]
iP [10µM]
BA [10µM]
NAA [10µM]
NAA [10µM], Kinetin [10µM]
ABA [10µM]
ABA [10µM], BA [10µM]
CL- B+ G+
CL+ B- G+
CL+ B+G-
CL+ B- G-
CL- B- G-

Figure 23: Bud and gametophore formation in mutant *P. patens* lines ectopically expressing *PpCHK1* fused to *GFP*. Transgenic lines were grown for 30 days on media supplemented with different phytohormones. Shown are the colony phenotype and the protonema phenotype (inset) with bud (if present). Indicated in the colony image is the occurrence of callus-like buds (CL), buds (B) and gametophores (G) with + if present and – if not present. The blue arrow in the picture indicates a normal bud and blue arrowheads indicate callus-like buds. These annotations have been derived from a larger picture represented by the inset. The bottom line of the colony picture corresponds to 2,3 cm; the bottom line of the inset corresponds to 1 mm.

300-fold. While the *PpCHK2* transcript was elevated to 6,5-fold, the *PpCHK4* transcript maintained its moderate up-regulation (3,6-fold). In contrast to the moderate up-regulation of the *PpCHK1* transgene, the N-terminal fusion line 35S::GFP:PpCHK1 #27N20 showed high levels of the transcript (71-fold up-regulation). The *PpCHK2* and *PpCHK4* transcripts were again not significantly altered and *PpCHK3* and *PpRR11* were up-regulated to 9,5-fold and 6,1-fold respectively.
In summary the transcriptional analysis of the transgene *PpCHK1* in the WT background surprisingly did not reveal a common regulation pattern of the analyzed transcripts.

Effects of different phytohormones on P. patens ectopically expressing PpCHK1

For further clues on the role of PpCHK1 in *P. patens*, the macroscopic phenotype of the transgenic lines on medium supplied with different phytohormones was analyzed. Since one of the best studied effects of cytokinin in *P. patens* is the formation of buds – the initials of gametophores developed later (Bopp and Brandes 1964; Brandes and Kende 1968; Reski and Abel 1985) – transgenic lines were analyzed for their response to cytokinin in the media by bud formation. Normal bud formation in the WT takes about 14 days. Mutant analysis was done after 30 days in order to also monitor the progression of gametophore development. It has also been reported that an excess of cytokinin leads to the formation of callus-like buds that eventually develop a gametophore (Bopp and Brandes 1964; Brandes and Kende 1968). Other phytohormones also play a role in the process of bud formation, such as ABA (which has an inhibiting effect) and auxin (which promotes bud formation) (von Schwartzenberg 2009).

The application of different cytokinins to the medium resulted in the formation of callus-like buds in the WT, the double knockout mutant (*Ppchk1 Ppchk2*), and in all C-terminally fused lines (Figure 23). The N-terminally fused line 35S::GFP:PpCHK1 #27N20 developed normal buds when grown on medium containing 1 µM kinetin, and on medium containing any cytokinin at 10 µM the mutant did not grow and eventually died. This hypersensitivity at high cytokinin concentrations could be caused by the strong overexpression of the *PpCHK1* transcript (Figure 22, B). The application of auxin (10 µM NAA) to the medium caused the C-terminally fused lines to have less gametophores, and the N-terminal fusion line

A

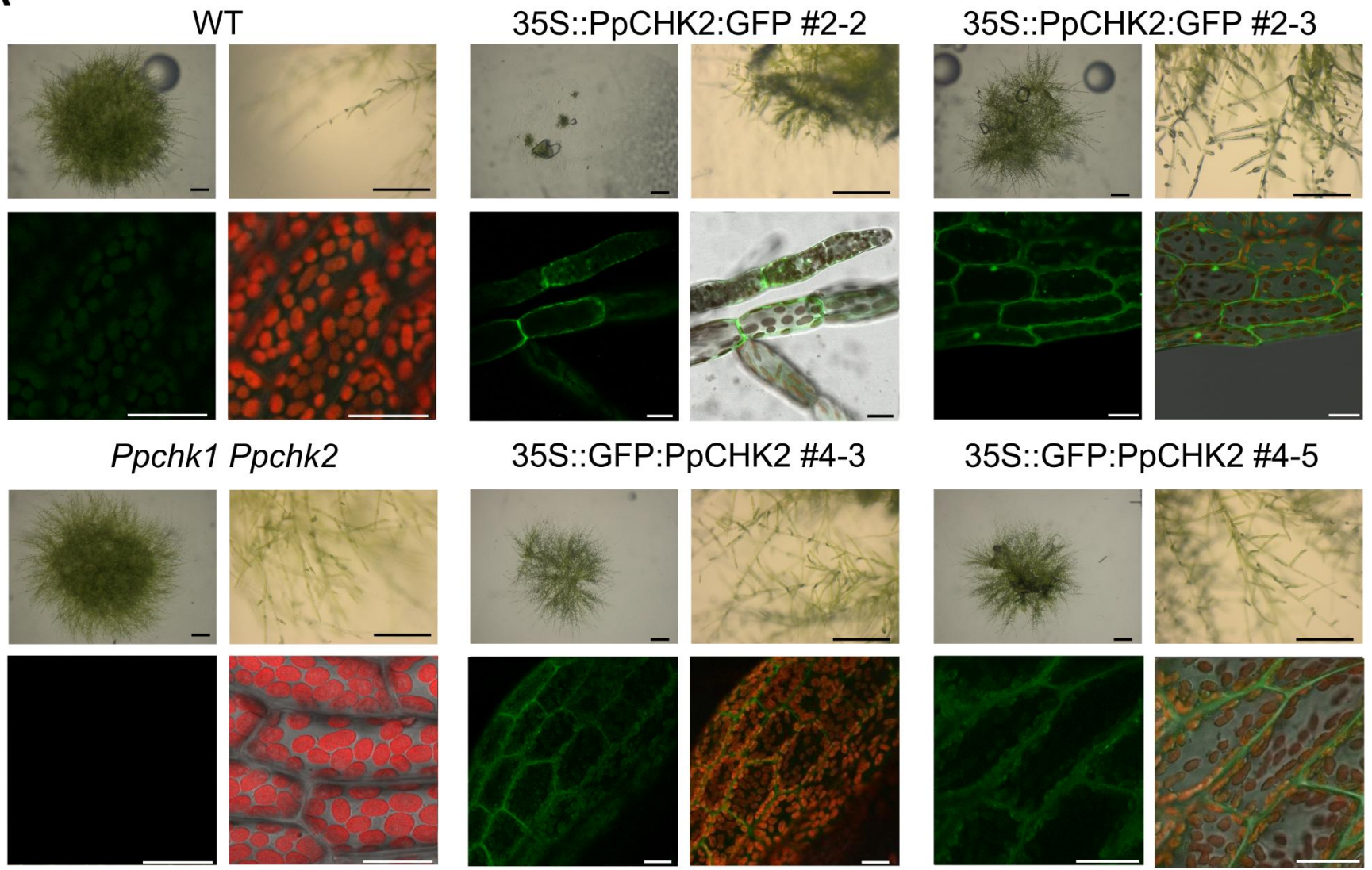
WT
35S::PpCHK2:GFP #2-2
35S::PpCHK2:GFP #2-3
Ppchk1 Ppchk2
35S::GFP:PpCHK2 #4-3
35S::GFP:PpCHK2 #4-5

B

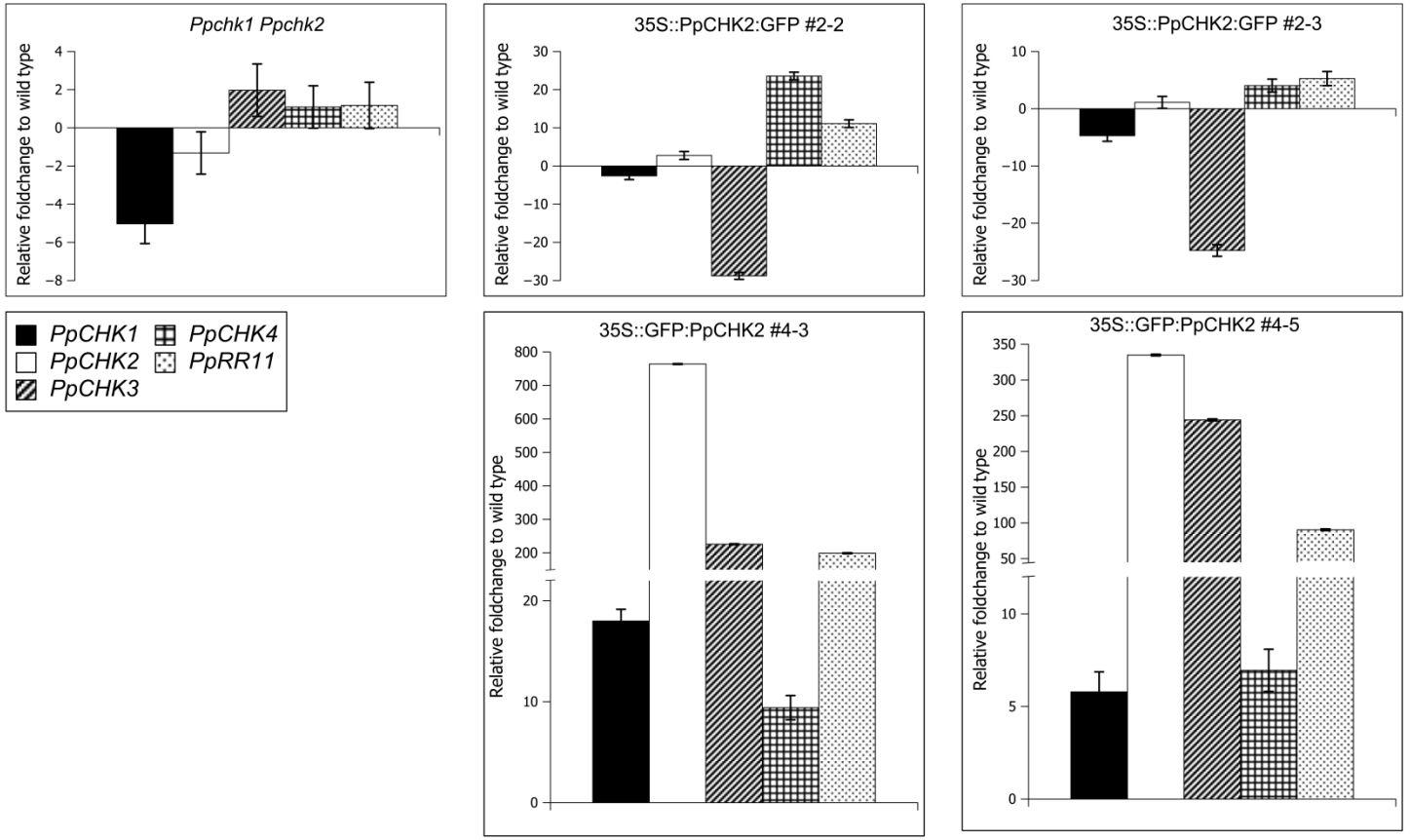

Figure 24: *PpCHK2* ectopically expressed in *P. patens*. A) Phenotypical description of the analyzed lines. Upper pictures show growth on BCD medium after 14 days. Lower pictures are taken from plants in long-term culture on BCD plates. Scale bars: upper left quadrant, 1mm; upper right quadrant, 0,5 mm; lower quadrants, 25 µm. Lower pictures indicate GFP signal (left) and the overlay of GFP, autofluorescence of the chloroplasts and the bright field image (right). **B)** qRT-PCR analysis of genes associated with cytokinin signaling in the respective transgenic line. Protonema and gametophore tissue was harvested from continuous cultures, RNA was isolated and qRT-PCR was carried out like described in section 2.5.1 and 2.2.1 respectively. WT levels were set to 1 and results are given as fold change compared to WT.

35S::GFP:PpCHK1 #27N20 to have irregularly shaped gametophores, compared to the mock treatment. The equimolar application of auxin and cytokinin (NAA and kinetin, 10 µM) copied the phenotypes of the sole application of cytokinin in the C-terminally fused lines. The phenocopy of the cytokinin phenotype was not observed in the 35S::GFP:PpCHK1 #27N20 mutant. Sole application of cytokinin heavily inhibited growth in this line, while the application of auxin allowed bud and gametophore formation. The application of auxin and cytokinin together formed callus-like buds that gave rise to gametophores. In this case it seems that the application of NAA (whilst cytokinin is also present) restored growth. The application of ABA to the medium only resulted in an inhibition of gametophore development in the transgenic line 35S::PpCHK1:GFP #1N4 and the protonema of this mutant grew very dense. All other plants, including the controls, still developed buds and gametophores. The simultaneous application of ABA and cytokinin (benzyladenine) copied the cytokinin phenotype of the transgenic lines, by developing callus-like buds and no gametophores. Only the double knockout mutant *Ppchk1 Ppchk2* developed gametophores, while gametophore development was inhibited when only benzyladenine was supplemented to the medium of *Ppchk1 Ppchk2*. Dense protonema growth with callus-like buds also resulted after the application of ABA and benzyladenine to the WT. Dense protonema was observed in the 35S::PpCHK1:GFP #1N4 mutant when only applying ABA.

Altogether, the four *GFP*-fused *PpCHK1* transgenic lines showed in three lines GFP fluorescence and all transgenic lines were altered in their chloroplast shape and/or distribution. The investigation of transcripts putatively involved in cytokinin signaling did not show clear patterns of regulation. Growth of the generated transgenic lines of *GFP* fusions with *PpCHK1* were affected by cytokinin, auxin and ABA.

Phenotypical description of P. patens ectopically expressing PpCHK2

The effect of PpCHK2 on *P. patens* growth was investigated by the analysis of ectopically expressed *GFP* fusions to the N- or C-terminus of the cytokinin receptor. *P. patens* was transformed with a construct encoding the respective promoter, receptor and tag fusion arrangement and the integration of the construct in use into the *P. patens* genome was investigated by PCR. All selected lines were positive for the construct's integration (Appendix Figure 3, A). Macroscopic phenotype analysis on BCD medium indicated a severely affected protonema growth in the transgenic line 35S::PpCHK2:GFP #2-2, which formed small colonies. All other lines, independent of GFP fusion orientation, grew similarly to the WT, developing buds and seeming to have a more branched protonema (Figure 24 A, upper left quadrant). Zooming to protonema resolution confirmed protruding protonema growth in all transgenic lines under investigation (Figure 24 A, upper right quadrant). Microscopic analysis

confirmed a common pattern of GFP fluorescence in all transgenic lines, displaying, namely the distribution of the GFP signal throughout the cell and possibly also at the plasma membrane of the cell. This fluorescence extended inside the cell, especially around the chloroplasts, and while the C-terminally fused lines also showed a fluorescent signal in the nucleus area, this was not the case for the N-terminally fused lines (Figure 24 A, lower quadrants). These observations were not verified by additional markers and should therefore be treated as preliminary. Additionally, the distribution and number of chloroplasts in the 35S::PpCHK2:GFP #2-2 protonema was unpredictable (Figure 24 A, upper right quadrant of 35S::PpCHK2:GFP #2-2); one protonema thread was filled with larger chloroplasts, another harbored drop shaped chloroplasts, and the third branch was tightly packed with chloroplasts (Figure 24 A, lower quadrants). The second C-terminally fused transgenic line, 35S::PpCHK2:GFP #2-3, had visibly less chloroplasts in one cell than the WT, and these chloroplasts lost their round shape. While the N-terminally fused line 35S::GFP:PpCHK2 #4-3 did not exhibit an altered appearance with regard to chloroplasts, the transgenic line 35S::GFP:PpCHK2 #4-5 displayed an elongated shape in its chloroplasts (Figure 24 A, lower quadrants).

Despite the clear GFP signal in all transgenic lines, the transcriptional analysis indicated only slight (2,7-fold) or no (1,1-fold) up-regulation above the threshold (2,5-fold) of the C-terminally fused *PpCHK2* transcript in 35S::PpCHK2:GFP #2-2 and 35S::PpCHK2:GFP #2-3, respectively (Figure 24, B), although both N-terminally fused transgenic lines had highly increased *PpCHK2* transcript levels. The absence of extensive up-regulation of the C-terminally fused receptor was also evident from the fusion constructs with the cytokinin receptor *PpCHK1* (Figure 22, B). Further investigation of the transcription of the other receptors (see explanation in the PpCHK1 section) and the potential output indicator *PpRR11* in the C-terminally fused *PpCHK2* transgenic lines showed differentially expressed cytokinin signaling components. In the transgenic line 35S::PpCHK2:GFP #2-2, the transcript of *PpCHK1* was insignificantly altered (2,5-fold down-regulated) and *PpCHK4* was 25-fold up-regulated. The *PpCHK3* transcript was effectively down-regulated to 28-fold below WT levels and *PpRR11* up-regulated to 11-fold of WT levels (Figure 24, B). The transgenic line 35S::PpCHK2:GFP #2-3 exhibited a similar pattern, where *PpCHK1* and *PpCHK3* were down-regulated to 4,7-fold and 24-fold less than in the WT, while *PpCHK4* and *PpRR11* were up-regulated to 4- and 5,2-fold of WT levels respectively (Figure 24, B). Contrary to the C-terminally fused transgenic lines, the expression of the N-terminally fused *PpCHK2* receptor resulted in higher transcript levels (Figure 22, B). The transgenic lines 35S::GFP:PpCHK2 #4-3 and 35S::GFP:PpCHK2 #4-5 also confirmed these findings by showing extensively up-regulated transcription of *PpCHK2*, *PpCHK3* and *PpRR11* and moderate up-regulation of *PpCHK1* and *PpCHK4* (transgenic line 35S::GFP:PpCHK2 #4-3: *PpCHK1*, 17-fold; *PpCHK2*,

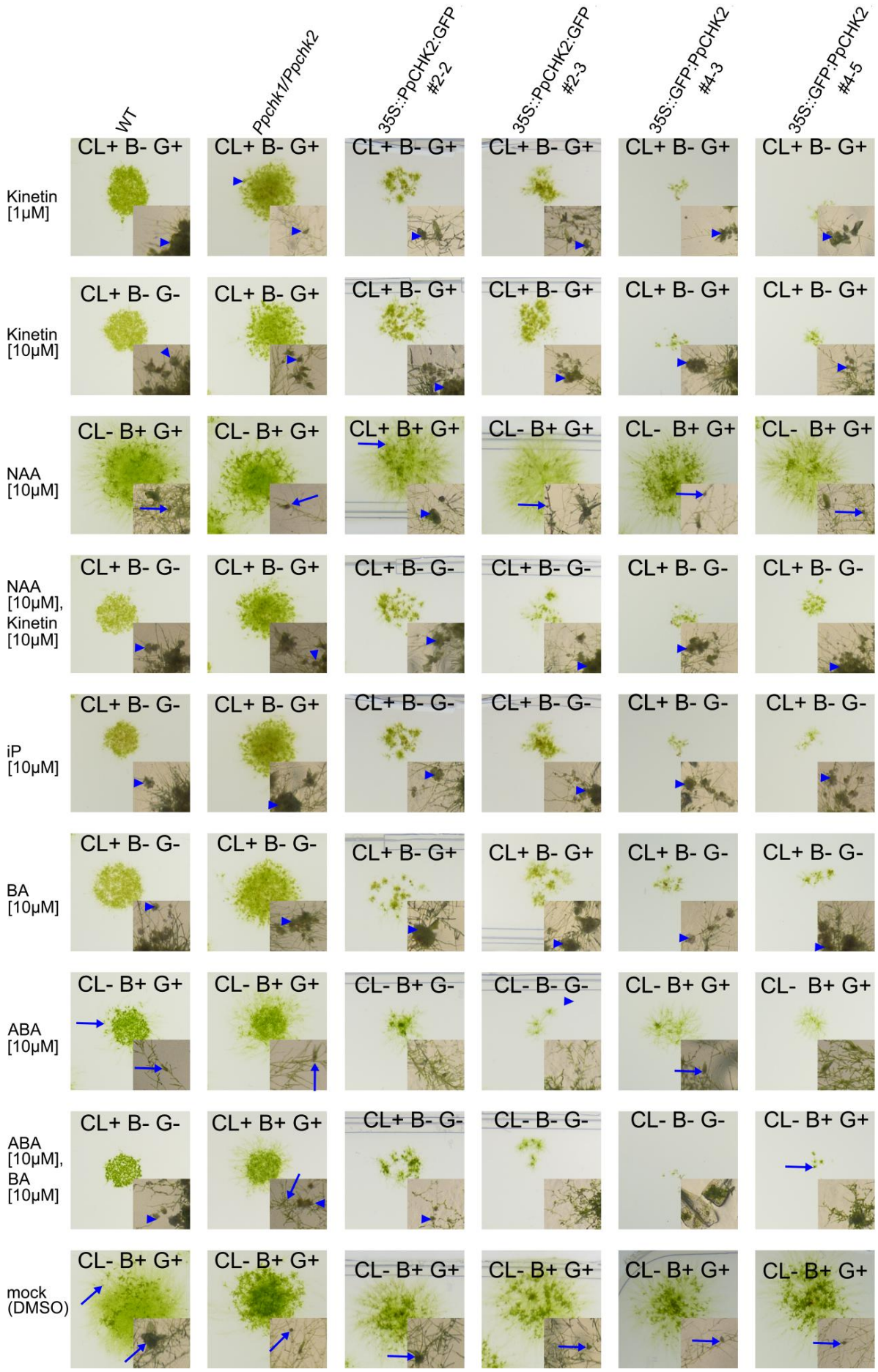
WT
Ppchk1/Ppchk2
35S::PpCHK2:GFP #2-2
35S::PpCHK2:GFP #2-3
35S::GFP:PpCHK2 #4-3
35S::GFP:PpCHK2 #4-5
Kinetin [1μM]
Kinetin [10μM]
NAA [10μM]
NAA [10μM], Kinetin [10μM]
iP [10μM]
BA [10μM]
ABA [10μM]
ABA [10μM], BA [10μM]
mock (DMSO)
CL+ B- G+
CL+ B- G+
CL+ B- G+
CL+ B- G+
CL+ B- G+
CL+ B- G+
CL+ B- G-
CL+ B- G+
CL+ B- G+
CL+ B- G+
CL+ B- G+
CL+ B- G+
CL- B+ G+
CL- B+ G+
CL+ B+ G+
CL- B+ G+
CL- B+ G+
CL- B+ G+
CL+ B- G-
CL+ B- G+
CL+ B- G-
CL+ B- G-
CL+ B- G-
CL+ B- G-
CL+ B- G-
CL+ B- G+
CL+ B- G-
CL+ B- G-
CL+ B- G-
CL+ B- G-
CL+ B- G-
CL+ B- G+
CL+ B- G+
CL+ B- G-
CL+ B- G-
CL+ B- G-
CL+ B- G-
CL- B+ G+
CL- B+ G+
CL- B+ G-
CL- B- G-
CL- B+ G+
CL- B+ G+
CL+ B- G-
CL+ B+ G+
CL+ B- G-
CL- B- G-
CL- B- G-
CL- B+ G+
CL- B+ G+
CL- B+ G+
CL- B+ G+
CL- B+ G+
CL- B+ G+
CL- B+ G+

Figure 25: Bud and gametophore formation in mutant *P. patens* lines ectopically expressing *PpCHK2* fused to *GFP*. Transgenic lines were grown for 30 days on media supplemented with different phytohormones. Shown are the colony phenotype and the protonema phenotype (inset) with bud (if present). Indicated in the colony image is the occurrence of callus-like buds (CL), buds (B) and gametophores (G) with + if present and – if not present. The blue arrow in the picture indicates a normal bud and blue arrowheads indicate callus-like buds. These annotations have been derived from a larger picture represented by the inset. The bottom line of the colony picture corresponds to 2,3 cm; the bottom line of the inset corresponds to 1 mm.

764-fold; *PpCHK3*, 225-fold; *PpCHK4*, 9,4-fold and *PpRR11*, 198-fold; transgenic line 35S::GFP:PpCHK2 #4-5: *PpCHK1*, 5,7-fold; *PpCHK2*, 334-fold; *PpCHK3*, 244-fold; *PpCHK4*, 6,9-fold and *PpRR11*, 90,4-fold; Figure 24, B).

Effects of different phytohormones on P. patens ectopically expressing PpCHK2

The macroscopic phenotype of the transgenic lines on medium supplied with different phytohormones was also analyzed (Figure 25). The response of the transgenic lines to the application of 1 µM kinetin and isopentenyladenine was no different to the WT. Both formed callus-like buds and gametophores when exposed to kinetin, and callus-like buds upon isopentenyladenine exposure. While the WT failed to form gametophores on medium supplemented with 10 µM kinetin, the knockout and the overexpressing lines still did. This uniform response among the transgenic lines changed when benzyladenine was applied to the medium. The C-terminally fused lines formed callus-like buds and gametophores, whereas the N-terminally fused lines, resembling the WT, remained in the callus-like bud stage. The addition of auxin generally retarded gametophore development, but also induced callus-like bud formation in the transgenic line 35S::PpCHK2:GFP #2-2. The simultaneous application of auxin and cytokinin in turn abolished gametophore formation in all plants under investigation whilst still inducing callus-like buds. The application of ABA led to less protonema growth in the WT and the knockout mutant, while both formed buds and gametophores. The N-terminally fused mutants had an appearance comparable to the WT, whereas the C-terminally fused mutant 35S::PpCHK2:GFP #2-2 formed only buds and the transgenic line 35S::PpCHK2:GFP #2-3 did not form buds at all. A comparable phenotype was observed when benzyladenine was applied in addition to ABA. Mutant 35S::PpCHK2:GFP #2-2 had callus-like buds and mutant 35S::PpCHK2:GFP #2-3 did not form buds of any kind. The transgenic line 35S::GFP:PpCHK2 #4-3 failed to form both buds and gametophores and transgenic line 35S::GFP:PpCHK2 #4-5 formed normal buds and gametophores under these conditions.

Area growth of transgenic lines ectopically expressing PpCHK1 or PpCHK2 in P. patens

In addition to its effects on the macroscopic phenotype of *P. patens* transgenic lines regarding bud and gametophore formation, the phytohormone treatment also affected colony

growth. Area growth was chosen as a parameter for this investigation (a short introduction on how the area growth was calculated will be given in the following). Area growth primarily reflects the growth of *P. patens* protonema. The gametophores grow vertically to the agar surface and are therefore not quantifiable in a photograph from above the agar plate. Despite the lack of the third dimension in this analysis, gametophores that unfolded their leaves above the protonema – thereby masking the underlying protonema – were also regarded as live tissue and taken into account in the investigation.
Additionally to the above mentioned phytohormones, other factors that have been shown to be connected to cytokinin signaling were also analyzed. Mutants were grown on media either deficient in or supplemented with substances affecting a) their hormone status, b) their energy status by altering the C to N ratio (Thelander *et al.,* 2005) or the chloroplast (Reutter *et al.,* 1998) (chloroplast division was shown to be inhibited by ampicillin (Kasten and Reski 1997; Katayama *et al.,* 2003)), and c) the micronutrient status of Ca^{2+} (Saunders 1994; Schumaker and Dietrich 1998; Brenner *et al.,* 2005) and of phosphate (Repp *et al.,* 2004). Osmotic stress was also applied to the plants because an effect of cytokinin and cytokinin receptors on osmotic stress response has been shown in *A. thaliana* (Tran *et al.,* 2010)).

Each plant's area growth was analyzed at three different time points over a period of 30 days (see section 2.5.4.5). Area growth was calculated as the quotient of the initial colony sized (3 days after transfer to the medium) and the actual colony size at the respective time point. The resulting area growth values were plotted for each treatment onto a half-logarithmic scale (plots for all PpCHK1 mutants in the WT background on all media are depicted in the Appendix Figure 4, and plots for all PpCHK2 mutants in the WT background on all media are depicted in the Appendix Figure 5) but comparison of the curves was rather complex. Another parameter for comparison therefore seemed desirable. The area growth curves described an exponential increase in area size and exponential growth can be described using an e-function (for details please refer to section 2.5.4.5). Approximation of the area growth curves was carried out using an e-function and the derived, specific growth constants of each transgenic line are compared in Table 25. Since the approximation did not take into account the sometimes high standard deviations of the area growth data points and the deviation of the area growth curve from the ideal exponential progression, this comparison can only serve to find general trends.

The comparison of the specific growth constants (Table 25) showed a slight growth promoting effect for the generated transgenic lines on the control media (BCD, III and mock treatment) compared to the WT. The application of cytokinin to the growth medium seemed to repress growth compared to the mock treatment and this effect was more pronounced in the transgenic lines, with the exception of transgenic line 35S::PpCHK1:GFP #1N32 at low

Table 25: Specific growth constants inferred from *P. patens* transgenic lines ectopically expressing *PpCHK1* or *PpCHK2* in the WT background are compared to the WTs growth constant. Given is the relative fold change to the WT. The effect of the treatment is indicated by the red (repressed growth) or the blue (enhanced growth) frame of the WT line. If the transgenic line showed an altered growth effect by the treatment, this is indicated with the respective color frame in the individual cell. Color code of the background of the cells indicates the fold change (at the bottom of the table).

Cytokinin receptor	GFP fusion site	Line number	Growth medium																
			BCD	III	mock (DMSO)	Kinetin [1 µM]	Kinetin [10 µM]	BA [10 µM]	Isopentenyl-adenine [10 µM]	NAA [10 µM]	NAA [10 µM], Kinetin [10 µM]	ABA [10 µM]	ABA [10 µM], BA [10 µM]	Ampicillin	Ampicillin, Glc [2%]	Ammonium tartrate	$NaCl_2$	Sorbitol	Calcium deficiency	Phosphate deficiency
PpCHK1	C-terminus	1N32	1,2	1,3	1,1	0,1	0,5	0,5	0,5	2,3	0,6	2,3	1,5	1,3	1,0	43,3	1,2	5,9	2,9	1,2
		1N4	1,4	1,4	1,4	0,5	0,7	0,5	1,1	0,2	1,0	7,3	1,6	2,9	1,0	8,8	9,3	2,5	6,2	0,1
		1N76	1,2	1,1	1,1	0,3	0,5	0,8	0,7	1,8	0,8	0,1	1,2	0,5	0,5	47,3	1,4	6,7	1,2	3,0
	N-terminus	27N20	1,2	1,4	0,9	1,4	1,3	1,5	1,6	4,0	1,4	1,2	2,3	2,0	0,3	65,0	0,2	2,3	0,0	3,5
PpCHK2	C-terminus	2-3	1,9	1,6	1,4	0,6	0, 6	0,2	1,0	8,2	1,2	0,4	1,0	1,6	0,4	80,0	0,2	2,1	9,3	2,9
		2-2	1,4	1,4	1,3	0,5	1,1	0,9	0,9	0,1	0,9	4,2	1,6	0,23	0,5	4,1	0,5	2,7	4,3	0,3
	N-terminus	4-3	1,5	1,4	1,4	0,6	1,3	1,5	1,6	2,9	1,5	4,1	3,0	0,1	1,2	9,1	2,9	0,1	0,1	1,3
		4-5	1,5	1,6	1,4	0,7	1,0	1,1	1,4	7,6	1,2	0,0	2,3	1,9	0,9	49,1	1,1	1,7	2,6	1,5
		WT	1,0	1,0	1,0	1,0	1,0	1,0	1,0	1,0	1,0	1,0	1,0	1,0	1,0	1,0	1,0	1,0	1,0	1,0
		delta	0,9	0,9	0,9	0,1	0,3	0,3	0,4	0,4	0,4	1,7	0,2	2,7	0,9	54,2	1,7	2,6	1,8	2,0
			<1,0		1,0	1,50	3,0		difference (treatment-control) = Δ						repressed growth				enhanced growth	
			quotient (Δ mutant / Δ WT)																	

cytokinin levels. Furthermore the application of auxin to the growth medium seemed to have a mostly growth promoting effect on the transgenic lines, with the exception of transgenic line 35S::GFP:PpCHK2 #4-3, while auxin treatment was slightly growth inhibiting in the WT. The inhibitory effect of auxin seemed to be restored by the simultaneous application of cytokinin and auxin. A similar, balancing effect seemed to be present when ABA and cytokinin were applied simultaneously, whereas the sole application of ABA had diverse effects, sometimes promoting growth and sometimes repressing. The supplementation of ammonium tartrate to the growth medium had strong effects on growth, but was not clearly either promoting or inhibiting. All other treatments exhibited a rather diverse response that did not allow any conclusions on their effect.

3.1.9. Characterization of transgenic lines ectopically expressing *PpCHK1* or *PpCHK2* in *Ppchk1 Ppchk2 P. patens* plants

To investigate and better delineate the roles of PpCHK1 and PpCHK2, both were transformed into the mutant background *Ppchk1 Ppchk2*. The analysis was repeated as described above. The following description will start with transgenic lines generated with GFP fusions to *PpCHK1*.

Phenotypical description of Ppchk1 Ppchk2 P. patens ectopically expressing PpCHK1

Firstly, PCR-based analysis showed all selected lines to be positive for the presence of the construct (see Appendix Figure 3, B). The generation of stable lines with the construct of GFP fused to the C-terminus of the receptor protein yielded various stable lines (shown here: three selected lines), but the construct consisting from N-terminally fused GFP to the receptor generated only one line (35S::GFP:PpCHK1 [*Ppchk1 Ppchk2*], #21-2). In the following, generated transgenic lines will be referenced with the construct and the unique line number, but the mutant background [*Ppchk1 Ppchk2*] will not be given for better readability. All lines were analyzed on their macroscopic phenotype regarding the formation of gametophores (Figure 26 A, upper left quadrant) and the distribution of chloronemal and caulonemal protonema (Figure 26 A, upper right quadrant) as previously explained. For reference, the WT was included as well as the double knockout *Ppchk1 Ppchk2*. After 14 days growing on standard BCD medium, both control strains developed gametophore initials (buds), but neither developed gametophores. This was also true for the C-terminal fusion line 35S::GFP:PpCHK1 #18-3 and the N-terminal fusion line 35S::PpCHK1:GFP #21-2. In contrast, the C-terminal fusion lines 35S::GFP:PpCHK1 #18-2 and 35S::GFP:PpCHK1 #18-8 did not develop gametophores but were forming protonema. A closer look at the protonema

revealed that the C-terminally fused mutants 35S::GFP:PpCHK1 #18-2 and 35S::GFP:PpCHK1 #18-3, as well as the N-terminal fusion line #21-2, formed caulonemal filament that had a brownish color (as has been observed before in the WT (Knoop 1978)) and gave rise to heavily branched chloronema. The transgenic line 35S::GFP:PpCHK1 #18-8 had both cell types: caulonemal protonema in the first and second cell from the tip, and then onwards only chloronemal protonema. All C-terminally fused mutants had irregular shaped protonema cells. The cellular composition of fully developed gametophores were also analyzed, if present (Figure 26 A, lower quadrants). The transgenic lines, with the exception of line 35S::GFP:PpCHK1 #18-8, had round shaped chloroplasts like the WT that seemed, in the case of 35S::GFP:PpCHK1 #18-2 and 35S::GFP:PpCHK1 #18-3, to be less in number while still being the normal size (data not shown for protonema, but also applies to gametophore as shown in (Figure 26 A, lower right quadrants). The transgenic line 35S::GFP:PpCHK1 #18-8 did not form gametophores and exhibited more drop shaped chloroplasts in overall distorted protonema cells. The GFP signal was evident in all C-terminal fusion lines and located in each line to smaller, line shaped patches primarily on the outside of the chloroplasts. No further analysis on the subcellular localization with markers was performed and results should be treated preliminarily. The N-terminally fused line 35S::PpCHK1:GFP #21-2 indicated a GFP signal pattern similar to the one found when *GFP:PpCHK1* was expressed in the WT background, with distributed small speckles over the whole cell but without perinuclear localization.

The transcriptional analysis of the *PpCHK1* overexpresser lines in the background of the *Ppchk1 Ppchk2* mutant indicated a complementation of the *PpCHK1* down-regulation to at least WT levels (compare to Figure 26, B). The transgenic line 35S::GFP:PpCHK1 #18-2 also showed WT-level transcription for all receptors in the analysis, while the *PpRR11* was up-regulated to 6-fold of WT levels. The transgenic line 35S::GFP:PpCHK1 #18-3 indicated a slight up-regulation of the *PpCHK3* and *PpCHK4* transcripts to 3,8- and 2,7-fold respectively, whereas the *PpRR11* was elevated to 4,7-fold of WT levels. Based on the transcriptional analysis, the transgenic line 35S::GFP:PpCHK1 #18-8 exhibits the strongest up-regulation of the C-terminally fused lines (*PpCHK1*, 3,3-fold; *PpCHK2*, 3,2-fold; *PpCHK3*, 11,8-fold; *PpCHK4*, 12,8-fold and *PpRRA11*, 30,9-fold) and also had the most pronounced phenotype, namely the lack of gametophores and distorted protonema cells. The N-terminal fusion line 35S::PpCHK1:GFP #21-2 exhibited a high up-regulation of the *PpCHK1* transcript, but this up-regulation only resulted in a low up-regulation of the other components under investigation compared to the up-regulation of 111-fold of WT levels (*PpCHK2*, 5,3-fold; *PpCHK3*, 10,2-fold; *PpCHK4*, 3,9-fold and *PpRRA11*, 3,4-fold). Based on these results and the results from the receptor expression in the WT background, it seems that the C-terminally fused transcript of *PpCHK1* is only limitedly inducible by the insertion of an overexpression

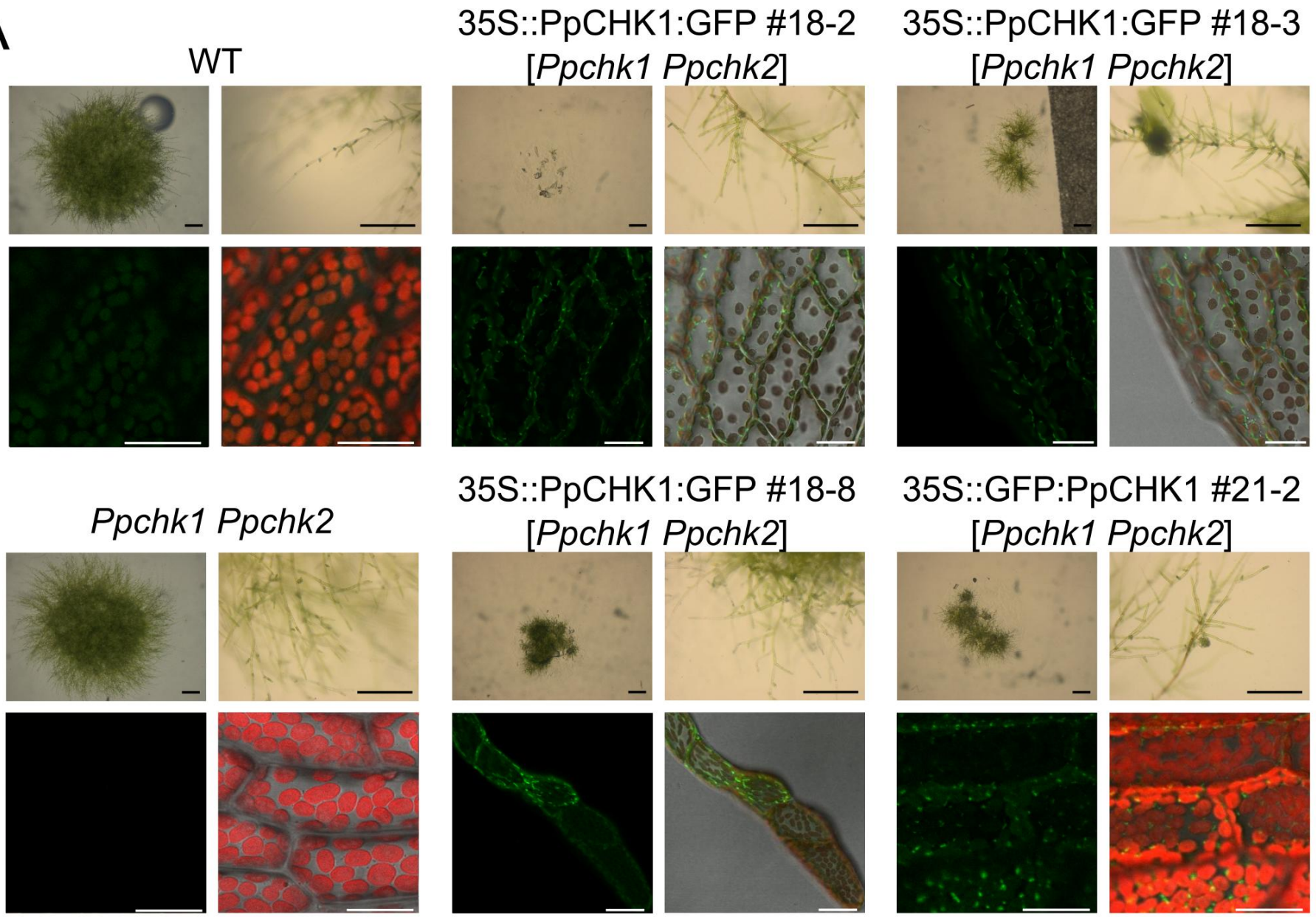
A
WT
35S::PpCHK1:GFP #18-2
[Ppchk1 Ppchk2]
35S::PpCHK1:GFP #18-3
[Ppchk1 Ppchk2]
Ppchk1 Ppchk2
35S::PpCHK1:GFP #18-8
[Ppchk1 Ppchk2]
35S::GFP:PpCHK1 #21-2
[Ppchk1 Ppchk2]

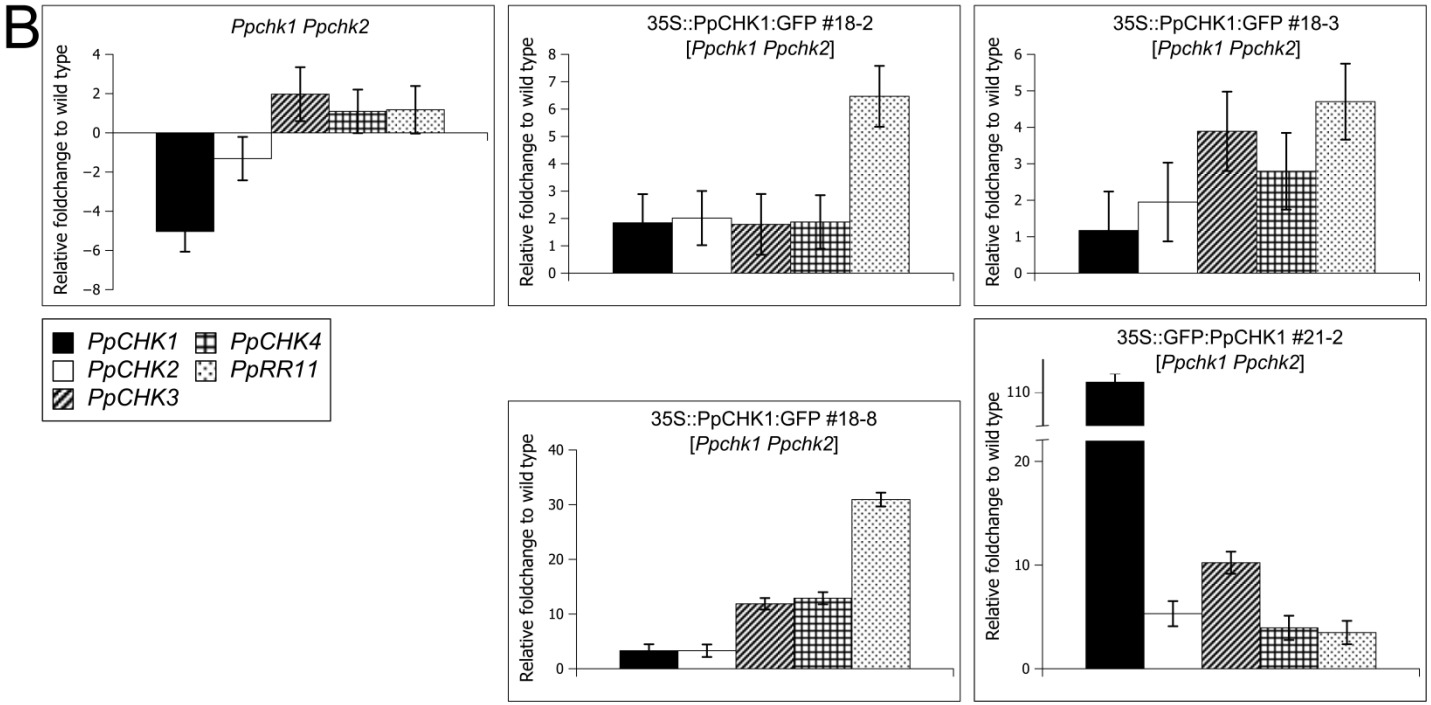

Figure 26: ***PpCHK1*** **ectopically expressed in** ***P. patens [Ppchk1 Ppchk2]*****. A)** Phenotypical description of the analyzed lines. Upper pictures show growth on BCD medium after 14 days. Lower pictures are taken from plants in long-term culture on BCD plates. Scale bars: upper left quadrant, 1mm; upper right quadrant, 0,5 mm; lower quadrants, 25 µm. Lower pictures indicate GFP signal (left) and the overlay of GFP, autofluorescence of the chloroplasts and the bright field image (right). **B)** qRT-PCR analysis of genes associated with cytokinin signaling in the respective transgenic line. Protonema and gametophore tissue was harvested from continuous cultures, RNA was isolated and qRT-PCR was carried out as described in sections 2.5.1 and 2.2.1 respectively. WT levels were set to 1 and results are given as fold change compared to WT.

construct. This might be due to potentially existing tight regulatory networks that keep the cytokinin signaling system balanced.

For further information about the transgenic lines, they were analyzed after 30 days on media supplemented with different phytohormones (detailed explanation see above). The overexpression of fusion constructs of *GFP* to the C-terminus of *PpCHK1* in the WT background led to the formation of callus-like buds when the medium was supplemented with cytokinin (Figure 23). A striking difference was found concerning the transgenic line 35S::GFP:PpCHK1 #18-8, which did not form buds upon cytokinin application and seemed to be cytokinin insensitive. For the other C-terminally fused *PpCHK1* transgenic lines in the *Ppchk1 Ppchk2* background the formation of callus-like buds was limited to isopentenyladenine- and benzyladenine-supplemented medium which then gave rise to gametophores, while kinetin-supplemented medium led to the formation of normal buds that also gave rise to gametophores (Figure 27). The application of 1 µM kinetin to the medium of the 35S::PpCHK1:GFP #21-2 N-terminally fused line had no effect, and the addition of 10 µM kinetin induced normal budding and subsequent gametophore development. Normal budding and gametophore development was also the result of applying isopentenyladenine to the growth medium, whereas the addition of benzyladenine did not induce bud formation in this transgenic line (Figure 27). Taken together it seems that transgenic line 35S::PpCHK1:GFP #21-2 is less sensitive towards cytokinin.

The second phytohormone in the analysis, auxin, led to less gametophores compared to the mock control when analyzed in the WT background (Figure 23). The application of auxin (10 µM NAA) to the mutants in the knockout background also caused less budding and gametophores in the transgenic line 35S::GFP:PpCHK1 #18-2 and 35S::PpCHK1:GFP #21-2, while the mutants 35S::GFP:PpCHK1 #18-3 and 35S::GFP:PpCHK1 #18-8 were without buds and gametophores entirely (Figure 27). When auxin and cytokinin (NAA and kinetin) were applied to the mutant's medium, 35S::GFP:PpCHK1 #18-2 and 35S::GFP:PpCHK1 #18-3 formed callus-like buds as well as normal buds and gametophores, while 35S::GFP:PpCHK1 #18-8 retained its bare protonema growth observed under both control and cytokinin treatment conditions. The transgenic line 35S::PpCHK1:GFP #21-2 did not form buds or gametophores (Figure 27). The application of ABA to the medium resulted in bud formation in the one mutant (35S::GFP:PpCHK1 #18-8) that had so far not formed buds even when supplemented with cytokinin or auxin (or both). Budding and gametophore formation were also evident in the other C-terminally fused lines, while the N-terminally fused line 35S::PpCHK1:GFP #21-2 did not leave the protonema stage (Figure 27). Collective application of ABA and cytokinin (benzyladenine) retained the ABA pattern, where the C-terminally fused lines had WT-comparable dense protonemal growth and the N-terminal fusion line eventually died (Figure 27).

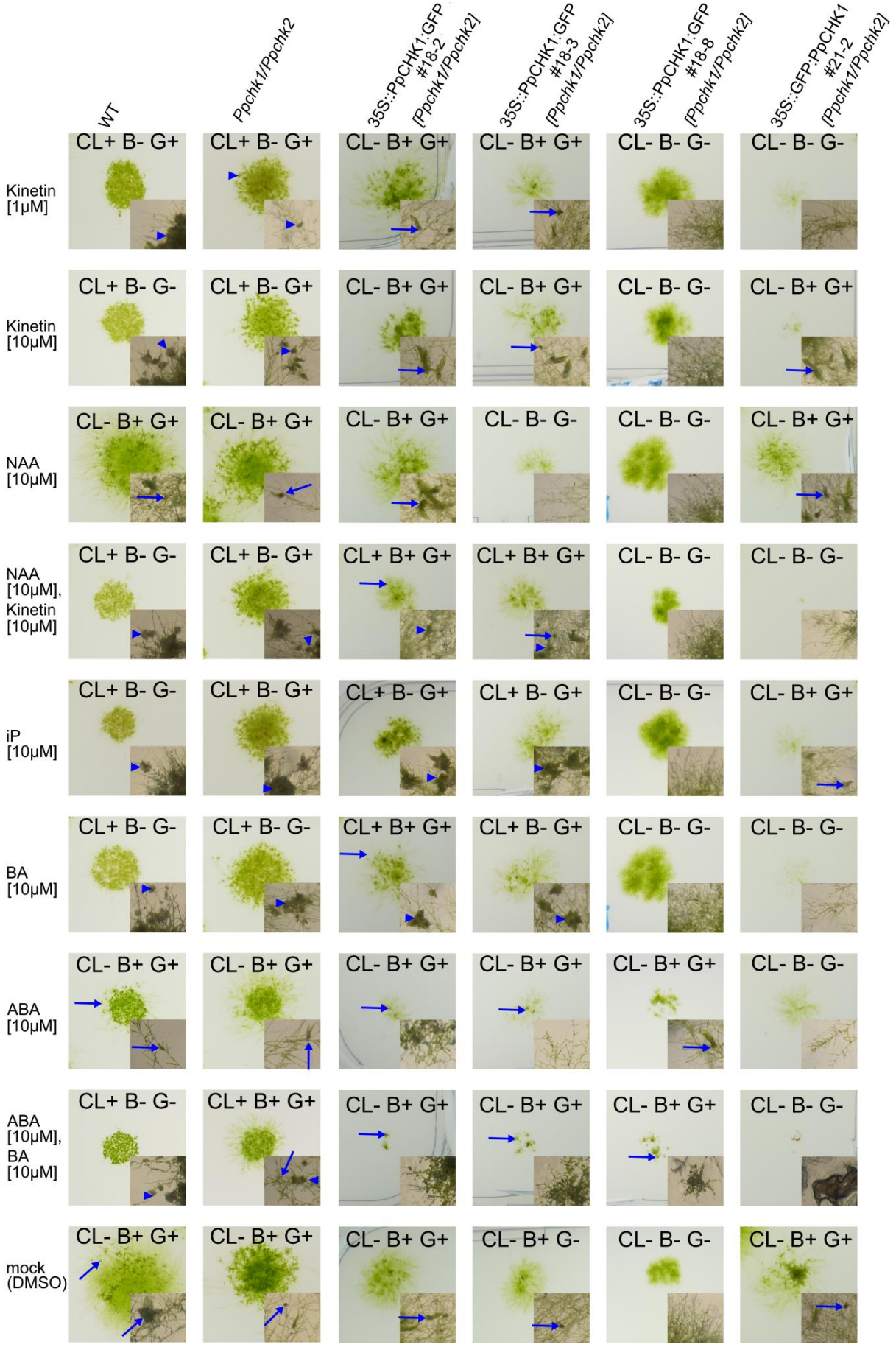
WT
Ppchk1/Ppchk2
35S::PpCHK1:GFP #18-2 [Ppchk1/Ppchk2]
35S::PpCHK1:GFP #18-3 [Ppchk1/Ppchk2]
35S::PpCHK1:GFP #18-8 [Ppchk1/Ppchk2]
35S::GFP:PpCHK1 #21-2 [Ppchk1/Ppchk2]
Kinetin [1μM]
CL+ B- G+
CL+ B- G+
CL- B+ G+
CL- B+ G+
CL- B- G-
CL- B- G-
Kinetin [10μM]
CL+ B- G-
CL+ B- G+
CL- B+ G+
CL- B+ G+
CL- B- G-
CL- B+ G+
NAA [10μM]
CL- B+ G+
CL- B+ G+
CL- B+ G+
CL- B- G-
CL- B- G-
CL- B+ G+
NAA [10μM], Kinetin [10μM]
CL+ B- G-
CL+ B- G+
CL+ B+ G+
CL+ B+ G+
CL- B- G-
CL- B- G-
iP [10μM]
CL+ B- G-
CL+ B- G+
CL+ B- G+
CL+ B- G+
CL- B- G-
CL- B+ G+
BA [10μM]
CL+ B- G-
CL+ B- G-
CL+ B+ G+
CL+ B- G+
CL- B- G-
CL- B- G-
ABA [10μM]
CL- B+ G+
CL- B+ G+
CL- B+ G+
CL- B+ G+
CL- B+ G+
CL- B- G-
ABA [10μM], BA [10μM]
CL+ B- G-
CL+ B+ G+
CL- B+ G+
CL- B+ G+
CL- B+ G+
CL- B- G-
mock (DMSO)
CL- B+ G+
CL- B+ G+
CL- B+ G+
CL- B+ G-
CL- B- G-
CL- B+ G+

Figure 27: Bud and gametophore formation in mutant *P. patens* lines *[Ppchk1 Ppchk2]* ectopically expressing *PpCHK1* fused to GFP, Transgenic lines were grown for 30 days on media supplemented with different phytohormones. Shown are the colony phenotype and the protonema phenotype (inset) with bud (if present). Indicated in the colony image is the occurrence of callus-like buds (CL), buds (B) and gametophores (G) with + if present and – if not present. The blue arrow in the picture indicates a normal bud and blue arrowheads indicate callus-like buds. These annotations have been derived from a larger picture represented by the inset. The bottom line of the colony picture corresponds to 2,3 cm; the bottom line of the inset corresponds to 1 mm.

Phenotypical description of Ppchk1 Ppchk2 P. patens ectopically expressing PpCHK2

The transgenic lines generated from *PpCHK2* constructs, fused to *GFP* either on the C-terminal or on the N-terminal side of the receptor in the background of the *Ppchk1 Ppchk2* mutant, were analyzed for the presence of the construct in the genomic DNA by PCR (Appendix Figure 3). The phenotypical description of the transgenic lines grown on standard BCD medium was strikingly dependent on the fusion orientation. C-terminally fused transgenic lines showed protonema growth with slightly enhanced branching and developed gametophores, while N-terminally fused transgenic lines grew a dense protonema, with no indication of gametophore formation (Figure 28 A, upper left quadrant). More detailed investigation of protonema from C-terminally fused transgenic lines did not reveal obvious changes compared to WT. The N-terminally fused transgenic lines, in turn, all had distorted, malformed protonema cells that irregularly branched and curved (Figure 28 B, upper right quadrant). Because of the deformation it was not possible to clearly distinguish caulonemal and chloronemal cells. All transgenic lines had a clear GFP signal that was potentially located to the plasma membrane region, copying the potential subcellular localization of PpCHK2 found in the *P. patens* WT background and partially co-localized with the autofluorescence of the chloroplasts in all transgenic lines. No further analysis was undertaken to elaborate the observed patterns, and subcellular localization should be regarded as preliminary. Furthermore, abnormal chloroplast shapes were found in all N-terminally fused transgenic lines.

The transcriptional regulation of the above described PpCHK2 mutants in the *Ppchk1 Ppchk2* background broke the previously anticipated moderate regulation pattern of the C-terminally fused lines by displaying a significant up-regulation of the C-terminally fused *PpCHK2* transcript to 21-fold and 39-fold in the transgenic lines 35S::PpCHK2:GFP #19-1 and 35S::PpCHK2:GFP #19-3, respectively (Figure 28, B). This up-regulation (*PpCHK3*, 45-fold; *PpCHK4*, 4-fold; *PpRR11*, 23-fold of WT levels in the transgenic line 35S::PpCHK2:GFP #19-1 and *PpCHK3*, 142-fold; *PpCHK4*, 7,1-fold; *PpRR11*, 32,7-fold of WT levels in the transgenic line 35S::PpCHK2:GFP #19-3; Figure 28, B) was accompanied by an insignificant change in the *PpCHK1* transcript but extensive up-regulation of *PpCHK3*, high up-regulation of *PpRR11* and moderate up-regulation of *PpCHK4* in both transgenic lines. Related patterns were also found in the N-terminally fused transgenic lines 35S::GFP:PpCHK2 #22-3 and

35S::GFP:PpCHK2 #22-8, although the *PpCHK2* transcript was induced to much higher levels (834-fold and 56-fold of WT levels respectively) and the transcript of *PpCHK3* was up-regulated to 46-fold and 6,1-fold (Figure 28, B). According to the pattern observed in the C-terminally fused lines, the *PpCHK1* transcript was expressed at levels not significantly different from the WT in the transgenic lines 35S::GFP:PpCHK2 #22-3 and 35S::GFP:PpCHK2 #22-8 and unaffected in 35S::GFP:PpCHK2 #22-9. The transcript of the potential cytokinin receptor *PpCHK4* was up-regulated to 3,9-fold in the 35S::GFP:PpCHK2 #22-3 mutant and not regulated beyond threshold limits in the 35S::GFP:PpCHK2 mutants #22-8 and #22-9. The potential signaling output indicator *PpRR11* was induced in all transgenic lines, to 107-fold, 19-fold and 24-fold of WT levels in the N-terminally fused transgenic lines 35S::GFP:PpCHK2 #22-3, 35S::GFP:PpCHK2 #22-8 and 35S::GFP:PpCHK2 #22-9, respectively (Figure 28, B). The transgenic line 35S::GFP:PpCHK2 #22-9 had a distinguished transcriptional pattern from the other two N-terminally fused transgenic lines with regard to *PpCHK1* and *PpCHK3* – both transcripts were down-regulated to 5-fold and 16-fold below WT levels respectively – while *PpCHK2* was up-regulated to 113-fold of WT levels (Figure 28, B). The regulation pattern of transgenic line 35S::GFP:PpCHK2 #22-9 to transcriptional profiles of the overexpression in the WT background, indicates a resemblance to resembles the transcriptional profiles of the C-terminally fused transgenic lines 35S::PpCHK2:GFP #2-2 and (to an even greater extent) 35S::PpCHK2:GFP #2-3 (Figure 24, C).

Effects of different phytohormones on Ppchk1 Ppchk2 P. patens ectopically expressing PpCHK2

The analysis of gametophore and bud formation after 30 days revealed that transgenic lines with integrated N-terminally fused PpCHK2 receptor constructs always maintained their protonemal growth and failed to form buds (and therefore also gametophores) under any hormone treatment. The applied hormones seemed to have an effect on protonema growth, altering their density, but these alterations were beyond the scope of this analysis and deserve further investigation (Figure 29). Once again, all N-terminally fused transgenic lines failed to form buds upon cytokinin treatment, a fact already implied by the overexpression of *PpCHK1* in the double knockout mutant in the C-terminally fused transgenic line 35S::GFP:PpCHK1 #18-8 under cytokinin and auxin treatment and the N-terminal fusion line 35S::PpCHK1:GFP #21-2 under low (1 µM) kinetin and benzyladenine treatment (Figure 27). While overexpression of *PpCHK1* indicated this feature in both fusion orientations, *GFP* fused to the C-terminus of *PpCHK2* did not change the sensitivity of the mutants to cytokinin treatment. The application of kinetin to the growth medium indicated that the C-terminally fused transgenic lines 35S::PpCHK2:GFP #19-1 and 35S::PpCHK2:GFP #19-3 are less

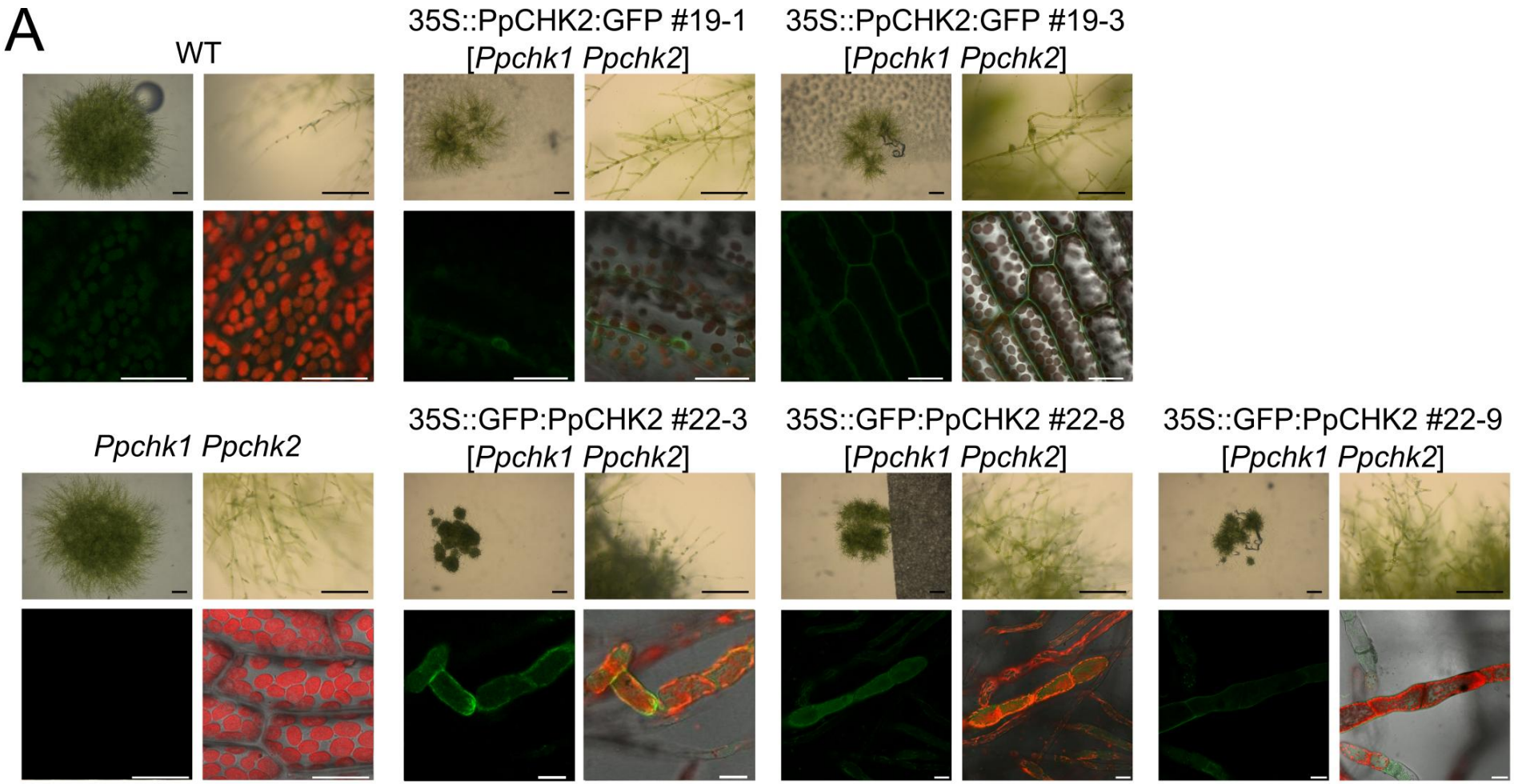
A
WT
35S::PpCHK2:GFP #19-1
[Ppchk1 Ppchk2]
35S::PpCHK2:GFP #19-3
[Ppchk1 Ppchk2]
Ppchk1 Ppchk2
35S::GFP:PpCHK2 #22-3
[Ppchk1 Ppchk2]
35S::GFP:PpCHK2 #22-8
[Ppchk1 Ppchk2]
35S::GFP:PpCHK2 #22-9
[Ppchk1 Ppchk2]

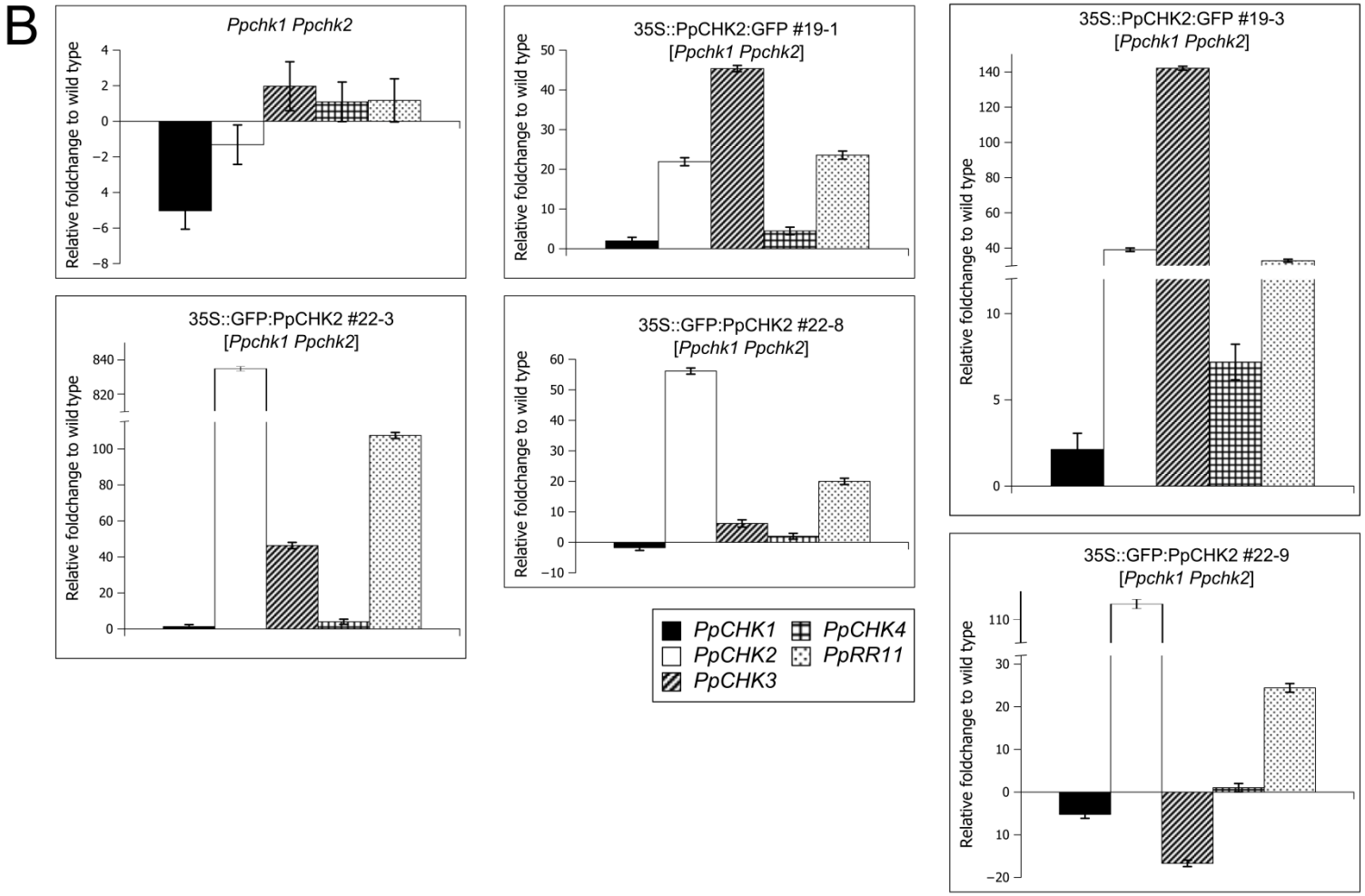

Figure 28: ***PpCHK2*** **ectopically expressed in** ***P. patens [Ppchk1 Ppchk2]*****. A)** Phenotypical description of the analyzed lines. Upper pictures show growth on BCD medium after 14days. Left quadrant, scale bar 1mm; right quadrant, scale bar 0,5mm. Lower pictures indicate GFP signal (left) and the overlay (right). **B)** qRT-PCR analysis of genes associated with cytokinin signaling in the respective transgenic line. Protonema and gametophore tissue was harvested from continuous cultures, RNA was isolated and qRT-PCR was carried out as described in section 2.5.1 and 2.2.1 respectively. WT levels were set to 1 and results are given as fold change compared to WT.

susceptible to kinetin treatment. Transgenic line 35S::PpCHK2:GFP #19-1 did not form callus-like buds at all, while transgenic line 35S::PpCHK2:GFP #19-3 formed callus-like buds and normal buds and gametophores after treatment with a high concentration of kinetin (Figure 29). The application of isopentenyladenine and benzyladenine clearly induced callus-like bud formation and gametophore formation in the C-terminal fusion lines, of which gametophore formation is impaired in the WT. When auxin (NAA) was added to the growth medium of the C-terminally fused transgenic lines, less gametophores were formed. The simultaneous application of kinetin and auxin induced bud formation in both the C-terminally fused transgenic lines, but only allowed gametophore formation in the transgenic line 35S::PpCHK2:GFP #19-3, which previously formed callus-like buds when treated with 10 µM kinetin. Surprisingly this very mutant was affected by the application of ABA, which suppressed bud and gametophore formation, while transgenic line 35S::PpCHK2:GFP #19-1 developed normal buds and gametophores. The simultaneous application of ABA and benzyladenine showed reduced cytokinin sensitivity by forming normal buds in the transgenic line 35S::PpCHK2:GFP #19-3 and a complete loss of bud formation in the transgenic line 35S::PpCHK2:GFP #19-1.

Figure 29: Bud and gametophore formation in mutant *P. patens* lines *[Ppchk1 Ppchk2]* ectopically expressing *PpCHK2* fused to GFP, Transgenic lines were grown for 30 days on media supplemented with different phytohormones. Shown are the colony phenotype and the protonema phenotype (inset) with bud (if present). Indicated in the colony image is the occurrence of callus-like buds (CL), buds (B) and gametophores (G) with + if present and - if not present. The blue arrow in the picture indicates a normal bud and blue arrowheads indicate callus-like buds. These annotations have been derived from a larger picture represented by the inset. The bottom line of the colony picture corresponds to 2,3 cm; the bottom line of the inset corresponds to 1 mm.

Area growth of transgenic lines ectopically expressing PpCHK1 or PpCHK2 in P. patens

Analogous to the analysis of the overexpressing transgenic lines in the WT background, the growth assay (see section 2.5.4.5 for detailed description) was conducted to investigate the transgenic lines in the double knockout *Ppchk1 Ppchk2* background. Mutants were grown on medium with an altered supply of a) phytohormones, b) carbon, nitrate or substances affecting the chloroplast, and c) the micronutrient Ca^{2+} and phosphate, as well as d) applying osmotic stress to the plants. Area growth was analyzed at three different time points over a period of 30 days. The resulting area growth values were plotted for each treatment onto a half-logarithmic scale (plots for all PpCHK1 mutants in the double knockout *Ppchk1 Ppchk2* background on all media are depicted in the Appendix Figure 4 and plots for all PpCHK2 mutants in the double knockout *Ppchk1 Ppchk2* background on all media are depicted in the Appendix Figure 7) but for comparison specific growth constants of each transgenic line are compared in Table 26. As before, this comparison can only serve to find general trends.
The comparison of the specific growth constants (Table 26) showed, as seen in the WT background, a slight growth promoting effect for the transgenic lines compared to the double knockout (*Ppchk1 Ppchk2*) background. A clear inhibiting effect of cytokinin was not evident from the comparison of the individual growth constants; in some lines, cytokinin treatment was even seen to have a growth promoting effect. A pattern regarding the transgenic line or the type of cytokinin could not be found. Further treatments were also inconclusive, with the exception of the simultaneous application of auxin and cytokinin and ABA and cytokinin. As with the double knockout mutant background, both treatments caused uniform growth repression. This was especially pronounced in the ABA and cytokinin treatment. It should be noted that the WT plants grown on ABA and cytokinin medium showed a comparable regulation to the double knockout background.

Table 26: Specific growth constants inferred from *P. patens* transgenic lines ectopically expressing *PpCHK1* or *PpCHK2* in the double knockout *Ppchk1 Ppchk2* background are compared to the double knockouts *Ppchk1 Ppchk2* growth constant. Given is the relative fold change to the double knockout *Ppchk1 Ppchk2*. The effect of the treatment is indicated by the red (repressed growth) or the blue (enhanced growth) frame of the double knockout *Ppchk1 Ppchk2* line. If the transgenic line showed an altered growth effect by the treatment, this is indicated with the respective color frame in the individual cell. Color code of the background of the cells indicates the fold change (at the bottom of the table).

Cytokinin receptor	GFP fusion site	Line number	Growth medium																	
			BCD	III	mock (DMSO)	Kinetin [1 µM]	Kinetin [10 µM]	BA [10 µM]	Isopentenyl-adenine [10 µM]	NAA [10 µM]	NAA [10 µM], Kinetin [10 µM]	ABA [10 µM]	ABA [10 µM], BA [10 µM]	Ampicillin	Ampicillin, Glc 2%	Ammonium tartrate	$NaCl_2$	Sorbitol	Calcium deficiency	Phosphate deficiency
PpCHK1	C-terminus	18-3	1,5	1,6	1,5	1,0	0,9	0,3	1,0	5,6	0,0	2,4	5,3	1,5	2,70	0,3	1,5	1,6	1,4	1,7
		18-2	1,7	1,5	1,8	1,0	1,3	0,6	1,4	1,2	0,9	2,9	9,7	0,2	6,0	0,3	0,1	1,3	1,3	1,1
		18-8	1,4	1,4	1,3	1,3	0,7	0,1	0,8	1,3	0,2	2,8	8,1	0,5	0,3	0,3	0,2	0,8	2,9	1,0
	N-terminus	21-2	1,6	1,7	1,6	3,6	2,6	0,7	1,0	3,0	5,0	0,8	15,9	0,4	2,3	0,7	0,6	2,1	0,2	0,1
PpCHK2	C-terminus	19-1	1,5	1,5	1,8	1,7	1,7	1,3	1,6	0,4	1,2	3,2	7,7	2,0	2,1	0,7	2,1	1,4	0,6	1,7
		19-3	1,5	1,5	1,8	0,6	2,0	3,1	2,1	11,1	1,0	2,3	5,9	1,4	3,1	0,4	1,8	1,9	0,4	1,2
	N-terminus	22-3	1,0	0,9	1,0	0,2	1,0	0,2	1,3	3,9	0,8	0,8	6,2	0,1	0,6	0,7	0,6	0,2	0,6	1,1
		22-8	1,1	1,2	1,2	1,3	0,3	0,0	0,7	3,0	0,0	2,0	6,6	0,3	0,9	1,1	3,0	1,2	3,2	2,6
		22-9	1,2	1,2	1,1	2,1	0,0	2,4	0,1	8,0	0,3	0,6	5,6	0,8	5,9	0,1	2,0	1,3	0,9	0,3
Ppchk1 Ppchk2			1,0	1,0	1,0	1,0	1,0	1,0	1,0	1,0	1,0	1,0	1,0	1,0	1,0	1,0	1,0	1,0	1,0	1,0
WT/(*Ppchk1 Ppchk2*)			1,1	1,1	1,2	9,5	3,2	2,9	2,3	2,2	2,3	0,6	5,2	0,4	1,1	0,0	0,6	0,4	0,6	0,5

<1, 0 | 1, 0 | 1,5 | 3,0 | difference (treatment - control) = Δ | repressed growth | enhanced growth

quotient (Δ mutant / Δ *Ppchk1 Ppchk2*)

3.2. Evolution of the cytokinin circuitry

The cytokinin signaling system, the formation and the depletion of the signaling molecule cytokinin is best understood in the model plant *A. thaliana*, although other plants have contributed to current understanding (Hellmann *et al.,* 2010). Despite the addition of details from different plant species, our knowledge about the origin of this signaling system is still limited. That is why in the second part of this project the evolution of the cytokinin signaling system was investigated. During the course of the project, further studies about the evolution of the cytokinin signaling system became available. Pils and Heyl published a bioinformatic analysis of the core components of the cytokinin signaling pathway in published chlorophyte, bryophyte and angiosperm genomes, investigating their occurrence and their phylogeny (Pils and Heyl 2009). Their central conclusion was that cytokinin receptors are found only in the land plant lineage and first occurred in the last common ancestor of angiosperms and the moss *P. patens*, the two of which diverged roughly 400 MYA. Other components such as type-A RRs (RRAs) were limited to the land plant lineage, and type-B RRs (RRBs) were present in all organisms investigated. The type-C RRs (RRCs) formed a clade well distinguished from the group of RRAs and RRBs. The group of RRCs was composed of many non-canonical (lacking the canonical his) RRCs. Hence, this clade was regarded as the ancient RRs (Pils and Heyl 2009).

3.2.1. Phylogenetic analysis of protein domains of cytokinin signaling components

Given the occurrence and the phylogeny of the different components of the cytokinin signaling system (Pils and Heyl 2009), the next question that arose was how those components formed in the first place. Proteins are made from subunits – protein domains – and it is well known that the domain composition of a protein may change during evolution (Vogel *et al.,* 2004a; Alm *et al.,* 2006). Hence the domain composition of a protein does not only influence the structure and the function of the protein, but is also its evolutionary footprint (Vogel *et al.,* 2004a). One model that describes the formation of new pathways is the 'toolbox' model, where the inventor organism first has to incorporate all necessary 'tools' (protein domains) before a pathway may be brought into being (Maslov *et al.,* 2009). Accordingly, the following analysis investigates the phylogenetic relationship of protein domains that are involved in cytokinin signaling – that is, those that are found in cytokinin signaling components. Another advantage of the domain-based approach was that EST data, specifically charophyte EST data, could be incorporated into the analysis to narrow the gap of genome data from early diverging algae.

A dataset was assembled comprising of EST from three charophyte algae, genome and EST data from 12 chlorophyte algae, eight land plant genomes, 11 bacterial genomes and genome and EST data for 13 unicellular eukaryotes (further information about the dataset may be found in Table 23 and section 9.1). It has been suggested that the TCS was brought into plants during the first endosymbiosis (Frebort *et al.,* 2011; Spichal 2012). Even though no cytokinin signaling-related genes were found in cyanobacteria, recent results on the phylogenetic distribution of cytokinin oxidases/dehydrogenases (*CKX*) genes have discovered a related gene in a cyanobacterium, indicating a possible origin of cytokinin metabolism genes via primary endosymbiosis (Frebort *et al.,* 2011). Therefore, selected cyanobacteria and bacteria genomes of the different divisions were also included in the dataset. Furthermore, it has been reported that the slime mold *Dictyostelium discoideum* encodes a histidine kinase containing a CHASE domain in its genome (*DhkA*) (Mougel and Zhulin 2001). The function of this receptor is involved in sporulation (Wang *et al.,* 1999) and sporulation is triggered by cytokinin addition. Therefore *D. discoideum* was also included in the dataset. The resulting dataset was analyzed in its entirety for the occurrence of the relevant domains from the cytokinin signaling pathway. Additionally, since the occurrence of *CKX* genes in cyanobacteria also added information to the evolutionary history of the cytokinin system, other domains related to cytokinin metabolism (from IPT- and LOG-proteins of cytokinin anabolism) were also included in the analysis.

3.2.2. Phylogenetic analysis of receptor domains reveals new clade of potential cytokinin receptors and indicates algal origin of the cytokinin signaling system

The first domain investigated was the CHASE domain, which is part of the cytokinin sensing receptor in *A. thaliana* and located at the N-terminus of the protein. The phylogenetic tree of all CHASE domains found in the dataset showed a clade containing well known cytokinin receptors from angiosperms, and *S. moellendorfii* and *P. patens* (Figure 30). Proteins in this clade will be referred to as classical cytokinin receptors. Surprisingly, this clade had a sister clade of eight *P. patens* CHASE domains and one *M. polymorpha* CHASE domain (see Figure 30). To assess whether these proteins were pseudogenes, EST evidence of the respective protein was analyzed in the cosmoss database[4]. Seven of the eight genes were actively transcribed and this clade was regarded as biologically relevant (see Figure 30). Furthermore, the phylogenetic tree consisted of four chlorophyte, two cyanobacterial and two *D. discoideum* CHASE domains. In the next step, residues of the CHASE domain, known to have a function in cytokinin binding (Heyl *et al.,* 2007), were analyzed for their conservation (Figure 30, 3). While the clade including the classical cytokinin receptors showed a high

[4] www.cosmoss.org

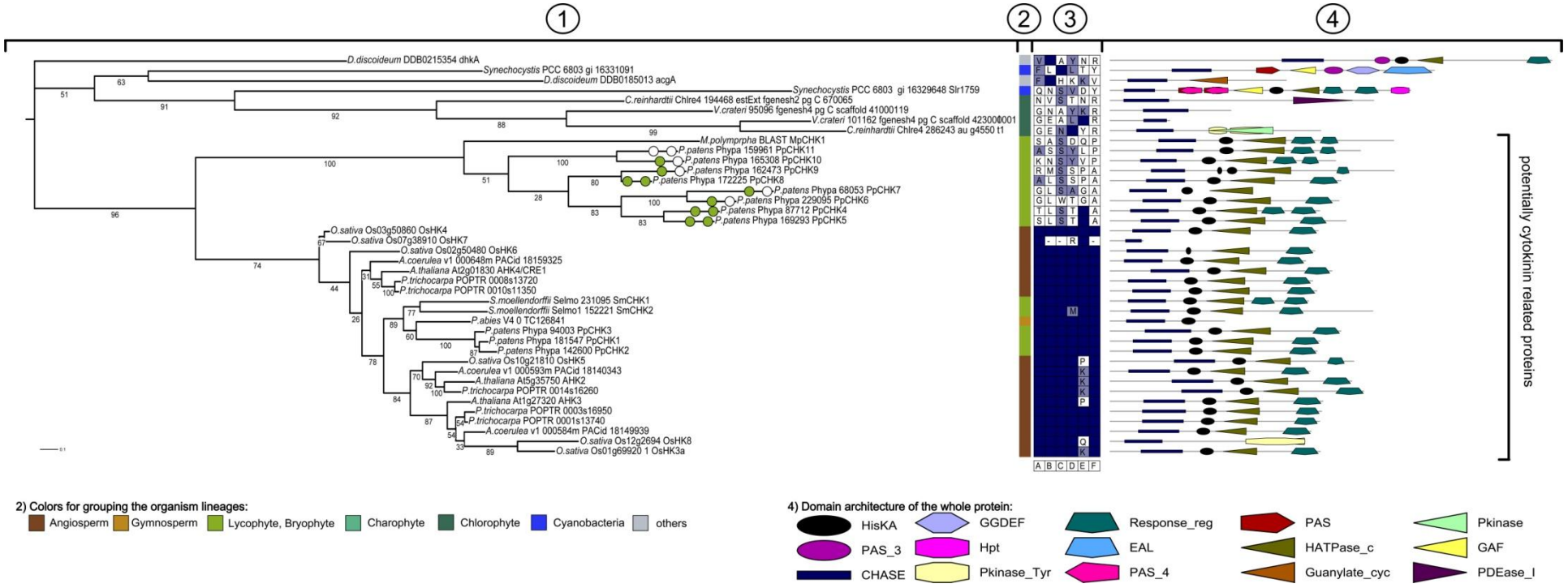

Figure 30: The phylogenetic tree of CHASE domains reveals a new subfamily of potential plant cytokinin receptors. (1) The Cyclase/ Histidine kinase Associated Sensory Extracellular (CHASE) domain (PF03924) sequences from all organisms under investigation were aligned (using MAFFT) and a phylogenetic tree using maximum likelihood was inferred using RAxML (for details see Material and Methods section 2.6.2). Circles on the branches of the phylogenetic tree indicate EST evidence. Open circle, no evidence; green circle, EST evidence. The circle toward the branch end indicates EST evidence from *F. hygrometica* and the circle towards the root indicates *P. patens* EST evidence. **(2)** Organism lineage color code **(3)** Conservation of amino acids involved in cytokinin binding in the CHASE domain (Heyl *et al.,* 2007). Dark blue shows identity to the reference protein AHK4, light blue marks conservative substitution, white boxes symbolize no conservation related to the respective position in the CHASE sequence of AHK4. **(4)** Domain architecture of the whole respective protein. Protein domains: Abbreviations of the domains are according to the Pfam-database (http://pfam.sanger.ac.uk): HisKA, PF00512; GGDEF, PF00990; Response_reg, PF00027; PAS, PF00989; Pkinase, PF00069; PAS 3, PF08447; Hpt, PF01627; EAL, PF00563; HATPase c, PF02518; GAF, PF01590; CHASE, PF03924; Pkinase Tyr, PF07714; PAS 4, PF08448; Guanylate_cyc, PF00211; PDEase I, PF00233.

degree of conservation compared to AHK4, the amino acid sequence of the new clade of bryophyte receptors is more divergent at those positions. A similar conservation pattern was found when amino acids found to be important for the structure or the binding to cytokinin (Hothorn*, et al.* 2011) were analyzed (Appendix Figure 8). However, the divergence of these residues was in a range comparable to the other CHASE domains from *Chlorophytes*, cyanobacteria, and of slime mold origin. Next, the analysis of the domain composition of each whole respective protein revealed a common pattern: all land plant CHASE domains were part of proteins whose domain architecture resembled the classical cytokinin receptors known from *A. thaliana* (see section 3.2.2), with the exception of one rice protein (CHARK). More information about CHARK has been reported before (Han *et al.,* 2004). The domain architecture of proteins from the chlorophyte, cyanobacterial or slime mold clades indicated that multiple domains had been added or changed compared to the classical cytokinin receptors. In some cases only one domain was identified and it is possible that these represent only fragments of proteins due to poor annotation. The similarity between the domain architecture of the protein and the phylogenetic tree of the CHASE domain shows that the evolutionary footprint of the protein (Vogel *et al.,* 2004a) is not limited to the domain architecture of the CHASE domain-containing proteins in the dataset, but extends into the sequence of the CHASE domain itself.

To test whether sequence conservation gives a result analogous to the domain architecture, other domains that were part of the cytokinin receptors were also analyzed and phylogenetic trees were calculated (for details please refer to section 2.6.2). The resulting phylogenetic trees of the Histidine kinase domain, the HATPase domain and the RR domain were evaluated and clades containing the cytokinin receptors were marked (for details please refer to section 2.6.4). Furthermore, clades containing known signaling proteins from *A. thaliana* were marked, including CKI1 and CKI2, the osmosensor AHK1, phytochromes, and ethylene receptors (Hutchison and Kieber 2002). These clades will be further referred to as functional clades. Subtrees including these functional clades are depicted in Figure 31.

The comparison of the functional clades derived from each domain further corroborated that the phylogenetic tree of the single domains corresponds to the domain architecture of the whole protein. All functional clades of the compared domains were recapitulated by each domain independently (compare Figure 31, D, outer three color stripes), with the exception of one protein in the functional clades of CKI1 and AHK1. Surprisingly, the phylogenetic tree of the RR domain (Figure 31, D) showed evidence of two charophyte RR domains in the functional clade of the cytokinin receptors. These RR domains suggested for the first time the potential existence of CHASE domain-containing receptors in Charophytes. Whether these

A: Histidinkinase domain

B: HATPase domain

C: Response regulator domain

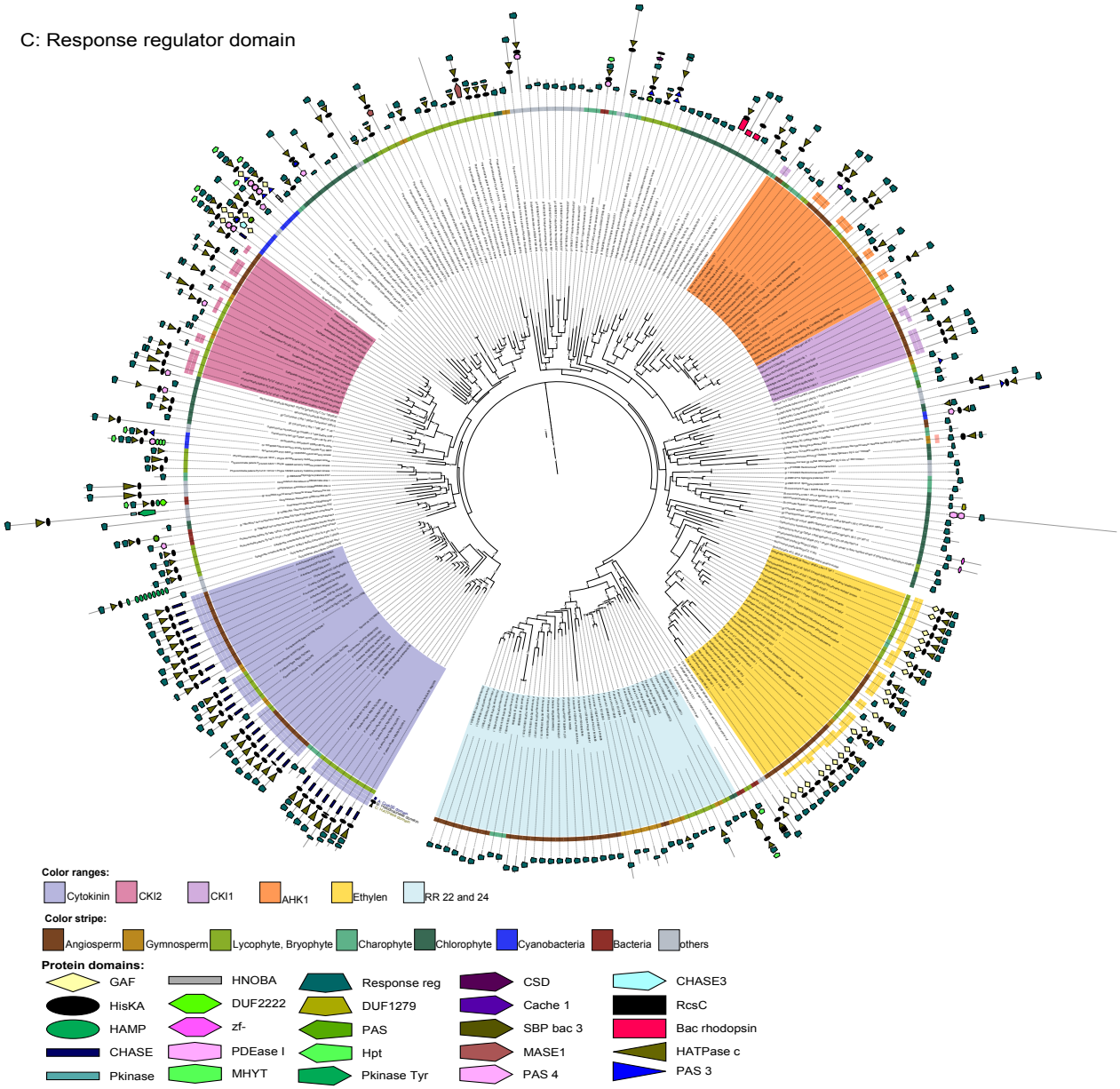

Figure 31: Phylogenetic sub-trees for different domains of hybrid histidine kinases. Sequences of the **(A)** HisK, **(B)** HATPase or **(C)** Response regulator domains were aligned (using MAFFT) and a maximum likelihood tree was calculated using RAxML. In these trees clades were colored according to known plant gene functions associated with the respective protein (for more information see the materials and method section 2.6.2). Subtrees with the relevant clades are shown for comparison of the clades only. Depicted in radial order from the inside to the outside are: maximum likelihood subtree of the RR domain; protein names of the respective protein; functional clades; color code for the organism lineage; color code of the functional clade of the respective protein found in the CHASE-domain tree; color code of the functional clade of the respective protein found in the HK-domain tree; color code of the functional clade of the respective protein found in the HATPase-domain tree; domain architecture of the whole respective protein. A scalable version of this figure can be found in the electronic version of this thesis. Protein domains: Abbrev. of the domains are according to the Pfam-database (http://pfam.sanger.ac.uk): GAF, PF01590; HNOBA, PF07701; Response_reg, PF00027; CSD, PF00313; CHASE3, PF05227; HisKA, PF00512; DUF2222, PF09984; DUF1279, PF06916; Cache1, PF02743; RcsC, PF09456; HAMP, PF00672; zf-, zf-DOF, PF02701; PAS, PF00989; SBP bac 3, PF00497; Bac rhodopsin, PF01036; CHASE, PF03924; PDEase I, PF00233; Hpt, PF01627; MASE1, PF05231; HATPase c, PF02518; Pkinase, PF00069; MHYT, PF03707; Pkinase Tyr, PF07714; PAS 4, PF08448; PAS 3, PF08447.

EST derived sequences (gi 299517909 *Spirogyra pratensis* EST; gi 299514768 *Spirogyra pratensis* EST) belong to proteins that comprise of the same domain architecture as the classical cytokinin receptors was not possible to determine from the dataset as the ESTs were not long enough to cover other domains. Even though these ESTs were not verified proteins with a domain architecture of cytokinin receptor proteins, another result further corroborated the possibility that charophyte algae have CHASE domain-containing receptors: the analysis of the HATPase domain also contained an EST from the charophyte algae *Spirogyra pratensis* amongst the functional clade of cytokinin receptors (gi 299511131 *Spirogyra pratensis* EST). This EST was also not long enough to find other domains, and so it is not clear whether the HATPase domain and one of the RR domains belong to the same protein.

The phylogenetic tree derived from all RR domains in the data set (Appendix Figure 9) included, additionally to the above mentioned functional clades, a clade containing the type-C RR proteins (RRCs) (Figure 31) as well as RR domains from all organisms of the land plant lineage. The domain composition analysis of the whole protein showed that the majority of the proteins are single-domain proteins, whereas two proteins also included a HATPase domain. The occurrence of the additional HATPase domain and the position of the RRCs as a sister clade to the receptors made it tempting to speculate that RRCs may be degenerated receptor proteins (Appendix Figure 10).

Altogether, the above presented results imply that the domains necessary for the formation of a cytokinin receptor protein were present in all ancestors of the land plant lineage and also in cyanobacteria. They were assembled into a receptor protein with the domain architecture of the classical cytokinin receptors in progenitors of charophyte algae (as indicated by the RR domains in the functional clade of cytokinin receptors) and land plants, however not in chlorophyte algae.

3.2.3. Phylogenetic analysis of domains derived from response regulator and histidine phosphotransfer proteins

Response regulator proteins

The above described RR domain subtree included the receptor RR domains and the RR domains from type-C RR (RRCs) proteins. The full tree of RR domains from the dataset (see Appendix Figure 9), also included the type-A (RRA) and type-B (RRB) RR domains. The subtree containing the RR domain of RRAs and RRBs is shown in Figure 32. The previous analysis of Pils and Heyl (2009) gathered all RRAs and RRBs, filtered them according to known component characteristics and showed their relatedness to each other. In contrast to this prefiltering, the analysis described here included all RR domains present in the dataset. The domain composition of the whole protein and the existence of the canonical Asp were not prerequisite for the analysis. The subtree including the functional clades of RRAs and RRBs also included another clade composed of known pseudo-RRs (PRRs). Members of this clade have been shown to be involved in circadian rhythm (Mizuno 2004; Mizuno and Nakamichi 2005; Satbhai *et al.,* 2011). The PRRs have been phylogenetically analyzed with regard to their component group and members of the PRRs from *P. patens* have been shown to possess the canonical Asp (Satbhai *et al.,* 2011). The other two functional clades recapitulated findings from Pils and Heyl (2009). RRBs include proteins from chlorophyte algae, while RRAs are limited to the land plant lineage (Figure 32). No charophyte algae RRA was found among the RRAs. Other than in previous analyses (Pils and Heyl 2009), non-canonical RRs were also found in the functional clade of RRAs. It should be noted that RR domains without the canonical Asp appear to be partial proteins and RR domains from the poorly annotated genome of *P. abies* (Figure 32, 4). In contrast to the RRAs, the degree of divergence at the canonical residue was much higher in the functional clades of RRBs and PRRs (Figure 32, 3). The analysis of the domain architecture of the respective whole protein indicated that the functional clade of RRAs includes only single-domain proteins, while the functional clades of RRBs and PRRs consist of proteins showing their characteristic domain architecture. The domain architecture of RRBs consists of the RR domain together with an MYB-DNA binding-related domain and the domain architecture of PRRs comprises the RR domain together with

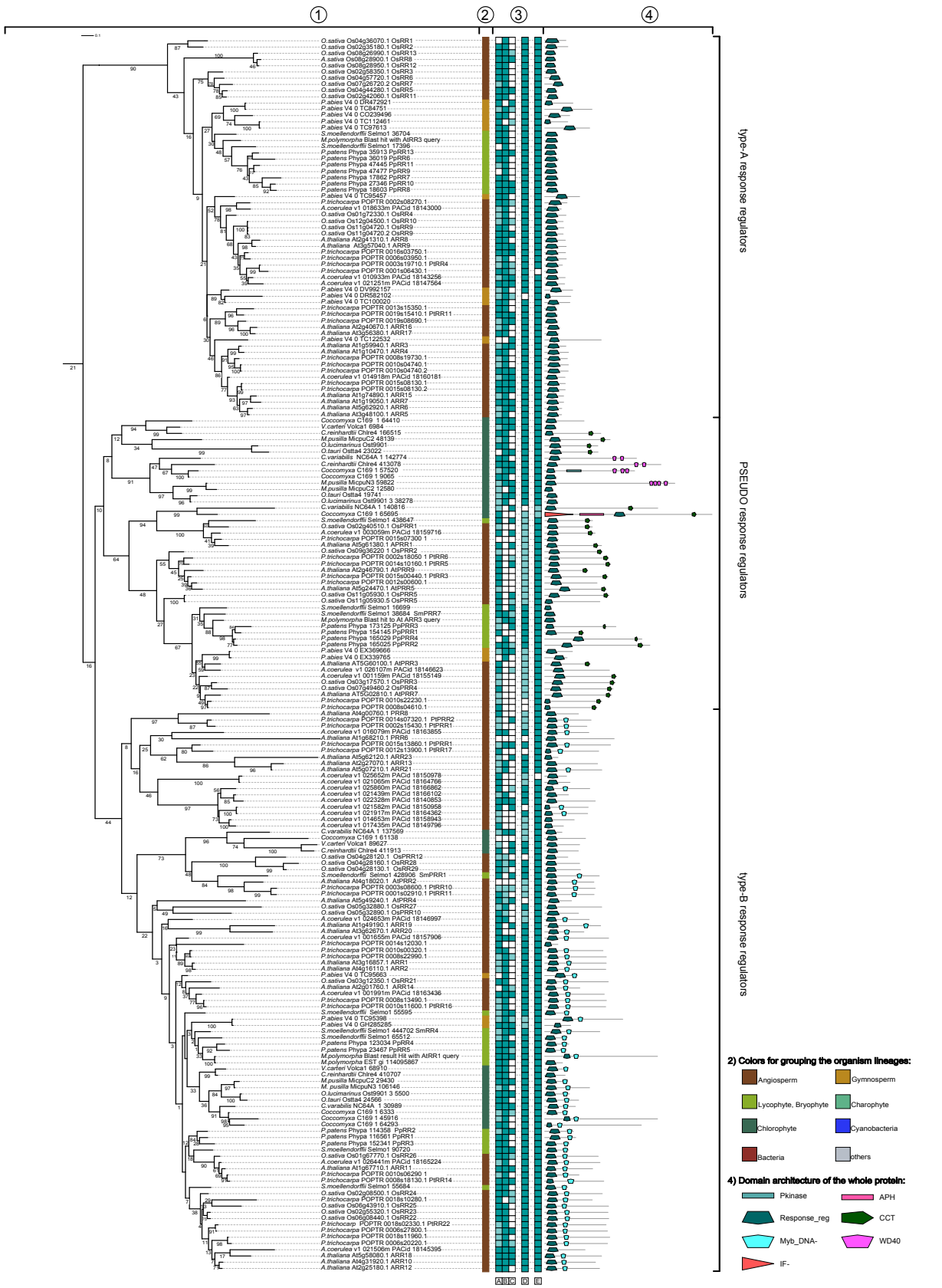

Figure 32: Phylogenetic subtree of the response regulator domain recapitulates the separation of type-A and -B RRs. (1) The response regulator domain sequences from all organisms under investigation were aligned (using MAFFT) and a phylogenetic tree using maximum likelihood was inferred with RAxML. Shown is the subtree containing the RR from the type-A and type-B (for details see the Material and Methods section 2.6.2).**(2)**

Organism lineage color code **(3)** Conservation of amino acids of the DDK-motive (first D positions ABC, second D position D, K position E; the positions A and C indicate the occurrence of a Asp at either one or two aa upstream and downstream of the conserved D). Dark blue shows conservation, light blue marks conservative substitution, white boxes symbolize no conservation. **(4)** Domain architecture of the whole respective protein (Abbrev. of the domains are according to the Pfam-database (http://pfam.sanger.ac.uk): Pkinase, PF00069; APH, PF01636; Response_reg, PF00027; CCT, PF06203; Myb_DNA, PF00249; WD40, PF00400; IF-2B, PF01008). A scalable graphic is available in the electronic file.

a CCT or WD40 domain. Both functional clades were interspersed with single-domain proteins that contained only the RR domain. Further investigation of the DDK motif revealed that the ability to function in the TCS, namely the conservation of the canonical Asp residue, is not dependent on the domain architecture since RRBs as well as PRRs have non-canonical and canonical members. The canonical members of the PRRs found in *P. patens* have previously been described and analyzed with regard to the function in the TCS (Satbhai *et al.,* 2011). *In vitro* experiments showed that PpPRRs were phosphorylated by the *E. coli* HPT (ArcB), and so could act in the TCS (Satbhai *et al.,* 2011). The results presented here show that the classification of RRs into the three subgroups of RRA, RRB and RRC is not dependent on the domain architecture (since single-domain proteins were found in all functional clades), but should be derived from phylogenetic analyses.

Histidine phosphotransfer proteins

In the above described work, domains from the receptor protein and the last two steps in the signaling cascade (RRBs and RRAs) have been described. Intermediate to those are the HPT proteins that transfer the molecular signal (the phosphoryl group) to the next component. The dataset (see section 2.6.1) was analyzed for the existence of HPT domains and a phylogenetic tree was calculated (for details please refer to section 2.6.2). This tree separated the HPT domains into distinct clades of organisms from the land plant lineage and chlorophyte algae. The land plant clade of the tree incorporated two HPT domains derived from EST evidence of the charophyte algae *C. orbicularis*. The analysis of the conservation of the canonical His in the HPT proteins found its conservation in all proteins except for gymnosperms and angiosperms (Figure 33, 3). In *A. thaliana* the protein without the canonical his, AHP6, was shown to have a negative regulatory function in the cytokinin signaling system (Mähönen *et al.,* 2006a). Further inspection of the organism lineage distribution revealed another surprise, namely the HPT domain derived from EST evidence of the bryophyte *M. polymorpha* amongst cyano- and bacterial HPT domains (*M. polymorpha* EST gi 114081174). This *M. polymorpha* HPT domain had a canonical His which indicated functionality in the TCS, and the domain architecture of the whole protein indicated that this protein also contained a RR domain. The phylogenetic analysis of all RR domains placed the RR domain of this EST in a sister clade of the RRCs together with bacterial and slime mold

RR domains (Figure 31). No further information was available about the protein corresponding to the EST.

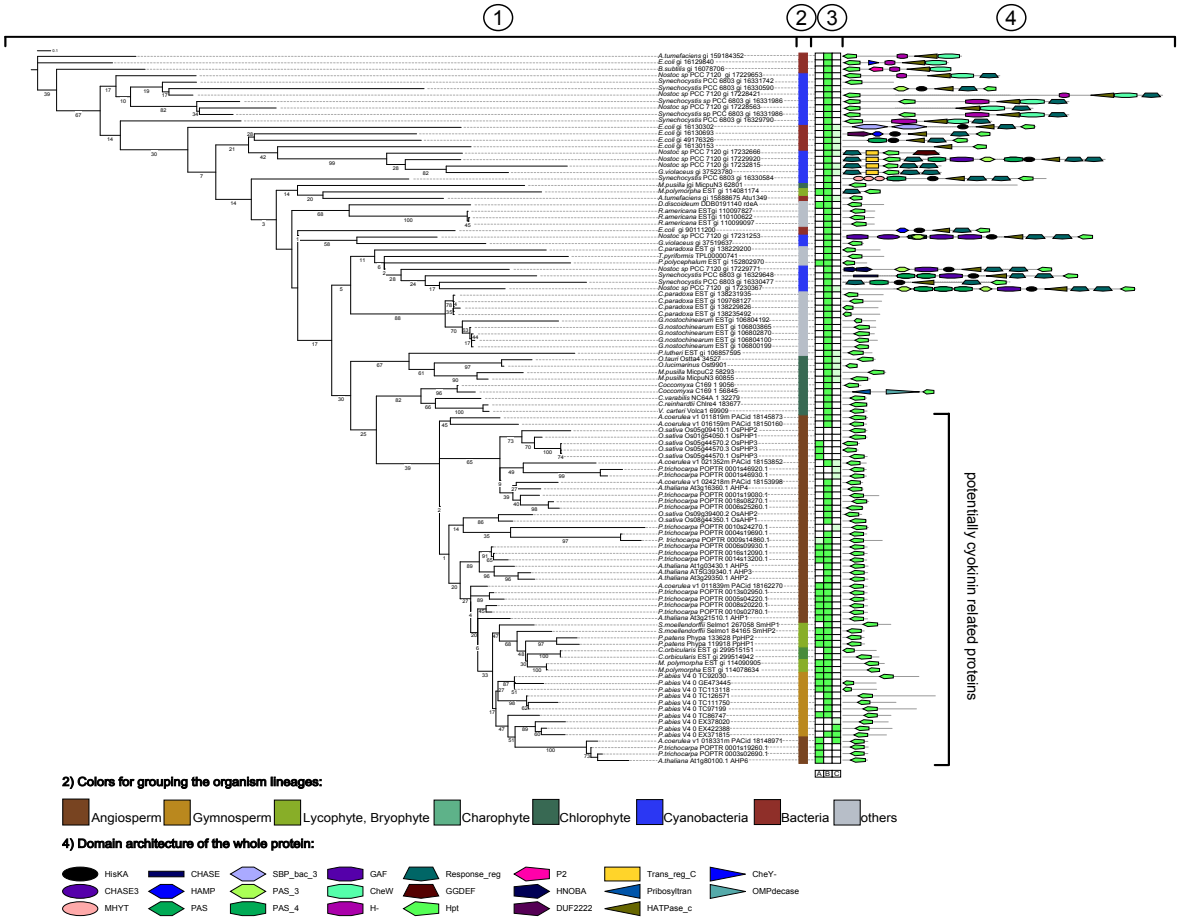

Figure 33 Phylogenetic tree of the HPT domain. (1) Sequences of the HPT domains were aligned (using MAFFT) and a maximum likelihood tree was calculated with RAxML. For details please refer to section 2.6.2. **(2)** Organism lineage color code **(3)** Conservation of the canonical his. Position B represents the conical his; the positions A and C indicate the occurrence of a His at either one or two aa upstream and downstream of the conserved D). Dark green shows conservation, light green marks conservative substitution, white boxes symbolize no conservation. **(4)** Domain architecture of the whole respective protein Abbreviations of the domains are according to the Pfam-database (http://pfam.sanger.ac.uk): HisKA, PF00512; CHASE, PF03924; SBP bac 3, PF00497; GAF, PF01590; Response_reg, PF00027; P2, PF07194; Trans_reg_C, PF00486; CheY-, CL0304; CHASE3, PF05227; HAMP, PF00672; PAS 3, PF08447; CheW, PF01584; GGDEF, PF00990; HNOBA, PF07701; Pribosyltran, PF000156; OMPdecase, PF00215; MHYT, PF03707; PAS, PF00989; PAS 4, PF08448; H-, PF02895; Hpt, PF01627; DUF2222, PF09984; HATPase c, PF02518. A scaleable graphic is available in the electronic file.

3.2.4. Phylogenetic analysis of domains derived from enzymes involved in cytokinin metabolism

The use of the cytokinin molecule as a growth regulator is not only dependent on a functional signaling system, the presence of the molecule itself must also be tightly regulated (Hutchison and Kieber 2002). In the following, the *A. thaliana* cytokinin metabolism will be used as a reference. In the plant *A. thaliana*, this is achieved via two key enzymes involved in anabolism (the LOG and IPT enzymes) and one key enzyme of catabolism (the CKX enzyme). In the following analysis, the characteristic domains of the three key enzymes of

cytokinin metabolism were investigated for their occurrence in the dataset. Respective domains were aligned and a phylogenetic tree was calculated (see section 2.6.2).

The phylogenetic tree of the lysine decarboxylase domain (LDC domain; see Appendix Figure 11), characteristic for LOG proteins, had three distinct clades and included the LDC domains of all organism lineages with the exception of charophyte algae. Domains that were part of the general clade originated from chlorophyte, bryophyte, gymnosperm and angiosperm LDC domains (see Appendix Figure 11, general). A possible function of the respective proteins in the general clade is associated with amino acid biosynthesis (Jander and Joshi 2009). The general clade was separated from two more clades by bacterial, slime mold and chlorophyte LDC domains. These two clades contained LDC domains from proteins previously found to be LOG proteins (Kurakawa *et al.,* 2007; Kuroha *et al.,* 2009). All proteins in these two clades came from the land plant lineage. One of the two clades (see Appendix Figure 11, II) consisted solely of angiosperm and gymnosperm protein domains and the other (see Appendix Figure 11, I) included LDC domains from bryophytes but no algae LDC domains.

The next key enzyme in the analysis was the IPT enzyme. The phylogenetic tree was generated in the same way as described in section 2.6.2 and separated into two distinct clades: one with known IPT enzyme domains (Kakimoto 2001; Takei *et al.,* 2001; Yevdakova and von Schwartzenberg 2007; Frebort *et al.,* 2011; Patil and Nicander 2013) and one other clade (Appendix Figure 12). The two clades containing the adenylate- and the tRNA-IPT enzymes did not separate into clades according to the assigned functions of the respective proteins. While the tRNA-ITP IPT9 of *A. thaliana* located as a sister of the bryophyte tRNA-IPT domains (Appendix Figure 12, I), the tRNA-IPT domain of the AtIPT2-enzyme was included in the clade that contained mainly adenylate-IPTs (Appendix Figure 12, II). The phylogenetic tree contained protein domains from slime mold proteins in all clades, but domains from chlorophyte algae were only present in the tRNA-IPT clade (Appendix Figure 12, I), and in the third clade bacterial tRNA-IPT domains were separated from plant IPT domains.

The domain characteristic of the cytokinin degrading enzyme CKX (FAD and cytokinin binding, PF09265) was also analyzed and the phylogenetic tree (Appendix Figure 13) showed three different clades. Two clades incorporated domains from known CKX enzymes (Mok and Mok 2001; Werner *et al.,* 2001; Gu *et al.,* 2010; Frebort *et al.,* 2011) and the third clade included, additionally to two domains from rice CKXs and one from *A. coerula* CKX, one domain from *Nostoc spp.* CKX. The other two clades with domains from *A. thaliana* CKX enzymes divided into a clade including AtCKX7 and two other angiosperm CKXs (one from rice and one from poplar) and the bryophyte and lycophyte CKXs (Appendix Figure 13, I),

and the other clade included only angiosperm CKXs and one *P. abies* CKX (Appendix Figure 13, II).

Taken together, the domain analysis of the metabolism proteins indicated a common pattern. All phylogenetic trees were divided into three clades: one clade with predominantly angiosperm domains, one clade with angiosperm and bryophyte domains and one clade with bacterial domains. Interestingly, the analysis did not identify any charophyte algae domains belonging to one of the three enzymes and chlorophyte algae domains were limited to the anabolism enzymes.

3.3. Characterization of members of the new receptor clade: PpCHK4 and MpCHK1

The phylogenetic analysis of the different domains involved in cytokinin signaling revealed a new clade of potential cytokinin receptors. The analysis in this section investigated whether these proteins function as cytokinin receptors, although sequence comparison of the amino acids critical for cytokinin binding showed a substantial divergence (Figure 30, 3 and Appendix Figure 8, 3). The newly identified clade of potential cytokinin receptors contained eight *P. patens* proteins, of which seven were actively transcribed, and one sequence from *M. polymorpha* (see Figure 30). As a candidate protein for subsequent functional analysis, PpCHK4 – for which with an equal amount of information was available compared to PpCHK5 – from the *P. patens* proteins and the *M. polymorpha* protein were selected.

First it was investigated whether cytokinin binds to these proteins in an *in vivo* binding assay (described in section 2.4.7). The receptor proteins are expressed in *E. coli* KMI002 cells (Table 2) and incubated with radioactively-labeled cytokinin. Specific cytokinin binding was calculated from the radioactive signal after incubation with an excess of non-labeled cytokinin. While cytokinin binding to the GST:PpCHK4 protein (139 kDa) was not detectable in the biological replicates, cytokinin binding was shown when GST:MpCHK1 (143 kDa) was investigated (see Figure 34). It should be noted that GST:PpCHK4-specific binding showed high standard deviations and weak protein expression in the immunoblot (Figure 34). Moreover, GST:PpCHK4 was shown to bind to cytokinin in this assay when a preselection for *E. coli* colonies that activated a reporter gene dependent on cytokinin presence was carried out ((Gruhn *et al.,* 2014); assay carried out by M. Halawa).

In the next step, another *in vivo* system was used to assess the ability of the two receptor proteins to activate TCS downstream components (for a detailed description of the assay, please refer to section 2.4.8). In this assay, a reporter gene is fused to the promoter of an *E. coli* TCS target gene. If cytokinin binds to the expressed receptor, the TCS can be activated and this activation modulates the reporter gene transcription. Both potential

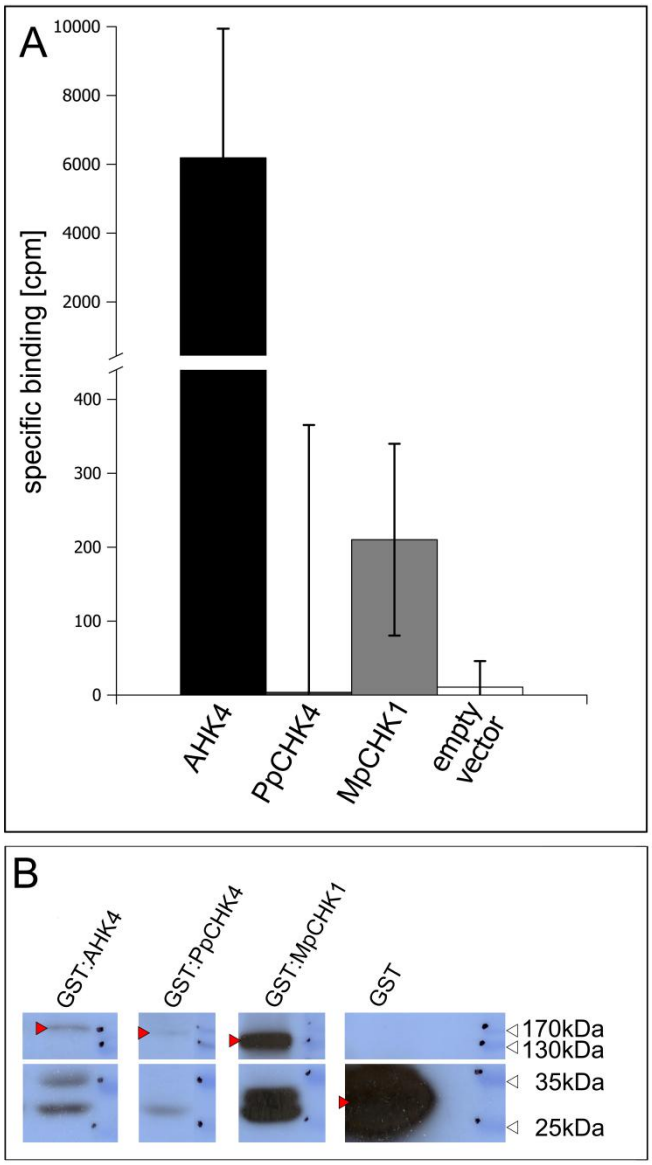

Figure 34: *M. polymorpha* receptor GST:MpCHK1 binds to *trans*-[2-^{3}H]zeatin. A: *In vivo* binding assay. All receptors were expressed as GST-fusion proteins in *E. coli*. The specific binding to *trans*-[2-^{3}H]zeatin was analyzed according to (Mizuno and Yamashino 2010). Shown are biological replicates (n = 3) and their standard deviation (whiskers). **B:** Expression control of the fusion proteins analyzed in A. Immunoblot detection was carried out using the pellet of 1 mL bacterial culture that was separated by SDS-PAGE and blotted to a PVDF membrane. GST-containing bands were detected using a GST-specific antibody (Santa Cruz Biotechnology, Heidelberg). White arrowheads mark the position of the protein marker (PageRuler™ Prestained Protein Ladder (Fermentas, St. Leon-Rot)), red arrowheads mark the full-length receptor protein band.

cytokinin receptor proteins activated the reporter gene in a concentration-dependent manner. Highest reporter gene activity was found for both receptors when *trans*-zeatin was applied (see Figure 36). The reporter gene activity measured upon the treatment with the other tested cytokinins had overlapping standard deviations and a conclusion about the binding preferences of PpCHK4 and MpCHK1 could therefore not be drawn.

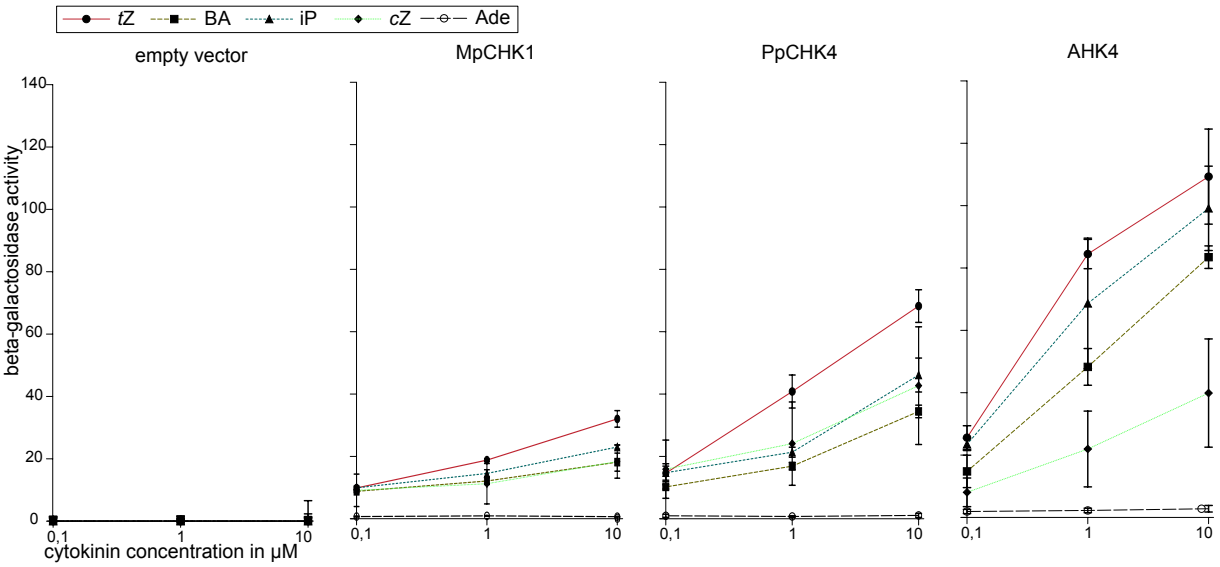

Figure 35: Potential cytokinin receptors MpCHK1 and PpCHK4 activate the TCS in dependence of cytokinin. The *E. coli* strain KMI002 was transformed with the respective receptor. PpCHK4 and MpCHK1 activated the reporter gene in a concentration-dependent manner. The positive control, *A. thaliana* AHK4 induced the reporter gene activity to a high extend. Shown are average values of three biological replicates and their standard deviation (whiskers). The experiment was performed by M. Halawa (Gruhn *et al.,* 2014). A scaleable graphic is available in the electronic file.

The above presented results show that MpCHK1 and PpCHK4 have the ability to activate a TCS in response to cytokinin. Whether this is also true *in planta* was investigated next. The two receptor proteins were expressed in *A. thaliana* protoplasts and cytokinin-dependent activation of the *A. thaliana* cytokinin signaling system was tested using the PTA (detailed

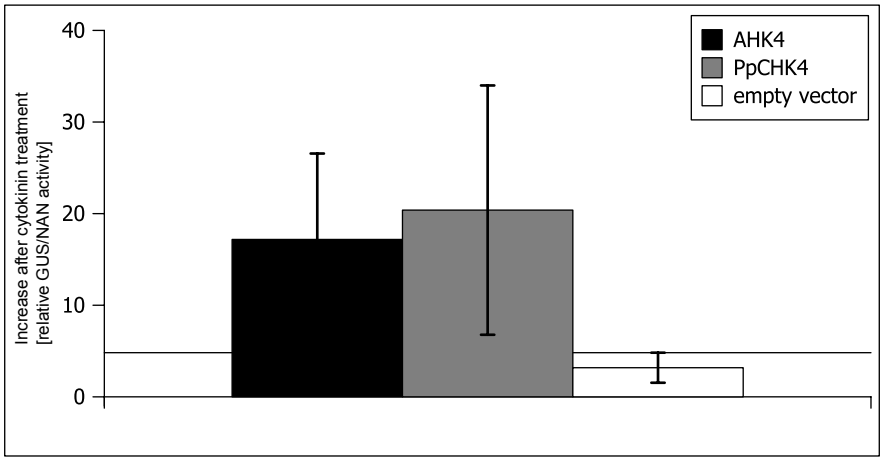

Figure 36: *P. patens* cytokinin receptor PpCHK4 activates the cytokinin-dependent TCS in *A. thaliana*. Cytokinin perception-deficient protoplasts (*ahk2-5 ahk3-7*) (Riefler *et al.,* 2006) were co-transformed with the cytokinin-responsive *ARR2* (effector), the *ARR6* promoter fused to *β*-glucuronidase (reporter), *35S::NAN* (internal reference) and the indicated cytokinin receptor (activator) under the 35S promoter. Protoplasts were incubated overnight either with or without trans-zeatin; *ARR6* promoter *trans*-activation was subsequently measured. Results were normalized by the internal reference and the specific activity upon cytokinin treatment was calculated (normalized reporter activity with cytokinin minus normalized reporter activity without cytokinin). Depicted results are mean values of three biological replicates (n = 3) and whiskers represent standard deviation.

description may be found in section 2.5.2.3). The receptor protein PpCHK4 activated the cytokinin signaling system after *trans*-zeatin addition (see Figure 36), while the GFP:MpCHK1 fusion protein did not activate the cytokinin signaling system (see Figure 37).

In summary, biochemical experiments showed that GST:PpCHK4 is able to activate TCS downstream components in a cytokinin concentration-dependent manner and that PpCHK4 activated the cytokinin signaling system *in planta*. The GST:MpCHK1 protein bound to cytokinin (Figure 34) and activated downstream TCS components in the bacterial assay (Figure 35), though this could not be shown *in planta* using GFP:MpCHK1 (Figure 37).

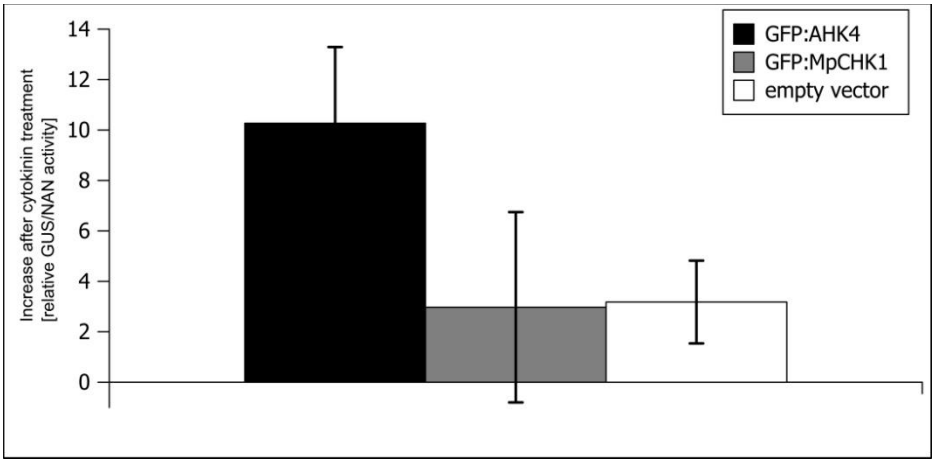

Figure 37: *M. polymorpha* receptor MpCHK1 does not activate the cytokinin-dependent TCS in *A. thaliana*. Cytokinin perception-deficient protoplasts (*ahk2-5 ahk3-7*) (Riefler *et al.,* 2006) were co-transformed with the cytokinin-responsive *ARR2* (effector), the *ARR6* promoter fused to *β*-glucuronidase (reporter), *35S::NAN* (internal reference) and the indicated cytokinin receptor (activator). Protoplasts were incubated overnight either with or without *trans*-zeatin; *ARR6* promoter *trans*-activation was subsequently measured. Results were normalized by the internal reference and the specific activity upon cytokinin treatment was calculated (normalized reporter activity with cytokinin minus normalized reporter activity without cytokinin). Depicted results are mean values of three biological replicates (n = 3) and whiskers represent standard deviation.

Ligand binding and signal transduction in dependency of cytokinin suggested that both proteins might play a role in cytokinin signaling. A protein's localization to the appropriate subcellular compartment is necessary for fulfilling its designated function. The vector constructs encoding GFP fusion proteins of GFP:PpCHK4 and GFP:MpCHK1 were transiently transformed into *N. benthamiana* leaves and fluorescence was analyzed in epidermal cells. The GFP:MpCHK1 protein showed fluorescence in the perinuclear region and co-localized with the plasma membrane dye FM4-64 (Figure 38). The fluorescence of GFP:PpCHK4, localized to the region of the nucleus, marked a network-like structure and co-localized with the plasma membrane dye FM4-64 (Figure 38).

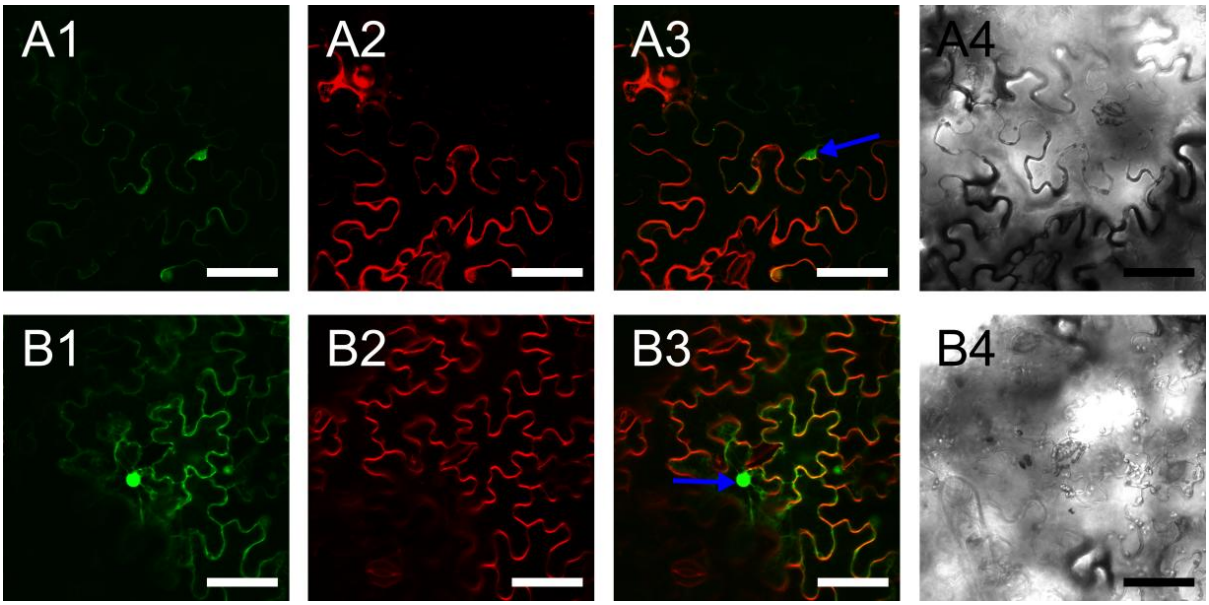

Figure 38: Subcellular localization of the MpCHK1 and the PpCHK4 protein fused to GFP expressed in *N. benthamiana* leaves. A1-4, GFP:MpCHK1; **B1-4**, GFP:PpCHK4; Both receptor proteins show a partial overlap (A3 and B3) with the plasma membrane stained by FM4-64 (A2 and B2). GFP:MpCHK1 also indicates fluorescence in the perinuclear space (A1 and A3), while GFP:PpCHK4 shows a strong fluorescence in the nucleus and marks a network-like structure (possibly associated with the ER) (B1 and B3). All constructs are driven by the 35S CaMV promoter, were transformed into *A. tumefaciens* and infiltrated into *N. benthamiana* leaves. Fluorescence was analyzed five days after infiltration in prepared leaf epidermal cells. Blue arrow marks the perinuclear space. First pictures show GFP fluorescence exited at 488 nm, emission detected at 509 nm ; A2 and B2 show fluorescence at 625-665 nm of FM4-64 dye, staining the plasma membrane; A3 and B3 show overlay from fluorescent channels; A4 and B4 show bright field image. Scale bars correspond to 50 µm.

To find out whether the observed fluorescence derived from the full length fusion protein, the cytosolic and membrane-enriched fraction were subjected to immunodetection and both fusion proteins were detected only in the membrane-enriched fraction (see Appendix Figure 14).

Taken together, the above described results indicate that both proteins may serve as cytokinin receptors, and that the newly identified clade of receptor proteins incorporates potential candidates to function as cytokinin receptors.

4. Discussion

4.1. Characterization of the *Physcomitrella patens* cytokinin receptors PpCHK1, PpCHK2 and PpCHK3

Previous bioinformatic analyses have identified three putative cytokinin receptors in *P. patens* (Pils and Heyl 2009). The characterization of these hybrid histidine kinases was the subject of the first part of this work. In general, the three *P. patens* genes shared the domain architecture that characterizes cytokinin receptors in *A. thaliana*, and so were suitable candidates to fulfill the same function in *P. patens*. The *P. patens* cytokinin receptors share 43-48% sequence identity with AHK2, AHK3, and AHK4 proteins (Appendix Table 3), therefore it was plausible that they also shared similar functionality. Besides the information gathered from the protein sequence, the characterization of a protein as a cytokinin receptor is dependent, first, on the binding of cytokinin to the respective protein and, second, on the output of the signal into the appropriate signaling system. To investigate these properties, well established assays were used which show that cytokinin as a ligand can bind to receptor proteins (Romanov and Lomin 2009); that the respective cytokinin receptor candidate translates the cytokinin binding into the activation of a TCS (Mizuno and Yamashino 2010) and that the respective receptor activates an AtTCS reporter (Choi *et al.,* 2010). Ultimately, the *A. thaliana ahk2 ahk3* double knockout mutant was used to analyze the complementation capacity of a cytokinin receptor (Caesar *et al.,* 2011; Stolz *et al.,* 2011; Wulfetange *et al.,* 2011a) on the whole plant level.

4.1.1. *P. patens* cytokinin receptors PpCHK1 and PpCHK2 bind to cytokinin

The first step in characterizing the putative receptors as cytokinin binding receptors was to analyze the binding of *trans*-zeatin to the putative receptors in an *E. coli in vivo* binding assay (Romanov *et al.,* 2005). This assay has effectively shown the binding of the CHASE domain of AHK2, and of AHK3 and AHK4 to cytokinin (Romanov *et al.,* 2006; Stolz *et al.,* 2011), as well as the binding of the maize cytokinin receptors ZmHK1, ZmHK2 and ZmHK3a to cytokinin (Lomin *et al.,* 2011). The binding of the putative receptors PpCHK1 and PpCHK2 to *trans*-zeatin, representing a cytokinin abundant in *A. thaliana,* was detected (see Figure 8, A), providing the first evidence that PpCHK1 and PpCHK2 fulfill the requirements of a cytokinin receptor. It should be noted that the variant of the assay used here is strictly qualitative.

Cytokinin binding was not detected when PpCHK3 was investigated (see Figure 8, A), but the immunoblot showed the protein to be expressed (Figure 8, B). Besides protein expression, the correct folding of the protein can influence ligand binding. This was not analyzed for the expressed PpCHK3 protein. AHK4, the most studied cytokinin receptor, has been investigated for its folding of the CHASE domain by circular dichroism (Wulfetange *et al.,*

2011b) and by crystallization (Hothorn *et al.,* 2011). Analogous experiments of the PpCHK3 protein could be carried out, but would require the laborious expression and purification of the protein. Influences on protein folding by the addition of the N-terminal GST tag are possible, but since PpCHK1 and PpCHK2 allowed cytokinin binding when being expressed as a GST-fusion protein, the effect of the GST tag fused to PpCHK3 seems less likely to be the reason for the absence of cytokinin binding.

In both *A. thaliana* and maize it has been shown that different cytokinin receptors have different ligand specificities (Spichal *et al.,* 2004; Yonekura-Sakakibara *et al.,* 2004; Romanov *et al.,* 2006; Lomin *et al.,* 2011). Thus, it might be possible that cytokinins other than *trans*-zeatin would bind to PpCHK3. While the ligand specificity of the *P. patens* cytokinin receptors might reveal important implications for which cytokinin is more relevant to *P. patens*, the results presented here, namely the capacity of PpCHK1 and PpCHK2 to function as cytokinin receptors, demonstrate the general ability to bind cytokinin.

4.1.2. *P. patens* cytokinin receptor PpCHK3 activates TCS components *in vivo*

Besides the binding of the ligand, a receptor needs to translate the binding into a biological signal. Hybrid histidine kinases translate the ligand binding by phosphorylation of the downstream component, an HPT protein (Figure 3). The cytokinin receptors AHK4 and AHK3 have previously been show to efficiently phosphorylate HPT YojN of the *E. coli* TCS, thereby complementing the Δrcsc-YojN-RcsB TCS in a cytokinin concentration-dependent manner (Suzuki *et al.,* 2001a; Yamada *et al.,* 2001). This assay was therefore used to analyze the signal transduction capacity of the *P. patens* PpCHK1, PpCHK2 and the PpCHK3 proteins. The PpCHK3 receptor did activate the TCS in a concentration-dependent manner (Figure 9). The cytokinin concentration-dependent increase in activation is important in this assay since the AtCKI1 protein, a hybrid histidine kinase which does not bind to cytokinin, activates the *E. coli* TCS independent of the presence of cytokinin at a steady state (Yamada *et al.,* 2001). The activation of the TCS by PpCHK3 indirectly implies the binding of the cytokinin ligand to the receptor.

The PpCHK1 and PpCHK2 proteins did not activate the *E. coli* TCS (Figure 9). What differences between the binding assay and the signal transduction assay lead to the TCS activation by *trans*-zeatin via PpCHK3 but not via PpCHK1 and PpCHK2 could not be deduced from the assay. Importantly, *PpCHK2* expressed without a tag in the analogous assay activated the reporter gene (Ishida *et al.,* 2010). However, the cytokinin receptors AHK2 and AHK3 were inactive in the *Δrcsc E. coli* mutant (Suzuki *et al.,* 2001a), even though their biological function has been shown in various experiments *in planta* (Hwang and Sheen 2001; Nishimura *et al.,* 2004; Riefler *et al.,* 2006; Stolz *et al.,* 2011), but later the activation of

the reporter gene has also been shown for AHK3 (Spichal *et al.,* 2004). Since cytokinin binding to the PpCHK1 and PpCHK2 receptor have been shown in the binding assay (discussed in section 4.1.1), the absence of reporter activation may be caused by incompatibility of PpCHK1 and PpCHK2 with the *E. coli* HPT despite cytokinin binding or by the fusion of the GST tag to the receptor, though this seems less likely because PpCHK3 was also expressed as fusion protein with the GST tag. Nevertheless, both assays were carried out in different *E. coli* genotypes and deviations due to the genotype cannot be excluded. It is also possible that PpCHK1 and PpCHK2 proteins were not sufficiently expressed in this assay, or that they were expressed but not correctly folded. Misfolded proteins might then lead to no binding of the ligand or to a loss of phosphotransfer function.

4.1.3. PpCHK1 and PpCHK2 activate the cytokinin signaling cascade *in planta*

In the above discussed assays (section 4.1.1 and 4.1.2) it was shown that cytokinin binds to PpCHK1 and PpCHK2 and that PpCHK3 converts cytokinin presence into a TCS output. Since these data relied on *E. coli*-based assays, the next step was to examine the activity of the receptors *in planta*. Hwang and Sheen (2001) report that the fusion of the RRA *ARR6* promoter to the reporter gene luciferase was responsive to cytokinin treatment in *A. thaliana* protoplasts, while the simultaneous expression of a cytokinin receptor increased reporter gene activity after cytokinin treatment. This was also shown by Choi *et al.* (2010), who also included an effector in the protoplast transactivation assay (PTA). Similar to the results in the *in vivo* binding assay (Figure 8, A), PpCHK1 and PpCHK2 were able to activate the *A. thaliana* TCS (AtTCS) in the PTA (Figure 10). This means that PpCHK1 and PpCHK2 are cytokinin receptors that bind cytokinin, and that they activate the cytokinin signal transduction system of *A. thaliana* in dependence of cytokinin. Surprisingly, no activation of the AtTCS was found in the assay when PpCHK3 was investigated. A possible reason might be the insufficient expression of *PpCHK3*, perhaps due the absence of the transgene in the protoplast. Controls for transformation efficiency indicated a sufficient transformation rate (data not shown) so this possibility seems less likely. Immunoblot experiments with isolated protein from *A. thaliana* protoplasts could be carried out to clarify whether the lack of activation was caused by the lack of protein. Alternatively, the lack of activation could be due to incorrect folding of the protein or an incompatibility of the PpCHK3 receptor with the AtTCS components. Analyses to gather information about the correct folding have been described before (section 4.1.1). Compatibility of the receptor protein with the AtTCS components, which mean that phosphotransfer from the receptor to the HPT requires binding of the HPT proteins to the receptor, could be investigated by analyzing the protein-protein interactions with yeast-two-hybrid experiments or bimolecular fluorescence complementation methods

(Kerppola 2006), or by carrying out phosphor transfer studies (Suzuki *et al.,* 1998) with the relevant components.

4.1.4. Subcellular localization of the *P. patens* cytokinin receptors

To investigate the subcellular localization of PpCHK1, PpCHK2 and PpCHK3 these receptors were transiently expressed as fusion proteins to GFP in tobacco epidermis cells.

The localization of PpCHK1 and PpCHK2 largely concentrated on the perinuclear space (Figure 13), a region linked to the ER (Sparkes *et al.,* 2009). This is in line with previous subcellular localization experiments of the cytokinin receptors of *A. thaliana* (Caesar *et al.,* 2011; Wulfetange *et al.,* 2011a). However, a co-localization with an ER marker protein (Nelson *et al.,* 2007) that contained the HDEL ER-retention signal and the AtWAK2 signal peptide (He *et al.,* 1999) was inconclusive due to the unclear localization of the marker protein in co-expressing cells (data not shown). Co-localization with other ER marker proteins in order to verify the ER localization of PpCHK1 and PpCHK2 is left for future research. In accordance with the potential localization to the ER, the computational prediction program WoLF PSORT for plant proteins (Horton *et al.,* 2007) predicted an ER-retention signal in the receptor protein sequences (Appendix Table 6). In addition to the potential ER-located fluorescent signal, fluorescent speckles were found (Figure 13) that could not be associated with a cellular compartment or structure. Further experiments are needed to conclude on the relevance of these fluorescent signals. PpCHK2 partially co-localized to FM4-64 dye, which is staining the plasma membrane, a result also found for AHK3 (Kim *et al.,* 2006; Wulfetange *et al.,* 2011a)). A localization of PpCHK1 to the plasma membrane was not shown (Figure 13, A and C), and so PpCHK1 subcellular localization is comparable to the subcellular localization of AHK2 and AHK4 (Caesar *et al.,* 2011; Wulfetange *et al.,* 2011a). These results imply that PpCHK1 and PpCHK2 potentially localize to the same compartment in tobacco cells as *A. thaliana* cytokinin receptors.

The localization to the perinuclear region indicates a possible ER-localization (Sparkes *et al.,* 2009) of the PpCHK3 protein but should be verified in the future by co-localization with an ER marker protein (Batoko *et al.,* 2000). In addition to the potential ER localization, PpCHK3 proteins showed a partial co-localization with the FM4-64 stained plasma membrane and the formation of fluorescent speckles, independently of its fusion orientation (Figure 13, H and I). The fluorescent pattern observed for the GFP fusion proteins of PpCHK3 corresponds with the localization pattern of the AHK3 *A. thaliana* cytokinin receptor (Kim *et al.,* 2006; Wulfetange *et al.,* 2011a).

4.1.5. *P. patens* cytokinin receptors PpCHK1 or PpCHK2 complement the cytokinin signaling-deficient *A. thaliana ahk2 ahk3* mutant

To investigate the potential for *P. patens* cytokinin receptors to complement a deficiency of the *A. thaliana* cytokinin receptors (*ahk2 ahk3*), fusion proteins of *PpCHK1* or *PpCHK2* with *GFP* were ectopically expressed in *A. thaliana* plants lacking the endogenous *AHK2* and *AHK3* receptors (the correct sequence of *PpCHK3* was not yet available). It is known that the expression of a functional cytokinin receptor in these plants can complement the mutant phenotype (Caesar *et al.,* 2011; Stolz *et al.,* 2011; Wulfetange *et al.,* 2011a). All tested *A. thaliana* plants transcribed the respective *PpCHK1* or *PpCHK2* fusion construct at a high rate (Figure 15) and were further analyzed for six parameters known to be altered in the *ahk2 ahk3* mutant (Riefler *et al.,* 2006; Brenner *et al.,* 2012; Kang *et al.,* 2012; Brenner pers. communication). For the discussion of the results obtained in the complementation experiments, the two most robust morphological parameters and one molecular parameter in the experiment are, the rosette diameter, the stem height and the transcriptional regulation of *ARR16* (Brenner *et al.,* 2012; Brenner pers. communication). Results from complementation experiments revealed that GFP fusion proteins of PpCHK1 and PpCHK2 can partially complement the *ahk2 ahk3* phenotype (Figure 16 and Figure 17), and that from the extent of complementation it seems that the PpCHK1 GFP fusion protein has a stronger effect on both compared morphological parameters than the PpCHK2 GFP fusion protein. Even though the comparison of the WT, the double knockout mutant *ahk2 ahk3* and the generated transgenic lines involved different parameters, a common pattern leading to conclusions about specific PpCHK1 or PpCHK2 roles could not be found. These were specially looked for given that specific roles are known for AHK2, AHK3 and AHK4 (Riefler *et al.,* 2006). Altogether PpCHK1 or PpCHK2 fusion proteins to GFP partially complement the *ahk2 ahk3* phenotype.

The next step is to determine what, exactly, is causing this partial complementation. Partial complementation is less likely to result from limited amounts of protein as mRNA amounts were highly elevated (Figure 15). Sufficient protein expression is also likely to have occurred since the partial complementation of the mutant phenotype indicates the presence of the protein. To verify this assumption, immunoblot analyses of the isolated PpCHK protein in use could be carried out.

If protein levels were sufficient, at least two different reasons might cause the partial complementation. Firstly, technical reasons might lead to compromised protein function, or secondly the biological function of the protein might be altered. Technically the properties of the GFP fusion protein with *P. patens* receptors could be insufficient for total complementation. The potential alteration of the properties of a protein fused to the GFP tag is considered a general disadvantage of the fusion (Moore and Murphy 2009). To this end, I have shown before that the addition of the GFP tag to the cytokinin receptor protein

negatively influences its activation capacity in the cytokinin signaling system of *A. thaliana* protoplasts (Figure 11 and Figure 12). In the PTA the fusion orientation was influencing activation but an effect on complementation was absent in the comparison of the C- and N-terminal fusion lines (as exemplified by the rosette diameter of the complementation with PpCHK1 in Figure 16, A).

Surprisingly, and in contrast to the PTA results, both mutant lines transformed with the N-terminal fusion construct of *PpCHK1* displayed a weaker complementation regarding the rosette diameter than the C-terminally fused PpCHK1 proteins. No such effect was observed when *PpCHK2* was used for complementation (Figure 17). Since the other parameters under investigation did not show a fusion site-dependent complementation pattern, it seems that the fusion site of the GFP to the *P. patens* receptor affects specific aspects of the complementation, and further experiments should be carried out also without the fusion to a tag. The fact that PTA results were affected by the fusion site of the GFP tag could indicate that factors different from the one that lead to the activation of the *ARR6* promoter contributed to the complementation on the whole plant level in *A. thaliana*. This is likely to be the case since the *ARR6* promoter has been shown to be a good indicator for transcriptional activation after cytokinin treatment (Hwang and Sheen 2001; Choi *et al.,* 2012), but does not represent the entirety of all cytokinin-regulated genes (Brenner *et al.,* 2012; Brenner and Schmülling 2012).

Secondly, biological factors that could contribute to the receptor-driven cytokinin response are a) the dimerization of the receptor proteins, and b) the interaction with other signaling components. With regards to (a), it has been shown that *A. thaliana* cytokinin receptors form hetero- and homodimers (Dortay *et al.,* 2006; Wulfetange *et al.,* 2011a), but the relevance of these heterodimers in cytokinin signaling has so far not been elucidated. From bacterial histidine kinases it is known that heterodimerization occurs under experimental conditions, but have no biological relevance (Capra and Laub 2012). Since the biological relevance of heterodimers in plants cannot be excluded, it is possible that incompatibility of the PpCHK1 or PpCHK2 protein with AHK4 would potentially not restore the same functions as AHK2 or AHK3. For (b), interactions with other proteins (a multitude of proteins have been shown to interact with the different cytokinin receptors in *A. thaliana* (Dortay *et al.,* 2008)), and more specifically the downstream components, are likely to influence complementation since the interaction of the downstream components is prerequisite to phosphotransfer. To gain insights on the interacting partners of the PpCHK1 and PpCHK2 proteins, protein-protein interaction experiments (such as the previously suggested yeast-two hybrid or bimolecular fluorescence complementation experiments (Kerppola 2006)) could to be carried out.

Another biological factor that could potentially influence the complementation of the *ahk2 ahk3* mutant is the ectopic expression of *PpCHK1* and *PpCHK2*. It has been shown that the expression domains of cytokinin receptors, while sometimes overlapping, can also occur

temporally and spatially distinguished from one another (Higuchi *et al.,* 2004; Nishimura *et al.,* 2004; Riefler *et al.,* 2006). Furthermore, the *AHK4* gene expressed under the promoter of *AHK2* only partially complemented the *ahk2 ahk3* mutant, while *pAHK3:AHK4* did not complement the mutant phenotype at all (Stolz *et al.,* 2011). Taking these findings into account, the partial complementation of the *PpCHK1*- and *PpCHK2*-expressing plants show the receptors' ability to function in the *A. thaliana* cytokinin signaling system.

In order to account for possible disadvantages of the ectopic expression of *PpCHK1* or *PpCHK2*, it was investigated whether *PpCHK1* and *PpCHK2* can complement the lack of the *AHK2* and *AHK3* receptors when they are expressed in the expression domain of the lacking *A. thaliana* cytokinin receptors (*ahk2 ahk3*). *PpCHK1* was expressed under the control of the promoters of both *AHK2* and *AHK3* in turn, while *PpCHK2* was expressed under the control of the promoter of *AHK3*. In these analyses the GFP tag was replaced by the smaller myc tag, which was located at the C-terminus of the receptor protein.The generation of homozygote *A. thaliana* plants seemed to be impossible when the *PpCHK1* receptor was expressed in the domains of either *AHK2* or *AHK3*. While *PpCHK1* transgenic plants failed to yield primary transformants in the expression domain of *AHK3*, heterozygote *pAHK2::PpCHK1* plants were viable, but all potentially homozygote plants died (Figure 18). The effect of *PpCHK1* expression during embryo development was not analyzed in this study. In principle a role of the cytokinin receptor-driven cytokinin response in the development of *A. thaliana* embryos has been suggested by the fact that *A. thaliana* cytokinin receptor mutants germinated earlier than WT plants (Riefler *et al.,* 2006). Furthermore, cytokinin signaling has been monitored with a synthetical cytokinin reporter construct derived from a six-times concatenated core motif of AtRRB promoters fused to luciferase, and was found to be active during embryo development and especially during root stem-cell system establishment (Müller and Sheen 2008). Also AHK4 plays a role during embryo development (Mähönen *et al.,* 2000) and a gain-of-function allele of *AHK2* was found to reduce fertility in the embryo of *A. thaliana* (Jensen 2013). Further analyses are needed to investigate whether the deleterious effect of PpCHK1 on root growth is based on altered root stem cell establishment during embryo development.

Additionally, it should be noted that the potentially homozygote *pAHK2:PpCHK1* plants seem to be not only impaired in proper root formation, but also in root growth (Figure 18, C), and cytokinin is known to be involved in root growth (Werner *et al.,* 2001; Werner *et al.,* 2003; Miyawaki *et al.,* 2004; Riefler *et al.,* 2006; Argyros *et al.,* 2008; Heyl *et al.,* 2008). The exogenous application of cytokinin inhibits root growth (Beemster and Baskin 2000). Interference with cytokinin signaling, such as the knockout of one or two RRBs (Sakai *et al.,* 2001; Argyros *et al.,* 2008), one or two receptors (Riefler *et al.,* 2006), or depletion of cytokinin (Werner *et al.,* 2001; Werner *et al.,* 2003), leads to enhanced root growth and renders the respective mutants insensitive to cytokinin root growth inhibition. The root

growth-stimulating effect of the mutants is lost by the knockout of more components, such as the triple cytokinin receptor mutant *ahk2 ahk3 ahk4* (Nishimura *et al.,* 2004). The *wol* mutant (Mähönen *et al.,* 2000) which is a mutant allele of the *AHK4* cytokinin receptor locked in the phosphatase state (Mähönen *et al.,* 2006b), is also compromised in root development. Therefore the observed phenotype in the *pAHK2:PpCHK1* plants may be caused by two alternative scenarios:

In the first, PpCHK1 is functional as a cytokinin receptor, binds *trans*-zeatin (compare to section 4.1.1) which is predominant in the root (Hirose *et al.,* 2008), and activates the cytokinin signaling pathway extensively, thereby inhibiting root growth to a level were survival of the plant is not possible. Supporting this hypothesis is the fact that the 2124 bp *pAHK2* promoter (Stolz *et al.,* 2011) is more active than the native *AHK2* promoter, which may be due to the lack of additional regulatory elements in the applied *pAHK2* promoter (Jensen 2013). However, plants expressing *PpCHK1 GFP* fusion constructs under the *35S* promoter only rarely showed this effect. Whether the addition of the GFP tag to the receptor protein limited receptor function and therefore enabled plant growth remains to be investigated.

In the second scenario, the striking phenotype concerning the root in *pAHK2:PpCHK1* plants leads to the hypothesis that PpCHK1 may share the phosphatase quality with AHK4 in the absence of cytokinin (Mähönen *et al.,* 2006b) and AHK4 is known to have a predominant role in the root (Mähönen *et al.,* 2000; Inoue *et al.,* 2001). If PpCHK1 had this ability and had different ligand specificities, PpCHK1 would drain phosphoryl signals from the AtTCS system in the *AHK2* or *AHK3* domain and might establish a phenotype similar to the *wol* mutant. This hypothesis relies on different ligand specificities between the *A. thaliana* cytokinin receptors and PpCHK1. Since these hypotheses are highly speculative, it is necessary to investigate the cytokinin binding specificities of PpCHK1 and PpCHK2 (as suggested previously), and to discover whether any of the *P. patens* cytokinin receptors have phosphatase activity in the absence of the ligand, analogously to previous experiments showing the phosphatase activity of AHK4 (Suzuki *et al.,* 1998; Mähönen *et al.,* 2006b).

Conclusions on the function of PpCHK1 with respect to the organ, namely the roots, cannot be drawn because *P. patens* does not form roots. Rhizoids, organs that are sometimes referred to as “root like” structures, grow by tip growth (Sakakibara *et al.,* 2003; Bonhomme *et al.,* 2013), which differs substantially from multicellular root growth and the prior root stem-cell establishment in *A. thaliana.*

To compare the complementation assay of ectopic *PpCHK2* expression and the expression in the native expression domain of *AHK3*, the rosette diameter seems the most stable parameter among the *ahk2 ahk3* allelic transgenic lines due to significant changes in all PpCHK-expressing lines and can therefore be used for comparison. This comparison is especially interesting regarding the *35S::PpCHK2:GFP* lines and the *pAHK3::PpCHK2:myc*

lines. The GFP PpCHK2-fused lines exhibited a rosette diameter of 54-60% of WT, while *PpCHK2:myc* in the domain of *AHK3* restored 80% of the WT rosette diameter. Whether this increase is due to the limited expression domain or due to the exchange of the GFP to the myc tag cannot be concluded from the experiment. The activation loss of receptors fused to GFP in the PTA experiment (Figure 11 and Figure 12) indicates that the choice of the tag contributes at least partially to the observed differences. Conclusions about the effect of the GFP tag may be gained by repeating the complementation analysis under the *AHK3* promoter with GFP tag.

Taken together, the complementation experiments of the *ahk2 ahk3* double knockout mutant show that both *P. patens* receptors PpCHK1 and PpCHK2 have the ability to function as cytokinin receptors in *A. thaliana*.

4.1.6. Cytokinin receptors in *P. patens*

After collecting evidence that the predicted *P. patens* receptors PpCHK1, PpCHK2 and PpCHK3 have the ability to function as cytokinin receptors, the expression of all three was compared in protonema and gametophore tissue. The three receptors showed almost equal expression levels in both tissue types (Figure 21). This result was unexpected, as all EST evidence available for *PpCHK3* came from gametophore tissue (Appendix Table 2) and the PCR verification of the full-length transcript was only possible after changing the template from protonema- to gametophore-derived cDNA (PCR was carried out by the group of K. von Schwartzenberg, Universität Hamburg, (von Schwartzenberg *et al.,* in preparation)). It should be noted that the tissue was harvested from agar plates grown for different growth periods. This means that protonema and gametophores were the dominating tissue types, but it was not an exclusive isolate. A repetition of the experiment with a different method for sample harvest may enable the generation of cDNA exclusively from one tissue-type, and would then increase the resolution of the transcriptional differences between protonema and gametophores. However, the differences in *PpCHK1*, *PpCHK2* and *PpCHK3* transcripts between the two tissues must be small, because a difference in the current samples would be traceable otherwise. Why EST data for *PpCHK3* are only available from gametophore tissue remains unclear, and since the experimental procedure of the generation of the ESTs is not available it is not possible to understand the differences between the EST data and the transcript analysis.

PpCHK1 and *PpCHK2* fusion constructs with *GFP* under the 35S promoter were transformed into wild type and *Ppchk1 Ppchk2 P. patens* plants (*PpCHK3* was not available at this point). The transformation of *P. patens* with the N-terminally fused *GFP:PpCHK1* constructs generated only one line in WT *P. patens* and one in the mutant background, while

GFP:PpCHK2 generated multiple independent lines in WT *P. patens* and the mutant background. All previous attempts to localize the GFP fusion protein of PpCHK1 or PpCHK2 in *P. patens* protoplasts had failed. The strong effect of PpCHK1 is supported by the strong effect of PpCHK1 in the complementation of the *ahk2 ahk3 A. thaliana* mutants (section 3.1.3) and the PTA experiments (section 3.1.4). Experiments that suggest a role of cytokinin in the process of protoplast regeneration were carried out by Xiao *et al.* (2012), showing that *PpIPT9* is up-regulated during protoplast regeneration. How the cytokinin receptors PpCHK1 and PpCHK2 influence protoplast regeneration is not clear and should be investigated in the future.

4.1.6.1. Expression of GFP fusion proteins of PpCHK1 and PpCHK2 alters chloroplast development in WT *P. patens*

All transgenic lines were investigated for their phenotype in the protonema and the gametophore stages; and the transgenic lines generated with *GFP* fusion constructs of *PpCHK1* exhibited normal appearance. Among the transgenic lines transformed with *GFP* fusion constructs to *PpCHK2*, one line formed protonema but no buds.
A microscopic analysis of the generated transgenic lines revealed deregulation of the normal round shape of the chloroplast and of the chloroplast size and number. These effects were found in three of the four *PpCHK1* transgenic lines (Figure 22) and in all *PpCHK2* transgenic lines (Figure 24). The subcellular localization of the PpCHK1 or PpCHK2 receptor GFP fusion protein in the *P. patens* transgenic lines generated in the WT background might possibly be located at the plasma membrane, which would be consistent with the subcellular localization pattern found by investigating transiently-expressing tobacco epidermis leaves (Figure 13), but future experiments with appropriate marker proteins are needed. Furthermore immunoblot analyses of protein extracts from the generated transgenic lines should provide evidence on whether the full-length fusion protein is present in the generated mutants.

Research in *Physcomitrella* has postulated cytokinin's effect on plastid development since as early as 1979 (Ashton *et al.,* 1979a). Other information about cytokinin action in *P. patens* plastids came from the mutant PC22, generated by X-ray irradiation of *P. patens* spores (Abel *et al.,* 1989). Mutant PC22 has normal amounts of cytokinin compared to the WT (Reutter *et al.,* 1998), but is defective in the traits *plastid division* (*pdi*, and therefore possesses a mega chloroplast) and *gametophore development* (*gad*). The defect in *pdi* can be partially compensated by exogenous cytokinin (isopentenyladenine), resulting in multiple smaller chloroplasts which are still about five times as big as WT chloroplasts (Reski *et al.,* 1991; Kasten *et al.,* 1997). The defect in *pdi* can also be rescued by blue light (Reski *et al.,* 1991; Reutter *et al.,* 1998), and is fully restored after transgenic expression of *Agrobacterium IPT* (Reutter *et al.,* 1998). These results led to the conclusion that cytokinin signaling might

be affected in this mutant (Reutter *et al.,* 1998). The locations of the genes affected by the mutations in PC22 are still unknown. Further analyses of PC22 revealed that *Filamentous temperature-sensitive Z* (*FtsZ*) genes (a family consisting of four members: *PpFtsZ1-1*, *PpFtsZ1-2*, *PpFtsZ2-1* and *PpFtsZ2-2*) are involved in chloroplast division (Strepp *et al.,* 1998; Kiessling *et al.,* 2000; Gremillon *et al.,* 2007). The proteins FtsZ2-1:GFP and FtsZ2-2:GFP were localized to network-like structures around the chloroplasts and in the cytosol connecting the chloroplasts to each other in WT and PC22 protoplasts (Strepp *et al.,* 1998; Kiessling *et al.,* 2004). This fluorescent pattern was increased after cytokinin treatment in the case of FtsZ2-1:GFP, and slightly increased for FtsZ2-2:GFP in PC22 protonema (Suppanz *et al.,* 2007). The localization of the FtsZ:GFP proteins, their function in chloroplast division and shape, their response to cytokinin, and their potential overlap of protein localization with the PpCHK1 protein make the investigation of the interplay between these proteins interesting for future cytokinin research in *P. patens*.

Besides the microscopic evaluation, the *P. patens* transgenic lines (transformed with constructs encoding *GFP* fusions to either *PpCHK1* or *PpCHK2*) were also analyzed for transcriptional regulation of the transgene. In contrast to the C-terminally fused receptor constructs, a high overexpression of the transcript of N-terminal fusions of GFP to the receptor was observed in transgenic lines generated with *PpCHK1* and *PpCHK2* (Figure 22 and Figure 24 respectively), and raised the question of whether the receptors influenced the regulation of their own transcription. The finding that *P. patens* cytokinin receptors are regulated at the transcriptional level is in line with the transcriptional response of *AHK4* in *A. thaliana* , which was down-regulated in *A. thaliana* with reduced cytokinin status (Brenner *et al.,* 2005), and up-regulated after long (24 hours) cytokinin treatment (Rashotte *et al.,* 2003). In rice, the cytokinin receptor homolog to *AHK4* (*OsHK4*) was also up-regulated after induction with cytokinin (Tsai *et al.,* 2012). The authors suggested that this was due to a proposed phosphatase activity of this receptor, which would enable a fast reset of the cytokinin signaling pathway upon cytokinin depletion. In light of these findings, it is very interesting to investigate whether all three *bona fide* cytokinin receptors in *P. patens* have phosphatase activity (as suggested before).

From the transcriptional analyses of the transgenic lines, it is evident that all transgenic lines were altered at the transcriptional level with respect to the other investigated, potentially cytokinin signaling-related genes (these include *PpCHK1*, *PpCHK2*, *PpCHK3*, *PpCHK4* and *PpRR11*; Figure 22, B and Figure 24, B). The regulation of the potentially cytokinin signaling-related genes indicated, in turn, that those genes are in fact a part of a system that responds to the alterations induced by the transformation of the transgene. Additionally to the transcriptional regulation, all transgenic lines were tested on their response to different phytohormones (Figure 23 and Figure 25). Although the transgenic lines responded

differently to the applied hormones, no patter extended to all transgenic lines generated from one receptor. Conclusions about the consequences in individual transgenic lines await the clarification of the integration site of the transgene.

Altogether, three and all of the transgenic lines transformed with constructs of *GFP* fused to *PpCHK1* or *PpCHK2* showed altered chloroplast distribution or shape respectively. Additionally, the fact that chloroplast distribution or shape and GFP fluorescence occurred in transgenic lines of both receptors and both fusion orientations led to the conclusion that the *P. patens* cytokinin receptors might have a function related to chloroplast distribution and shape. This hypothesis is further supported by literature concerning cytokinin's effect in connection with chloroplasts in *P. patens.*

4.1.6.2. Expression of GFP fusion proteins of PpCHK1 and PpCHK2 in *Ppchk1 Ppchk2 P. patens*

The double knockout mutant *Ppchk1 Ppchk2* was used to generate stable mutants with 35S promoter driven fusion constructs of *GFP* to the receptors *PpCHK1* and *PpCHK2* (*PpCHK3* was not available at the time). Macroscopic phenotype investigations found the protonema to be altered in all PpCHK1 lines (Figure 26, A, upper quadrants), including the formation of brown pigments, deformed cells and more branching. Furthermore, one line exclusively formed protonema. The *PpCHK2*-expressing mutants showed more branching of the protonema in the case of C-terminally fused lines and pure protonema growth in all three N-terminally fused *PpCHK2* lines (Figure 28, A, upper quadrants). The strong effect of PpCHK2 in the double knockout mutant background corresponds well the transcriptional analysis. In the presence of *PpCHK1* (in the WT background), transcriptional up-regulation of *PpCHK2* was only present in conjunction with *PpCHK1* up-regulation (Figure 24). In the double knockout mutant *PpCHK2* was much more up-regulated and independent of *PpCHK1* (Figure 28). This finding is in accordance with the stronger effect of PpCHK1 than of PpCHK2 in the *A. thaliana ahk2 ahk3* mutant (section 3.1.3). On the cellular level, *PpCHK1* or *PpCHK2* transgenic lines had less or deformed chloroplasts in protonema and gametophore cells (Figure 26, A, lower right quadrants; Figure 28, A, lower quadrants) and GFP fluorescence was evident in all generated lines, but the localization of the *P. patens* cytokinin receptors PpCHK1 and PpCHK2 is not clear and needs further investigation (as suggested before). The linkage with chloroplast shape and distribution was also evident in the transgenic lines of *PpCHK1* or *PpCHK2* in the double knockout mutant background, as previously observed in the WT background. A role for PpCHK1 and PpCHK2 receptors in chloroplast development therefore seems likely. These observations should be analyzed in more detail, in order to gain insights into the regulatory functions of the cytokinin receptors in *P. patens*.

On the transcriptional level, *PpCHK1* transcripts of the C-terminally fused mutants were reverted to but not above WT levels, while the *PpCHK1* transcript in N-terminally fused transgenic lines was overexpressed (Figure 26, B), recapitulating the transgene regulation found in the WT background. In contrast to the *PpCHK1* mutants, all *PpCHK2* transcripts were up-regulated compared to WT levels in the PpCHK2 mutants (Figure 28, B). Altogether, the transcriptional comparison of the transgenic lines with the WT and the double knockout indicated that the three *P. patens* cytokinin receptors *PpCHK1*, *PpCHK2* and *PpCHK3* respond to the overexpression of *PpCHK1* or *PpCHK2* on the transcriptional level. Future experiments have been described previously and might shed light on the functionality of this regulatory circuit.

The *PpCHK1* and *PpCHK2* transgenic lines in the double knockout background (*Ppchk1 Ppchk2*) were further investigated on media supplemented with different hormones, but there was no common regulatory pattern for *PpCHK1* transgenic lines in the double knockout background. N-terminally fused transgenic lines of *PpCHK2* in the double knockout background were arrested in protonemal growth and never formed gametophores during the 30 day growth period. This drastic phenotype was consistent in all three transgenic lines and in all hormone treatments. The complete insensitivity to cytokinin in transgenic lines of GFP:PpCHK2 in the double knockout background is potentially based on a highly activated cytokinin signaling system that prevents the cytokinin response by locking the cytokinin signaling system via the negative feedback loop. To this end it has been shown that rice calli which overproduce the cytokinin receptor *OsHK6* do not green in response to cytokinin, and it has been suggested that the negative feedback loop of the cytokinin signaling system is responsible for this behavior (Choi *et al.,* 2012). Furthermore, such a highly activated system would require the presence of cytokinin, and it has been shown that the *A. thaliana* mutant *ahk2-3 ahk3-5* has higher levels of cytokinins than the WT (Riefler *et al.,* 2006), which would indicate a regulatory mechanism that increases cytokinin content in the case of low cytokinin signaling. This kind of regulation is also apparent in the *Ppchk1 Ppchk2* mutant, where levels of *trans*-zeatin-type and *cis*-zeatin-type cytokinins are elevated (von Schwartzenberg *et al.,* in preparation). How this may influence the response to other hormones such as auxin or ABA was not revealed by the hormone treatment analysis. But since auxin and ABA have antagonistic effects on cytokinin in *P. patens* development (Christianson 2000; von Schwartzenberg 2009), one could imagine that the effect of *PpCHK2* in the *Ppchk1 Ppchk2* background, with higher levels of cytokinin in the double knockout (von Schwartzenberg *et al.,* in preparation), could flood *P. patens* with cytokinin signaling and possibly drown the signals of ABA or auxin. Why PpCHK1 does not show this kind of stronger activity can only be speculated. If PpCHK1 was able to restore appropriate cytokinin levels, but not PpCHK2, this could explain the observed phenotypes.

In summary, the following conclusions and hypotheses can be made after the analysis of *PpCHK1* or *PpCHK2* overexpression in *P. patens*:

1) GFP fusion proteins of PpCHK1 and PpCHK2 are at least partially functional in *P. patens*, irrespective of their fusion side, because all mutants in the WT background respond more strongly to the cytokinin stimulus than the WT.

2) Results generated from gain-of-function experiments indicate that PpCHK1 and PpCHK2 might play a role in chloroplast development. The majority of the generated transgenic lines were altered in their chloroplast distribution or chloroplast shape. This hypothesis is supported by the literature, which denotes a regulation of chloroplast development that might involve PpFtsZ.

3) It is not clear whether PpCHK1 and PpCHK2 have phosphatase activity. Since mutants were generated in the WT background, which should not be altered in cytokinin levels, and the *Ppchk1 Ppchk2* double knockout background, which contains elevated levels of cytokinin, all generated transgenic lines were not cytokinin deficient and phosphatase activity should have been inactive.

4.1.6.3. Establishment of the area growth assay and its use to analyze *P. patens* mutants that express *PpCHK1* or *PpCHK2*

The area growth assay was established to monitor alterations that affect *P. patens* growth independent of the classical budding assay (Christianson 2000). A similar approach was published by Thelander *et al.* (2005), which characterizes protonema growth in-depth (Thelander *et al.,* 2005). Since cytokinin research has a long tradition in mosses (Gorton and Eakin 1957; Gorton *et al.,* 1957), but nothing was known about the molecular mechanism behind cytokinin's effect, the desired assay was meant to highlight the effect of the perturbation caused by the transgene as a general hint for further, more detailed experiments. Area growth of the transgenic lines was monitored for 30 days and individual area growth curves were compared (Appendix Figure 4, Appendix Figure 5, Appendix Figure 6, Appendix Figure 7). Due to the multitude of conditions and mutants, comparison of this data was demanding and another method of comparison was desirable. Since all area growth curves had an exponential area growth curve progression, area growth curves were approximated by an e-function and specific growth constants (Monod 1949) were deduced (see section 2.5.4.5). While this provided a comparable measure of these mutants' performance under given conditions, several parameters are neglected in this kind of presentation. First of all, the subject of the analysis is the two-dimensional expansion of area colonized by the respective mutant. Due to length of the growth period (30 days), some of the

plants formed gametophores and, naturally, grew in three dimensions. This growth was only measured when the gametophore expanded beyond the boundaries of the protonema. The formation of gametophores has furthermore been reported to influence protonema growth (Reski 1998). Secondly, three biological replicates were analyzed and in some cases high standard deviations were detected (Appendix Figure 4, Appendix Figure 5, Appendix Figure 6, Appendix Figure 7). These deviations were not considered for the approximation of the area growth curve with the e-function, and this approximation does not represent the true progression of the area growth curve. Clearly, the comparison of the derived specific growth constants is a crude way to compare area growth performance of the transgenic lines. Definite conclusions from the presented data are not possible and therefore the derived hypotheses require repeated experiments with more replicates to qualify the statistical relevance of the observed patterns.

In the following, the area growth assay results of the transgenic lines generated in the WT background will be discussed first. The relevant results and conditions will be briefly reviewed and then discussed in the context of current knowledge about the respective growth condition. Finally, transgenic lines generated in the double knockout background will be discussed in the same manner.

The results of the area growth assay of transgenic lines generated in the WT background indicated a general growth-promoting effect by the expression of PpCHK1 or PpCHK2 fusion proteins. This suggests functionality of the respective cytokinin receptor, because cytokinin treatment was followed by a stronger growth reduction than in the WT in all transgenic lines, with the exception of PpCHK1 #1N32 under 1 µM kinetin application. The influence of auxin was highlighted in the transgenic lines generated in the WT background (Table 25), where seven of eight transgenic lines had derived area growth constants that indicated a growth-promoting effect of auxin, while in the WT the derived area growth constant indicated a growth reduction after treatment with auxin (Table 25). It is known that auxin has an antagonistic effect to cytokinin during bud formation in *P. patens* (von Schwartzenberg 2009). Since high concentrations of cytokinin are known to inhibit *P. patens* growth (Ashton *et al.,* 1979b), auxin might cause a growth promotion in the generated transgenic lines.
The regulation of developmental processes through a close interaction of counteracting auxin and cytokinin has also been shown in *A. thaliana* and has recently been reviewed (El-Showk *et al.,* 2013). Similar regulatory mechanisms might be in effect here. On the other hand, direct transcriptional regulation after cytokinin treatment included auxin transcriptional repressors (IAA), AXR1 (which is involved in the degradation of IAA), and auxin efflux carriers (PINs) in *A. thaliana* (Brenner *et al.,* 2005; Brenner *et al.,* 2012), and such direct connection between cytokinin and auxin was not found in *P. patens* (Erxleben 2010; own results, data not shown). *P. patens* also does not exhibit polar auxin transport (Fujita *et al.,* 2008). The monitoring of

auxin action via *pGH3* or p*DR5* reporter fusion constructs in *P. patens* (Bierfreund *et al.,* 2003) applied to the generated transgenic lines might give insights on whether auxin distribution is altered due to enhanced cytokinin signaling.

The interaction of ABA and cytokinin was not indicated by the sole treatment of the transgenic lines with ABA, but when ABA and cytokinin were applied together to the generated mutants in the WT background, the area growth-inhibiting effect of cytokinin at a high concentration ((Ashton *et al.,* 1979b) and Table 25) was more pronounced in all transgenic lines. It is known that the application of ABA counteracts the formation of buds and instead favors the formation of tnema (short lived cells with sparse cytoplasm) or brachycyst cells (vegetative spores; Goode *et al.,* 1993) by intercalary division of protonema cells at a concentration of 100 µM (Decker *et al.,* 2006). In the area growth experiment 10 µM ABA were applied to the medium and it is possible that protonema tip growth was inhibited and intercalary cell division was about to be initialized. The growth-inhibiting effect of cytokinin and the potential tip growth-inhibiting effect of ABA could then synergistically alter the derived area growth constant. Further experiments with a higher dose of ABA or prolonged cultivation time could give insights into whether the onset of intercalary cell division was the reason for area growth inhibition. Apart from the synergistic effect of cytokinin and ABA observed here, the germination rate of the single *Arabidopsis* cytokinin receptor mutants *ahk2* or *ahk3* was reduced on medium containing ABA, indicating that cytokinin signaling acts as a negative regulator of ABA (Tran *et al.,* 2007). To elucidate the interaction of ABA and cytokinin in *P. patens*, it would be interesting to investigate tnema or brachycyte formation in different receptor knockout mutant combinations (generated and discussed in (von Schwartzenberg *et al.,* in preparation)).

The derived growth constants from transgenic lines generated in the WT background grown with an additional source of nitrogen (ammonium tartrate) indicated a growth-promoting effect in seven out of eight transgenic lines. Previous experiments demonstrated that the supplementation of ammonium tartrate to the medium does not increase dry weight and cell proliferation, but has an effect on the development – namely, it keeps *P. patens* protonema cells in the chloronema state, and hence acts as a growth regulator (Jenkins and Cove 1983; Hohe *et al.,* 2002; Schween *et al.,* 2003). Furthermore, cytokinin has been shown to inhibit chloronema differentiation into caulonema type protonema (Thelander *et al.,* 2005). The characterization of *PpNRT2* genes (a class of high affinity nitrate transporters) also contributed to this end, as it was found that, in contrast to higher plants, ammonium is a more potent inhibitor of the transcriptional regulation of nitrate transporters than nitrate (Tsujimoto *et al.,* 2007). This suggests a difference between nitrogen content control mechanisms in *A. thaliana* and *P. patens*. Consistent with the lack of literature concerning PpNRT1 proteins, Blast (Altschul *et al.,* 1997) with the AtNRT1-1 protein sequence (At1g12110.1) did not yield

a significant hit on the *P. patens* proteome[5], while Blast of the protein sequence of AtAMT1-1, an ammonium transporter (At4g13510.1), indentified five potential ammonium transporters in *P. patens*. In *A. thaliana* and maize it has been shown that cytokinin biosynthesis is increased after nitrate treatment, which is mediated in *A. thaliana* by the transcriptional up-regulation of *AtIPT3* (Takei *et al.,* 2002; Takei *et al.,* 2004). The up-regulation of RRAs in response to nitrate are possibly a result of increased cytokinin levels, which then affect nitrogen metabolism (Sakakibara *et al.,* 2006). While nitrate induced *AtIPT3* transcript levels after short nitrate treatment, ammonium only induced *AtIP3* after long-term treatment (11 days) (Takei *et al.,* 2004). Whether a similar mechanism to the up-regulation of cytokinin biosynthesis genes occurs in *P. patens* treated with ammonium is unknown, but ammonium's tendency to act as growth regulator could be established in a similar way to *A. thaliana* (ammonium →IPT → cytokinin signaling). This could also explain growth promotion, because cytokinin at physiological levels acts as a growth promoter, and only high levels of cytokinin inhibit growth (Ashton *et al.,* 1979b). Negating this hypothesis is the fact that bud formation, the typical cytokinin response, does not occur at elevated levels under ammonium treatment. Furthermore AtIPT3 belongs to the group of adenylate-IPTs and no report was found on tRNA-IPT enzyme response to nitrate stimulus. This is important because *P. patens* encodes exclusively tRNA-IPTs in its genome, hence it is questionable whether the different enzymes are regulated in a similar way. Further experiments on the interplay of ammonium and cytokinin biosynthesis might give insights on the nitrogen ←→ cytokinin regulation in *P. patens*. In general, cytokinin and nitrogen interaction in *A. thaliana* occurs mainly with cytokinin and nitrate (Sakakibara *et al.,* 2006), and recent studies have found cytokinin to be involved in nitric oxide (NO) degradation (Liu *et al.,* 2013) and S-nitrosylation of cytokinin signaling components (Feng *et al.,* 2013). Even though NO biosynthesis enzymes are present in *P. patens* (Plant metabolite network, PMN 8.0[6]), as well as an S-nitrosoglutathione reductase gene (Xu *et al.,* 2013), the mechanisms discovered in *A. thaliana* remain to be shown in *P. patens*. All other treatments (ampicillin; ampicillin and Glc [2%]; $NaCl_2$; sorbitol; calcium deficiency; phosphate deficiency) investigated with the mutant lines in the WT background generated such a variety of derived area growth constants that a conclusion cannot be drawn.

The monitoring of the area growth of transgenic lines generated from the *Ppchk1 Ppchk2* double knockout mutants indicated a general growth-promoting effect due to the expression of PpCHK1- or PpCHK2-GFP fusion proteins (Table 26) similar to the transgenic lines generated in the WT background (Table 25). Unlike the WT background, the application of cytokinin did not reveal a clear growth-inhibiting effect, and was in fact sometimes growth-

[5] http://www.cosmoss.org/bm/BLAST?type=0
[6] http://pmn.plantcyc.org/MOSS/NEW-IMAGE?type=PATHWAY&object=PWY-4983

promoting. Patterns that would allow for the explanation of the observed effects were not recognized, and instead indicate a disturbed response to cytokinin of the transgenic lines when compared to the WT. Other conclusions cannot be derived from the results under cytokinin treatment and any hypothesis would require the repetition of the experiment with more replicates.

4.2. Evolution of the cytokinin circuitry

The objective in the second part of the project was to increase our understanding of the evolution of the cytokinin signaling system. Previous analyses by Pils and Heyl (2009) demonstrated that *P. patens* was the earliest-diverging plant that encoded all components of the cytokinin signaling system in its genome, and that chlorophyte algae genomes encode some TCS components. While these were important results for the experimental design of this project, the nonexistence of genomic data of early diverging organisms in the land plant lineage, namely the charophyte algae, caused a gap in information on the evolution of the TCS in these organisms. The occurrence of components from the TCS, both in chlorophyte algae (Duplessis *et al.,* 2007; Pils and Heyl 2009) and in land plants, opened the possibility that the common ancestor of both lineages already had TCSs or that both lineages separately acquired them. In general, it is thought that the TCS entered the plant cell via primary endosymbiosis (Koretke *et al.,* 2000; Duplessis *et al.,* 2007; Spichal 2012), which means that the common ancestor of Chlorophytes and Streptophytes had a TCS. Thus the existence of TCS is not by itself an answer to the question of when the cytokinin signaling system was established. The answer to this question might be given by charophyte algae, which split very early from the land plant lineage (Wodniok *et al.,* 2011). The presented analysis therefore included data from charophyte algae in order to potentially gain insights into, firstly, how the cytokinin signaling system was established, and secondly, whether the TCS components found in chlorophyte algae potentially share a common ancestor with progenitors of the cytokinin signaling system. Due to the lack of genomic data from charophyte algae, the inclusion of EST data was necessary. While genomic data allow the alignment of predicted genes, EST data are fragments of the mRNA (Nagaraj *et al.,* 2007) and the alignment of ESTs together with transcripts would influence alignment quality by inserting many gaps. This was one of the reasons why the phylogenetic analysis was limited to protein domains which were extracted from the proteomes and the EST data. Moreover, the protein domains as structural and functional subunits of a protein (Vogel *et al.,* 2004a) underlie a selective force which is higher than in the interconnecting regions between the conserved domains – these connecting regions could potentially induce the formation of gaps in the alignment, thereby lowering the quality of the analysis. In order to determine when the cytokinin signaling system was established, it was important to determine whether the

investigated organism has the ability to regulate the abundance of the potential signaling molecule cytokinin. Due to the chemical nature of cytokinin as a derivative of adenine, cytokinins can be generated from the breakdown of tRNAs with a modified adenine adjacent to the anticodon (Koenig *et al.,* 2002), and tRNAs with such a modification have been found in all organisms except *Archae* (Persson *et al.,* 1994). This is why the existence of cytokinin in an organism alone does not give insights on its use as a hormone. Only cytokinin as a hormone requires coordinated synthesis, a signal transduction system for its perception and specific degradation to reset the pathway. Domains of cytokinin metabolism proteins were incorporated therefore into the analysis as well.

The available data were screened for the phylogenetic analysis, protein domains of interest were excised from the data and aligned before a phylogenetic tree was constructed. The use of protein domains allowed the integration of EST data into the analysis, but – due to the length of the protein domains, their characteristic as structural and functionally conserved subunits of a protein (Vogel *et al.,* 2004a), and the multitude of organisms in the analysis – bootstrap support of the branches was limited. The incorporation of many organisms is a known challenge in phylogenetic analyses (Nei 1996; Friedman *et al.,* 2008). A selection of the maximum likelihood phylogenetic trees generated here was also constructed with Bayesian interference method and reconciled the main clades of the investigated trees (Gruhn *et al.,* 2014). Furthermore, the reliability of the results obtained in this study is often supported by the presence of proteins with known biological function in one phylogenetic clade together with a grouping of proteins with other biological functions in another clade.

4.2.1. Phylogenetic analysis of protein domains incorporated in cytokinin signaling components

4.2.1.1. Insights on the evolution of cytokinin receptors

The analysis began with the investigation of the first component of the TCS in cytokinin signaling, the cytokinin receptors. They are composed of multiple protein domains (Figure 4; Inoue*, et al.* 2001; Suzuki*, et al.* 2001a; Yamada*, et al.* 2001), and phylogenetic analyses have been carried out for each domain independently (Figure 30 and Figure 31). All phylogenetic trees generated based on the protein domains found in cytokinin receptors showed the existence of eight additional histidine kinases from *P. patens* and one histidine kinase from *M. polymorpha* that incorporate a CHASE domain (Figure 30 and Figure 31). The domains derived from these proteins clustered together in a sister clade, clearly distinct from the already known cytokinin receptors from land plants and from *P. patens* in any of the generated phylogenetic trees (Figure 30 and Figure 31). In the following, members of this clade will be referred to as new potential cytokinin receptors. While the eight proteins from

clade will be referred to as new potential cytokinin receptors. While the eight proteins from *P. patens* were already annotated as histidine kinases (Rensing *et al.,* 2008), the histidine kinase from *M. polymorpha* was derived from a Blast search (Altschul *et al.,* 1990) generated with the query sequence of *AHK4* on the *M. polymorpha* genome (J. Bowman, Monash University, Australia[7]). The eight new potential cytokinin receptors of *P. patens* had not previously been annotated as potential cytokinin receptors; the domain search program previously used for the annotation of the *P. patens* genome was HMMer2 using PFAM HMM profiles release 20.0 (Rensing *et al.,* 2008), whereas this analysis was conducted with a later version (HMMer3) that was able to predict the CHASE domains in the respective proteins based on PFAM HMM profile release 24.0 (Table 24). The same applies to chlorophyte algae, which were previously thought to lack CHASE domain-containing receptors (Pils and Heyl 2009); this analysis identified two CHASE domain-containing receptors in each of *V. carteri* and *C. reinhardtii*. To exclude any errors caused by the locally emphasized prediction of domain boundaries by the new HMMer3 program, the domain boundaries of all hits were analyzed with HMMer2.

Additional information on these newly identified potential cytokinin receptors was gathered from the comparison of their amino acid sequence to amino acids known to be involved in cytokinin binding (Heyl *et al.,* 2007; Hothorn *et al.,* 2011). As already indicated by the clear separation and the long branch between the two clades in the phylogenetic tree (Figure 30), these residues were comparatively diverged in all new potential cytokinin receptors, compared to the *bona fide* cytokinin receptors (Figure 30 and Appendix Figure 8), hence there was no indication that these receptor proteins were functionally conserved. For example, one amino acid (Appendix Figure 8, 3, column M) that leads to a total loss of binding in the AtAHK4 protein when it is altered (Heyl *et al.,* 2007) was conserved in the *bona fide* cytokinin receptor clade and in two members of the new potential cytokinin receptors, but lost in the other members of the new potential cytokinin receptor proteins. Similar differences were observed for the other amino acids, which were compared. Whether these potential cytokinin receptors are able to bind cytokinin despite the divergence of the CHASE domain was investigated by the analysis of one new potential *P. patens* cytokinin receptor and the *M. polymorpha* receptor of this clade. The results of these studies indicated a function of these proteins as cytokinin receptors and will further be discussed in section 4.3. Whether one of the receptors from *Synechocystis* PCC6803 (gi:16329648; Slr1759), identified in the course of this analysis, could bind cytokinin was subject to a more detailed analysis carried out by M. Halawa (Freie Universität Berlin, research group Heyl). This protein and its domain architecture has previously been described, as Slr1759, and though a clear function of this

[7] since this service is not publically available, the sequence was provided to J. Bowman, Monash University, Australia, who ran the Blast search and returned the results as a kind gift (http://monash.edu/science/about/schools/biological-sciences/staff/bowman)).

receptor was not shown, experimental data hint at a function in redox perception which is related to photosynthetic and metabolic activity (Nodop *et al.,* 2006; Michel *et al.,* 2009). The comparison of the position of Slr1759 in the phylogenetic trees of the different receptor domains could not associate Slr1759 with a functional clade (a functional clade is defined as a clade to which members of the clade have been assigned the respective function in experiments (section 2.6.4)). The analysis by M. Halawa showed the absence of cytokinin binding (M. Halawa, personal communication). The relevance of this particular gene should therefore be investigated in more detail because it may represent an ancestral gene which was preserved in cyanobacteria and lost in plants. However, the lack of evidence from other cyanobacteria (which were also included in this analysis, such as *G. violaceus*) highlights the importance of investigating Slr1759 before speculating about its implications for the origin of cytokinin signaling TCS in plants.

The existence of more potential cytokinin receptors in *P. patens* was a surprise, since three *bona fide* cytokinin receptors are encoded in the *P. patens* genome (Pils and Heyl 2009). While this was unexpected, *P. patens* has been shown to encode more histidine kinases in its genome than other plants (Rensing *et al.,* 2008). The reasons for this expansion (our analysis provides evidence for 56 histidine kinase domains derived from *P. patens*, compared to 14 histidine kinase domains from *A. thaliana* in the dataset) are not known. Whether or not other basal land plants such as *M. polymorpha* also have more histidine kinases, and where they cluster in a phylogenetic tree, remains an interesting question for future research. Additionally, it would be interesting to investigate whether an expansion of the histidine kinase family is also present in *S. moellendorfii*, which is placed evolutionarily between *P. patens* and seed plants. From our analysis of the dataset, which gave evidence for 22 histidine kinase domains in the *S. moellendorfii* genome (data not shown), it was not possible to infer whether these 22 histidine kinase domains represent independent proteins, or if splicing variants are instead incorporated in this number. This should be clarified before drawing any conclusions on the evolution of histidine kinases in *S. moellendorfii*. But in any case this number is lower than the 56 histidine kinases found in *P. patens*, and more within the range of the 14 histidine kinase domains of *A. thaliana*.

Besides the question about specific roles of the identified potential cytokinin receptors, a broader perspective on what caused the expansion of the potential cytokinin receptors suggests the possibility of a more general evolutionary principle underlying the expansion. A more general evolutionary principle that might contribute to the expansion of histidine kinases in *P. patens* is highlighted by the fact that the cytokinin receptors incorporate two supradomains (Vogel *et al.,* 2004b) which are among the 200 most duplicated supradomains (Vogel *et al.,* 2004a). The occurrence of one supradomain, the HATPase domain of HSP 90 Chaperone/DNA Topoisomerase II/Histidinekinase, and Che-Y-like supradomain, is known in histidine kinases (Dutta and Inouye 2000; Vogel *et al.,* 2004a; Vogel *et al.,* 2004b). The

second supradomain, the double PAS supra domain, was revealed by the crystal structure of AHK4 CHASE domain (Hothorn *et al.,* 2011), which is structurally similar to two PAS-like domains (Ponting and Aravind 1997). Cytokinin receptors therefore incorporate two supradomains that are often expanded during the course of evolution. It will be an interesting question for future research what leads to the expansion of these often duplicated supradomains and whether there might be a common evolutionary principle.

The investigation of the different domains of cytokinin receptors also delivered some first clues on the existence of histidine kinases in charophyte algae, which might share their domain architecture with cytokinin receptors. The analysis of the RR domain showed two *Spirogyra pratensis* RR domain sequences clustered in the functional clade of the cytokinin receptors (Figure 31, C). This was further corroborated by the identification of a *Spirogyra* HATPase domain in the functional clade of the cytokinin receptors (Figure 31, B). The phylogenetic tree was constructed only with domain sequences that were different from each other – protein domains that were 100% identical were omitted from the analysis because they would not provide additional information and usually derive from splicing variants of the same gene. The occurrence of two EST derived RR domains therefore indicated that two different proteins include a RR domain. That these proteins have a domain architecture similar to cytokinin receptors is tempting to speculate – all other full-length proteins in the clade of cytokinin receptors shared the same domain architecture – but only the extension of these ESTs will provide insight on the existence of putative cytokinin receptors in *S. pratensis*. Whether the EST derived HATPase domain of *S. pratensis* is part of one of the proteins that contain the RR domain, or represents a different protein, could not be concluded from the available sequences because no overlap between the three ESTs could be found (data not shown). However, these protein domains indicate the possibility that charophyte algae possess potential cytokinin receptors and provide a good starting point to identify the latter in the *Spirogyra* genome, once it becomes available. The presence of potential cytokinin receptors in charophyte algae would then point to an early establishment of potential cytokinin receptors in the streptophyte lineage.

4.2.1.2. Type-C response regulators might derive from receptor proteins

Another key result of the analysis contributed to our understanding of the evolution of cytokinin receptors. The phylogenetic tree generated from the RR domains showed functional clades for different histidine kinases characterized in *A. thaliana*, including cytokinin receptors, ethylene receptors, CKI1 and CKI2 receptors, AHK1 osmosensors and phytochromes (Yeh and Lagarias 1998; Hutchison and Kieber 2002; Lohrmann and Harter 2002; Schaller *et al.,* 2002; Mizuno 2005; Tran *et al.,* 2007; Schaller *et al.,* 2011). Next to

these functional clades with well described proteins, a clade containing the known type-C response regulators (RRCs; Figure 31, C) grouped. The occurrence of the RRCs as a sister clade to the TCS-derived histidine kinases in plants has already been shown (Schaller *et al.,* 2002; Kiba *et al.,* 2004). These results only included *A. thaliana* RR domains and were not commented on in the respective publication. While the phylogenetic tree presented here contains RR domains of different organisms (Figure 31, C), the previous analyses support the positioning of the RRCs as a sister clade to the receptors. The presence of two proteins, one from *S. moellendorfii* and one from spruce (both also contained a HATPase domain), indicates a possible origin of these RRCs from receptors. This is also in accordance with the fact that *ARR22* overexpresser (*ARR22ox*) mutants (Gattolin *et al.,* 2006; Horák *et al.,* 2008) phenotypically resemble the *wol* phenotype (Mähönen *et al.,* 2000), that is, they are dwarf plants with compromised root development. The resemblance of *ARR22ox* mutants with the *wol* plants suggests that the phosphatase activity of AHK4 is established via its RR domain, which was indeed absent after mutation of the canonical Asp in the AHK4 RR domain (Mähönen *et al.,* 2006b). This is also in accordance with the idea that ARR22 (an RRC) plays a role as a negative regulator in cytokinin signaling (Kiba *et al.,* 2004; Gattolin *et al.,* 2006; Horák *et al.,* 2008), possibly by taking over the phosphoryl group from the AHP proteins (Kiba *et al.,* 2004) to themselves, and subsequent dephosphorylation. Furthermore the RRCs share the domain architecture with the RRAs in *A. thaliana*, but are not inducible by cytokinin treatment, indicating that AtRRAs and AtRRCs have a different role in the cytokinin signaling system. It would be interesting to study the consequences of the expression of RRC from different species in *A. thaliana* to determine if the respective protein phenocopies the *ARR22* overexpression phenotype. To investigate whether RRCs are functional as phosphatases in cytokinin receptors, one could imagine that domain swap experiments, such as those presented for the AHKs N-terminal CHASE domain (Stolz *et al.,* 2011) with the C-terminal response regulator domains of the receptor and the RR domain of the RRCs would give insights. Furthermore phosphatase assay as shown for AHK4 by Mähönen, *et al.* (2006), conducted with RRCs might elucidate a similar regulatory mechanism of RRCs and phosphatase active cytokinin receptors.

4.2.2. Phylogenetic analysis of domains derived from downstream cytokinin signaling components

4.2.2.1. The response regulator domain

The response regulator domain is not only part of the cytokinin receptor, it also occurs in the downstream cytokinin signaling components – the RRBs and the RRAs. The phylogenetic tree of all RR domains in the dataset therefore included RRBs and RRAs (Appendix Figure 9). The subtree containing RRBs and RRAs also included the PRRs (Figure 32). The analysis

of the topology of the tree within the functional clades is beyond the resolution of the analysis, due to low bootstrap support, but coincides with previous results (Schaller *et al.,* 2002; Pils and Heyl 2009; Satbhai *et al.,* 2011). No charophyte RR proteins were found in the phylogenetic subtree of RRBs, RRAs and PRRs (Figure 32). Concerning RR proteins of charophyte algae, the investigation of ESTs is not sufficient to conclude on the absence of RR proteins from charophyte proteomes. Therefore the presence of RR proteins should be investigated once a complete charophyte algae genome is available. The phylogenetic distribution of these putative charophyte RR proteins is of special interest, because the presence of RRAs in addition to RRBs and RRCs would indicate the origin of RRAs from charophyte algae, while the absence of RRAs and presence of RRBs and PRRs would indicate the origin of the RRAs and, with that, the origin of the complete cytokinin signaling pathway in the last common ancestor of land plants. The phylogenetic clustering and analysis of the canonical DDK motif showed that the phylogenetic grouping of the cytokinin signaling components is not dependent on the conservation of the motif. The conservation of the domain architecture among RRs was clearly separated according to their biological function, with the exception of single-domain proteins that occurred in all functional clades (Figure 32). Furthermore, non-canonical as well as canonical RR domains have been identified in all functional clades, but non-canonical members of the RRAs are limited to spruce, which might reflect a suboptimal genome annotation. The previously applied criteria for how to group a RR protein (conventional criteria: RRBs consist of a RR and a Myb-DNA binding related domain; RRAs are single RR domain proteins (Imamura *et al.,* 1999) and PRRs are non-canonical proteins and have a CCT or WD40 domain (Mizuno 2004)) are not consistent with the phylogenetic distribution of the RR domains. Only recently, it has been suggested that annotation of the component group should be inferred from the phylogenetic relationship of the protein rather than from its domain architecture (Heyl *et al.,* 2013). For example, the *P. patens* PRRs, which have been annotated as PRRs because of their domain architecture (Satbhai *et al.,* 2011), have been shown to act as oscillators that coordinate the physiological response to the light-dark shift in *P. patens* (Holm *et al.,* 2010), and are also functional for phosphate transfer (and carry the DDK motif) in an *in vitro* assay (Satbhai *et al.,* 2011). Future research on *P. patens* cytokinin signaling should, due to the acceptance of the phosphoryl group, take into account the PRRs.

In general, investigations on the functions of proteins from a) chlorophyte algae, and b) proteins that do not match the conventional criteria of RR protein grouping, will provide insights on the relevance of these proteins in the TCS-regulated functions. Concerning (a), proteins of chlorophyte algae, conservation of the biological function in other proteins from the same functional clade would indicate a common origin of these proteins from a common ancestor protein that is likely to have had these properties already. Conversely, the absence

of functionally conserved RR proteins in chlorophyte algae might indicate a neo-functionalization of the respective protein in Streptophytes. With respect to (b), the functions of the single-domain proteins found among the RR proteins in comparison to the known RRA proteins should show whether the domain architecture or the sequence similarity of the RR domain directs protein function. However, it has only recently been shown that RR proteins from a different phylogenetic subgroup among the RRBs may complement the *arr1 arr12* mutant of *A. thaliana*, while members of the same RRB-subgroup did not (Hill *et al.,* 2013). It should be noted that RRBs also carry a MYB-DNA binding-related domain necessary for function and the phylogenetic relationship of this domain has not been investigated in this study, so the ability to complement might be indicated by sequence similarity of the MYB-DNA binding-related domains.

4.2.2.2. Histidine phosphotransfer proteins

The phylogenetic analysis of the HPT domain showed a cluster of single-domain proteins from land plants in the dataset including charophyte algae. The presence of single-domain HPT proteins in charophyte algae contributes to the idea that a complete TCS was present in charophyte and chlorophyte algae, and hence also in ancient green algae. This cluster included proteins from the cytokinin signaling system (Figure 33). The rest of the tree consisted of proteins of chlorophyte algae, bacteria, cyanobacteria, other organisms and one of bryophyte origin. The corresponding full length proteins displayed a wide array of additional domains, but also few single domain proteins were found among these, which often derived from EST sequences. Due to the nature of EST, as parts of the mRNA, these domains may represent larger proteins than predicted from the EST sequence (Figure 33, 4). This part of the tree also included an HPT domain from *M. polymorpha* that derived from a two-domain EST. The translated amino acid sequence of this EST was used as a query for Blast (Altschul *et al.,* 1997) of the non-redundant database at the NCBI, and returned a 100% match to a histidine kinase of *Pseudomonas fluorescens* (Sequence ID: ref|WP_003217742.1). It may therefore be regarded as a contamination. This is further corroborated by the position of the respective RR domain in the RR domain tree among other bacterial RR domains.

The analysis of the canonical His of the HPT domain identified non-canonical members exclusively among vascular plants. Since the non-canonical AHP6 protein was shown to be a negative regulator in cytokinin signaling (Mähönen *et al.,* 2006a), it seems that this kind of regulation was established during evolution of the vascular plants. The presence of negative regulatory HPT proteins in vascular plants is in line with the theory that vascular plants created more complex hormone signaling networks to coordinate growth of their complicated body plan (Rensing *et al.,* 2008).

4.2.3. Phylogenetic analysis of domains derived from enzymes involved in cytokinin metabolism

The analysis of protein domains from IPT-, LOG- and CKX-proteins, which are involved in cytokinin metabolism, revealed a pattern in phylogenetic tree topology. All three phylogenetic trees had two clades in common: i) a clade that included protein domains from vascular plants, bryophytes and lycophytes ('clade I'), and ii) a clade that included solely protein domains from vascular plants ('clade II'). No protein domain derived from charophyte algae was found in these phylogenetic trees. Furthermore, IPT and LOG phylogenetic trees contained a clade of general metabolism protein domains which are most likely not involved in cytokinin biosynthesis. It has previously been proposed that a more complex hormone signaling network was established in vascular plants to coordinate the growth of their complicated body plan (Rensing *et al.,* 2008) and the separation into clades I and II seem to corroborate this theory.

4.3. Characterization of members of the new receptor clade: PpCHK4 and MpCHK1

In section 3.2.1 and 4.2.1.1 I describe the discovery of a group of potential cytokinin receptors. Two proteins were chosen from these nine potential cytokinin receptors as candidate proteins for further analysis (section 3.2.1). Both genes were synthesized according to their gene models (for details on the synthesized DNA sequence please refer to section 9.2.6 and 9.2.7). This synthesis, in contrast to classical cloning, carries the disadvantage that the synthesized sequences may not be correct. Until the cDNA sequence can be verified from biological samples, there is considerable uncertainty about the composition of the resulting protein and its properties. Owing to these caveats, positive results of the analyses can be taken as a hint towards correct annotation of the gene and functionality of the respective protein; negative results, however, may reflect the inadequate annotation of the gene.

Both potential cytokinin receptors were analyzed in the cytokinin binding assay. While cytokinin (*trans*-zeatin) bound to MpCHK1 at significant levels, cytokinin binding to PpCHK4 was not significant and high standard deviations indicated the presence of cytokinin binding in some samples but not others (Figure 34, A). Furthermore, protein blot analysis showed comparatively low levels of the PpCHK4 protein compared to MpCHK1 (Figure 34, B). The expression of a functional cytokinin receptor (*AHK4*) in *E. coli* has previously been difficult, and closer analysis revealed that a high rate of mutations were introduced into the *AHK4* gene, rendering it non-functional (Nielsen 2005). A preselection of the colony to be tested was therefore established in the assay which would activate a reporter gene in the presence

of a functional cytokinin receptor and cytokinin, before proceeding to the binding assay. These experiments were carried out by M. Halawa and showed cytokinin binding to the PpCHK4 receptor. It can be concluded that both potential cytokinin receptors bound cytokinin.

To investigate whether the two potential cytokinin receptors can also translate the cytokinin binding into a TCS signal, both receptors were analyzed in the *E. coli* complementation assay (2.4.8). Both receptor proteins activated the reporter gene. While PpCHK4 clearly activated the TCS reporter gene compared to the positive control, MpCHK1 activated the reporter gene only weakly (Figure 35). Furthermore, the reporter gene activation by PpCHK4 suggested that this receptor binds with different specificities to the different applied cytokinins. Among the tested cytokinins, *trans*-zeatin was the most effective activator of the reporter gene (Figure 35). This result is very interesting and should be investigated further, because the crystal structure of AHK4s CHASE domain revealed certain residues to be involved in the binding of *trans*-zeatin (Hothorn *et al.,* 2011), and the amino acids in the respective positions of the CHASE domain of the new potential cytokinin receptors are significantly less conserved than in the *bona fide* cytokinin receptors (Appendix Figure 8, position K to M). Nevertheless, since PpCHK4 is able to bind *trans*-zeatin, there seem to be other structural features in the CHASE domain of PpCHK4 that still enable the binding of *trans*-zeatin. As a result of these experiments, M. Halawa is currently pursuing the crystallization of the CHASE domain of PpCHK4, to determine whether other amino acid changes in the CHASE domain enable the binding of *trans*-zeatin in PpCHK4 despite the divergence of the amino acids responsible for *trans*-zeatin binding in AHK4.

While my results confirmed PpCHK4's ability to function as cytokinin receptor, they do not give a definite answer for MpCHK1. It should be noted that AHK2 also fails to activate the TCS in bacteria (Suzuki *et al.,* 2001a), but cytokinin binds to the CHASE domain of the AHK2 receptor (Stolz *et al.,* 2011), and AHK2 is generally accepted as a true cytokinin receptor (Nishimura *et al.,* 2004; Riefler *et al.,* 2006). There are possible causes of weak activation of the reporter gene in the *E. coli* complementation assay. Firstly, as mentioned above, it is not clear whether the DNA sequence used to express the protein encodes for that protein's correct sequence – the sequence is not supported by biological data (i.e. ESTs) and deviations from it would influence the correct folding and directly affect the functionality of the protein. The binding of cytokinin does not contradict this hypothesis, because the ligand binding (CHASE) domain may be correctly annotated and it has been shown that the expression of the CHASE domain by itself is sufficient to bind cytokinin (Heyl *et al.,* 2007; Hothorn *et al.,* 2011). Secondly, the weak activation of the reporter gene may be due to histidine kinase activity that is independent from cytokinin binding. However, such constitutive activation was present when CKI1 was analyzed in this assay (Yamada *et al.,*

2001) and showed a high level of reporter gene activation, so this possibility seems less likely. Furthermore, and contradictory to an unspecific activation, is the significant increase of reporter gene activity dependent on cytokinin concentration, which should be unaffected in the case of cytokinin-independent activation of the reporter gene. Thirdly, the corresponding protein levels have not been shown for the tested *E. coli* extracts, and the low activation of MpCHK1 may reflect less receptor protein in the sample.

Both receptors were shown to bind cytokinin and potentially activated the TCS in *E. coli*, and so were good candidates to act in cytokinin sensing *in planta*. To test whether PpCHK4 or MpCHK1 have the ability to activate the AtTCS, both proteins were expressed in *A. thaliana* protoplasts of *ahk2 ahk3* double receptor knockout plants. While PpCHK4 activated the AtTCS to the same extent as AHK4, no activation was shown when MpCHK1 was expressed as an N-terminal fusion protein to GFP (Figure 36 and Figure 37). It should be noted that previous experiments showed that fusion proteins of PpCHK1, PpCHK2 and AHK4 to GFP had weaker activation capacity than the corresponding unfused receptor proteins (Figure 11 and Figure 12). Taking into account the weak activation of the *E. coli* TCS by MpCHK1, it may be the case that MpCHK1 activates the AtTCS at a low level, and that this activation is abolished by the fusion to GFP. Experiments with the untagged MpCHK1 protein and a higher number of samples to generate a statistically more robust result could give insights into whether or not this is actually the case.

The subcellular localization of N-terminal fusion proteins of the two potential cytokinin receptors PpCHK4 and MpCHK1 to GFP were investigated and found to partially co-localize to the FM4-64 stained plasma membrane (Figure 38). Both fusion proteins showed a localization that corresponds to the subcellular localization of AHK3 (Kim *et al.,* 2006; Wulfetange *et al.,* 2011a). Furthermore, the localization to the plasma membrane and the ER is supported by the subcellular fractionation of the proteins of the analyzed tobacco cells (Appendix Figure 14). Fusion proteins of PpCHK4 and MpCHK1 with GFP were only detectable in the membrane-enriched fraction. The localization of the PpCHK4 protein to the same compartment as the *bona fide* cytokinin receptors raises questions over the extent to which PpCHK4 overlaps in its functionality with the *bona fide* cytokinin receptors of *P. patens*. It would be an interesting question for future research to investigate the specific function of the new potential cytokinin receptors, to gain insight on why such a high number of cytokinin receptors are present in *P. patens*. On the other hand, the localization of the PpCHK1 and PpCHK2 proteins in *P. patens* stable lines differed from the localization in tobacco cells (section 3.1.1 and 3.1.4). Future research should therefore focus on the localization of the new potential cytokinin receptors compared to the *bona fide* cytokinin receptors in *P. patens*, in order to identify whether there are differences in the subcellular localization of the receptor

proteins, which would in turn indicate different specializations of the proteins. Regarding MpCHK1, the congruent subcellular localization supports the idea of MpCHK1 as a functional cytokinin receptor. However, localization studies with the *P. patens* cytokinin receptor indicated differences between the tobacco and the native system, and a repetition of the localization study in *M. polymorpha* would therefore be preferential.

Even though the presented data strongly suggest that PpCHK4 and MpCHK1 are cytokinin receptors, the biological role of the new potential cytokinin receptor in *P. patens* is unclear as *bona fide* cytokinin receptors are also encoded in the genome (Rensing *et al.,* 2008; Pils and Heyl 2009). Furthermore, the triple knockout mutant *Ppchk1 Ppchk2 Ppchk3* is insensitive to cytokinin (isopentenyladenine) in the budding assay (von Schwartzenberg *et al.,* in preparation). More experiments investigating the triple knockout mutant *Ppchk1 Ppchk2 Ppchk3* on the activity of different cytokinins in the budding assay might give insights into whether and where the new potential cytokinin receptors could play a biological role. Additionally, more information on all the cytokinin receptors in *P. patens*, such as their temporal and spacial expression patterns during plant development, might give insights into differences between the receptor proteins.

Analogous to the first functional annotation of AHK4 (Inoue *et al.,* 2001; Suzuki *et al.,* 2001a; Yamada *et al.,* 2001), the results presented above show the functionality of the two potential cytokinin receptors as genuine cytokinin receptors, hence these two proteins may be labeled as such. Whether this also applies to the other seven PpCHK proteins in the new receptor clade remains to be confirmed.

4.4. Potential avenues for research in cytokinin signaling in *P. patens* and the evolution of cytokinin signaling

4.4.1. Future research on cytokinin signaling in *P. patens*

4.4.1.1. *P. patens* cytokinin receptors

This study shows that the two investigated (of three total) *bona fide* cytokinin receptors in *P. patens* fulfill the requirements of cytokinin receptors and have the ability to complement the *ahk2 ahk3* knockout mutant in *A. thaliana* (section 3.1). Furthermore, *P. patens* has a more complex signaling system for cytokinin because, additionally to the three cytokinin receptors, eight other receptors were identified with the same domain architecture. Of these eight receptors, one member was shown to be functional in the TCS of *E. coli* and activated a reporter gene via the AtTCS (section 3.3). However, the role of this cytokinin receptor in *P. patens* remains unclear. An increased number of receptors could indicate a more complex array of input signals leading to the same output (Capra and Laub 2012). While this

hypothesis is derived from evolutionary insights about TCSs in general, this would imply different specificities of the ligand-sensing CHASE domain in the cytokinin receptors. Up until now, different ligand specificities have been observed for the CHASE domains of AHK2, AHK3 and AHK4 (Yamada *et al.,* 2001; Romanov *et al.,* 2005; Romanov *et al.,* 2006; Stolz *et al.,* 2011), but experimental data are not enough to predict ligand specificities of a CHASE domain from the amino acid sequence. Even though the crystal structure of the AHK4 CHASE domain showed the involvement of different amino acids in cytokinin binding (Hothorn *et al.,* 2011), the binding of PpCHK4 to *trans*-zeatin – despite the divergence of amino acids shown to be critical for *trans*-zeatin binding in AHK4 (Appendix Figure 8) – suggests that more information about the different CHASE domains are needed to understand which region of the CHASE domain or which amino acids are responsible for the establishment of ligand specificity. It will therefore be interesting to investigate binding specificities of the different known CHASE domains in order to identify common sequential or structural properties of the domains with similar ligand specificities. Experimental work in this direction has begun with the attempt to crystallize the CHASE domain of PpCHK4 (M. Halawa, Freie Universität Berlin).

4.4.1.2. Cytokinin signaling in *P. patens*

While it was initially thought that the TCS of *P. patens* was less complex than in *A. thaliana* due to its limited number of components (Pils and Heyl 2009), more potential components have been found at the output level of the cytokinin signaling pathway than previously anticipated (Satbhai *et al.,* 2011). The PpPRR proteins are regulated in circadian rhythm (Holm *et al.,* 2010) and are canonical RR proteins, and so may also function in the TCS pathway (Satbhai *et al.,* 2011). It should be noted that, so far, there are no data available that show the transcriptional regulation of RRAs upon cytokinin treatment in *P. patens*. One experiment carried out with isopentenyladenine, for potential induction of the cytokinin signaling system in *P. patens*, did not identify RRAs or other TCS components to be transcriptionally up-regulated after isopentenyladenine treatment (Erxleben 2010). During the course of my project, induction experiments were also conducted using the cytokinin kinetin, and up-regulation of the *PpRR11* transcript was shown in qRT-PCR analyses (data not shown). This RRA was therefore included in the analysis of the cytokinin receptor-overproducing *P. patens* transgenic lines, which had altered transcript levels of *PpRR11* compared to the WT (Figure 22, Figure 24, Figure 26 and Figure 28). It should be noted that microarray experiments after kinetin treatment did not verify the induction of *PpRR11* (preliminary results, data not shown).

Concluding from the multitude of potential cytokinin receptors (Figure 30), the possibility of TCS signal transduction via PRRs that are associated with circadian rhythm (Satbhai *et al.,*

2011), and the questionable inducibility of the RRAs after cytokinin treatment, it seems as if cytokinin signaling is regulated differently in *P. patens* than in *A. thaliana*. Similar to cytokinin signaling, components from ABA, auxin and gibberellin signaling have been identified in *P. patens* (Yasumura *et al.,* 2007; De Smet *et al.,* 2011; Hanada *et al.,* 2011), but the respective analogous regulatory pathways were not identified in *P. patens*. The difference between the cytokinin signaling system in *P. patens* and *A. thaliana* (as a representative of vascular plants) is further corroborated by the analysis of the phosphoproteome after cytokinin stimulus in *P. patens* (Heintz *et al.,* 2006). While 50% of the identified proteins were of unknown function, the authors come to the conclusion that cytokinin treatment leads to rapid phosphorylation of proteins in plastids (Heintz *et al.,* 2006). Even though the importance of cytokinin action on plastids was also found in *A. thaliana* by similar experiments (Cerny *et al.,* 2011), the regulated proteins overlapped only in two cases (Cerny *et al.,* 2011), highlighting the difference in the molecular cytokinin response in these two organisms.

4.4.1.3. Biological role of PpCHK1 and PpCHK2

Attempts to find the biological role of PpCHK1 and PpCHK2 by overexpressing the respective receptor in *P. patens* WT and the double knockout *Ppchk1 Ppchk2* mutant indicated a role for both receptors in the regulation of chloroplast shape and division (section 4.1.5). Although the underlying mechanisms remain to be discovered, a potential regulatory cue was inferred from the literature (involving the PpFtsZ protein, for details please refer to section 4.1.5), which need further investigation. In a more general context, chloroplast development has been seen to be affected by the cytokinin status of a plant before (Werner *et al.,* 2008; Cortleven and Valcke 2012), and the involvement of cytokinin was shown by inducing changes of thylakoids (Seyer *et al.,* 1975), grana (Naito *et al.,* 1981), chloroplast ripening in conjunction with light (Axelos and Péaud-Lenoel 1980; Colijn *et al.,* 1982), regulation of plastid protein levels (Axelos and Péaud-Lenoel 1980; Lew and Tsuji 1982; Axelos *et al.,* 1984), and transcription in chloroplasts (Kasten *et al.,* 1997; Zubo *et al.,* 2008). However, the molecular modes of action underlying these processes have not been discovered yet.

Further functions of cytokinin signaling in *P. patens* might be identified by generating a mutant of the least common cytokinin signaling component, which are the two *P. patens HPT* genes. The generation of the *Pphpt1 Pphpt2* double knockout mutant to abolish cytokinin signaling would possibly abolish the TCS-mediated cytokinin response in *P. patens*, thus providing important clues on TCS-mediated cytokinin response in *P. patens*. Such an approach was already pursued in *A. thaliana*, where the quintuple HPT knockout mutant forms a dwarf plant (Hutchison *et al.,* 2006; Deng *et al.,* 2010). The generation of the triple knockout receptor mutant in *P. patens* (von Schwartzenberg *et al.,* in preparation) was aimed at producing a similar effect, but, as we now know, the potential cytokinin receptors might

compensate for the knockout of the *bona fide* receptors. The generation of the double knockout *Pphpt1 Pphpt2* mutant would therefore be an important milestone in the elucidation of cytokinin signaling in *P. patens*.

4.4.2. Implications for research on the evolution of the cytokinin signaling system

The investigation of the evolution of the cytokinin signaling system brought two major novelties to light: first, the *P. patens* genome encodes for more potential cytokinin receptors than anticipated (compare to section 4.4.1); second, the genome of the charophyte algae *S. pratensis* might encode for potential cytokinin receptors (section 4.2.1.1). Regarding the cytokinin signaling system as a whole, the potential existence of cytokinin receptors in charophyte algae and the presence of HPTs makes it tempting to speculate that the full cytokinin signaling toolset already exists in charophyte algae. But potential IPT and LOG proteins and CKX enzyme were not identified in charophyte algae.

Altogether, this work presents evidence that PpCHK1, PpCHK2 and PpCHK4, as well as MpCHK1, are cytokinin receptors. Furthermore, it indicates that PpCHK1 and PpCHK2 play a role in chloroplast development in *P. patens*, and that cytokinin signaling is regulated differently in *P. patens* than it is in *A. thaliana*. The analysis of the phylogeny of the cytokinin signaling system identified a new group of cytokinin receptors in *P. patens* and suggests the possible existence of cytokinin receptors in charophyte algae.

5. Summary

Cytokinins are important plant hormones and as such they trigger a wide range of responses in plants. Cytokinins are perceived by membrane-located histidine kinases and transduce the signal via the His-to-Asp phosphorelay system, which also includes histidine phosphotransfer proteins and response regulators. The cytokinin signal transduction system is well understood in higher plants, but knowledge about the molecular principles of cytokinin signal transduction in basal land plants is limited.

The first part of this project therefore investigated the first step of signal transduction in the basal land plant *P. patens.* Experiments on the functionality of the bioinformatically predicted *P. patens* cytokinin receptors showed that PpCHK1 and PpCHK2 bind cytokinin, and that PpCHK3 converts cytokinin presence into a two-component system output in *E. coli* cells. Transient expression in tobacco also suggests that the *P. patens* cytokinin receptors PpCHK1, PpCHK2 and PpCHK3 could fulfill a similar function to the *A. thaliana* cytokinin receptors, concluded mainly from its localization. Furthermore, the *A. thaliana ahk2 ahk3* double knockout mutant was used to analyze the complementation capacity of two cytokinin receptors on the whole plant level. This complementation experiment showed that both tested *P. patens* receptors (PpCHK1 and PpCHK2) have the ability to function as cytokinin receptors in *A. thaliana*.
Generated mutant lines of *P. patens*, transformed with GFP fusion constructs of *PpCHK1* or *PpCHK2*, showed changes in chloroplast distribution or shape in transgenic lines of both receptors and both fusion orientations, which led to the conclusion that the *P. patens* cytokinin receptors might have a function related to chloroplast distribution and shape. Altogether, it was shown that PpCHK1 and PpCHK2 are functional cytokinin receptors. While their function in *P. patens* seems involved in chloroplast development, these receptors are able to fulfill a function analogous to cytokinin receptors in *A. thaliana*, but a role in chloroplast development was not apparent in *A. thaliana*.

The objective of the second part of the project was to increase our understanding of the evolution of the cytokinin signaling system. For analysis, a domain-based approach was chosen. To gain insights into the origin and evolution of the cytokinin regulatory system, key components of the cytokinin signaling pathway and of cytokinin metabolism were identified in the genomes or EST data of different species ranging from bacteria and algae to modern land plants.
The first domain investigated was the CHASE domain, which is part of the cytokinin sensing receptor. The phylogenetic tree of all CHASE domains found in the dataset showed a clade containing well known cytokinin receptors. Surprisingly, this clade had a sister clade of eight *P. patens* and one *M. polymorpha* CHASE domains. These new potential cytokinin receptors were also identified by an analysis of the other protein domains in the cytokinin receptors.

Experimental investigation of two representatives from the newly identified potential cytokinin receptors showed their functionality in cytokinin binding and signal transduction into a TCS output. Additionally, there is evidence for the most C-terminal domain of the cytokinin receptor, the response regulator (RR) domain in charophyte algae, which could possibly be part of a receptor protein. The results imply that the domains necessary for the formation of a cytokinin receptor protein were present in the ancestors of the land plant lineage and also in cyanobacteria. These domains were assembled into a receptor protein with the domain architecture of the classical cytokinin receptors in progenitors of charophyte algae and land plants. Furthermore, the obtained results indicate that type-C RR proteins might derive from receptor proteins.

Regarding the downstream signaling components from the cytokinin signaling system, single-domain proteins were identified among the three RR protein groups (type-A, type-B and pseudo RR proteins), which contrasts with the current guidelines on how to group RR proteins. Analysis of the metabolism proteins indicated that charophytes might encode biosynthesis genes in their genomes, while the classical cytokinin catabolism gene (cytokinin oxidase/dehydrogenase, CKX) was absent from chlorophyte genomes and charophyte EST collections. Altogether this analysis accumulated hints on the existence of a potential cytokinin signaling system in charophyte algae, while *P. patens* remains the earliest-diverging plant to also incorporate a full set of cytokinin metabolism enzymes according to current data.

6. Zusammenfassung

Cytokinine sind wichtige Pflanzenhormone und als solche haben sie verschiedene Auswirkungen auf die Pflanze. Cytokinine werden von membranständigen Histidinekinasen erkannt und das Signal wird mittels eines His-zu-Asp *Phosphorelays* weitergeleitet. Die Weiterleitung involviert anschließend ein Phosphatresttransfer von einem Histidinphosphotransferprotein zu einem Responseregulatorprotein. Während das Cytokininsignaltransduktionssystem in höheren Pflanzen gut erforscht ist, sind Informationen über das Cytokininsignaltransduktionssystem in primitiven Landpflanzen rar.

Im ersten Teil dieser Arbeit wurde deshalb der erste Schritt der Cytokininsignaltransduktion in der basalen Landpflanze *P. patens* untersucht. Untersuchungen der Funktionalität der bioinformatisch vorhergesagten Cytokininrezeptoren zeigen, dass PpCHK1 und PpCHK2 Cytokinin binden und das PpCHK3, in *E. coli* die Präsenz von Cytokinin in ein Signal des Zwei-Komponenten-Systems konvertieren kann. Die transiente Expression von *P. patens* Cytokininrezeptoren in Tabak legt nahe, dass PpCHK1, PpCHK2 und PpCHK3 eine ähnliche Funktion wie die *A. thaliana* Cytokininrezeptoren haben könnten, da sich ihre Lokalisation konserviert darstellt. Anschließend wurde die Komplementationskapazität von zwei *P. patens* Cytokininrezeptoren auf die *A. thaliana ahk2 ahk3* doppel *knockout* Mutante untersucht. In diesem Experiment zeigen die beiden *P. patens* Cytokininrezeptoren (PpCHK1 und PpCHK2), dass sie als Cytokininrezeptoren in *A. thaliana* wirken können.
Hergestellte *P. patens* Mutanten, transformiert mit GFP-fusions Konstrukten von *PpCHK1* oder *PpCHK2* zeigten veränderte Chloroplastenform oder -verteilung in transgenen Pflanzen beider Fusionsrichtungen und führten zu der Schlussfolgerung, dass die *P. patens* Cytokininrezeptoren in *P. patens* möglicherweise eine Funktion während dieser Prozesse haben. Zusammengenommen wurde gezeigt, dass *P. patens* Cytokininrezeptoren PpCHK1 und PpCHK2 funktionelle Cytokininrezeptoren sind. Während sie in *P. patens* an der Entwicklung von Chloroplasten beteiligt sein könnten, können sie in *A. thaliana* die Funktion nativer Cytokininrezeptoren übernehmen, aber eine Rolle bei der Chloroplastenentwicklung konnte in *A. thaliana* nicht festgestellt werden.

Zweck des zweiten Teils dieser Arbeit war es das Wissen über die Evolution des Cytokininsignaltransduktionssystems zu erweitern. Zur Untersuchung wurde ein Ansatz basierend auf Proteindomänen gewählt. Um Einsichten in die Entstehung und die Evolution des regulatorischen Systems von Cytokinin zu erlangen, wurden Kernkomponenten des Cytokininsignaltransduktionssystems und des Cytokinin-Metabolismus in dem vorliegenden Datensatz, aus Genom- und *Expressed Sequence Tag (EST)*-Daten verschiedener Spezies von Bakterien über Algen bis hin zu modernen Landpflanzen identifiziert.
Zuerst wurde die ligandenbindende CHASE Domäne der Cytokininrezeptoren untersucht. Der phylogenetische Baum aller CHASE Domänen zeigte eine Klade bekannter

Cytokininrezeptoren. Überraschenderweise hatte diese Klade eine Schwesterklade, welche acht *P. patens* und eine *M. polymorpha* CHASE Domäne beinhaltete. Diese neuen, potentiellen Cytokininrezeptoren wurden auch von weiteren Domänen, die Teil eines Cytokininrezeptors sind, identifiziert. Die experimentelle Beschreibung zweier Repräsentanten aus der Klade der neuen, potentiellen Cytokininrezeptoren zeigte die Funktionalität dieser Rezeptoren bei der Bindung von Cytokinin und die Signalweiterleitung bei Cytokinin Präsenz in ein Signal des Zwei-Komponenten-Systems. Außerdem wurde die C-terminale Domäne des Cytokininrezeptors, die Responseregulator Domäne in Charophyceae identifiziert, die möglicherweise Teil eines Cytokininrezeptors sein könnte. Die generierten Ergebnisse weisen darauf hin, dass alle Domänen zur Zusammensetzung eines Cytokininrezeptors bereits in den Vorfahren der Landpflanzen und in Cyanobakterien vorhanden waren. Diese Domänen könnten zu einem Protein mit der Domänen-Architektur klassischer Cytokininrezeptoren in Vorläufern von Charophyceae und Landpflanzen assembliert worden sein. Weiterhin weisen die Ergebnisse darauf hin, dass Typ-C Responseregulator Proteine möglicherweise von Rezeptoren abstammen.

Bezüglich der weiteren Signalkomponenten des Cytokininsignaltransduktionssystems wurden Proteine mit nur einer Proteindomäne in allen drei Gruppen der Responseregulator Proteine (Typ-A, Typ-B und Pseudo Responseregulator Proteine) identifiziert und stellen damit geltenden Richtlinien zur Einteilung dieser Gruppen in Frage. Die Analyse der Proteine, beteiligt am Metabolismus von Cytokinin legte nahe, dass Charophyceae Gene zur Biosynthese von Cytokinin im Genom enthalten könnten, während klassische Katabolismus Gene (wie die Cytokininoxidase/-dehydrogenase) in Chlorophyceae Genomen und Charophyceae *EST*-Kollektionen nicht vorhanden waren. Zusammengenommen wurden Hinweise auf die Existenz eines potentiellen Cytokininsignaltransduktionssystems in Charophyceae gesammelt, während *P. patens*, nach derzeitigem Stand, die am frühsten divergierende Landpflanze bleibt, die auch ein komplettes Set von Cytokinin Metabolismus Genen codiert.

7. Publications

Hellmann, E., Gruhn, N. and Heyl, A. (2010). "The more, the merrier: Cytokinin signaling beyond *Arabidopsis*." Plant Signaling and Behaviour **5**(11): 1365-1371.

Gruhn, N. and Heyl, A. (2013). "Updates on the model and the evolution of cytokinin signaling." Current Opinion in Plant Biology **16**(5): 569-574.

Gruhn, N., Halawa, M., Snel, B., Seidel, M. F. and Heyl, A. (2014). "A new subfamily of putative cytokinin receptors is revealed by an analysis of the evolution of the two-component signaling system of plants." Journal of Plant Physiology.

8. Acknowledgements

Danksagung

Ich möchte mich bei Dr. Heyl und Prof. Schmülling bedanken, für die Möglichkeit am Institut für Angewandte Genetik zu forschen und zu promovieren.
Ihre fortwährende Hilfestellung und Begleitung hat eine sehr offene Arbeitsatmosphäre geschaffen.

Desweiteren möchte ich mich bei den Mitgliedern der Prüfungskommission bedanken.

Liebe, mir bekannten Labor106-ler: Vielen Dank für die Tage, Wochen oder Jahre, in denen wir Spaß und Frust geteilt haben.

Bedanken möchte ich mich auch bei allen Mitarbeitern, die mir von Ihrer wertvollen Zeit etwas abgegeben haben, wenn ich eine Frage hatte.
Insbesondere bei Prof. Schuster für Rat und Tat in Computerangelegenheiten, bei Dr. Gerdemann-Knörck für Hinweise zur Protoplastierung und bei Cordula Braatz für jede erdenkliche Hilfe bei Laborarbeiten und vielem mehr...

Dank geht auch an die Mitarbeiter des Instituts.
An alle wie Sie sind, weil die dadurch entstehende wundervolle, sehr fördernde und kollegiale Stimmung die beste Motivation ist.

Bedanken möchte ich mich bei Dr. Snel und Dr. Seidel für ihre exzellente Betreuung der bioinformatischen Analyse. Vielen Dank an alle Mitglieder der AG Snel und der TBB für die herzliche Aufnahme während meinem Aufenthalt bei Euch.

Ich möchte mich auch bei Dr. von Schwartzenberg und Fr. Lindner bedanken, für die freundschaftliche und zuverlässige Zusammenarbeit.

Ich danke James S. Cunningham für die sehr hilfreichen Kommentare zu meinem Manuskript.

Ich bedanke mich bei meiner Familie und meinen Freunden für Eure Unterstützung!

Vielen Dank an die Volkswagen Stiftung für die finanzielle Unterstützung dieses Projektes.

9. Appendix

9.1. Data acquisition:

Data for the phylogenetic analysis was retrieved from different databases. An overview of the used databases is found in Appendix Table 1.

Appendix Table 1: Overview of the databases used to generate the dataset for the phylogenetic analysis of the project. Given is the trivial name, the provider, the URL of the respective database and a reference if available.

Species	Source	URL	Reference
Agrobacterium tumefaciens	GB	http://www.ncbi.nlm.nih.gov/Taxonomy/Browser/wwwtax.cgi?id=176299	
Amphidinium operculatum	TbestDB	http://amoebidia.bcm.umontreal.ca/pepdb/pep.php	
Aquilegia coerula	Phytozome	ftp://ftp.jgi-psf.org/pub/JGI_data/phytozome/v6.0/Acoerulea/annotation/	
Arabidopsis thaliana	TAIR	ftp://ftp.arabidopsis.org/home/tair/Sequences/blast_datasets/TAIR9_blastsets/	
Bacillus subtilis	GB	http://www.ncbi.nlm.nih.gov/bioproject/76	
Chlamydomonas reinhardtii	JGI DOE	http://genome.jgi-psf.org/Chlre4/Chlre4.download.ftp.html	(Merchant *et al.,* 2007)
Chlorella variabilis sp. NC64A	GB	http://www.ncbi.nlm.nih.gov/nuccore?term=txid554065[Organism%3Anoexp]	(Blanc *et al.,* 2010)
Coccomyxa C169	JGI DOE	http://genome.jgi-psf.org/Coc_C169_1/Coc_C169_1.info.html	
Coleochaete orbicularis	GB	http://www.ncbi.nlm.nih.gov/nucest	(Timme and Delwiche 2010)
Corynebacterium glutamicum	GB	http://www.ncbi.nlm.nih.gov/genome/?term=Corynebacterium%20glutamicum%20ATCC%2013032	
Cyanophora paradoxa	GB	http://www.ncbi.nlm.nih.gov/sites/entrez?db=nucest&cmd=Search&dopt=DocSum&term=txid2762[Organism%3Anoexp]	(Reyes-Prieto *et al.,* 2006)
Dictyostelium discoideum	Dictybase	http://dictybase.org/db/cgi-bin/dictyBase/download/blast_databases.pl	
Dunaliella salina	GB	http://www.ncbi.nlm.nih.gov/sites/entrez?db=nucest&cmd=Search&dopt=DocSum&term=txid3046[Organism%3Anoexp]	
Escherichia coli K12	GB	http://www.ncbi.nlm.nih.gov/genome?term=Escherichia%20coli%20str.%20K-12%20substr.%20MG1655	
Glaucocystis nostochinearum	GB	http://www.ncbi.nlm.nih.gov/nucest/?term=Glaucocystis+nostochinearum	(Reyes-Prieto *et al.,* 2006)
Gloeobacter violaceus	GB	http://www.ncbi.nlm.nih.gov/genome?term=Gloeobacter%20violaceus%20PCC%207421	
Helicosporidium sp. ex Simulium jonesi	GB	http://www.ncbi.nlm.nih.gov/sites/entrez?db=nucest&cmd=Search&dopt=DocSum&term=txid145475[Organism%3Anoexp]	(de Koning *et al.,* 2005)
Heterocapsa triquetra	GB	http://www.ncbi.nlm.nih.gov/sites/entrez?cmd=PureSearch&db=nucest&term=txid66468[orgn]%20AND%20gbdiv_est[prop]	(Waller *et al.,* 2006)
Isochrysis galbana	GB	http://www.ncbi.nlm.nih.gov/sites/entrez?cmd=PureSearch&db=nucest&term=txid37099[orgn]%20AND%20gbdiv_est[prop]	

Species	Source	URL	Reference
Lotharella amoeboformis	TbestDB	http://amoebidia.bcm.umontreal.ca/pepdb/pep.php	
Marchantia polimorpha Blast results	JGI DOE		
Marchantia polymorpha	GB	http://www.ncbi.nlm.nih.gov/nucest?term=%28txid3197[orgn]%20AND%20gbdiv_est[prop]%29	(Yamato *et al.,* 2007)
Mesostigma viride	GB	http://www.ncbi.nlm.nih.gov/sites/entrez?db=nucest&cmd=Search&dopt=DocSum&term=txid41882[Organism%3Anoexp]	(Nedelcu *et al.,* 2006)
Micromonas pusilla CCMP1545	JgI DOE	http://genome.jgi-psf.org/MicpuC2/MicpuC2.info.html	(Worden *et al.,* 2009)
Micromonas pusilla RCC299	JGI DOE	http://genome.jgi-psf.org/MicpuN3/MicpuN3.download.ftp.html	
Mycobacterium tuberculosis	GB	http://www.ncbi.nlm.nih.gov/genome/?term=Mycobacterium%20tuberculosis%20F11	
Neisseria meningitidis	GB	http://www.ncbi.nlm.nih.gov/genome?term=Neisseria%20meningitidis%20MC58	
Nostoc PCC7120	GB	http://www.ncbi.nlm.nih.gov/genome?term=Nostoc%20sp.%20PCC%207120	
Oryza sativa	Phytozome	ftp://ftp.jgi-psf.org/pub/JGI_data/phytozome/v6.0/Osativa/annotation/	(Ouyang *et al.,* 2007)
Ostreococcus tauri	JGI DOE	http://genome.jgi-psf.org/Ostta4/Ostta4.download.ftp.html	(Derelle *et al.,* 2006; Palenik *et al.,* 2007)
Otreococcus lucimarinus	JGI DOE	http://genome.jgi-psf.org/Ost9901_3/Ost9901_3.info.html	(Palenik *et al.,* 2007)
Pavlova lutheri	GB	http://www.ncbi.nlm.nih.gov/sites/entrez?cmd=PureSearch&db=nucest&term=txid2832[orgn]%20AND%20gbdiv_est[prop]	
Physarum polycephalum	GB	http://www.ncbi.nlm.nih.gov/sites/entrez?cmd=PureSearch&db=nucest&term=txid5791[orgn] AND gbdiv_est[prop]	(Glöckner *et al.,* 2008)
Physcomitrella patens	cosmoss.org	https://www.cosmoss.org/physcome_project/wiki/Downloads	(Rensing *et al.,* 2008)
Polytomella parva	GB	http://www.ncbi.nlm.nih.gov/sites/entrez?db=nucest&cmd=Search&dopt=DocSum&term=txid51329[Organism%3Anoexp]	
Populus trichocarpa	Phytozome	ftp://ftp.jgi-psf.org/pub/JGI_data/phytozome/v5.0/Ptrichocarpa/annotation/	
Porphyra haitanensis	GB	http://www.ncbi.nlm.nih.gov/sites/entrez?db=nucest&cmd=Search&dopt=DocSum&term=txid76159[Organism%3Anoexp]	
Porphyra yezoensis	GB	http://www.ncbi.nlm.nih.gov/sites/entrez?db=nucest&cmd=Search&dopt=DocSum&term=txid2788[Organism%3Aexp]	
Prototheca wickerhamii	GB	http://www.ncbi.nlm.nih.gov/sites/entrez?db=nucest&cmd=Search&dopt=DocSum&term=txid3111[Organism%3Anoexp]	(Borza *et al.,* 2005)

Species	Source	URL	Reference
Reclinomonas americana	GB	http://www.ncbi.nlm.nih.gov/sites/entrez?cmd=PureSearch&db=nucest&term=txid48483[orgn]%20AND%20gbdiv_est[prop]	
Selaginella moellendorffii	GB	http://www.ncbi.nlm.nih.gov/sites/entrez?db=nucest&cmd=Search&dopt=DocSum&term=txid88036[Organism%3Anoexp]	
Spirogyra pratensis	GB	http://www.ncbi.nlm.nih.gov/sites/entrez?db=nucest&cmd=Search&dopt=DocSum&term=txid332123[Organism%3Anoexp]	(Timme and Delwiche 2010)
Spruce V4.0 */ Picea abies*	TIGR	http://compbio.dfci.harvard.edu/cgi-bin/tgi/gimain.pl?gudb=spruce	
Streptococcus pyogenes	GB	http://www.ncbi.nlm.nih.gov/genome?term=Streptococcus%20pyogenes%20M1%20GAS	
Synechocystis PCC6803	GB	http://www.ncbi.nlm.nih.gov/genome?term=Synechocystis%20sp.%20PCC%206803	
Tetrahymena thermophila	GB	http://www.ncbi.nlm.nih.gov/nucest?term=%28txid5911[orgn]%20AND%20gbdiv_est[prop]%29	
Trimastix pyriformis	TbestDB	http://amoebidia.bcm.umontreal.ca/pepdb/searches/organism.php?orgID=TP	
Volvox carteri	JGI DOE	http://genome.jgi-psf.org/Volca1/Volca1.download.ftp.html	(Prochnik *et al.,* 2010)

9.2. *P. patens* cytokinin receptor DNA and Protein sequence selection

9.2.1. *P. patens* cytokinin receptors

At the beginning of this project different database entries were accessible that belong to three potential cytokinin receptors from Physcomitrella patens. The different annotations were compared by multiple sequence alignment (MSA) using ClustalW (Thompson *et al.,* 1994).

9.2.2. *P. patens* cytokinin histidine kinase 1

Different gene annotations of *PpCHK1* were loaded from the respective database and compared to each other.

9.2.2.1. *PpCHK1* Entry from Gen Bank

The *PpCHK1* gene was taken from the GenBank database[8] with the following CDS:

Physcomitrella patens subs. *P. patens* cytokinin receptor AtAHK4-like protein (CRE1) mRNA, complete coding sequence; Sequence ID: ref|XM_001761701.1|Length: 3398 .

9.2.2.2. *PpCHK1* Entry from Joint Genome Institute

The *PpCHK1* gene taken from the JGI (Joint Genome Institute) database[9] with the following CDS: jgi|Phypa1_1|142600|e_gw1.194.71.1

ATGCACAGGGCTACTGGCTCTGGACGGCTAGGGGTAAAATGGTGGAAGGATTCAGGAA
TTACCTGTATTAAGCCTAAACAGAAGGATTCTGAAGCTGGATCCAGGTATGGTCATAATT
GGCATACTATAGCATTCATCATGTGGGTGGTTTTTATGGGTGCTGTTTCTGTGTCCGTTT
ATTTCGCCATGAGATTCGACATGCTTGAACGAAGAAGAGAAAATCTTGCGAACATGTGC
GAGGGACGGGCTCGTATGCTTGAGGAGCAATTCAAGGCAAGTATGAACCATGTCAGAG
CACTCACGGCTCTTCTCACTACTTTTCATCTTGGCAAGCAGCCCTCAGCCATCAATCAG
GAAACCTTTGCTACCTATGCTGAAAGAACAGCATTTGAAAGACCGTTGATGAGTGGGGT
TGCATATGCCGAGAGAGTCCTTCATGCGAATCGAAACTTGTTCGAGTCGAAACATGGCT
GGACTATCAAGGAAATGTTTTCTAAAGAAAAGCAGCGAGATTTTGACGAATACGCCCCA
ACTACCATGACTCAAGAGACTCTCTCCCATTTGACGTCTCTTGATATGATGTCTGGTCAG
GAAGATCGCGAAAATATCATACGAGCGCGAGAGTCGGGAAAAGGAGCTTTGACGAACC
CCTTCAGGTTACTGGAGTCTAAGCATCTTGGAGTAGTGTTTACGTTCGCTGTATACACCA
CAGACCTGCCAGAAGATGCAACAAAGGAGGACCGAATTAAAGCAACCGCTGGTTATCT
GGGTGGAGCCTTTGACGTCGAAACGCTTGTGGAGAATCTTCTTCGACAAATGGCTGGTA
GTCAGATTATTGCGGTCAACGTATATGACATTACAAATGAAACGATGCCTCTTGTGATGT
ATGGCTACACCAACGTTGAAAAAATGCAAAGCACATATGTCAGCGACTTGGACTTTGGA
GACCCTGCCCGTAGGCATGAAATGCGGTGCAGGTTTAAAGAGGATGCGTTGCCTCCTT
GGACAGCCATATCCACTTCTATAGGTATATTTGTAATCGCATTTTTGGTCGGACACATGC
TACATGCTTCAAGGAACCGAATCGATAAAGTAGAAGAAAACTGTCGCATATTTCAGGAG

[8] http://www.ncbi.nlm.nih.gov/nuccore
[9] http://www.jgi.doe.gov

CTTAAGATGCGTGCAGATGATGCTGTTATAGCGAAGTCTCAGTTCTTGGCAACTGTGTC
TCACGAGATTCGGACTCCAATGAATGGTGTTCTAGGAATGCTTCAAATGTTGATAGACAC
TCCGCTGAATCCAGCGCAATTAGACTATGCCCAAACTGCTTTAGCCAGTGGAAAAGCAC
TTATCAACCTCATAAATGAGGTCCTTGATCAGGCTAAGATTGAATCGGGCCGTCTAGAAT
TTGAGCATGTTCCCTTTGATTTGCGTGCCATCCTTGACGATGTGCTCTCCCTCTTCCATG
GAAAATCAAGAGCTTCGGGCATCGAGTTAGCGGTTTACGTTTCTGCGAGGGTTCCCAAA
ATTCTCGTTGGTGACCCTGGTCGTTTTCGGCAGATCATCACCAATCTCGTTGGCAATTC
CATCAAAGTAATCATTTGTTCTAAATGCCTCAACTTGCTTTATATGTCACATTTCACCGAA
GCTGGTCACATTTTTGTTTGCGTTCATTTGAATGAAGACGTCAACATGGTGATGGATGG
GAGTGGAGGTGATGCTGACGATACTATGGATGGGGAAGTTGAAAGTGCCGGACCGCTG
AATGACATGAACTACCGATTTAACACCCTTAGTGGCAGAGAAACTGCTGATTACCGAAA
CAGCTGGGAAATGTTTGAGCGACTGCTTGCGCAAGAACAGTCACACAATGATACTTGGA
GTTACTCCGACTCGAGCGATGTTGTGAATCTGGTGGTCAGTGTGGAGGATACAGGTGT
GGGTATACCCTTACACGTACAAGACCGTGTCTTTACCCCCTTCATGCAGGCTGACAGCT
CAACATCTAGAAATTACGGAGGCACTGGAATAGGACTAAGCATCAGCCGGTGTTTAGTA
GAGCTTATGTCAGGGGAGATGGGCTTTGTTAGTCGTCCTAAAGTGGGGTCCACATTCAC
ATTCACTGTGGAATTGCAACGTGTACCCGCCAATATACCCGAAAGGATCCTTAGAGAGG
GCAGGAACAGTTATCTACAAACGCCGCCACTAACTACTTGTTTCCAAGGAATGCGTGTA
CTCGTTGTGGATGGCAGAAAAGTCCGCTGTGAAGTCACTCGCCATCATTTAAAGAGGCT
CGGACTCCAGGTTGAGGTCGCCCACACTGTTAGTGAGGCTGCCGAGATTCTTTCTACA
GTGGCTGACCAAGGCACTTGCAGCTCAAGGGGTTCACGAAATATCGAAATGATTTTCGT
GGACAAGGACGCTTGGGGTCCTGGAACTGGGATGAATTTTAGAAGCTTGCTTGGTGAA
ATGATTCAATCCATGAAGAGGATGGTTCTAGTTGCGACATCAATGACGGATATGGAGCT
TGGGATGGTGAAAGCCAGCGGATTTGTGGATACTGTTGTTAGGAAACCACTTCGAGCAA
GCTTGATAGCTGCTTGTCTCAAGCAGATTCTTGGGGTTGGGGACAGGAGCCGAGACCA
AGAGCAGGAGTTGCGGAGTGGGGTTACTTCTCTACAGACTCTTTTATATGGAAAACGGA
TTCTCGTGGTTGATGATAATCCCGTGAATCGAAAGGTTGCAGCTGGGGCTCTGCACAAG
TATGGGGCTCAAGTTGAGTGTGTTTACAGTGGAAGAGCTGCTATCCAGAAGTTGAAGCC
TCCCCACAATTTCGATGCCTGTTTTATGGACGTGCAGATGCCAGAAATGGATGGTTTCG
AGGCTACAGGGTTAATAAGGAAGGCGGAGGCTGCAGCCGCAGAGAGAGGCCAAGCAG
CGGGATTGCCAACCTTTAAACGCCGACTGCATGTGCCGATCCTGGCAATGACAGCTGA
CGTTATTCAAGCTACCTCCGAAGAATGTATGCGCTGTGGCATGGATGGCTACGTGGCTA
AGCCATTTGACGAACATCAGCTTTACCAAGCGGTTGCCAAGCATTTCTTCGACGTGAAC
TAA

9.2.2.3. *PpCHK1* Entry from www.cosmoss.org

Pp1s50_141V2.1 Phypa_181547 cytokinin receptor AtAHK4-like protein.

9.2.2.4. *PpCHK1* from Nogue Lab

The following CDS was obtained from the Nogue Lab (INRA, France) and found to be deposited at the NCBI[10]: DQ389162.

9.2.3. Comparison of the different gene models of *PpCHK1*

The different annotations were compared (see Appendix Figure 1) and evaluated. Since there was only one sequence that actually derived from a biological sample, and the other annotations were computationally inferred, based on other genomes, this sequence was regarded as more relevant and further work was always related to DQ389162.

[10] http://www.ncbi.nlm.nih.gov/nuccore

Appendix Figure 1: ClustalW-alignment of different *PpCHK1* annotations. Gene annotations were taken from databases (see section 9.2.2.1 to 9.2.2.4) and resulting protein sequences were subjected to the alignment. The computationally derived sequences (JGI, GenBank, cosmoss) indicate two gaps where the biological sample (Nogue) codes for the protein.

9.2.4. *P. patens* cytokinin histidine kinase 2

9.2.4.1. *PpCHK2* from GenBank

PpCHK2 entry in GenBank[11]: NCBI Reference Sequence: XM_001775579.1.

9.2.4.2. *PpCHK2* from JGI

PpCHK2 entry from the JGI[12]: e_gw1.194.71.1

ATGCACAGGACAACAGGACCTGGGCGATTGGGGGTGAATTGGTGGAAGGATACAGGG
ATTTCTTACATTAGACCTACTTACAAGGATTCAGAAGCTAGATCCAGGTATGGCCACAAT

[11] http://www.ncbi.nlm.nih.gov/nuccore/XM_001775579.1
[12] http://www.jgi.doe.gov

TGGCATACTAAAGCTTTCGTTGTGTGGGTGGTTTTTATGGGAGCTGTTTCTCTATCCGTT
TTTCTGGCCATGAGATTCGACATGCTGGAGCGGAGAAGAGAGAATCTTGCAAACATGTG
CGAGGGACGGGCCCGCATGCTTGAGGAGCAATTCAAGGCCAGCATGAACCACGTTAGA
GCACTTACAGCTCTTCTCACTACCTTTCATCTTGGCAAGCAACCCTCAGCTATTAATCAG
GAAACATTTGCTACCTATGCTGAAAGAACAGCTTTTGAGAGGCCGTTGATGAGTGGTGT
TGCATTTGCTGAACGAGTGCTGCATGCGAATCGGAAATTGTTCGAGTCAGCACATGGCT
GGACTATAAAGGAAATGTATTCGAAAGATCTTCAACAAGATTTCGACGAATATGCCCCAA
CCACAATGTCTCAGAAGTCTCTCTCGTATTTAACCTCTCTTGATATGATGTCTGGCCAGG
AGGATCGCGAAAATATTATTCGAGCGCGAGAGTTAGGGAAAGGTGCTTTAACCAAGCCA
TTCAGGCTTCTGGAATCTAAGCATCTTGGAGTGGTGTTCACCTTCGCCGTCTACTGCAC
AGACCTACATGATGATGCGAAAAAGGAAGATCGGATCAAAGCAACTGCCGGGTATCTTG
GAGGTGCTTTTGACGTCGAAACACTTGTGGAGAATCTGCTTCGTCAAATGGCTGGTAGT
CAAATTATTGCCGTCAATGTGTACGACATCACCAACGAGACCATGCCTCTTGTGATGTAT
GGCCATACCAATGTTGAGAAGTCAAAAAACACGTATGTCAGCAGCTTGGATTTCGGAGA
TCCGGCGCGAAGGCATGAAATGCGTTGCAGGTTTAAAGAGGATGCATTACCTCCTTGGA
CAGCCATATCCACTTCAATAGGTATATTTGTGATAGCGTTTTTGGTTGGACACATGCTAC
ATGCGTCAAGAAACCGAATTGACAAGGTTGAAGAAAATTGTCGCATATTTCAGGAGCTA
AAGATGCGCGCAGATGATGCCGTCATAGCGAAGTCTCAGTTTCTGGCGACAGTATCACA
TGAAATTCGGACCCCCATGAATGGTGTTCTAGGAATGCTTAATATGTTGACGAATACTCG
GCTGAATCCAGCACAGTTAGACTACGCCCGAACTGCTTTAGCGAGTGGCAAAGCACTTA
TCAATCTTATCAATGAGGTCCTTGATCAAGCAAAAATTGAATCAGGCCGTGTAGAGCTTG
AACACGTTCCATTTGATTTGCGTGCCATCCTTGACGATGTACTCTCTCTCTTCCATGGGC
AATCAAGAGATTCAGGTATCGAGCTGGCAGTTTACGTCTCTGCGAAAGTTCCTAAGATT
CTCGTCGGCGACCCTGGTCGATTTCGGCAGATCATCACCAATCTCGTTGGCAATTCCAT
CAAATTCACCGAAGCTGGTCACATTTTTGTTTGCGTTCATCTCAATGAGGATGTCAACAA
CTTGATGGATGGGGATGAAGGTGAAGCCGATGACACTCTGGATGGGGAGGTTGAAAGT
GCCGGACCTCTGACGGACATGAACTACCGATTCAACACCCTTAGTGGCAGAGAAACTG
CTGATTACCGAAACAGCTGGGAAATGTTTGAGCGACTGCTCGCTCAAGAAAAGTCACAT
CGATCAGGTGTAGACCAAGATACTCGGAATTACTGTGACTTAAATGGGGCGGTGAATCT
GGTGATCAGTGTCGAAGATACAGGTGTTGGTATACCCCTGCATGTACAAGACCGTGTCT
TTATGCCCTTCATGCAGGCCGACAGTTCAACATCAAGAAATTATGGAGGAACAGGAATT
GGACTAAGCATAAGCCGTTCCTTAGTAGACCTCATGTCAGGGGAGATGGAGTTTGTTAG
TCATCCTAAAGTGGGGTCCACATTCACGTTTACTGCAGAATTACAACGTGTACCTGCAAA
TGTACCCGAACATATCCTCAGAGAAGGCAGAAACTGTTATCTACAAACGCCGCCGCTAA
CTACGTGTTTCCAAGGAATGCGTGTACTGGTAGTGGATGGCCGAAAAGTCCGCTGTGAA
GTCACTCGACATCATTTGCAGAGGCTTGGACTTCGGGTATTGCCGTCTGTGTCCTGCTC
TTCTATCTTTTTTTCGATTTTTAAGGAACTTTTAATTTATTGTGAAGTTATTTCAGATATTG
AATTGATTTTTGTGGACAAGGACGCTTGGGGTCCTGGAACGTGGGTGAATTTTCGAAGT
CTTCTTACTGAAAGTTTCATCGGCCAATTGAGTCACAACCAAACGACATCAATGAATGAG
ATGGAGCTTAGTGTGGTCAAGGCTAGCGGATTTGTCGATACTGTTGTTCGGAAACCTCT
TCGAGCAAGCTTGGTAGCTGCTTCCCTCGAGGAGATACTTGGGGTTGGGGATGGGGGC
CGGGATCAAGGGCAGAATTTACAGGGGGGAATTAATTCCCTTCAGAACCTCTTAACTGG
GAAAAGAATTCTTGTGGTTGATGACAATCCCGTGAATCGTAAGGTTGCTGCCGGGGCCC
TCAATAAGTACGGCGCCCAAGTTGACTGTGTTAACAGTGGGAGAGCTGCGATCCAAAGT
TTGAAGCCTCCGCACAATTACGATGCCTGTTTTATGGATGTGCAAATGCCAGAAATGGA
TGGTTTTGAGGCCACAAGATTAATAAGGAAGGCTGAAGCTGCAGCCGTAGACAATTGGC
AAGCAGGGAGATTCTCCTCTTTCGGACGCCGATTGCATGTGCCAATCCTGGCGATGACA
GCCGACGTCATTCAAGCCACATCGGAAGAGTGCATGCGCTGTGGAATGGATGGCTACG
TAGCTAAGCCCTTTGACGAGCATCATCTCTACCAAGCAGTTGCCAAGCACTTCTTCGGG
CCAAACTGA

9.2.4.3. *PpCHK2* from www.cosmoss.org

The sequence of *PpCHK2* from was taken from the cosmoss database[13] with the following identifier: Pp1s194_72V2.1 Phypa_142600 cytokinin receptor AtAHK4-like protein

9.2.4.4. *PpCHK2* from the Nogue Lab

The sequence of *PpCHK2* was deposited in the Uniprot database[14]: genomic DNA entry DQ389163.

9.2.4.5. Comparison of the different gene annotations of *PpCHK2*

The different annotations were compared (see Appendix Figure 2) and evaluated. Since there was only one sequence that actually derived from a biological sample, and the other annotations were computationally inferred, based on other genomes, this sequence was regarded as more relevant and further work was always related to DQ389163.

[13] www.cosmoss.org
[14] uniprot entry http://www.uniprot.org/uniprot/Q27PX3

Appendix Figure 2: ClustalW-alignment of different PpCHK2 annotations. Gene annotations were taken from databases (see section 9.2.4.1 to 9.2.4.4) and resulting protein sequences were subjected to the alignment. The computationally derived sequences (JGI, cosmoss) indicate two gaps where the biological sample (Nogue) codes for the protein.

9.2.5. *P. patens* cytokinin histidine kinase 3

The third *Physcomitrella patens* cytokinin receptor was only annotated in the JGI[15] genome sequencing project.

9.2.5.1. *PpCHK3* from JGI

fgenesh1_pg.scaffold_252000025

ATGAGACAAAGAAAACAGTTGATCAATCCCGATAGCAATCAAATGTCGAACCAGAGTGG
AGCCAGGAGCGGAGTCAGAAGTGAAGCTAGGAGGGGCTCAGAATCGAGCCCCTGCAT
ATCAAATGGGAGCTCTAGGTCAAAGGTCCCGCTGAAGTGTGGAAGTGGAGTATACATG
CATAGAACCACAGGGCCTGGGCGGCTTAGAGTAAAGTGGTGGAATGACTCAGGAAACA
CATATGTCAGGCCTACGTACAATGATTCCAAAGCAGGGCCTAGGTATGGCCACAATTGG
CACACTAAGGTTTTCGTTTTCTGGGTGGTTTTTATGGGCGCTGTCTCTCTATCTGTTTAC
TTCGCAATGAGATTTGACATGCTTGAACGGAGAAGGGAAAATCTTGCAAACATGTGCGA
AGGACGGGCTCGTATGCTTGAGGACCAATTTAAGGCAAGTATGAACCATGTGAGAGCTC
TTACTGCTCTTCTCACTACTTTTCATCTTGGCAAGCAACCTTCAGCAATTAATCAGGAAA
CATTTGCCACGTATGCTGCAAGAACAGCATTTGAGAGACCTTTGATGAGTGGCGTTGCA

[15] http://www.jgi.doe.gov

TATGCTGAAAGAGTGCTTCATGCTAATCGAGCAATGTTTGAGTTGACACATGGTTGGACT
ATCAAGGAAATGTTCTCAAAAGAACGACAACAAGATTTTGATGAATATGCTCCAACTACA
ATGTCTCAAGAGACCGTTTTTTACTTAACTTCACTCGACATGATGTCTGGTCAGGAGGAC
CGGGAGAATATTATCCGGGCACGAGAGTCTGGGAAGGGCGCTTTAACCAATCCCTTCA
GGTTACTAGAATCGAAGCATCTCGGCGTTGTATTCACTTTCGCTGTCTACTCCACTGACC
TACCCTTTGATGCAACGAAAGAAGATCGAATTAAAGCAACTGCCGGTTTACAAATTGGAA
ACAGAATTATTCTTGTGCAGTATATGGAATCCTCAAGAACCTCATGTACTATCACATGGA
AGCTATGCCTTAACTTTCTAGGAATTCATGACTGTCGCAGTTATCTCGGAGGTGCATTTG
ACGTCGAAACTCTTGTGGAGAATTTATTGCGTCAAATGGCTGGTAGCCAGATTATTGCG
GTAAATGTATACGACATCACCAACGACACAATGCCTCTTGTAATGTATGGCCATACTAAT
GTTGAAAGATCGGATAACACGTATGTCAGCCTTTTGGACTTCGGAGACCCATTACGCAA
TCATGAAATGCGGTGCAGGTTTAAAGAAGATGCGTTACCTCCTTGGACAGCCATTTCCA
CATCAATAGGCATATTTGTGATAGCGTTTTTGGTCGGACACATGTTACATGCATCTAGGA
ACCGGATTGACAAGGTAGAAGAAAATTGTCGGATATTCCAGGAGCTCAAGATGCGGGC
AGATGATGCTGTCATAGCGAAATCTCAGTTTCTGGCAACTGTCTCTCATGAAATACGGAC
GCCCATGAACGGTGTTCTAGGAATGCTTCAAATGTTGATGGATACTCCTTTGAATTCGAC
GCAGCTAGACTATGCTAGAACTGCTCAAGCAAGTGGCAAAGCACTCATCACCCTAATTA
ATGAGGTTCTAGACCAGGCCAAGATTGAATCAGGCCGTCTGGAGCTTGAGCATGTCCC
CTTCGATTTACGTGCTATCCTTGACGATGTACTCTCTCTCTTTCATGGAAAGTCGAGAGC
TTCAGGCATTGAGTTGGCAGTTTACGTCTCTGAGAAGGTCCCAAAAATTCTCATTGGCG
ACCCAGGTCGCTTTCGGCAGATAATTATTAATCTCGTTGGCAATTCTATCAAATTTACTG
AAGCAGGTCATATTTTTGTTTGCGTCCATCTGAATGAAGATGTAAATATGGTAATGGGTT
GGGATGGAGGTGATGCCGATGACACTCTAGATGGGGAGGTTGAAAGCGCTAGACCTCT
TATTGAAAAGGGGCATCAGTTCAATACTCTTAGTGGCAGAGAAACTGCTGACCTCCGAA
ATAGCTGGGAGATGTTTGAGCGACTGCTTACTCAAGAACAGTCATATCGGTCAGCTGGA
GATCGTGAGACATGGAATTATGATTCGAATGATGTTGTAGAACTGGTGGTTAGTGTAGA
GGACACTGGTGTTGGCATACCCTTGCATGTACAAGACCGTGTATTCACACCTTTCATGC
AGGCCGACAGCTCAACATCAAGAACCTACGGAGGCACAGGTATCGGACTAAGCATAAG
CCGATGCCTAGTGGAGCTTATGTCTGGAGAGATGGACTTTGTCAGTAGTCCTGGGGTG
GGATCTACTTTCACATTTACCGCAGAATTTCAACGAGTACCTGCAAATGTACCAGAGAGC
ATATTAAGAGAAGGCAGCAATTGCCTGTTACAAACGCCCCCATTACCTACTTGTTTTCAA
GGCATGCGTGTACTCGTAGTGGATGGTAGACAAGTTGAGGTCGCCCACTCCGTTCCTG
AGGCTGCTGAGCTTCTCACCACAGTGGTTAACCGCGGTTCTCGCGGTACTCGTAATTCG
CGTGGCTCCATTTCTGCGGACATCGAAATGATCTTTGTAGATAAGGATGCATGGGGTCC
AGGAACTGGGATGAATTTTCGGTCTCTTCTTTCTGAATGTTACATGGAGTCCCCCTCGA
GTTACCACAATGCACGAGCAAGTTACCAGTATCGGTTAACAGCAGGCAGGCTCCCCATA
GGATTTCAGGTTCATTCTATGCAGAAGATGGTTCTAGTTGCGACATCGATGAATGGGCT
GGAGCTTGAGATGGTGAAGGCTAGTGGATTTGTGGATACTGTTATTAGAAAACCTCTTC
GAGCAAGTTTGGTGGCTGCTTGCCTTAAGCAGATTCTTGGAGTGGGAGATGGGAGGGA
CCCAGGGCAGGAGTTACGGGGTGGAGTTAATTCTCTTCAGAACCTCTTATCTGGAAAAA
GAATTCTAGTGGTTGATGATAATCCCGTGAATCGAAAGGTAGCAGCCGGGGCTCTCAAC
AAGTATGGTGCTCAAGTTGAGTGTGTTCACAGCGGAAGAGCAGCAATCCAGAAGTTAAA
ACCTCCTCACAACTTTGATGCGTGTTTCATGGATGTGCAAATGCCAGAAATGGATGGTTT
TCAAGCAACGGGTTTGATAAGGAAAGCAGAAACTTTAGCCGCAGACCAGTGGCTAGCA
GCGGGTTTGCCAACCTTTGGAGTCCGATTTCATGTACCAATTTTGGCCATGACAGCGGA
CGTTATTCAAGCAACATCAGAAGAATGTATGCGTTGTGGTATGGATGGCTATGTGGCTA
AGCCTTTTGATGAACATCAGCTTTATCAGGCGGTTGCAAAGCATTTCTTCCAGGCGAATT
AA

EST evidence to the corresponding gene was found in the cosmoss database[16].

[16] www.cosmoss.org

Appendix Table 2: EST evidence of *PpCHK3* EST evidence to the *PpCHK3* gene annotated in the JGI genome draft fgenesh1_pg.scaffold_252000025.

EST identifier (cosmoss)	Tissue type
scaffold_252_PP015033075R_1_gth	Gametophore
scaffold_252_BY971077.1_1_gth	Upper half part of gametophores
scaffold_252_PPLS085C08.AB1_1_gth	Upper half part of gametophores

9.2.6. PpCHK4 to PpCHK11

P. patens receptor	cosmoss identifier
PpCHK4	Pp1s160_135V6.1
PpCHK5	Pp1s203_100V2.1
PpCHK6	Pp1s71_181V2.1
PpCHK7	Pp1s17_71V2.1
PpCHK8	Pp1s336_63V2.1
PpCHK9	Pp1s43_207V2.1
PpCHK10	Pp1s85_103V2.1
PpCHK11	Pp1s17_74V2.1

9.2.7. *Marchantia polymorpha* cytokinin histidine kinase 1

ATGTTATGCAACTCGGACGATGAAGAGCGCCATAGATGGCGCCGCGGTTGCAGATCGT
TGAGCCATTTGAAGGGGCTGAAGCGGACTTTTCCGTCCTGGAAGGAGATTAGGCAAAG
TCCCCGTAGAGCTGTGGCCGCCCAGTTGGTGTGCACCGCCATAGGATTCTTAACTGCA
GTTGGCGTGGGACTCGTTTTATTTCACAATTCTCTTCAAACACAGCGGCAAGAATTCAAG
CTGAAATGCAGCAATCGGCAGGAGATACTTATGGGAGAGGTAGCCAACAATCTAAACAC
GTCCTTCATGATACTGGGGCTGCTGGCAAGTGAACCCGATCTGACTCAGGAAGCGTGG
TTAGCATTTACTAATGAAACAGACTTTCTTAGACCAAGCACCCCTAGGGTGAGCTACATT
GAACTTATAACTGATAAAGAGAGAGCTGGGTTTGAGCTGGAATGGAACTCCTCGCTTTT
GATGATAGATGAGAAGCAAGAAGCAATTCCTATCAATTACACGGCCAAGGAGTATGCAC
CCATCATCTATGCTTCACAGACGGTGTTGTACGCTTTGCTGGTGGACGTCAGGTCATTT
CGTGCAATCAACCATACTTTGAACAATGCGAGAAATTCTGGGGCAATCGCTATGTCACC
ACCAGATCAGTACGGGACGATTTGGAGAGTCGGAACCTACTTACCTTATTTTGGGAACA
AGACACCAACAACGGTCGAGGAGCGGATAGAGATGTGCATTGGGTGGGTTGGTGTATC
ACTGGATGTTGAGAAGGTTTTTGGTACAGTCCTCTCAAGATATCAGGATGATGAAGACAT
GGATGCTGCTGTTGTATATCTCCCACAAAGCCGGGACGATTGGCTTCCTAGTCTCAACT
GTGTCCCCTCAGCATCTACTTGCGAATTGCCTGTCTATGACCCACAGTCAAGATTTGGT
CAAGAAAGCACAGCAACAATCGCATGGACCTATGCTTTTCAAAACTTTGAACTTAGATGC
TTTGCGACGAAGAGCATCAGGTTGAACGCACTGAGGAACGTTATAGCTTGGCCCATTCT
CATGATGATTGTTGTTCTACTCTGCTCCGTGATTGTTTACCTTGCAATCAAGAAAATGCA
AGCAATAGAGAAGCACATGTTCCAAGTGGAGAAGATGAATTTTGACTTAAGGGCAGCGA
AACAAGCTGCTGAGTCAGCGGACAAAGCGAAGTCTCGATTTCTGGCAACTGTTTCTCAT
GAAATAAGAACACCAATGAATGGAGTGATTGGGATGACGAACTTGCTTATGGGTACAGA
ACTGAGTGCACAACAGCATGAGTATGTTAAGATAGCCCAAGCAAGTGGCAATAATCTTG

TTTCTTTGATCAATGAAGTTCTTGACCTTTCGAAAATTGAGGCTGGGAAGATGGAGTTGG
AGTCAGTTCCTTTCGATCTTCGTGTAGAACTCGATGACTTGCTGTGTCTTTTCGAAGATA
AAGTGAATGAAAAGAAACTCGAAGTTTCTGCCCTAGTACACGATAGTGTACCTAGATGT
GTATATGGGGACCCTGGAAGACTTCGTCAGGTTCTCATCAATCTTGTTGGAAACTCCAT
GAAGTTCACAAAGCATGGTAGCATTTTTGTTTGCGTTCGTATTTATAACCCTCAAGAGGA
TACATTTAGTTCGATGTTAACATCATCACTTTCGTCTTCGCCTGCAAGCGAGGGTAGCCA
CAGAGGCAAGCGGCAATATGATGTTTCAAAGCTAGTTAAAATAGTAGAGAGTCGAGAAT
GGTCTGCTTCTGATATTAGGTTAGAAGGAGTAGGGGTAGTGGAAGCTATGGCACCAAGA
TTGAGCATGCAAGAAGGTCCACTAAACACGGAGGAAGCAGTTAAGAAATGGAGAAACTG
GGTGCCAAAGGCAGGGGTAGAAGGCGAAGATTCGGTTGAAGGCTCCAAAACTTTGTCA
CTGGTCATTTCTGTGGAGGACACAGGTATTGGCGTTCCTTCTCATCTTCAGCATCGGCT
GTTCCAGCCATTTCTTCAAGCGGATAGCAGCACATCTCGGGAGTTTGGTGGTACGGGC
ATTGGATTATCCATTTCCAAGAAATTGGTGGAACTAATGGGAGGGAAGCTTGACGTAAT
CAGTGCACCAGATGAAGGTAGCATATTTGAATTTACATTTAAGGTAGGTAAGGAACGCG
ATGTTGCAGACAAGGATGTAAAGCGTGAATGTGAAGGTTACGGAGAAGAAAACTTGAAA
GGGAGAAGAGTGCTCCTCGTCGACCAGCATTTTGTTAGGCAGGAGGTTGCTGCAAGTT
ATTTACGAAGGTTAGGTGTAATAGTGGAAGGTGTCAGCAACAGGCAAACAGCTCTGACT
TCCCTGTTAGAAAGCGATAGACCTCAGATTCACGCAGTCATACTGGATCTGCAAGGAAT
GGGAATGGATGAGGCCGTTCAACTGGTAAAATTAATGCGCAAGGAACAGCACCTGATGT
CTATCCCTGTATTAGCACTTTCATGTCCTTTAACCACCCCTTTGGAAAAGAAGGAGTTAT
ATGAGGCGGGTTTTTCACAAACTGTTTTCAAACCTATACGCCGCACGACGCTAGCTACT
GGGTTACTGCAAGCAGTGGGAATCTCTTTGCGACCACCAACGAAGACCGTGAATACAAA
TGCAAACATGTTGGCAGGGAAGAGGCTGTTAGTGGTGGATGACAACTTGATCAACCGTA
AGGTTGCACGCTCAATGTTGGCCCGTTATGGCGCAACTGTGGAGTGCGTGAATGGGGG
AGTAGAGGCGATTGAGGCCATAAAGAACAAAGCTGCGAACTTGCAATTTGATTTAATTTT
GATGGATATTCAGATGCCTGAGGTGGATGGTTGTGAAGCTACCAGAAGAATCCGTCGTT
GGGAGATTGAGAATTGCAGTTTCTGCCGAGCATCTGAAAGCAAAAAATGGGAGCAACAA
GCACCTCCTGGTGTTTTACAACAGTGTCCACACAGCAGAATACCAGTCGTAGCAGTCAC
TGCTGATGTTATGCAGGGCACTCATGAGATGTGCTTCGGCTCGGGCATGGATGATTACA
TGCCTAAGCCTCTCGATCAAAAAGTACTGCACCAGCTGTTGGTAAGGTTTTTACAAAACG
ACTTCATCAACCAGACAGGTCAATCAAGAAGAAGAAGTAAGACATTGGAAAGGGAATCT
GTGGCACAATGA

The coding sequence translated into protein sequence would result in the following sequence:

mlcnsddeerhrwrrgcrslshlkglkrtfpswkeirqsprravaaqlvctaigfltavgvglvlfhnslqtqrqefklkcsnrqeilmge
vannlntsfmilgllasepdltqeawlaftnetdflrpstprvsyielitdkeragfelewnssllmidekqeaipinytakeyapiiyasq
tvlyallvdvrsfrainhtlnnarnsgaiamsppdqygtiwrvgtylpyfgnktpttveeriemcigwvgvsldvekvfgtvlsryqdd
edmdaavvylpqsrddwlpslncvpsastcelpvydpqsrfgqestatiawtyafqnfelrcfatksirlnalrnviawpilmmivvll
csvivylaikkmqaiekhmfqvekmnfdlraakqaaesadkaksrflatvsheirtpmngvigmtnllmgtelsaqqheyvkiaq
asgnnlvslinevldlskieagkmelesvpfdlrvelddllclfedkvnekklevsalvhdsvprcvygdpgrlrqvlinlvgnsmkftk
hgsifvcvriynpqedtfssmltsslssspasegshrgkrqydvsklvkivesrewsasdirlegvgvveamaprlsmqegplnte
eavkkwrnwvpkagvegedsvegsktlslvisvedtgigvpshlqhrlfqpflqadsstsrefggtgiglsiskklvelmggkldvis
apdegsifeftfkvgkerdvadkdvkrecegygeenlkgrrvllvdqhfvrqevaasylrrlgvivegvsnrqtaltsllesdrpqihav
ildlqgmgmdeavqlvklmrkeqhlmsipvlalscplttplekkelyeagfsqtvfkpirrttlatgllqavgislrpptktvntnanmla
gkrllvvddnlinrkvarsmlarygatvecvnggveaieaiknkaanlqfdlilmdiqmpevdgceatrrirrweiencsfcrasesk
kweqqappgvlqqcphsripvvavtadvmqgthemcfgsgmddympkpldqkvlhqllvrflqndfinqtgqsrrrsktleresv
aq-

9.2.8. Comparison of the analyzed cytokinin receptors

The “classical” cytokinin receptors and the newly identified receptors of *P. patens* were compared to *AHK4* (At2g01830), *AHK3* (At1g27320) and *AHK2* (At5g35750) from *A. thaliana*.

Appendix Table 3: Sequence comparison of receptors from *P. patens* and *A. thaliana*. Shown are the percent identity and percent similarity of the proteins to each other. Percentages were calculated using MatGAT software package (Campanella *et al.,* 2003) with BLOSUM50 matrix, gap openening penalty 12, extending gap penalty 2.

	PpCHK 1	PpCHK 2	PpCHK 3	PpCHK 4	PpCHK 5	PpCHK 6	PpCHK 7	PpCHK 8	PpCHK 9	PpCHK 10	PpCHK 11	MpCHK 1	AHK 4	AHK 3	AHK 2
PpCHK1		85,3	76,6	29,5	28,5	28,9	25,5	30,0	24,7	30,8	27,7	30,0	47,5	48,0	43,8
PpCHK2	91,6		75,4	30,4	29,5	29,1	25,3	30,8	25,4	30,4	27,2	30,2	46,1	47,2	42,2
PpCHK3	83,3	82,7		29,2	28,4	28,9	25,4	29,3	25,7	29,3	27,5	30	46,5	46,2	43,1
PpCHK4	51,4	50,1	49,0		56,8	52,7	42,0	47,1	37,7	41,5	39,2	43,1	28,9	29,5	25,9
PpCHK5	46,9	47,3	48,8	69,3		51,1	40,0	44,0	38,4	39,4	40,6	41,8	29,0	29,9	27,5
PpCHK6	47,7	49,1	50,2	69,4	69,7		50,5	47,4	40,0	43,6	42,6	44,6	29,2	29,9	28,0
PpCHK7	45,8	46,4	44,5	61,0	57,0	65,8		36,0	31,6	33,9	33,9	35,2	24,0	25,1	22,9
PpCHK8	47,7	48,4	50,8	63,4	64,5	67,8	54,4		56,2	43,0	42,2	43,2	30,5	30,7	28,2
PpCHK9	39,6	40,4	41,1	51,3	55,1	54,8	46,3	66,1		36,9	36,2	36,3	25,9	25,2	23,9
PpCHK10	49,2	48,7	50,1	59,3	58,7	63,4	53,6	61,4	51,6		64,9	43,2	29,7	30,5	27,3
PpCHK11	45,4	46,1	46,7	55,9	59,3	60,2	50,2	59,5	53,3	73,4		41,5	28,7	28,3	27,0
MpCHK1	50.3	50.7	49.5	63.0	61.3	63.7	54.5	62.2	50.9	62.1	59.8		30,0	28,0	30,0
AHK4	65,6	65,4	64,2	48,4	49,0	50,4	45,6	51,6	42,1	51,6	48,3	53,1		48,9	46,5
AHK3	68,1	67,0	62,6	51,5	48,5	50,4	46,5	50,8	40,6	52,1	48,9	51,7	67,7		48,7
AHK2	60,7	59,5	61,1	45,2	47,9	48,0	40,6	50,3	43,1	47,7	48,9	47,4	63,9	64,5	
	% similarity		% identity												

Appendix Table 4: Possible phorphorylation sites of receptors from *P. patens* and *A. thaliana.* Predictions were made with NetPhos 2.0 program (www.cbs.dtu.dk/services/NetPhos-2.0 Blom *et al.,* 1999). Given is the potential number of phosphorylation sites at the respective amino acid. N-glycosylation sites were predicted with NetNGlyc program (http://www.cbs.dtu.dk/services/NetNGlyc/ Gupta *et al.,* 2004). Given are potential glycosylation sites with a probability of more than 50%.The isoelectric point of the proteins were calculated at the ExPASy bioinformatics resource portal (http://web.expasy.org/cgi-bin/compute_pi/pi_tool).

	possible phosphorylation			N-glycosylation	
Protein	Ser	Thr	Tyr	Asn	pI
PpCHK1	31	10	9	2	6,31
PpCHK2	31	11	8	1	6,36
PpCHK3	35	14	11	6	6,37
PpCHK4	34	9	9	9	7,52
PpCHK5	39	16	8	7	6,91
PpCHK6	42	13	5	6	8,27
PpCHK7	37	12	8	7	9,32
PpCHK8	50	16	12	12	8,04
PpCHK9	41	19	11	10	6,46
PpCHK10	27	8	12	7	6,19
PpCHK11	40	10	13	3	8,07
AHK4	49	9	9	6	5,88
AHK3	33	11	6	4	6,84
AHK2	40	17	7	4	5,90

Appendix Table 5: Subcellular localization prediction of receptors from *P. patens* and *A. thaliana* with targetP v1.1 Reliability classes range from one (best) to five (uncertain). Predictions were made with targetP program (http://www.cbs.dtu.dk/services/TargetP/) for plant sequences with default settings (Emanuelsson *et al.,* 2000).

Protein	target peptide			other	predicted	reliability class
	chloroplast	mitochondrial	secretory		localization	
PpCHK1	0,016	0,235	0,019	0,899	other	2
PpCHK2	0,017	0,420	0,006	0,812	other	4
PpCHK3	0,944	0,202	0,008	0,031	Chloroplast	2
PpCHK4	0,175	0,129	0,024	0,840	Other	2
PpCHK5	0,042	0,104	0,192	0,936	Other	2
PpCHK6	0,305	0,058	0,029	0,829	Other	3
PpCHK7	0,062	0,711	0,001	0,265	Mitochondrion	3
PpCHK8	0,026	0,188	0,071	0,436	Other	4
PpCHK9	0,652	0,031	0,013	0,701	Other	5
PpCHK10	0,003	0,805	0,027	0,744	Mitochondrion	5
PpCHK11	0,082	0,288	0,020	0,689	Other	3
AHK4	0,017	0,592	0,076	0,548	Mitochondrion	5
AHK3	0,003	0,017	0,980	0,124	Secretory	1
AHK2	0,357	0,154	0,020	0,835	other	3

Appendix Table 6: Subcellular localization prediction of receptors from *P. patens* and *A. thaliana* with WoLF PSORT scores range from twelve (best) to one (uncertain). Prediction were made with WoLF PSORT program for plant sequences at (http://wolfpsort.seq.cbrc.jp/) (Horton *et al.,* 2007). ER, Endoplasmatic reticulum.

Protein	ER retention signal at the N-terminus		plasma membrane	ER	other
	XXRR	KKXX			
PpCHK1	HRAT	-	10,5	3,0	cytoplasm (6,0)
PpCHK2	HRTT	-	8,5	5,0	cytoplasm (5,0)
PpCHK3	RQRK	-	7,5	4,0	vacuole (2,0) cytoplasm (4,5)
PpCHK4	none		9,0	3,0	nuclear (1,0)
PpCHK5	none		10,0	1,0	vacuole (2,0)
PpCHK6	MRMA	-	9,5	3,0	cytoplasm&nuclear (5,5)
PpCHK7	-	TFKG	7,0	4,0	vacuole (2,0)
PpCHK8	-	KSRS	10,0		vacuole (2,0) nuclear (1,0)
PpCHK9	none		2,0	3,0	chloroplast (3,5) cytoplasm&nuclear (2,5) nuclear (1,05) chloroplast&mitochondria (2,5)
PpCHK10	none		2,0	3,0	chloroplast (2,0) mitochondrial (1,0) cytoplasm&nuclear (3,0) nuclear (2,0)
PpCHK11	DRKG	GCKC	10,0	2,0	vacuole (2,0)
AHK4	RRDF	-	12,0	2,0	
AHK3	none		11,0	2,0	
AHK2	HRAT		13,0		

9.3. Detailed description of transgenic lines ectopically expressing *PpCHK1* or *PpCHK2* in *P. patens*

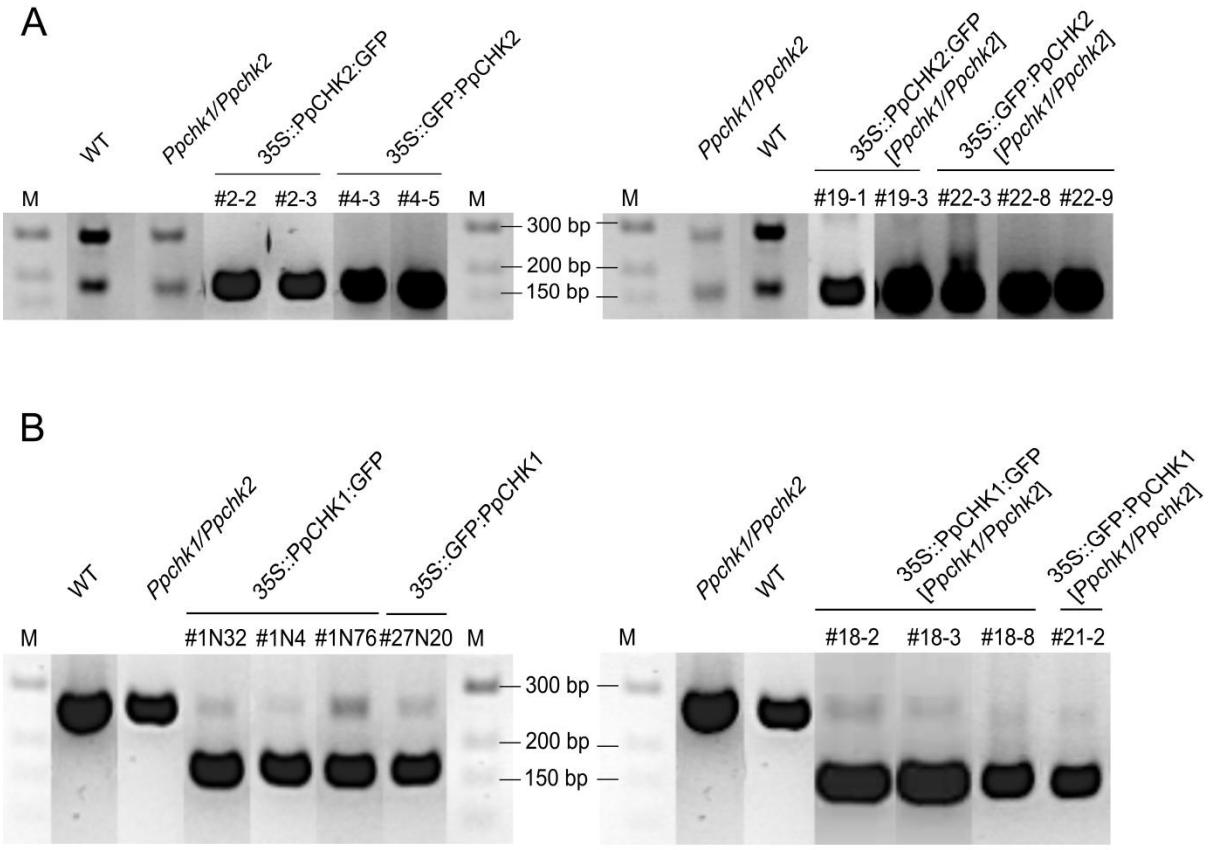

Appendix Figure 3: All *P. patens* transgenic lines carry a transgene. Plasmids encoding for the fusion of *PpCHK2* and *PpCHK1* with *GFP* under the 35S promoter were transformed in the WT (left) and the *Ppchk1 Ppchk2* (right) background. Genomic DNA was isolated and an intron spanning fragment of the receptor was amplified by PCR (38 cycles). **A)** *PpCHK2* PCR on genomic DNA with intron spanning primers, resulting in a band of 183 bp amplicon, when the intron was not amplified, as would be the case when the cDNA was integrated in the genome **B)** *PpCHK1* PCR on genomic DNA with intron spanning primers, resulting in a band of 176 bp amplicon, when the intron was not amplified, as would be the case when the cDNA was integrated in the genome.

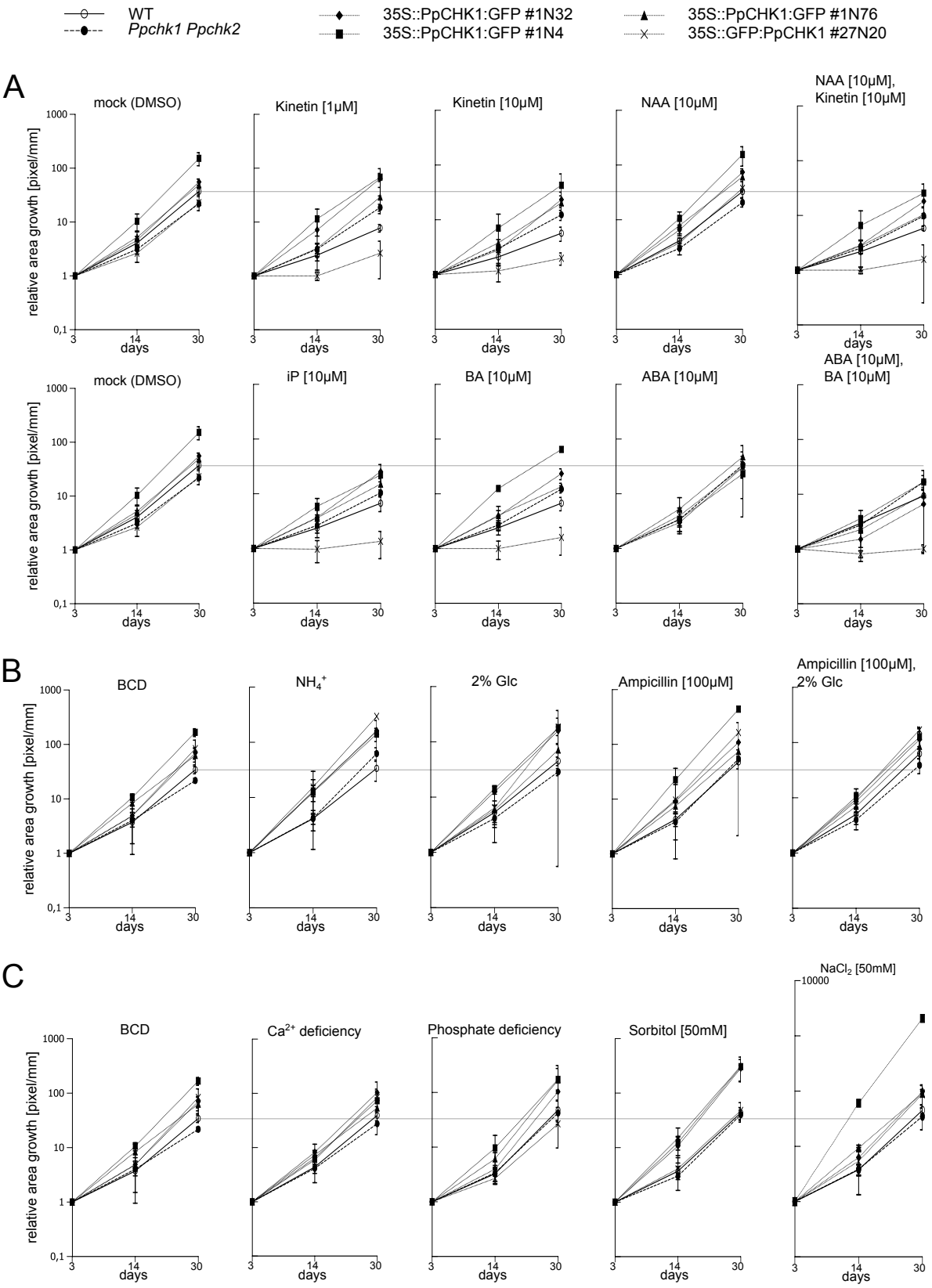

Appendix Figure 4: Growth analysis of the transgenic lines expressing PpCHK1 fusion protein to GFP. Transgenic lines were inoculated to medium supplemented with the respective substance and area with live tissue was analyzed after 3 days. Given is the increase of area covered with live tissue relative to the 3rd day. **A)** Area growth on different phytohormones. **B)** Area growth on media affecting energy supply. **C)** Area growth on media deficient of microelements Ca^{2+} and Phosphate as well as on media introducing osmotic stress. All analysis was done in three biological replicates. A scaleable graphic is available in the electronic file.

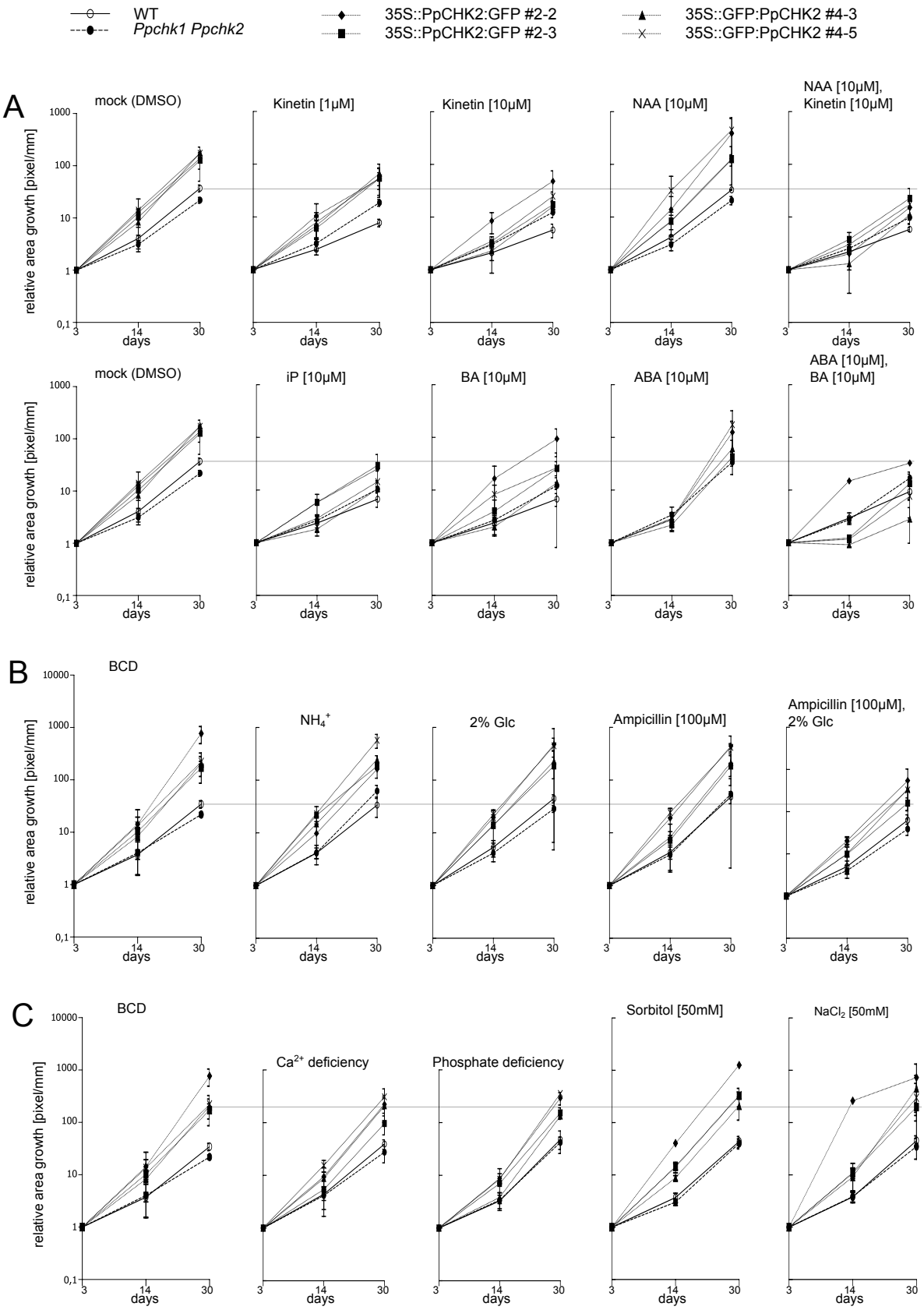

Appendix Figure 4: Growth analysis of the transgenic lines expressing PpCHK1 fusion protein to GFP. Transgenic lines were inoculated to medium supplemented with the respective substance and area with live tissue was analyzed after 3 days. Given is the increase of area covered with live tissue relative to the 3rd day. **A)** Area growth on different phytohormones. **B)** Area growth on media affecting energy supply. **C)** Area growth on media deficient of microelements Ca^{2+} and Phosphate as well as on media introducing osmotic stress. All analysis was done in three biological replicates. A scaleable graphic is available in the electronic file.

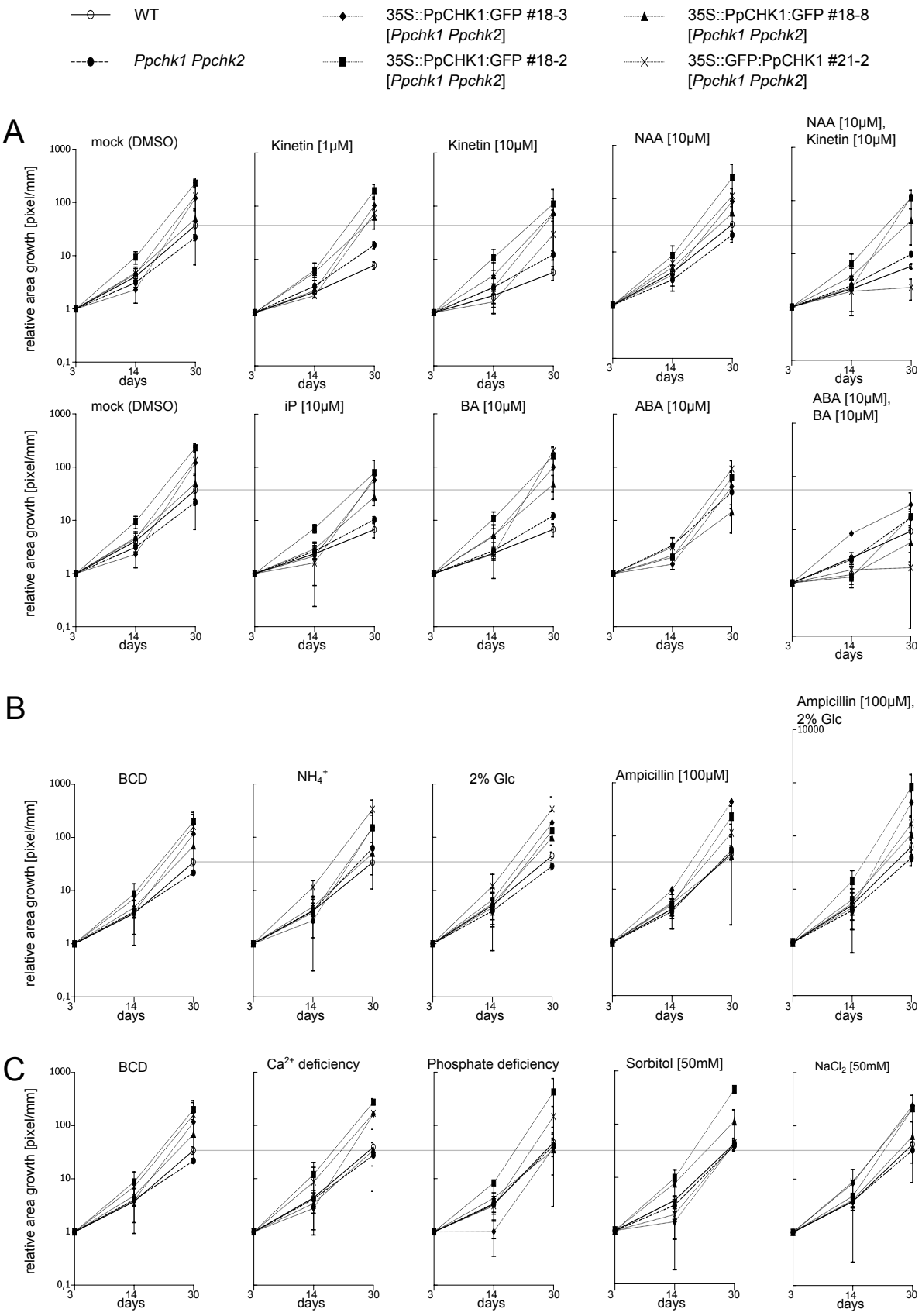

Appendix Figure 6: Growth analysis of the transgenic lines expressing PpCHK1 *[Ppchk1 Ppchk2]* fusion protein to GFP. Transgenic lines were inoculated to medium supplemented with the respective substance and area with live tissue was analyzed after 3 days. Given is the increase of area covered with live tissue relative to the 3rd day. **A)** Area growth on different phytohormones. **B)** Area growth on media affecting energy supply. **C)** Area growth on media deficientof microelements Ca^{2+} and Phosphate as well as on media introducing osmotic stress. All analysis was done in three biological replicates. A scaleable graphic is available in the electronic file.

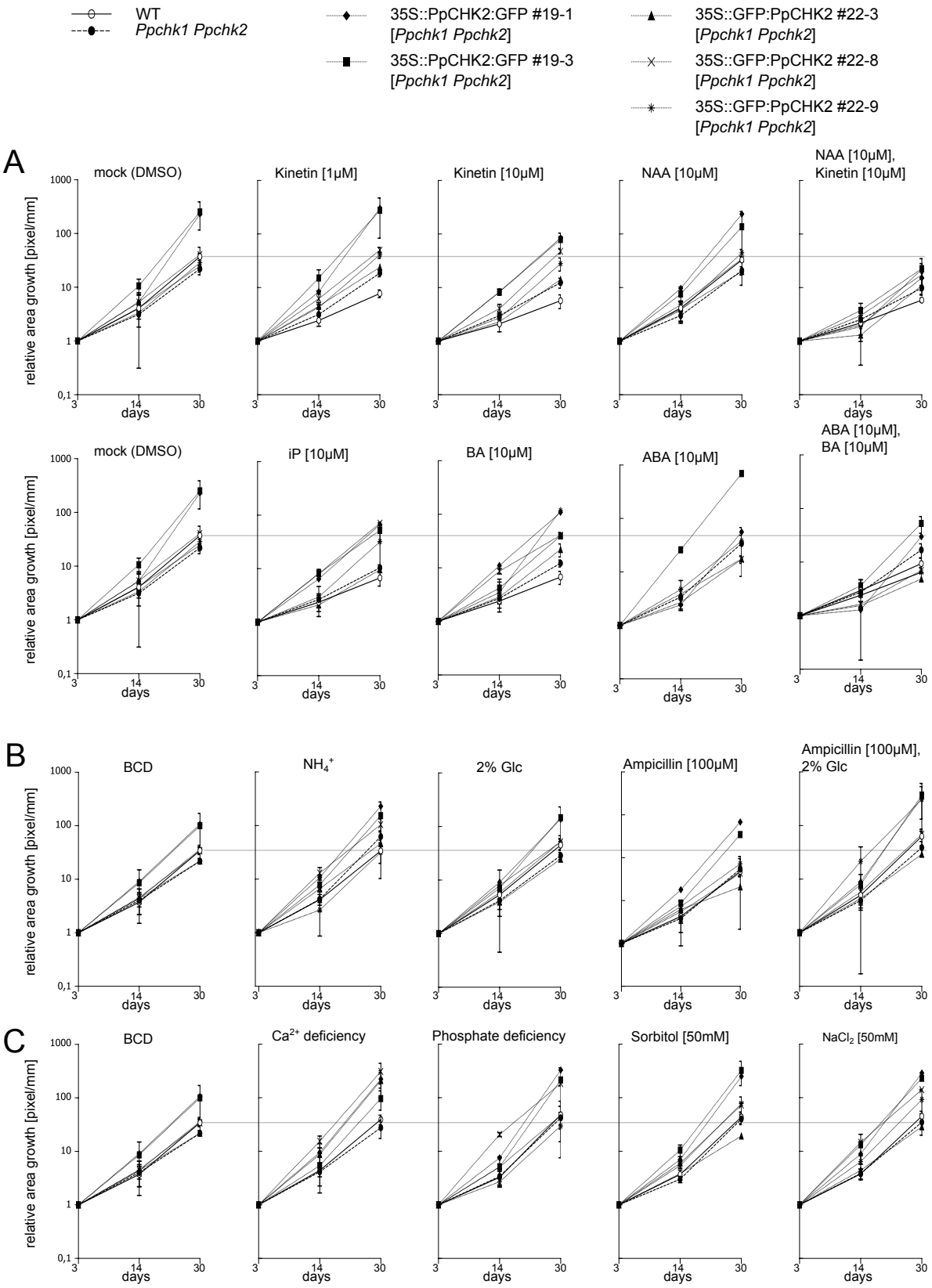

Appendix Figure 6: Growth analysis of the transgenic lines expressing PpCHK2 *[Ppchk1 Ppchk2]* fusion protein to GFP. Transgenic lines were inoculated to medium supplemented with the respective substance and area with live tissue was analyzed after 3 days. Given is the increase of area covered with live tissue relative to the 3rd day. **A)** Area growth on different phytohormones. **B)** Area growth on media affecting energy supply. **C)** Area growth on media deficientof microelements Ca^{2+} and Phosphate as well as on media introducing osmotic stress. All analysis was done in three biological replicates. A scaleable graphic is available in the electronic file.

9.4. Conservation of the CHASE domain residues

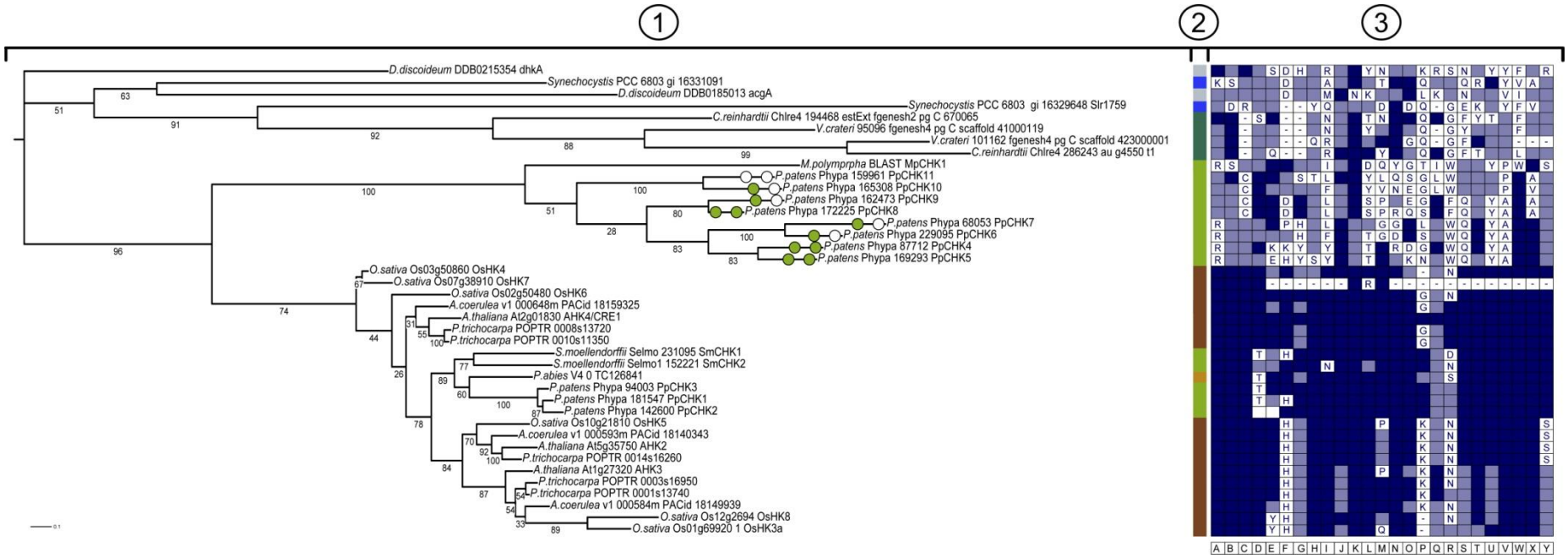

1) Maximum likelyhood tree of the CHASE-domain. Newly identified *Physcomitrella* proteins are marked with an open circle when no EST evidence could be found. Green circles mark EST evidence first in *Physcomitrella patens* and second in *Funaria hygrometica*.

2) Colors for grouping the organism lineages: Angiosperm, Gymnosperm, Lycophyte, Bryophyte, Charophyte, Chlorophyte, Cyanobacteria, others

3) Comparison of amino acids found to be relevant for cytokinin binding in the CHASE domain according to Horthorn *et al.,* 2011:

Position A, (Reference posistion of AHK4 is aa 223 (G) interacts with iP in crystalstructure)
Position B, (Reference posistion of AHK4 is aa 225 (A) interacts with iP in crystalstructure)
Position C, (Reference posistion of AHK4 is aa 227 (A) interacts with iP in crystalstructure)
Position D, (Reference posistion of AHK4 is aa 264 (V) interacts with iP in crystalstructure)
Position E, (Reference posistion of AHK4 is aa 271 (V) interacts with iP in crystalstructure)
Position F, (Reference posistion of AHK4 is aa 273 (Y) interacts with iP in crystalstructure; NOT critical for *t*Z mediated activation in E.coli assay)
Position G, (Reference posistion of AHK4 is aa 274 (L) interacts with iP in crystalstructure)
Position H, (Reference posistion of AHK4 is aa 279 (M) interacts with iP in crystalstructure; NOT critical for *t*Z mediated activation in E.coli assay; mutation caused a slight drop in binding (Heyl et al., 2007))
Position I, (Reference posistion of AHK4 is aa 285 (D) interacts with iP in crystalstructure)
Position J, (Reference posistion of AHK4 is aa 289 (I) interacts with iP in crystalstructure)
Position K, (Reference posistion of AHK4 is aa 303 (P) critical for *t*Z mediated activation in *E. coli* assay)
Position L, (Reference posistion of AHK4 is aa 304 (F) critical for *t*Z mediated activation in *E. coli* assay; mutation caused 40% drop in binding (Heyl *et al.,* 2007))
Position M, (Reference posistion of AHK4 is aa 305 (R) potential canidate to form a flap for the bindingpocket; mutation caused a loss of function (Heyl *et al.,* 2007))
Position N, (Reference posistion of AHK4 is aa 306 (L) critical for *t*Z mediated activation in *E. coli* assay)
Position O, (Reference posistion of AHK4 is aa 307 (L) forms H_2O bridge with iP; critical for *t*Z mediated activation in *E. coli* assay)
Position P, (Reference posistion of AHK4 is aa 308 (E) potential canidate to form a flap for the bindingpocket)
Position Q, (Reference posistion of AHK4 is aa 309 (T) potential canidate to form a flap for the bindingpocket)
Position R, (Reference posistion of AHK4 is aa 310 (H) potential canidate to form a flap for the bindingpocket)
Position S, (Reference posistion of AHK4 is aa 311 (H) potential canidate to form a flap for the bindingpocket)
Position T, (Reference posistion of AHK4 is aa 312 (L) potential canidate to form a flap for the bindingpocket)
Position U, (Reference posistion of AHK4 is aa 315 (V) interacts with iP in crystalstructure)
Position V, (Reference posistion of AHK4 is aa 317 (T) interacts with iP in crystalstructure; NOT critical for *t*Z mediated activation in *E. coli* assay; mutation caused 60% drop in binding (Heyl *et al.,* 2007))
Position W, (Reference posistion of AHK4 is aa 341 (Y) interacts with iP in crystalstructure)
Position X, (Reference posistion of AHK4 is aa 343 (G) interacts with iP in crystalstructure; critical for *t*Z mediated activation in *E. coli* assay)
Position Y, (Reference posistion of AHK4 is aa 345 (A) interacts with iP in crystalstructure)

Dark blue shows conservation compared to reference protein AHK4, light blue marks conserved aa group, white boxes do not show conservation related to AHK4.

Appendix Figure 8: Phylogenetic tree of the CHASE domain and conservation of residues involved in protein folding and ligand binding. (1) The CHASE domain sequences from all organisms under investigation were aligned and a phylogenetic tree using maximum likelihood was inferred, (for details see Material and Methods section 2.6).(2) Organism lineage color code (3) Conservation of amino acids of the CHASE domain that were highlighted by Hothorn and colleagues (2011) when the AHK4 crystal structure was resolved. Dark blue shows conservation, light blue marks conservative substitution, white boxes symbolize no conservation.

9.5. Full phylogenetic tree of the response regulator domains in the data set

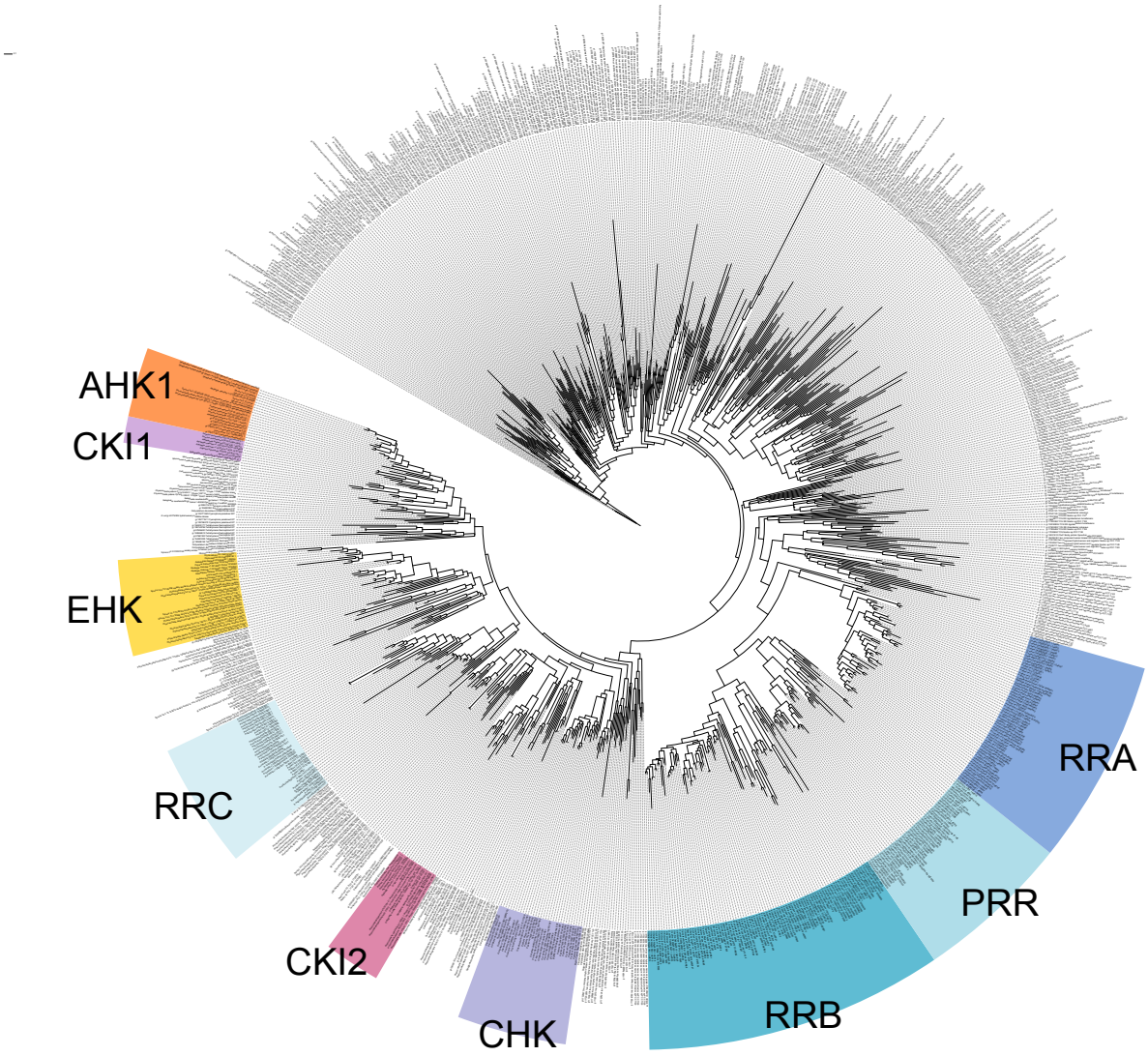

Appendix Figure 9: Phylogenetic tree of all response regulator (RR) domains in the dataset. The response regulator domain sequences from all organisms under investigation were aligned and a phylogenetic tree using a maximum likelihood was inferred. The clades were colored according to known plant gene functions associated with the respective protein. Abbreviations indicate the functionality of the respective clade (AHK1, AHK1 related histidine kinases; CHK, Cytokinin related histidine kinases; CKI1, CKI1 related Histidine kinases; CKI2, CKI2 related Histidine kinases; EHK, Ethylen related Histidine kinases ; RRA, type-A RRs; RRB, type-B RRs; RRC, type-C RRs; PRR, Pseudo-RRs). For details see the material and method section (2.6). A scaleable graphic will be available in the electronic file.

9.6. Phylogenetic analysis of RRCs

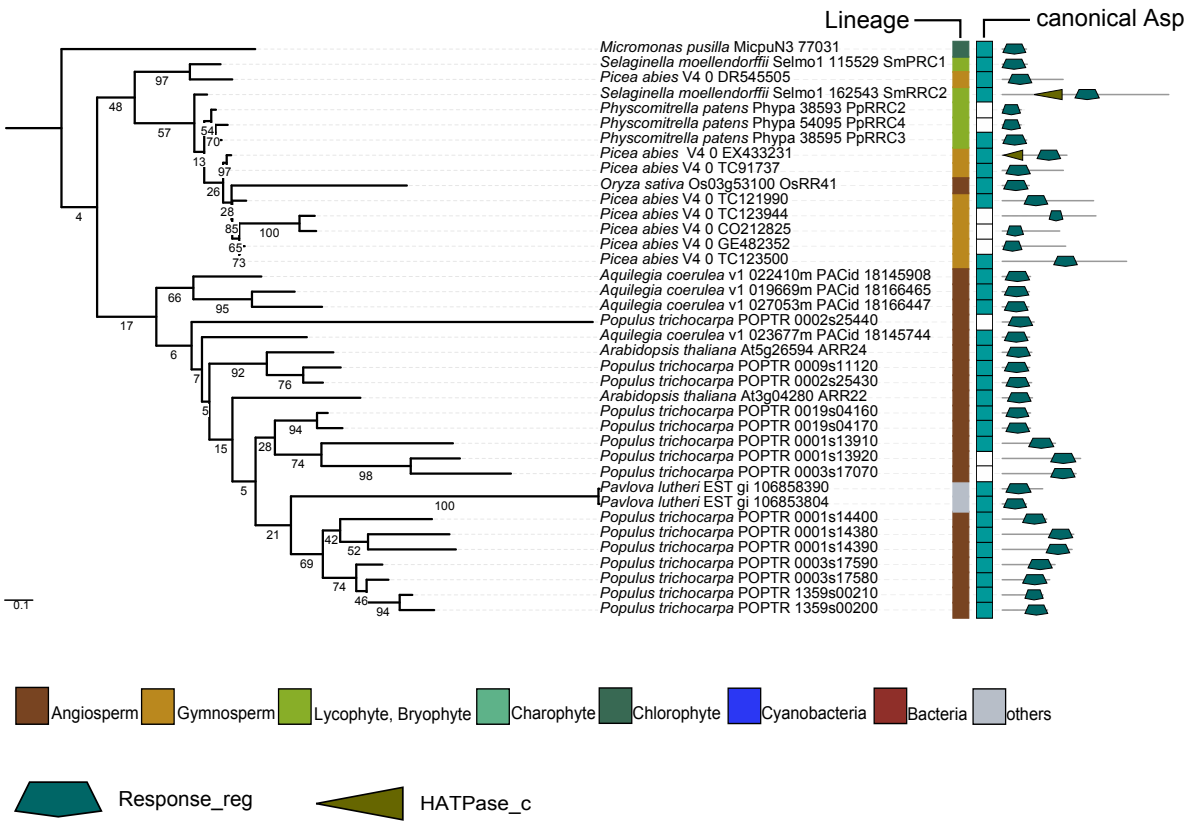

Appendix Figure 10: Phylogenetic tree of the type C response regulators (RRCs). The response regulator domain sequences from all organisms under investigation were aligned and a phylogenetic tree using a maximum likelihood was inferred, shown is the subtree containing the RRCs (for details see Material and Methods section). Domain architecture of the whole respective protein (Abbrev. of the domains are according to the Pfam-database (http://pfam.sanger.ac.uk): Response_reg, PF00027; HATPase c, PF02518).A scaleable graphic is available in the electronic file.

9.7. Phylogenetic analysis of cytokinin metabolism proteins

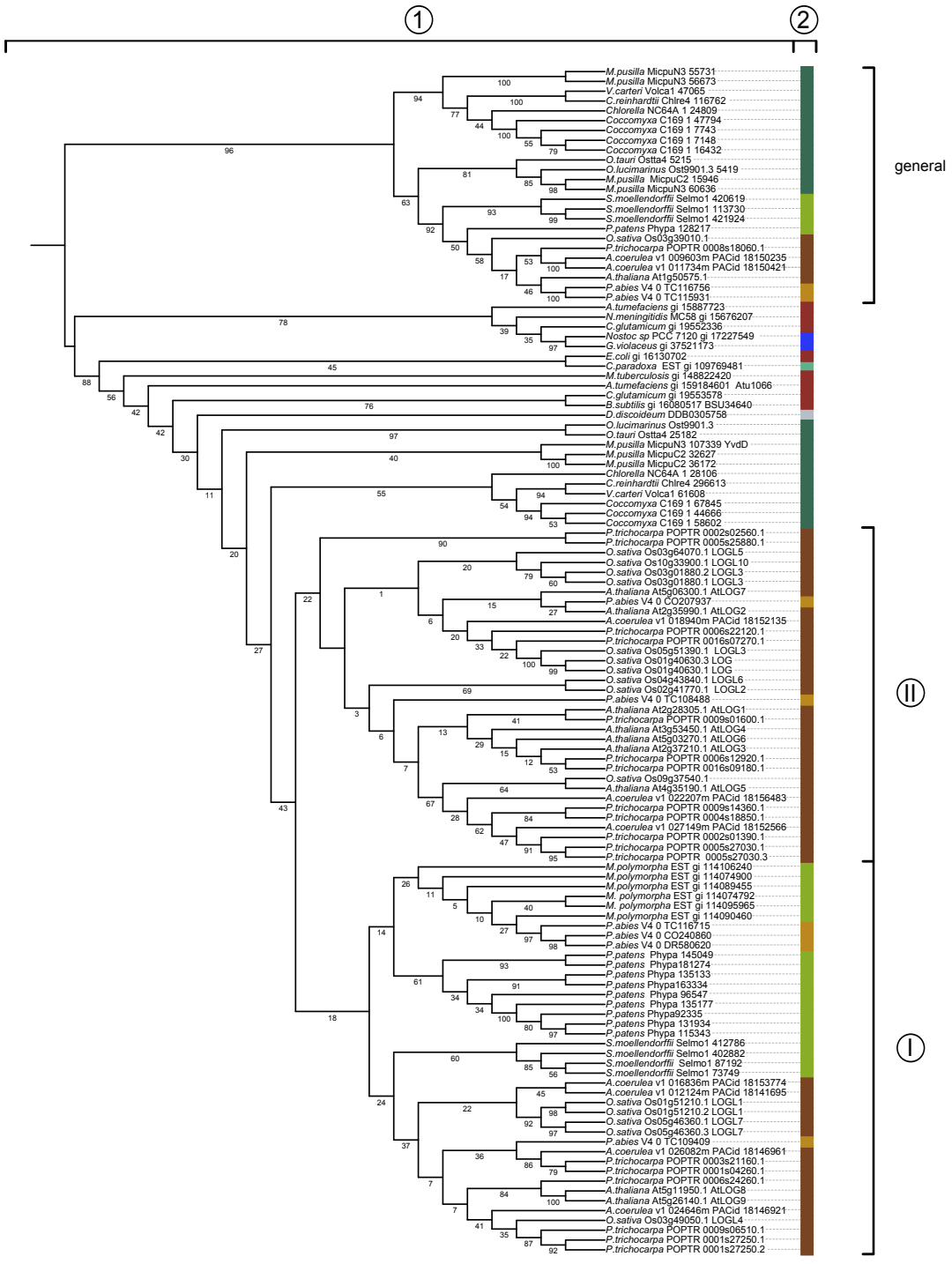

1) Maximum likelyhood tree of the Lysine decarboxylase-domain characteristic for LOG proteins.
2) Colors for grouping the organism lineages:

Angiosperm | Gymnosperm | Lycophyte, Bryophyte | Charophyte | Chlorophyte | Cyanobacteria | Bacteria | others

I) Clade with Angiosperm/Gymnosperm proteins also containing Lycophyte and Bryophyte proteins
II) The Angiosperm/Gymnosperm proteins clade

Appendix FIgure 11: Phylogenetic tree of the Lysine decarboxylase-domain reveals two subclasses of LOG proteins. (1) Sequences of the Lysine decarboxylase domains (Pfam-database (http://pfam.sanger.ac.uk): PFAM PF03641) were aligned using MAFFT and a maximum liklihood tree was calculated with RAxML program. (2) Organism lineage color code.

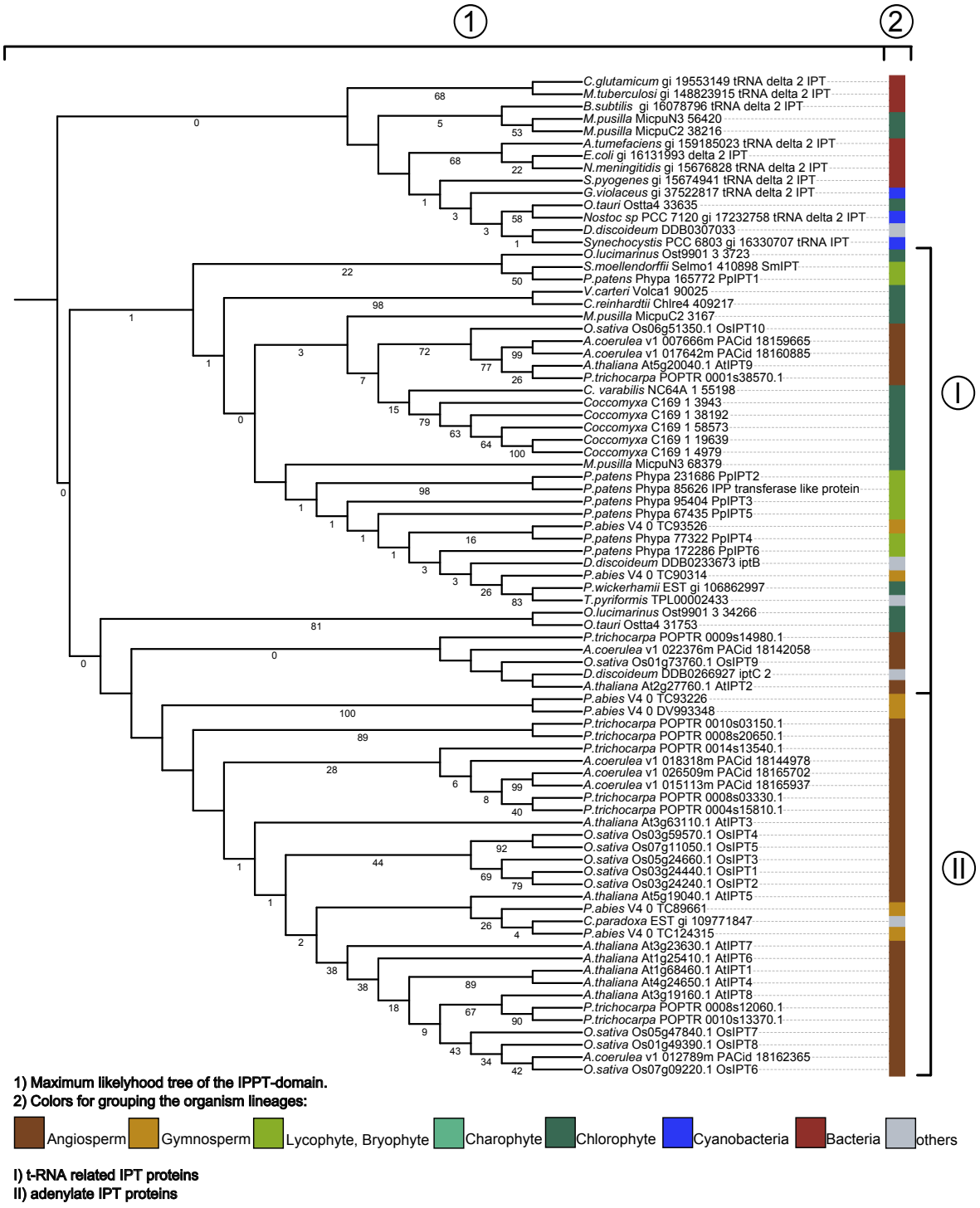

Appendix Figure 12: Phyolgenetic tree of the IPPT-domain reveals two subclasses of Isopentenyltransferase (IPT) proteins. (1) Sequences of the Lysine decarboxlase domains were aligned and a maximum likelihood tree was calculated. (2) Organism lineage color code. (I) Functional clade of t-RNA IPT proteins. (II) Functional clade of adenylate IPT proteins. A saleable graphic is available in the electronic file.

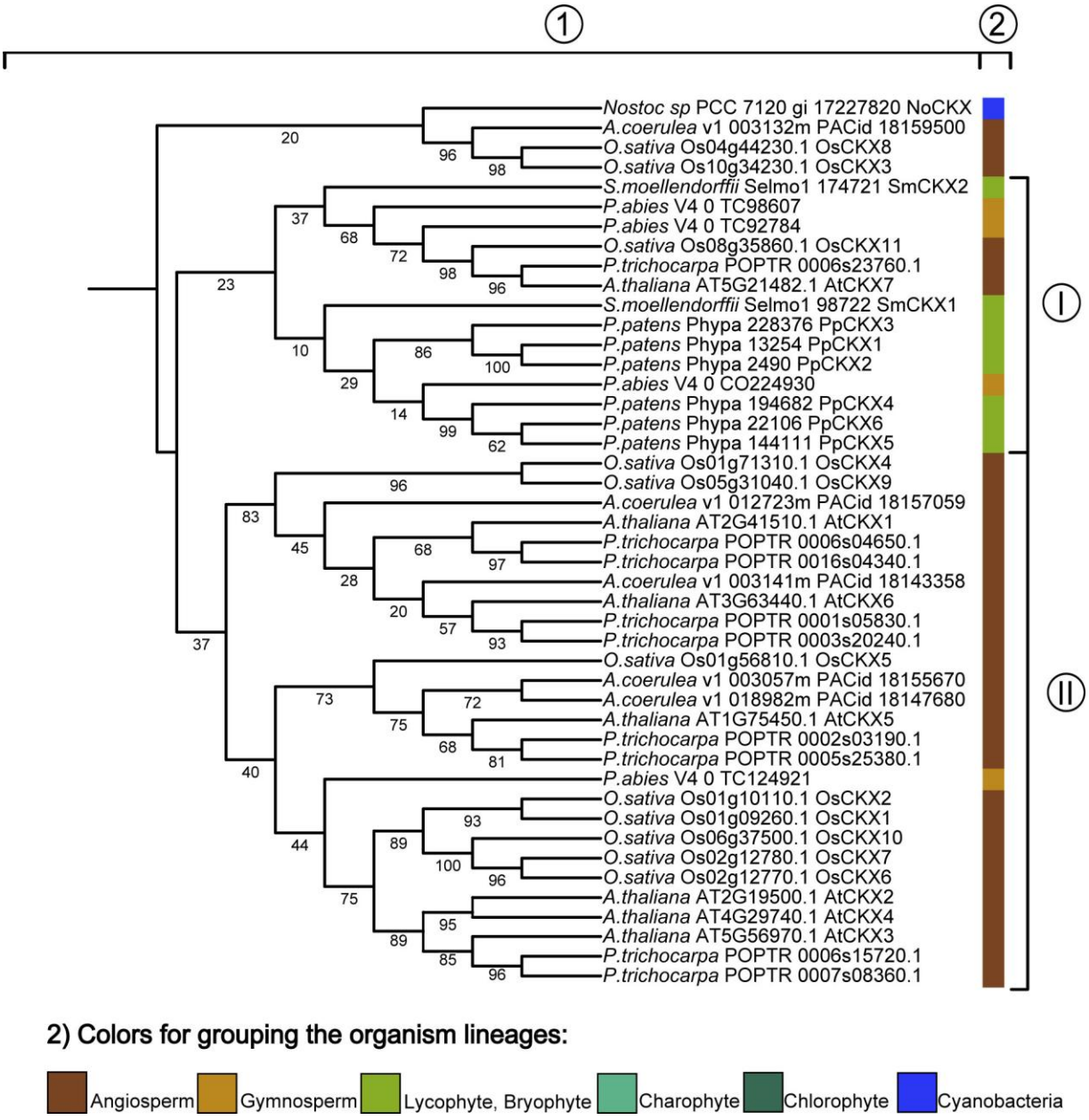

Appendix Figure 13: Phylogenetic tree of the CKX domain reveals two subclasses cytokinin oxidase/ dehydrogenase proteins. (1) Sequences of the cytokinin oxidase/dehydrogenase 1, FAD and cytokinin binding (PF09265) domains were aligned and a maximum likelihood tree was calculated. (2) Organism lineage color code. (I) Clade containing AtCKX7 (II) Clade of vascular plant CKX enzymes.

9.8. PpCHK1 and MpCHK1 are membrane associated

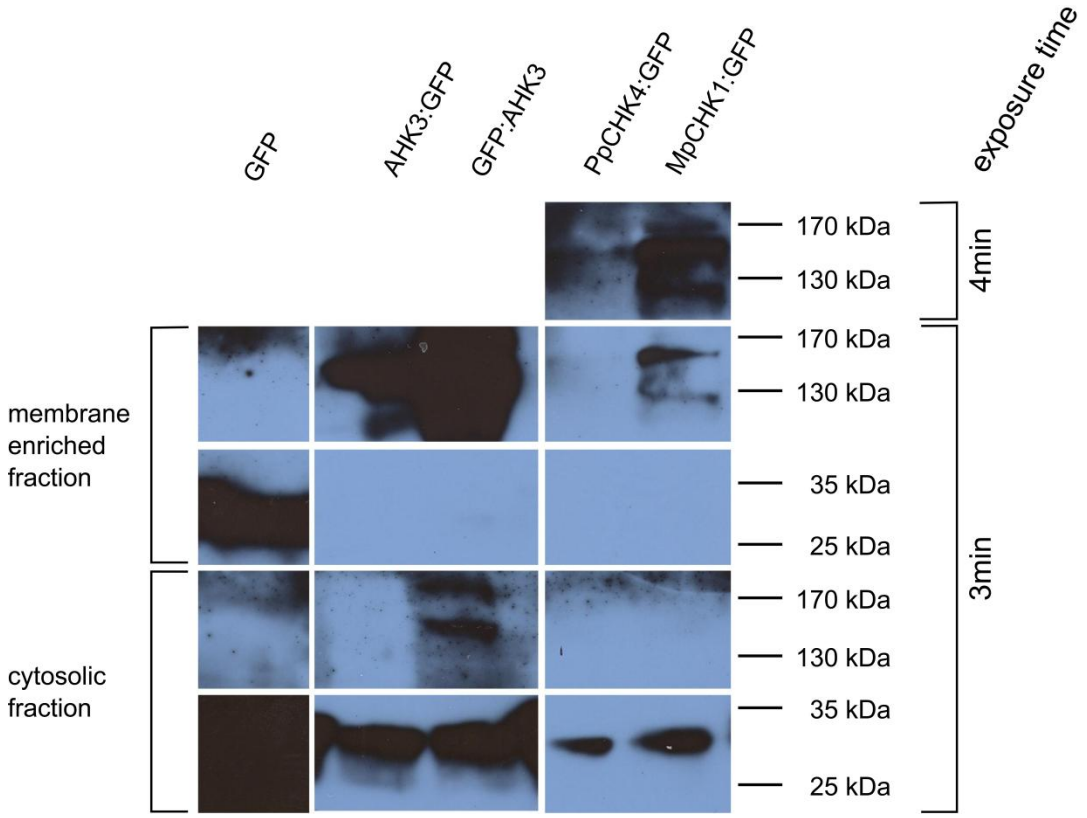

Appendix Figure 14: Cell fractionation and immunodetection of the new potential cytokinin receptors fused to GFP. *N. benthamiana* epidermis cells expressing the relevant fusion protein were harvested five days after infiltration and cell extracts were separated into a membrane enriched and a cytosolic fraction (see section 2.3.1). Subsequent to SDS-PAGE, Immunodetection of the fusion protein was carried out using anti-GFP Antibody (Roche Applied Science, Mannheim). Protein bands of any of the receptor fusion proteins were detected in the membrane enriched fraction. Protein sizes: GFP:AHK3 143 kDa; PpCHK4:GFP, 140 kDa; MpCHK1:GFP, 143 kDa. Free GFP was analyzed as a positive control for expression.

10. Abbreviations

Abbreviation	Explanation
A. thaliana	*Arabidopsis thaliana*
ABA	Abscisic acid
APS	Ammonium persulfate
BA	Benzyladenine
BAP	benzylaminopurine
bp	Base pair
CCT	CONSTANS, CO-like, and TOC1
CHASE	cyclase/histidine kinase associated sensory extracellular
CHK	CHASE domain containing histidine kinase receptor
CKX	Cytokinin Oxidase
cZ	*cis*-zeatin
DAG	Days after germination
DAPI	4´-6-diamino-2-phenylindole
ddH_2O	Bi-distilled, deionisized water
DMAPP	dimethylallylpyrophosphate
DMSO	Dimethyl sulfon oxide
DNA	Deoxyribonucleic acid
DTT	Dithiotreithol
E. coli	*Escherichia coli*
ECL	Enhanced Chemo Luminescence
ER	Endoplasmatic reticulum
EtOH	Ethylalcohol
GFP	Green fluorescent protein
GUS	β-glucuronidase
Glc	glucose
HisKA	Histidine kinase domain
HK	Hybrid histidine kinase
HRP	horse radish peroxidase
IPT	Isopentenyl transferase
IPTG	isopropyl-1-thio-β-D-galactopyranoside
LB	Luria Bertani broth
LOG	cytokinin riboside 5´-monophosphate phosphoribohydrolase
Mbp	mega base pairs
NAA	Naphtaleneacetic acid
nt	Nucleotide
o/n	Over night
P. patens	*Physcomitrella patens*
PCR	Polymerase chain reaction
PEG	Polyethylenglycole
PMSF	phenylmethanesulfonylfluoride
PTA	Protoplast transactivation assay

qRT-PCR	quantitative real time PCR
RE	Restriction enzyme
RNA	Ribonucleic acid
Rpm	Rounds per minute
RR	Response regulator
RRA	type-A response regulator
RRB	type-B response regulator
RRC	type-C response regulator
RT	Room temperature
S. cerevisiae	*Saccharomyces cerevisiae*
SDS	Sodium dodecyl sulfate
SDS-PAGE	SDS-polyacrylamidgelelectrophoresis
TBS	Tris-buffered saline
TCS	Two-component system
TEMED	N,N,N',N'-Tetramethylethylenediamine
tZ	*trans*-zeatin
wol	*Wooden leg*

11. References

Abel, W. O., Knebel, W., Koop, H. U., Marienfeld, J. R., Quader, H., Reski, R., Schnepf, E. and Spärlein, B. (1989). "A cytokinin-sensitive mutant of the moss, *Physcomitrella patens*, defective in chloroplast division." Protoplasma **152**(1): 1-13.

Akiyoshi, D. E., Klee, H., Amasino, R. M., Nester, E. W. and Gordon, M. P. (1984). "T-DNA of *Agrobacterium tumefaciens* encodes an enzyme of cytokinin biosynthesis." Proceedings of the National Academy of Sciences U S A **81**(19): 5994-5998.

Alm, E., Huang, K. and Arkin, A. (2006). "The evolution of two-component systems in bacteria reveals different strategies for niche adaptation." PLoS Computational Biology **2**(11): e143.

Alonso, J. M., Stepanova, A. N., Leisse, T. J., Kim, C. J., Chen, H., Shinn, P., Stevenson, D. K., Zimmerman, J., Barajas, P., Cheuk, R., Gadrinab, C., Heller, C., Jeske, A., Koesema, E., Meyers, C. C., Parker, H., Prednis, L., Ansari, Y., Choy, N., Deen, H., Geralt, M., Hazari, N., Hom, E., Karnes, M., Mulholland, C., Ndubaku, R., Schmidt, I., Guzman, P., Aguilar-Henonin, L., Schmid, M., Weigel, D., Carter, D. E., Marchand, T., Risseeuw, E., Brogden, D., Zeko, A., Crosby, W. L., Berry, C. C. and Ecker, J. R. (2003). "Genome-wide insertional mutagenesis of *Arabidopsis thaliana*." Science **301**(5633): 653-657.

Altschul, S. F., Gish, W., Miller, W., Myers, E. W. and Lipman, D. J. (1990). "Basic local alignment search tool." Journal of Molecular Biology **215**(3): 403-410.

Altschul, S. F., Madden, T. L., Schaffer, A. A., Zhang, J., Zhang, Z., Miller, W. and Lipman, D. J. (1997). "Gapped BLAST and PSI-BLAST: a new generation of protein database search programs." Nucleic Acids Research **25**(17): 3389-3402.

Anantharaman, V. and Aravind, L. (2001). "The CHASE domain: A predicted ligand-binding module in plant cytokinin receptors and other eukaryotic and bacterial receptors." Trends in Biochemical Sciences **26**(10): 579-582.

Anterola, A., Shanle, E., Mansouri, K., Schuette, S. and Renzaglia, K. (2009). Gibberellin precursor is involved in spore germination in the moss *Physcomitrella patens*. Planta. **229:** 1003-1007.

Argyros, R. D., Mathews, D. E., Chiang, Y. H., Palmer, C. M., Thibault, D. M., Etheridge, N., Argyros, D. A., Mason, M. G., Kieber, J. J. and Schaller, G. E. (2008). "Type B response regulators of *Arabidopsis* play key roles in cytokinin signaling and plant development." The Plant Cell **20**(8): 2102-2116.

Ashton, N. W., Champagne, C. E. M., Weiler, T. and Verkoczy, L. K. (2000). "The bryophyte *Physcomitrella patens* replicates extrachromosomal transgenic elements." New Phytologist **146**(3): 391-402.

Ashton, N. W., Cove, D. J. and Featherstone, D. R. (1979a). "The isolation and physiological analysis of mutants of the moss, *Physcomitrella patens*, which over-produce gametophores." Planta **144**(5): 437-442.

Ashton, N. W., Grimsley, N. H. and Cove, D. J. (1979b). "Analysis of gametophytic development in the moss, *Physcomitrella patens*, using auxin and cytokinin resistant mutants." Planta **144**(5): 427-435.

Auer, C. A. (1997). "Cytokinin conjugation: recent advances and patterns in plant evolution." Plant Growth Regulation **23**: 17-32.

Axelos, M., Barbet, J. and Péaud-Lenoel, C. (1984). "Influence of cytokinins on the biosynthesis of light-harvesting chlorophyll ab proteins in tobacco cell suspensions: Detection by radioimmunological assay." Plant Science Letters **33**(2): 201-212.

Axelos, M. and Péaud-Lenoel, C. (1980). "The apoprotein of the light-harvesting chlorophyll ab complex of tobacco cells as a molecular marker of cytokinin activity." Plant Science Letters **19**(1): 33-41.

Barker, E. I. and Ashton, N. W. (2013). "Heteroblasty in the moss, *Aphanoregma patens* (*Physcomitrella patens*), results from progressive modulation of a single fundamental leaf developmental programme." Journal of Bryology **35**(3): 185-196.

Barry, G. F., Rogers, S. G., Fraley, R. T. and Brand, L. (1984). "Identification of a Cloned Cytokinin Biosynthetic Gene." Proceedings of the National Academy of Science U S A **81**(15): 4776-4780.
Batoko, H., Zheng, H. Q., Hawes, C. and Moore, I. (2000). "A rab1 GTPase is required for transport between the endoplasmic reticulum and golgi apparatus and for normal golgi movement in plants." The Plant Cell **12**(11): 2201-2218.
Beemster, G. T. S. and Baskin, T. I. (2000). "STUNTED PLANT 1 Mediates Effects of Cytokinin, But Not of Auxin, on Cell Division and Expansion in the Root of *Arabidopsis*." Plant Physiology **124**(4): 1718-1727.
Benfey, P. N. and Chua, N.-H. (1990). "The cauliflower mosaic virus 35S promoter: combinatorial regulation of transcription in plants." Science **250**(4983): 959-966.
Bernard, P. and Couturier, M. (1992). "Cell killing by the F plasmid CcdB protein involves poisoning of DNA-topoisomerase II complexes." Journal of Molecular Biology **226**(3): 735-745.
Beutelmann, P. (1973). "Untersuchungen zur Biosynthese eines Cytokinins in Calluszellen von Laubmoossporophyten." Planta **112**(2): 181-190.
Bierfreund, N. M., Reski, R. and Decker, E. L. (2003). "Use of an inducible reporter gene system for the analysis of auxin distribution in the moss *Physcomitrella patens*." Plant Cell Reports **21**(12): 1143-1152.
Blanc, G., Duncan, G., Agarkova, I., Borodovsky, M., Gurnon, J., Kuo, A., Lindquist, E., Lucas, S., Pangilinan, J., Polle, J., Salamov, A., Terry, A., Yamada, T., Dunigan, D. D., Grigoriev, I. V., Claverie, J. M. and Van Etten, J. L. (2010). "The *Chlorella variabilis NC64A* genome reveals adaptation to photosymbiosis, coevolution with viruses, and cryptic sex." Plant Cell **22**(9): 2943-2955.
Blom, N., Gammeltoft, S. and Brunak, S. (1999). "Sequence and structure-based prediction of eukaryotic protein phosphorylation sites." Journal of Molecular Biology **294**(5): 1351-1362.
Bolte, S., Talbot, C., Boutte, Y., Catrice, O., Read, N. D. and Satiat-Jeunemaitre, B. (2004). "FM-dyes as experimental probes for dissecting vesicle trafficking in living plant cells." Journal of Microscopy **214**(Pt 2): 159-173.
Bonhomme, S., Nogué, F., Rameau, C. and Schaefer, D. (2013). "Usefulness of *Physcomitrella patens* for studying plant organogenesis. " Plant Organogenesis. D. De Smet, Humana Press. **959:** 21-43.
Bopp, M. and Brandes, H. (1964). "Versuche zur Analyse der Protonemaentwicklung der Laubmosse" Planta **62**: 116-136.
Borza, T., Popescu, C. E. and Lee, R. W. (2005). "Multiple metabolic roles for the nonphotosynthetic plastid of the green alga *Prototheca wickerhamii*." Eukaryotic Cell **4**(2): 253-261.
Brandes, H. and Kende, H. (1968). "Studies on cytokinin-controlled bud formation in moss protonemata." Plant Physiology **43**(5): 827-837.
Brenner, W. G., Ramireddy, E., Heyl, A. and Schmülling, T. (2012). "Gene regulation by cytokinin in *Arabidopsis*." Frontiers in Plant Science **3**: 8.
Brenner, W. G., Romanov, G. A., Köllmer, I., Bürkle, L. and Schmülling, T. (2005). "Immediate-early and delayed cytokinin response genes of *Arabidopsis thaliana* identified by genome-wide expression profiling reveal novel cytokinin-sensitive processes and suggest cytokinin action through transcriptional cascades." The Plant Journal **44**(2): 314-333.
Brenner, W. G. and Schmülling, T. (2012). "Transcript profiling of cytokinin action in *Arabidopsis* roots and shoots discovers largely similar but also organ-specific responses." BMC Plant Biology **12**: 112.
Brzobohaty, B., Moore, I., Kristoffersen, P., Bako, L., Campos, N., Schell, J. and Palme, K. (1993). "Release of active cytokinin by a beta-glucosidase localized to the maize root-meristem." Science **262**(5136): 1051-1054.
Burger, L. and van Nimwegen, E. (2008). "Accurate prediction of protein-protein interactions from sequence alignments using a Bayesian method." Molecular Systems Biology **4**: 165.
Caesar, K., Thamm, A. M., Witthoft, J., Elgass, K., Huppenberger, P., Grefen, C., Horak, J. and Harter, K. (2011). "Evidence for the localization of the *Arabidopsis* cytokinin receptors AHK3 and AHK4 in the endoplasmic reticulum." Journal of Experimental Botany.

Calvin, N. M. and Hanawalt, P. C. (1988). "High-efficiency transformation of bacterial cells by electroporation." Journal of Bacteriology **170**(6): 2796-2801.
Campanella, J. J., Bitincka, L. and Smalley, J. (2003). "MatGAT: an application that generates similarity/identity matrices using protein or DNA sequences." BMC Bioinformatics **4**: 29.
Capra, E. J. and Laub, M. T. (2012). "Evolution of two-component signal transduction systems." Annual Reviews of Microbiology **66**: 325-347.
Capra, E. J., Perchuk, B. S., Lubin, E. A., Ashenberg, O., Skerker, J. M. and Laub, M. T. (2010). "Systematic dissection and trajectory-scanning mutagenesis of the molecular interface that ensures specificity of two-component signaling pathways." PLoS Genetics **6**(11): e1001220.
Casino, P., Rubio, V. and Marina, A. (2009). "Structural insight into partner specificity and phosphoryl transfer in two-component signal transduction." Cell **139**(2): 325-36.
Cerny, M., Dycka, F., Bobalova, J. and Brzobohaty, B. (2011). "Early cytokinin response proteins and phosphoproteins of *Arabidopsis thaliana* identified by proteome and phosphoproteome profiling." Journal of Experimental Botany **62**(3): 921-937.
Chang, C., Kwok, S. F., Bleecker, A. B. and Meyerowitz, E. M. (1993). "*Arabidopsis* ethylene-response gene ETR1: similarity of product to two-component regulators." Science **262**(5133): 539-544.
Choi, J., Choi, D., Lee, S., Ryu, C. M. and Hwang, I. (2011). "Cytokinins and plant immunity: old foes or new friends?" Trends in Plant Science **16**(7): 388-394.
Choi, J., Huh, S. U., Kojima, M., Sakakibara, H., Paek, K. H. and Hwang, I. (2010). "The cytokinin-activated transcription factor ARR2 promotes plant immunity via TGA3/NPR1-dependent salicylic acid signaling in *Arabidopsis*." Developmental Cell **19**(2): 284-295.
Choi, J., Lee, J., Kim, K., Cho, M., Ryu, H., An, G. and Hwang, I. (2012). "Functional identification of OsHK6 as a homotypic cytokinin receptor in rice with preferential affinity for iP." Plant and Cell Physiology **53**(7): 1334-1343.
Chomczynski, P. and Sacchi, N. (1987). "Single-step method of RNA isolation by acid guanidinium thiocyanate-phenol-chloroform extraction." Analytical Biochemistry **162**(1): 156-159.
Christianson, M. L. (2000). "ABA prevents the second cytokinin-mediated event during the induction of shoot buds in the moss *Funaria hygrometrica*." American Journal of Botany **87**(10): 1540-1545.
Christianson, M. L. and Hornbuckle, J. S. (1999). "Phenylurea cytokinins assayed for induction of shoot buds in the moss *Funaria hygrometrica*." American Journal of Botany **86**(11): 1645-1648.
Chung, C. T., Niemela, S. L. and Miller, R. H. (1989). "One-step preparation of competent *Escherichia coli*: transformation and storage of bacterial cells in the same solution." Proceedings of the National Academy of Science U S A **86**(7): 2172-2175.
Clough, S. J. and Bent, A. F. (1998). "Floral dip: a simplified method for *Agrobacterium*-mediated transformation of *Arabidopsis thaliana*." The Plant Journal **16**(6): 735-743.
Colijn, C. M., Sijmons, P., Mol, J. M. M., Kool, A. J. and Nijkamp, H. J. J. (1982). "Light and benzylaminopurine induce changes in ultrastructure and gene expression in plastids of *Petunia hybrida* cell cultures." Current Genetics **6**: 129-135.
Cortleven, A., Noben, J. P. and Valcke, R. (2011). "Analysis of the photosynthetic apparatus in transgenic tobacco plants with altered endogenous cytokinin content: a proteomic study." Proteome Science **9**: 33.
Cortleven, A., Remans, T., Brenner, W. G. and Valcke, R. (2009). "Selection of plastid- and nuclear-encoded reference genes to study the effect of altered endogenous cytokinin content on photosynthesis genes in *Nicotiana tabacum*." Photosynthesis Research **102**(1): 21-29.
Cortleven, A. and Valcke, R. (2012). "Evaluation of the photosynthetic activity in transgenic tobacco plants with altered endogenous cytokinin content: lessons from cytokinin." Physiologia Plantarum **144**(4): 394-408.
Cove, D., Bezanilla, M., Harries, P. and Quatrano, R. (2006). "Mosses as model systems for the study of metabolism and development." Annual Reviews of Plant Biology **57**: 497-520.
Cove, D. J. (1984). "The role of cytokinin and auxin in protonemal development in *Physcomitrella patens* and *Physcomitrium sphaericum*." The Journal of the Hattori Botanical Laboratory = Hattori Shokubutsu Kenkyujo hokoku(55): 79-86.

Cui, Q., Purisima, E. O. and Wang, E. (2009). "Protein evolution on a human signaling network." BMC Systems Biology **3**: 21.
Cutcliffe, J. W., Hellmann, E., Heyl, A. and Rashotte, A. M. (2011). "CRFs form protein-protein interactions with each other and with members of the cytokinin signalling pathway in *Arabidopsis* via the CRF domain." Journal of Experimental Botany **62**(14): 4995-5002.
D'Agostino, I. B., Deruere, J. and Kieber, J. J. (2000). "Characterization of the response of the *Arabidopsis* response regulator gene family to cytokinin." Plant Physiology **124**(4): 1706-1717.
de Koning, A. P., Tartar, A., Boucias, D. G. and Keeling, P. J. (2005). "Expressed sequence tag (EST) survey of the highly adapted green algal parasite, *Helicosporidium*." Protist **156**(2): 181-190.
De Smet, I., Voss, U., Lau, S., Wilson, M., Shao, N., Timme, R. E., Swarup, R., Kerr, I., Hodgman, C., Bock, R., Bennett, M., Jurgens, G. and Beeckman, T. (2011). "Unraveling the evolution of auxin signaling." Plant Physiology **155**(1): 209-221.
Decker, E. L., Frank, W., Sarnighausen, E. and Reski, R. (2006). Moss systems biology en route: phytohormones in *Physcomitrella* development. Plant Biology. **8:** 397-405.
Dello Ioio, R., Nakamura, K., Moubayidin, L., Perilli, S., Taniguchi, M., Morita, M. T., Aoyama, T., Costantino, P. and Sabatini, S. (2008). "A genetic framework for the control of cell division and differentiation in the root meristem." Science **322**(5906): 1380-1384.
Deng, Y., Dong, H., Mu, J., Ren, B., Zheng, B., Ji, Z., Yang, W. C., Liang, Y. and Zuo, J. (2010). "*Arabidopsis* histidine kinase CKI1 acts upstream of histidine phosphotransfer proteins to regulate female gametophyte development and vegetative growth." The Plant Cell **22**(4): 1232-1248.
Depuydt, S. and Hardtke, C. S. (2011). "Hormone signalling crosstalk in plant growth regulation." Current Biology **21**(9): R365-R373.
Derelle, E., Ferraz, C., Rombauts, S., Rouze, P., Worden, A. Z., Robbens, S., Partensky, F., Degroeve, S., Echeynie, S., Cooke, R., Saeys, Y., Wuyts, J., Jabbari, K., Bowler, C., Panaud, O., Piegu, B., Ball, S. G., Ral, J. P., Bouget, F. Y., Piganeau, G., De Baets, B., Picard, A., Delseny, M., Demaille, J., Van de Peer, Y. and Moreau, H. (2006). "Genome analysis of the smallest free-living eukaryote *Ostreococcus tauri* unveils many unique features." Proceedings of the National Academy of Science U S A **103**(31): 11647-11652.
Dortay, H. (2006) Protein-Protein-Interaktionen im Zweikomponenten-Signalsystem von *Arabidopsis thaliana* Freie Universität Berlin Institut für Biologie - Angewandte Genetik
Dortay, H., Gruhn, N., Pfeifer, A., Schwerdtner, M., Schmülling, T. and Heyl, A. (2008). "Toward an interaction map of the two-component signaling pathway of *Arabidopsis thaliana*." Journal of Proteome Research **7**(9): 3649-3660.
Dortay, H., Mehnert, N., Bürkle, L., Schmülling, T. and Heyl, A. (2006). "Analysis of protein interactions within the cytokinin-signaling pathway of *Arabidopsis thaliana*." FEBS Journal **273**(20): 4631-4644.
Duplessis, M. R., Karol, K. G., Adman, E. T., Choi, L. Y., Jacobs, M. A. and Cattolico, R. A. (2007). "Chloroplast His-to-Asp signal transduction: a potential mechanism for plastid gene regulation in *Heterosigma akashiwo* (Raphidophyceae)." BMC Evolutionary Biology **7**: 70.
Dutta, R. and Inouye, M. (2000). "GHKL, an emergent ATPase/kinase superfamily." Trends in Biochemical Sciences **25**(1): 24-28.
Ehlert, A., Weltmeier, F., Wang, X., Mayer, C. S., Smeekens, S., Vicente-Carbajosa, J. and Dröge-Laser, W. (2006). "Two-hybrid protein-protein interaction analysis in *Arabidopsis* protoplasts: establishment of a heterodimerization map of group C and group S bZIP transcription factors." The Plant Journal **46**(5): 890-900.
Eklund, D. M., Thelander, M., Landberg, K., Staldal, V., Nilsson, A., Johansson, M., Valsecchi, I., Pederson, E. R., Kowalczyk, M., Ljung, K., Ronne, H. and Sundberg, E. (2010). "Homologues of the *Arabidopsis thaliana* SHI/STY/LRP1 genes control auxin biosynthesis and affect growth and development in the moss *Physcomitrella patens*." Development **137**(8): 1275-1284.
El-Showk, S., Ruonala, R. and Helariutta, Y. (2013). "Crossing paths: cytokinin signalling and crosstalk." Development **140**(7): 1373-1383.

Emanuelsson, O., Nielsen, H., Brunak, S. and von Heijne, G. (2000). "Predicting subcellular localization of proteins based on their N-terminal amino acid sequence." Journal of Molecular Biology **300**(4): 1005-1016.
Erxleben, A. (2010) Untersuchungen zu Cytokinin- und Auxin-regulaierten Entwicklungsprozessen in *Physcomitrella patens* (Hedw.) Bruch & Schimp Albert-Ludwigs-Universität Freiburg im Breisgau Fakultät für Biologie
Feng, J., Wang, C., Chen, Q., Chen, H., Ren, B., Li, X. and Zuo, J. (2013). "S-nitrosylation of phosphotransfer proteins represses cytokinin signaling." Nature Communications **4**: 1529.
Ferreira, F. J. and Kieber, J. J. (2005). "Cytokinin signaling." Current Opinion in Plant Biology **8**(5): 518-525.
Finet, C., Timme, R. E., Delwiche, C. F. and Marletaz, F. (2010). "Multigene phylogeny of the green lineage reveals the origin and diversification of land plants." Current Biology **20**(24): 2217-2222.
Finka, A., Saidi, Y., Goloubinoff, P., Neuhaus, J.-M., Zrÿd, J.-P. and Schaefer, D. G. (2008). "The knock-out of *ARP3a* gene affects F-actin cytoskeleton organization altering cellular tip growth, morphology and development in moss *Physcomitrella patens*." Cell Motility and the Cytoskeleton **65**(10): 769-784.
Finn, R. D., Clements, J. and Eddy, S. R. (2011). "HMMER web server: interactive sequence similarity searching." Nucleic Acids Research **39**(Web Server issue): W29-37.
Finn, R. D., Mistry, J., Tate, J., Coggill, P., Heger, A., Pollington, J. E., Gavin, O. L., Gunasekaran, P., Ceric, G., Forslund, K., Holm, L., Sonnhammer, E. L., Eddy, S. R. and Bateman, A. (2010). "The Pfam protein families database." Nucleic Acids Research **38**(Database issue): D211-222.
Frank, W., Ratnadewi, D. and Reski, R. (2005). "*Physcomitrella patens* is highly tolerant against drought, salt and osmotic stress." Planta **220**(3): 384-394.
Frebort, I., Kowalska, M., Hluska, T., Frebortova, J. and Galuszka, P. (2011). "Evolution of cytokinin biosynthesis and degradation." Journal of Experimental Botany **62**(8): 2431-2452.
Friedman, A., Janies, D. and Pol, D. (2008). Large-Scale Phylogenetic Analysis of Emerging Infectious Diseases. Tutorials in Mathematical Biosciences IV, Springer Berlin Heidelberg. **1922:** 39-76.
Fujita, T., Sakaguchi, H., Hiwatashi, Y., Wagstaff, S. J., Ito, M., Deguchi, H., Sato, T. and Hasebe, M. (2008). "Convergent evolution of shoots in land plants: lack of auxin polar transport in moss shoots." Evolution & Development **10**(2): 176-186.
Furusawa, C. and Kaneko, K. (2000). "Origin of complexity in multicellular organisms." Physical Review Letters **84**: 6130-6133.
Galperin, M. Y., Nikolskaya, A. N. and Koonin, E. V. (2001). "Novel domains of the prokaryotic two-component signal transduction systems." Federation of European Microbiological Societies Microbiology Letters **203**(1): 11-21.
Gan, S. and Amasino, R. M. (1995). "Inhibition of leaf senescence by autoregulated production of cytokinin." Science **270**(5244): 1986-1988.
Gattolin, S., Alandete-Saez, M., Elliott, K., Gonzalez-Carranza, Z., Naomab, E., Powell, C. and Roberts, J. A. (2006). "Spatial and temporal expression of the response regulators ARR22 and ARR24 in *Arabidopsis thaliana*." Journal of Experimental Botany **57**(15): 4225-4233.
Gerhäuser, D. and Bopp, M. (1990a). "Cytokinin Oxidases in Mosses: 1. Metabolism of Kinetin and Benzyladenine *in vivo*." Journal of Plant Physiology **135**(6): 680-685.
Gerhäuser, D. and Bopp, M. (1990b). "Cytokinin Oxidases in Mosses: 2. Metabolism of Kinetin and Benzyladenine *in vitro*." Journal of Plant Physiology **135**(6): 714-718.
Glöckner, G., Golderer, G., Werner-Felmayer, G., Meyer, S. and Marwan, W. (2008). "A first glimpse at the transcriptome of *Physarum polycephalum*." BMC Genomics **9**(1): 6.
Goode, J. A., Stead, A. D. and Duckett, J. G. (1993). "Redifferentiation of moss protonemata: an experimental and immunofluorescence study of brood cell formation." Canadian Journal of Botany **71**(11): 1510-1519.
Gordon, S. P., Chickarmane, V. S., Ohno, C. and Meyerowitz, E. M. (2009). "Multiple feedback loops through cytokinin signaling control stem cell number within the Arabidopsis shoot meristem." Proceedings of the National Academy of Science U S A **106**(38): 16529-16534.

Gorton, B. S. and Eakin, R. E. (1957). "Development of the gametophyte in the moss *Tortella caespitosa*." Botanical Gazette **119**(1): 31-38.
Gorton, B. S., Skinner, C. G. and Eakin, R. E. (1957). "Activity of some 6-(substituted) purines on the development of the moss *Tortella caespitosa*." Archives of Biochemistry and Biophysics **66**(2): 493-496.
Graham, L. E., Cook, M. E. and Busse, J. S. (2000). "The origin of plants: body plan changes contributing to a major evolutionary radiation." Proceedings of the National Academy of Science U S A **97**(9): 4535-4540.
Graham, L. K. and Wilcox, L. W. (2000). "The origin of alternation of generations in land plants: a focus on matrotrophy and hexose transport." Philosophical Transactions of the Royal Society B: Biological Sciences **355**(1398): 757-766.
Gremillon, L., Kiessling, J., Hause, B., Decker, E. L., Reski, R. and Sarnighausen, E. (2007). "Filamentous temperature-sensitive Z (FtsZ) isoforms specifically interact in the chloroplasts and in the cytosol of *Physcomitrella patens*." New Phytologist **176**(2): 299-310.
Gruhn, N., Halawa, M., Snel, B., Seidel, M. F. and Heyl, A. (2014). "A new subfamily of putative cytokinin receptors is revealed by an analysis of the evolution of the two-component signaling system of plants " Journal of Plant Physiology.
Gruhn, N. and Heyl, A. (2013). "Updates on the model and the evolution of cytokinin signaling." Current Opinion in Plant Biology **16**(5): 569-574.
Grunberg-Manago, M. (1999). "Messenger RNA stability and its role in control of gene expression in bacteria and phages." Annual Reviews of Genetics **33**: 193-227.
Gu, R., Fu, J., Guo, S., Duan, F., Wang, Z., Mi, G. and Yuan, L. (2010). "Comparative Expression and Phylogenetic Analysis of Maize Cytokinin Dehydrogenase/Oxidase (CKX) Gene Family." Journal of Plant Growth Regulation **29**(4): 428-440.
Gultekin, H. and Heermann, K. H. (1988). "The use of polyvinylidenedifluoride membranes as a general blotting matrix." Analytical Biochemistry **172**(2): 320-329.
Gupta, R., Jung, E. and Brunak, S. (2004). "Prediction of N-glycosylation sites in human proteins." In preparation.
Han, Q. M., Jiang, H. W., Qi, X. P., Yu, J. and Wu, P. (2004). "A CHASE domain containing protein kinase *OsCRL4*, represents a new *AtCRE1*-like gene family in rice." Journal of Zhejiang University Science **5**(6): 629-633.
Hanada, K., Hase, T., Toyoda, T., Shinozaki, K. and Okamoto, M. (2011). "Origin and evolution of genes related to ABA metabolism and its signaling pathways." Journal of Plant Research **124**(4): 455-465.
Hanahan, D. (1983). "Studies on transformation of *Escherichia coli* with plasmids." Journal of Molecular Biology **166**(4): 557-580.
Harford, J. B. and Bonifacino, J. S. (2009). Subcellular fractionation and isolation of organelles. Current Protocols in Cell Biology, John Wiley & Sons, Inc. **11:** 3.0.1–3.0.7.
Harrison, C. J., Roeder, A. H., Meyerowitz, E. M. and Langdale, J. A. (2009). "Local cues and asymmetric cell divisions underpin body plan transitions in the moss *Physcomitrella patens*." Current Biology **19**(6): 461-471.
Hass, C., Lohrmann, J., Albrecht, V., Sweere, U., Hummel, F., Yoo, S. D., Hwang, I., Zhu, T., Schafer, E., Kudla, J. and Harter, K. (2004). "The response regulator 2 mediates ethylene signalling and hormone signal integration in *Arabidopsis*." The EMBO Journal **23**(16): 3290-3302.
Hayashi, K., Horie, K., Hiwatashi, Y., Kawaide, H., Yamaguchi, S., Hanada, A., Nakashima, T., Nakajima, M., Mander, L. N., Yamane, H., Hasebe, M. and Nozaki, H. (2010). "Endogenous diterpenes derived from ent-kaurene, a common gibberellin precursor, regulate protonema differentiation of the moss *Physcomitrella patens*." Plant Physiology **153**(3): 1085-1097.
He, Z. H., Cheeseman, I., He, D. and Kohorn, B. D. (1999). "A cluster of five cell wall-associated receptor kinase genes, *Wak1-5*, are expressed in specific organs of *Arabidopsis*." Plant Molecular Biology **39**(6): 1189-1196.

Hedges, S. B., Blair, J. E., Venturi, M. L. and Shoe, J. L. (2004). "A molecular timescale of eukaryote evolution and the rise of complex multicellular life." BMC Evolutionary Biology **4**: 2.
Heintz, D., Erxleben, A., High, A. A., Wurtz, V., Reski, R., Van Dorsselaer, A. and Sarnighausen, E. (2006). "Rapid alteration of the phosphoproteome in the moss *Physcomitrella patens* after cytokinin treatment." Journal of Proteome Research **5**(9): 2283-2293.
Hejatko, J., Ryu, H., Kim, G. T., Dobesova, R., Choi, S., Choi, S. M., Soucek, P., Horak, J., Pekarova, B., Palme, K., Brzobohaty, B. and Hwang, I. (2009). "The Histidine Kinases CYTOKININ-INDEPENDENT1 and ARABIDOPSIS HISTIDINE KINASE2 and 3 Regulate Vascular Tissue Development in Arabidopsis Shoots." The Plant Cell **21**(7): 2008-2021.
Hellmann, E., Gruhn, N. and Heyl, A. (2010). "The more, the merrier: Cytokinin signaling beyond *Arabidopsis*." Plant Signaling and Behaviour **5**(11): 1365-1371.
Heyl, A., Brault, M., Frugier, F., Kuderova, A., Lindner, A. C., Motyka, V., Rashotte, A. M., Schwartzenberg, K. V., Vankova, R. and Schaller, G. E. (2013). "Nomenclature for members of the two-component signaling pathway of plants." Plant Physiol **161**(3): 1063-1065.
Heyl, A., Ramireddy, E., Brenner, W. G., Riefler, M., Allemeersch, J. and Schmülling, T. (2008). "The transcriptional repressor ARR1-SRDX suppresses pleiotropic cytokinin activities in *Arabidopsis*." Plant Physiology **147**(3): 1380-1395.
Heyl, A. and Schmülling, T. (2003). "Cytokinin signal perception and transduction." Current Opinion in Plant Biology **6**(5): 480-488.
Heyl, A., Werner, T. and Schmülling, T. (2006). Cytokinin metabolism and signal transduction. Plant Hormone Signaling. P. Hedden and S. G. Thomas. Oxford, Blackwell Publishing. **24:** 93-123.
Heyl, A., Wulfetange, K., Pils, B., Nielsen, N., Romanov, G. A. and Schmülling, T. (2007). "Evolutionary proteomics identifies amino acids essential for ligand-binding of the cytokinin receptor CHASE domain." BMC Evolutionary Biology **7**: 62.
Higuchi, M., Pischke, M. S., Mähönen, A. P., Miyawaki, K., Hashimoto, Y., Seki, M., Kobayashi, M., Shinozaki, K., Kato, T., Tabata, S., Helariutta, Y., Sussman, M. R. and Kakimoto, T. (2004). "*In planta* functions of the *Arabidopsis* cytokinin receptor family." Proceedings of the National Academy of Sciences U S A **101**(23): 8821-8826.
Hill, K., Mathews, D. E., Kim, H. J., Street, I., Wildes, S., Chiang, Y. H., Mason, M., Alonso, J., Ecker, J., Kieber, J. and Schaller, G. E. (2013). "Functional characterization of type-B response regulators in the *Arabidopsis* cytokinin response." Plant Physiology **162**: 212-224.
Hirano, K., Nakajima, M., Asano, K., Nishiyama, T., Sakakibara, H., Kojima, M., Katoh, E., Xiang, H., Tanahashi, T., Hasebe, M., Banks, J. A., Ashikari, M., Kitano, H., Ueguchi-Tanaka, M. and Matsuoka, M. (2007). "The GID1-mediated gibberellin perception mechanism is conserved in the Lycophyte *Selaginella moellendorffii* but not in the Bryophyte *Physcomitrella patens*." The Plant Cell **19**(10): 3058-3079.
Hirose, N., Takei, K., Kuroha, T., Kamada-Nobusada, T., Hayashi, H. and Sakakibara, H. (2008). "Regulation of cytokinin biosynthesis, compartmentalization and translocation." Journal of Experimental Botany **59**(1): 75-83.
Hoch, J. A. and Varughese, K. I. (2001). "Keeping signals straight in phosphorelay signal transduction." Journal of Bacteriology **183**(17): 4941-4949.
Hohe, A., Decker, E., Gorr, G., Schween, G. and Reski, R. (2002). "Tight control of growth and cell differentiation in photoautotrophically growing moss (*Physcomitrella patens*) bioreactor cultures." Plant Cell Reports **20**(12): 1135-1140.
Holm, K., Källman, T., Gyllenstrand, N., Hedman, H. and Lagercrantz, U. (2010). "Does the core circadian clock in the moss *Physcomitrella patens* (Bryophyta) comprise a single loop?" BMC Plant Biology **10**(1): 1-14.
Horák, J., Grefen, C., Berendzen, K. W., Hahn, A., Stierhof, Y. D., Stadelhofer, B., Stahl, M., Koncz, C. and Harter, K. (2008). "The *Arabidopsis thaliana* response regulator ARR22 is a putative AHP phospho-histidine phosphatase expressed in the chalaza of developing seeds." BMC Plant Biology **8**: 77.

Horstmann, V., Huether, C. M., Jost, W., Reski, R. and Decker, E. L. (2004). "Quantitative promoter analysis in *Physcomitrella patens*: a set of plant vectors activating gene expression within three orders of magnitude." BMC Biotechnology **4**: 13.
Horton, P., Park, K. J., Obayashi, T., Fujita, N., Harada, H., Adams-Collier, C. J. and Nakai, K. (2007). "WoLF PSORT: protein localization predictor." Nucleic Acids Research **35**(Web Server issue): W585-W587.
Hothorn, M., Dabi, T. and Chory, J. (2011). "Structural basis for cytokinin recognition by *Arabidopsis thaliana* histidine kinase 4." Nature Chemical Biology **7**(11): 766-768.
Hutchison, C. E. and Kieber, J. J. (2002). "Cytokinin signaling in *Arabidopsis*." The Plant Cell **14 Suppl**: S47-S59.
Hutchison, C. E., Li, J., Argueso, C., Gonzalez, M., Lee, E., Lewis, M. W., Maxwell, B. B., Perdue, T. D., Schaller, G. E., Alonso, J. M., Ecker, J. R. and Kieber, J. J. (2006). "The *Arabidopsis* histidine phosphotransfer proteins are redundant positive regulators of cytokinin signaling." The Plant Cell **18**(11): 3073-3087.
Hwang, I., Chen, H. C. and Sheen, J. (2002). "Two-component signal transduction pathways in *Arabidopsis*." Plant Physiology **129**(2): 500-515.
Hwang, I. and Sheen, J. (2001). "Two-component circuitry in *Arabidopsis* cytokinin signal transduction." Nature **413**(6854): 383-389.
Hwang, I., Sheen, J. and Müller, B. (2012). "Cytokinin signaling networks." Annual Reviews of Plant Biology **63**: 353-380.
Imamura, A., Hanaki, N., Nakamura, A., Suzuki, T., Taniguchi, M., Kiba, T., Ueguchi, C., Sugiyama, T. and Mizuno, T. (1999). "Compilation and characterization of *Arabiopsis thaliana* response regulators implicated in His-Asp phosphorelay signal transduction." Plant and Cell Physiology **40**(7): 733-742.
Imamura, A., Hanaki, N., Umeda, H., Nakamura, A., Suzuki, T., Ueguchi, C. and Mizuno, T. (1998). "Response regulators implicated in His-to-Asp phosphotransfer signaling in *Arabidopsis*." Proceedings of the National Academy of Sciences U S A **95**(5): 2691-2696.
Inoue, T., Higuchi, M., Hashimoto, Y., Seki, M., Kobayashi, M., Kato, T., Tabata, S., Shinozaki, K. and Kakimoto, T. (2001). "Identification of *CRE1* as a cytokinin receptor from *Arabidopsis*." Nature **409**(6823): 1060-1063.
Ishida, K., Yamashino, T., Nakanishi, H. and Mizuno, T. (2010). "Classification of the genes involved in the two-component system of the moss *Physcomitrella patens*." Bioscience, Biotechnology and Biochemistry **74**(12): 2542-2545.
Ishida, K., Yamashino, T., Yokoyama, A. and Mizuno, T. (2008). "Three type-B response regulators, ARR1, ARR10 and ARR12, play essential but redundant roles in cytokinin signal transduction throughout the life cycle of *Arabidopsis thaliana*." Plant and Cell Physiology **49**(1): 47-57.
Jameson , P. E. (1994). Cytokinin metabolism and compartmentation. Cytokinins: Chemistry, activity, and function. D. W. Mok and M. C. Mok. Boca Raton, CRC**:** 113-128.
Jander, G. and Joshi, V. (2009). "Aspartate-Derived Amino Acid Biosynthesis in *Arabidopsis thaliana*." The Arabidopsis Book: e0121.
Jenkins, G. I. and Cove, D. J. (1983). "Light requirements for regeneration of protoplasts of the moss *Physcomitrella patens*." Planta **157**(1): 39-45.
Jensen, H. (2013) Molecular characterization of dominant repressors of the cytokinin deficiency syndrome Freie Universität Berlin Institut für Biologie - Angewandte Genetik
Kakimoto, T. (2001). "Identification of plant cytokinin biosynthetic enzymes as dimethylallyl diphosphate: ATP/ADP isopentenyltransferases." Plant and Cell Physiology **42**(7): 677-685.
Kakimoto, T. (2003). "Perception and signal transduction of cytokinins." Annual Reviews of Plant Biology **54**: 605-627.
Kang, N. Y., Cho, C., Kim, N. Y. and Kim, J. (2012). "Cytokinin receptor-dependent and receptor-independent pathways in the dehydration response of *Arabidopsis thaliana*." Journal of plant physiology **169**(14): 1382-1391.

Karimi, M., De Meyer, B. and Hilson, P. (2005). "Modular cloning in plant cells." Trends in Plant Science **10**(3): 103-105.
Karimi, M., Inze, D. and Depicker, A. (2002). "GATEWAY vectors for *Agrobacterium*-mediated plant transformation." Trends in Plant Science **7**(5): 193-195.
Karol, K. G., McCourt, R. M., Cimino, M. T. and Delwiche, C. F. (2001). "The closest living relatives of land plants." Science **294**(5550): 2351-2353.
Kasten, B., Buck, F., Nuske, J. and Reski, R. (1997). "Cytokinin affects nuclear- and plastome-encoded energy-converting plastid enzymes." Planta **201**(3): 261-272.
Kasten, B. and Reski, R. (1997). "beta-Lactam antibiotics inhibit chloroplast division in a moss (*Physcomitrella patens*) but not in tomato (*Lycopersicon esculentum*)." Journal of Plant Physiology **150**(1-2): 137-140.
Katayama, N., Takano, H., Sugiyama, M., Takio, S., Sakai, A., Tanaka, K., Kuroiwa, H. and Ono, K. (2003). "Effects of antibiotics that inhibit the bacterial peptidoglycan synthesis pathway on moss chloroplast division." Plant and Cell Physiology **44**(7): 776-781.
Katoh, K., Asimenos, G. and Toh, H. (2009). "Multiple alignment of DNA sequences with MAFFT." Methods in molecular biology **537**: 39-64.
Keeling, P. J. (2010). "The endosymbiotic origin, diversification and fate of plastids." Philosophical transactions of the Royal Society of London. Series B, Biological sciences **365**(1541): 729-748.
Kenrick, M. K. and Crane, P. R. (1997). "The origin and early evolution of plants on land." Nature **389**: 33-39.
Kerppola, T. K. (2006). "Design and implementation of bimolecular fluorescence complementation (BiFC) assays for the visualization of protein interactions in living cells." Nature Protocols **1**(3): 1278-1286.
Kiba, T., Aoki, K., Sakakibara, H. and Mizuno, T. (2004). "*Arabidopsis* response regulator, *ARR22*, ectopic expression of which results in phenotypes similar to the *wol* cytokinin-receptor mutant." Plant and Cell Physiology **45**(8): 1063-1077.
Kiessling, J., Kruse, S., Rensing, S. A., Harter, K., Decker, E. L. and Reski, R. (2000). "Visualization of a cytoskeleton-like FtsZ network in chloroplasts." Journal of Cell Biology **151**(4): 945-950.
Kiessling, J., Martin, A., Gremillon, L., Rensing, S. A., Nick, P., Sarnighausen, E., Decker, E. L. and Reski, R. (2004). "Dual targeting of plastid division protein FtsZ to chloroplasts and the cytoplasm." EMBO Reports **5**(9): 889-894.
Kim, H. J., Ryu, H., Hong, S. H., Woo, H. R., Lim, P. O., Lee, I. C., Sheen, J., Nam, H. G. and Hwang, I. (2006). "Cytokinin-mediated control of leaf longevity by AHK3 through phosphorylation of ARR2 in *Arabidopsis*." Proceedings of the National Academy of Science U S A **103**(3): 814-819.
Kim, K., Ryu, H., Cho, Y. H., Scacchi, E., Sabatini, S. and Hwang, I. (2012). "Cytokinin-facilitated proteolysis of ARABIDOPSIS RESPONSE REGULATOR 2 attenuates signaling output in two-component circuitry." The Plant Journal **69**(6): 934-945.
Kim, P. M., Korbel, J. O. and Gerstein, M. B. (2007). "Positive selection at the protein network periphery: evaluation in terms of structural constraints and cellular context." Proceedings of the National Academy of Science U S A **104**(51): 20274-20279.
Kirby, J. and Kavanagh, T. A. (2002). "NAN fusions: a synthetic sialidase reporter gene as a sensitive and versatile partner for GUS." The Plant Journal **32**(3): 391-400.
Klein, B. (1967). "Versuche zur Analyse der Protonemaentwicklung der Laubmoose." Planta **73**(1): 12-27.
Knoop, B. (1978). "Multiple DNA contents in the haploid protonema of the moss *Funaria hygrometrica* sibth." Protoplasma **94**(3-4): 307-314.
Koenig, R. L., Morris, R. O. and Polacco, J. C. (2002). "tRNA is the source of low-level *trans*-zeatin production in *Methylobacterium spp.*" Journal of Bacteriology **184**(7): 1832-1842.
Komatsu, K., Nishikawa, Y., Ohtsuka, T., Taji, T., Quatrano, R. S., Tanaka, S. and Sakata, Y. (2009). "Functional analyses of the ABI1-related protein phosphatase type 2C reveal evolutionarily conserved regulation of abscisic acid signaling between *Arabidopsis* and the moss *Physcomitrella patens*." Plant Molecular Biology **70**(3): 327-340.

Koncz, C., Olsson, O., Langridge, W. H., Schell, J. and Szalay, A. A. (1987). "Expression and assembly of functional bacterial luciferase in plants." Proceedings of the National Academy of Science U S A **84**(1): 131-135.
Koretke, K. K., Lupas, A. N., Warren, P. V., Rosenberg, M. and Brown, J. R. (2000). "Evolution of two-component signal transduction." Molecular Biology and Evolution **17**(12): 1956-1970.
Krecek, P., Skupa, P., Libus, J., Naramoto, S., Tejos, R., Friml, J. and Zazimalova, E. (2009). "The PIN-FORMED (PIN) protein family of auxin transporters." Genome Biology **10**(12): 249.
Kurakawa, T., Ueda, N., Maekawa, M., Kobayashi, K., Kojima, M., Nagato, Y., Sakakibara, H. and Kyozuka, J. (2007). "Direct control of shoot meristem activity by a cytokinin-activating enzyme." Nature **445**(7128): 652-655.
Kuroha, T., Tokunaga, H., Kojima, M., Ueda, N., Ishida, T., Nagawa, S., Fukuda, H., Sugimoto, K. and Sakakibara, H. (2009). "Functional analyses of LONELY GUY cytokinin-activating enzymes reveal the importance of the direct activation pathway in *Arabidopsis*." The Plant Cell **21**(10): 3152-3169.
Laemmli, U. K. (1970). "Cleavage of structural proteins during the assembly of the head of bacteriophage T4." Nature **227**(5259): 680-685.
Lakatos, L., Szittya, G., Silhavy, D. and Burgyan, J. (2004). "Molecular mechanism of RNA silencing suppression mediated by p19 protein of tombusviruses." The EMBO Journal **23**(4): 876-884.
Lang, D., Zimmer, A. D., Rensing, S. A. and Reski, R. (2008). "Exploring plant biodiversity: the *Physcomitrella* genome and beyond." Trends in Plant Science **13**(10): 542-549.
Lee, D. J., Kim, S., Ha, Y. M. and Kim, J. (2008). "Phosphorylation of Arabidopsis response regulator 7 (ARR7) at the putative phospho-accepting site is required for ARR7 to act as a negative regulator of cytokinin signaling." Planta **227**(3): 577-587.
Leibfried, A., To, J. P., Busch, W., Stehling, S., Kehle, A., Demar, M., Kieber, J. J. and Lohmann, J. U. (2005). "WUSCHEL controls meristem function by direct regulation of cytokinin-inducible response regulators." Nature **438**(7071): 1172-1175.
Lerbs, S., Lerbs, W., Klyachko, N. L., G., R. E., Kulaeva, O. N., Wollgiehn, R. and Parthier, B. (1984). "Gene expression in cytokinin- and light-mediated plastogenesis of cucurbita cotyledons: ribulose-1,5-bisphosphate carboxylase/oxygenase." Planta **162**: 289-298.
Letham, D. S. (1963). "Zeatin, a Factor Inducing Cell Division Isolated from Zea Mays." Life Sciences **8**: 569-573.
Lew, R. and Tsuji, H. (1982). "Effect of Benzyladenine Treatment Duration on delta-Aminolevulinic Acid Accumulation in the Dark, Chlorophyll Lag Phase Abolition, and Long-Term Chlorophyll Production in Excised Cotyledons of Dark-Grown Cucumber Seedlings." Plant Physiology **69**(3): 663-667.
Lewis, L. A. and McCourt, R. M. (2004). "Green algae and the origin of land plants." American Journal of Botany **91**: 1535-1556.
Li, Y., Kurepa, J. and Smalle, J. (2013). "AXR1 promotes the Arabidopsis cytokinin response by facilitating ARR5 proteolysis." The Plant Journal: for Cell and Molecular Biology **74**(1): 13-24.
Liang, C., Xi, Y., Shu, J., Li, J., Yang, J., Che, K., Jin, D., Liu, X., Weng, M., He, Y. and Wang, B. (2004). Construction of a BAC library of *Physcomitrella patens* and isolation of a LEA gene. Plant Science. **167:** 491-498.
Lienard, D., Durambur, G., Kiefer-Meyer, M. C., Nogue, F., Menu-Bouaouiche, L., Charlot, F., Gomord, V. and Lassalles, J. P. (2008). "Water transport by aquaporins in the extant plant *Physcomitrella patens*." Plant Physiology **146**(3): 1207-1218.
Ligrone, R., Duckett, J. G. and Renzaglia, K. S. (2012). "Major transitions in the evolution of early land plants: a bryological perspective." Annals of Botany **109**(5): 851-871.
Liu, W. Z., Kong, D. D., Gu, X. X., Gao, H. B., Wang, J. Z., Xia, M., Gao, Q., Tian, L. L., Xu, Z. H., Bao, F., Hu, Y., Ye, N. S., Pei, Z. M. and He, Y. K. (2013). "Cytokinins can act as suppressors of nitric oxide in *Arabidopsis*." Proceedings of the National Academy of Science U S A **110**(4): 1548-1553.

Lohar, D. P., Schaff, J. E., Laskey, J. G., Kieber, J. J., Bilyeu, K. D. and Bird, D. M. (2004). "Cytokinins play opposite roles in lateral root formation, and nematode and Rhizobial symbioses." The Plant Journal **38**(2): 203-214.
Lohrmann, J., Buchholz, G., Keitel, C., Sweere, U., Kircher, S., Bäurle, I., Kudla, J., Schäfer, E. and Harter, K. (1999). "Differential Expression and Nuclear Localization of Response Regulator-Like Proteins from Arabidopsis thaliana1." Plant Biology **1**(5): 495-505.
Lohrmann, J. and Harter, K. (2002). "Plant two-component signaling systems and the role of response regulators." Plant Physiology **128**(2): 363-369.
Lomin, S. N., Yonekura-Sakakibara, K., Romanov, G. A. and Sakakibara, H. (2011). "Ligand-binding properties and subcellular localization of maize cytokinin receptors." Journal of Experimental Botany **62**(14): 5149-5159.
Lopez, P. J., Marchand, I., Joyce, S. A. and Dreyfus, M. (1999). "The C-terminal half of RNase E, which organizes the *Escherichia coli* degradosome, participates in mRNA degradation but not rRNA processing *in vivo*." Molecular Microbiology **33**(1): 188-199.
Lysenko, E., Pshybytko, N., Karavaiko, N., Yakovleva, L., Novikova, G., Kulaeva, O. and Kusnetsov, V. (2012). "Do plant chloroplasts contain histidine kinases?" Acta Physiologiae Plantarum **34**(3): 1153-1164.
Mähönen, A. P., Bishopp, A., Higuchi, M., Nieminen, K. M., Kinoshita, K., Tormakangas, K., Ikeda, Y., Oka, A., Kakimoto, T. and Helariutta, Y. (2006a). "Cytokinin signaling and its inhibitor AHP6 regulate cell fate during vascular development." Science **311**(5757): 94-98.
Mähönen, A. P., Bonke, M., Kauppinen, L., Riikonen, M., Benfey, P. N. and Helariutta, Y. (2000). "A novel two-component hybrid molecule regulates vascular morphogenesis of the *Arabidopsis* root." Genes and Development **14**(23): 2938-2943.
Mähönen, A. P., Higuchi, M., Tormakangas, K., Miyawaki, K., Pischke, M. S., Sussman, M. R., Helariutta, Y. and Kakimoto, T. (2006b). "Cytokinins regulate a bidirectional phosphorelay network in *Arabidopsis*." Current Biology **16**(11): 1116-1122.
Marella, H. H., Sakata, Y. and Quatrano, R. S. (2006). "Characterization and functional analysis of ABSCISIC ACID INSENSITIVE3-like genes from *Physcomitrella patens*." The Plant Journal **46**(6): 1032-1044.
Martin, W., Rujan, T., Richly, E., Hansen, A., Cornelsen, S., Lins, T., Leister, D., Stoebe, B., Hasegawa, M. and Penny, D. (2002). "Evolutionary analysis of *Arabidopsis*, cyanobacterial, and chloroplast genomes reveals plastid phylogeny and thousands of cyanobacterial genes in the nucleus." Proceedings of the National Academy of Science U S A **99**(19): 12246-12251.
Maslov, S., Krishna, S., Pang, T. Y. and Sneppen, K. (2009). "Toolbox model of evolution of prokaryotic metabolic networks and their regulation." Proceedings of the National Academy of Science U S A **106**(24): 9743-9748.
Mason, M. G., Li, J., Mathews, D. E., Kieber, J. J. and Schaller, G. E. (2004). "Type-B response regulators display overlapping expression patterns in *Arabidopsis*." Plant Physiology **135**(2): 927-937.
Mason, M. G., Mathews, D. E., Argyros, D. A., Maxwell, B. B., Kieber, J. J., Alonso, J. M., Ecker, J. R. and Schaller, G. E. (2005). "Multiple type-B response regulators mediate cytokinin signal transduction in *Arabidopsis*." The Plant Cell **17**(11): 3007-3018.
Merchant, S. S., Prochnik, S. E., Vallon, O., Harris, E. H., Karpowicz, S. J., Witman, G. B., Terry, A., Salamov, A., Fritz-Laylin, L. K., Marechal-Drouard, L., Marshall, W. F., Qu, L. H., Nelson, D. R., Sanderfoot, A. A., Spalding, M. H., Kapitonov, V. V., Ren, Q., Ferris, P., Lindquist, E., Shapiro, H., Lucas, S. M., Grimwood, J., Schmutz, J., Cardol, P., Cerutti, H., Chanfreau, G., Chen, C. L., Cognat, V., Croft, M. T., Dent, R., Dutcher, S., Fernandez, E., Fukuzawa, H., Gonzalez-Ballester, D., Gonzalez-Halphen, D., Hallmann, A., Hanikenne, M., Hippler, M., Inwood, W., Jabbari, K., Kalanon, M., Kuras, R., Lefebvre, P. A., Lemaire, S. D., Lobanov, A. V., Lohr, M., Manuell, A., Meier, I., Mets, L., Mittag, M., Mittelmeier, T., Moroney, J. V., Moseley, J., Napoli, C., Nedelcu, A. M., Niyogi, K., Novoselov, S. V., Paulsen, I. T., Pazour, G., Purton, S., Ral, J. P., Riano-Pachon, D. M., Riekhof, W., Rymarquis, L., Schroda, M., Stern, D., Umen, J., Willows, R., Wilson, N., Zimmer, S. L., Allmer, J., Balk, J., Bisova, K., Chen, C. J., Elias, M., Gendler, K., Hauser, C., Lamb, M. R., Ledford, H., Long, J. C., Minagawa, J.,

Page, M. D., Pan, J., Pootakham, W., Roje, S., Rose, A., Stahlberg, E., Terauchi, A. M., Yang, P., Ball, S., Bowler, C., Dieckmann, C. L., Gladyshev, V. N., Green, P., Jorgensen, R., Mayfield, S., Mueller-Roeber, B., Rajamani, S., Sayre, R. T., Brokstein, P., Dubchak, I., Goodstein, D., Hornick, L., Huang, Y. W., Jhaveri, J., Luo, Y., Martinez, D., Ngau, W. C., Otillar, B., Poliakov, A., Porter, A., Szajkowski, L., Werner, G., Zhou, K., Grigoriev, I. V., Rokhsar, D. S. and Grossman, A. R. (2007). "The *Chlamydomonas* genome reveals the evolution of key animal and plant functions." Science **318**(5848): 245-250.
Michael, L. C. and Christianson, M. L. (2000). "Control of morphogenesis in bryophytes" Bryophyte Biology, Cambridge University Press 199-224.
Michel, K. P., Schroder, A. K., Zimmermann, M., Brandt, S., Pistorius, E. K., Frankenberg-Dinkel, N. and Staiger, D. (2009). "The hybrid histidine kinase Slr1759 of the cyanobacterium *Synechocystis sp.* PCC 6803 contains FAD at its PAS domain." Archives of Microbiology **191**(6): 553-559.
Miller, C. O. (1958). "The Relationship of the Kinetin and Red-Light Promotions of Lettuce Seed Germination." Plant Physiology **33**(2): 115-117.
Miller, C. O., Skoog, F., Okumura, F. S., Von Saltza, M. H. and Strong, F. M. (1956). "Isolation, Structure and Synthesis of Kinetin, a Substance Promoting Cell Division." Journal of the American Chemical Society **78**(7): 1375-1380.
Miwa, K., Ishikawa, K., Terada, K., Yamada, H., Suzuki, T., Yamashino, T. and Mizuno, T. (2007). "Identification of amino acid substitutions that render the *Arabidopsis* cytokinin receptor histidine kinase AHK4 constitutively active." Plant and Cell Physiology **48**(12): 1809-1814.
Miyawaki, K., Matsumoto-Kitano, M. and Kakimoto, T. (2004). "Expression of cytokinin biosynthetic isopentenyltransferase genes in *Arabidopsis*: tissue specificity and regulation by auxin, cytokinin, and nitrate." The Plant Journal **37**(1): 128-138.
Miyawaki, K., Tarkowski, P., Matsumoto-Kitano, M., Kato, T., Sato, S., Tarkowska, D., Tabata, S., Sandberg, G. and Kakimoto, T. (2006). "Roles of Arabidopsis ATP/ADP isopentenyltransferases and tRNA isopentenyltransferases in cytokinin biosynthesis." Proceedings of the National Academy of Sciences U S A **103**(44): 16598-16603.
Mizuno, T. (2004). "Plant response regulators implicated in signal transduction and circadian rhythm." Current Opinion in Plant Biology **7**(5): 499-505.
Mizuno, T. (2005). "Two-component phosphorelay signal transduction systems in plants: from hormone responses to circadian rhythms." Bioscience, Biotechnology, and Biochemistry **69**(12): 2263-2276.
Mizuno, T. and Nakamichi, N. (2005). "Pseudo-Response Regulators (PRRs) or True Oscillator Components (TOCs)." Plant and Cell Physiology **46**(5): 677-685.
Mizuno, T. and Yamashino, T. (2010). "Biochemical characterization of plant hormone cytokinin-receptor histidine kinases using microorganisms." Methods in Enzymology **471**: 335-356.
Mok, D. W. and Mok, M. C. (2001). "Cytokinin metabolism and action." Annual Reviews of Plant Physiology and Plant Molecular Biology **52**: 89-118.
Monod, J. (1949). "The growth of bacterial cultures." Annual Reviews of Microbiology **3**: 371-394.
Moore, I. and Murphy, A. (2009). "Validating the location of fluorescent protein fusions in the endomembrane system." The Plant Cell **21**(6): 1632-1636.
Mougel, C. and Zhulin, I. B. (2001). "CHASE: An extracellular sensing domain common to transmembrane receptors from prokaryotes, lower eukaryotes and plants." Trends in Biochemical Sciences **26**(10): 582-584.
Müller, B. and Sheen, J. (2008). "Cytokinin and auxin interaction in root stem-cell specification during early embryogenesis." Nature **453**(7198): 1094-1097.
Nagaraj, S. H., Gasser, R. B. and Ranganathan, S. (2007). "A hitchhiker's guide to expressed sequence tag (EST) analysis." Briefings in Bioinformatics **8**(1): 6-21.
Naito, K., Ueda, K. and Tsuji, H. (1981). "Differential effects of benzyladenine on the ultrastructure of chloroplasts in intact bean leaves according to their age." Protoplasma **105**(3-4): 293-306.

Nedelcu, A. M., Borza, T. and Lee, R. W. (2006). "A land plant-specific multigene family in the unicellular *Mesostigma* argues for its close relationship to Streptophyta." Molecular Biology and Evolution **23**(5): 1011-1015.
Nei, M. (1996). "Phylogenetic analysis in molecular evolutionary genetics." Annual Reviews of Genetics **30**(1): 371-403.
Nelson, B. K., Cai, X. and Nebenfuhr, A. (2007). "A multicolored set of *in vivo* organelle markers for co-localization studies in *Arabidopsis* and other plants." The Plant Journal **51**(6): 1126-1136.
Nielsen, N. (2005) Funktionelle Charakterisierung der CHASE-Domäne des Cytokininrezeptors AHK4. Freie Universität Berlin Institut für Biologie - Angewandte Genetik
Nishimura, C., Ohashi, Y., Sato, S., Kato, T., Tabata, S. and Ueguchi, C. (2004). "Histidine kinase homologs that act as cytokinin receptors possess overlapping functions in the regulation of shoot and root growth in *Arabidopsis*." The Plant Cell **16**(6): 1365-1377.
Nishiyama, T. (2007). "Evolutionary Developmental Biology of Nonflowering Land Plants." International Journal of Plant Sciences **168**(1): 37-47.
Nishiyama, T., Fujita, T., Shin, I. T., Seki, M., Nishide, H., Uchiyama, I., Kamiya, A., Carninci, P., Hayashizaki, Y., Shinozaki, K., Kohara, Y. and Hasebe, M. (2003). "Comparative genomics of *Physcomitrella patens* gametophytic transcriptome and *Arabidopsis thaliana*: implication for land plant evolution." Proceedings of the National Academy of Science U S A **100**(13): 8007-8012.
Nodop, A., Suzuki, I., Barsch, A., Schroder, A. K., Niehaus, K., Staiger, D., Pistorius, E. K. and Michel, K. P. (2006). "Physiological and molecular characterization of a *Synechocystis sp.* PCC 6803 mutant lacking histidine kinase Slr1759 and response regulator Slr1760." Zeitschrift für Naturforschung C **61**(11-12): 865-878.
O`Donoghue, M.-T., Chater, C., Wallace, S., Gray, J. E., Beerling, D. J. and Fleming, A. J. (2013). "Genome-wide transcriptomic analysis of the sporophyte of the moss *Physcomitrella patens*." Journal of Experimental Botany **64**(12): 3567-3581.
Ouyang, S., Zhu, W., Hamilton, J., Lin, H., Campbell, M., Childs, K., Thibaud-Nissen, F. o., Malek, R. L., Lee, Y., Zheng, L., Orvis, J., Haas, B., Wortman, J. and Buell, C. R. (2007). "The TIGR Rice Genome Annotation Resource: improvements and new features." Nucleic Acids Research **35**(suppl 1): D883-D887.
Palenik, B., Grimwood, J., Aerts, A., Rouzé, P., Salamov, A., Putnam, N., Dupont, C., Jorgensen, R., Derelle, E., Rombauts, S., Zhou, K., Otillar, R., Merchant, S. S., Podell, S., Gaasterland, T., Napoli, C., Gendler, K., Manuell, A., Tai, V., Vallon, O., Piganeau, G., Jancek, S., Heijde, M., Jabbari, K., Bowler, C., Lohr, M., Robbens, S., Werner, G., Dubchak, I., Pazour, G. J., Ren, Q., Paulsen, I., Delwiche, C., Schmutz, J., Rokhsar, D., Van de Peer, Y., Moreau, H. and Grigoriev, I. V. (2007). "The tiny eukaryote *Ostreococcus* provides genomic insights into the paradox of plankton speciation." Proceedings of the National Academy of Sciences **104**(18): 7705-7710.
Patil, G. and Nicander, B. (2013). "Identification of two additional members of the tRNA isopentenyltransferase family in *Physcomitrella patens*." Plant Molecular Biology **82**(4-5): 417-426.
Persson, B. C., Esberg, B., Olafsson, O. and Björk, G. R. (1994). "Synthesis and function of isopentenyl adenosine derivatives in tRNA." Biochimie **76**(12): 1152-1160.
Pils, B. and Heyl, A. (2009). "Unraveling the evolution of cytokinin signaling." Plant Physiology **151**(2): 782-791.
Ponting, C. P. and Aravind, L. (1997). "PAS: a multifunctional domain family comes to light." Current Biology **7**(11): R674-R677.
Prigge, M. J. and Bezanilla, M. (2010). "Evolutionary crossroads in developmental biology: *Physcomitrella patens*." Development **137**(21): 3535-3543.
Prochnik, S. E., Umen, J., Nedelcu, A. M., Hallmann, A., Miller, S. M., Nishii, I., Ferris, P., Kuo, A., Mitros, T., Fritz-Laylin, L. K., Hellsten, U., Chapman, J., Simakov, O., Rensing, S. A., Terry, A., Pangilinan, J., Kapitonov, V., Jurka, J., Salamov, A., Shapiro, H., Schmutz, J., Grimwood, J., Lindquist, E., Lucas, S., Grigoriev, I. V., Schmitt, R., Kirk, D. and Rokhsar, D. S. (2010). "Genomic analysis of organismal complexity in the multicellular green alga *Volvox carteri*." Science **329**(5988): 223-226.

Proctor, M. C. F. and Tuba, Z. (2002). "Poikilohydry and homoihydry: antithesis or spectrum of possibilities?" New Phytologist **156**(3): 327-349.
Proust, H., Hoffmann, B., Xie, X., Yoneyama, K., Schaefer, D. G., Nogue, F. and Rameau, C. (2011). "Strigolactones regulate protonema branching and act as a quorum sensing-like signal in the moss *Physcomitrella patens*." Development **138**(8): 1531-1539.
Punwani, J. A., Hutchison, C. E., Schaller, G. E. and Kieber, J. J. (2010). "The subcellular distribution of the *Arabidopsis* histidine phosphotransfer proteins is independent of cytokinin signaling." The Plant Journal **62**(3): 473-482.
Puthiyaveetil, S. and Allen, J. F. (2009). "Chloroplast two-component systems: evolution of the link between photosynthesis and gene expression." Proceedings of the Royal Society B: Biological sciences **276**(1665): 2133-2145.
Qiu, Y. L., Li, L., Wang, B., Chen, Z., Knoop, V., Groth-Malonek, M., Dombrovska, O., Lee, J., Kent, L., Rest, J., Estabrook, G. F., Hendry, T. A., Taylor, D. W., Testa, C. M., Ambros, M., Crandall-Stotler, B., Duff, R. J., Stech, M., Frey, W., Quandt, D. and Davis, C. C. (2006). "The deepest divergences in land plants inferred from phylogenomic evidence." Proceedings of the National Academy of Science U S A **103**(42): 15511-15516.
Raleigh, E. A., Lech, K. and Brent, R. (1989). Selected Topics from Classical Bacterial Genetics. Current Protocols in Molecular Biology. F. Ausubel, R. Brent, R. E. Kingstonet al, Wiley. **1a:** 1.4.1-1.4.16.
Raleigh, E. A., Murray, N. E., Revel, H., Blumenthal, R. M., Westaway, D., Reith, A. D., Rigby, P. W. J., Elhai, J. and Hanahan, D. (1988). "McrA and McrB restriction phenotypes of some *E. coli* strains and implications for gene cloning." Nucleic Acids Research **16**(4): 1563-1575.
Ramireddy, E., Brenner, W. G., Pfeifer, A., Heyl, A. and Schmülling, T. (2013). "In planta analysis of a *cis*-regulatory cytokinin response motif in Arabidopsis and identification of a novel enhancer sequence." Plant and Cell Physiology **54**(7): 1079-1092.
Rashotte, A. M., Carson, S. D., To, J. P. and Kieber, J. J. (2003). "Expression profiling of cytokinin action in *Arabidopsis*." Plant Physiology **132**(4): 1998-2011.
Rashotte, A. M. and Goertzen, L. R. (2010). "The CRF domain defines cytokinin response factor proteins in plants." BMC Plant Biology **10**(74): 1471-2229.
Rashotte, A. M., Mason, M. G., Hutchison, C. E., Ferreira, F. J., Schaller, G. E. and Kieber, J. J. (2006). "A subset of *Arabidopsis* AP2 transcription factors mediates cytokinin responses in concert with a two-component pathway." Proceedings of the National Academy of Science U S A **103**(29): 11081-11085.
Rensing, S. A., Ick, J., Fawcett, J. A., Lang, D., Zimmer, A., Van de Peer, Y. and Reski, R. (2007). "An ancient genome duplication contributed to the abundance of metabolic genes in the moss *Physcomitrella patens*." BMC Evolutionary Biology **7**: 130.
Rensing, S. A., Lang, D., Zimmer, A. D., Terry, A., Salamov, A., Shapiro, H., Nishiyama, T., Perroud, P. F., Lindquist, E. A., Kamisugi, Y., Tanahashi, T., Sakakibara, K., Fujita, T., Oishi, K., Shin, I. T., Kuroki, Y., Toyoda, A., Suzuki, Y., Hashimoto, S., Yamaguchi, K., Sugano, S., Kohara, Y., Fujiyama, A., Anterola, A., Aoki, S., Ashton, N., Barbazuk, W. B., Barker, E., Bennetzen, J. L., Blankenship, R., Cho, S. H., Dutcher, S. K., Estelle, M., Fawcett, J. A., Gundlach, H., Hanada, K., Heyl, A., Hicks, K. A., Hughes, J., Lohr, M., Mayer, K., Melkozernov, A., Murata, T., Nelson, D. R., Pils, B., Prigge, M., Reiss, B., Renner, T., Rombauts, S., Rushton, P. J., Sanderfoot, A., Schween, G., Shiu, S. H., Stueber, K., Theodoulou, F. L., Tu, H., Van de Peer, Y., Verrier, P. J., Waters, E., Wood, A., Yang, L., Cove, D., Cuming, A. C., Hasebe, M., Lucas, S., Mishler, B. D., Reski, R., Grigoriev, I. V., Quatrano, R. S. and Boore, J. L. (2008). "The *Physcomitrella* genome reveals evolutionary insights into the conquest of land by plants." Science **319**(5859): 64-69.
Rensing, S. A., Rombauts, S., Van de Peer, Y. and Reski, R. (2002). "Moss transcriptome and beyond." Trends in Plant Science **7**(12): 535-538.

Repp, A., Mikami, K., Mittmann, F. and Hartmann, E. (2004). "Phosphoinositide-specific phospholipase C is involved in cytokinin and gravity responses in the moss *Physcomitrella patens*." The Plant Journal **40**(2): 250-259.
Reski, R. (1998). "Development, genetics and molecular biology of mosses." Botanica Acta(111): 1-15.
Reski, R. (1999). "Molecular genetics of *Physcomitrella*." Planta **208**(3): 301-309.
Reski, R. and Abel, W. O. (1985). "Induction of budding on chloronemata and caulonemata of the moss, Physcomitrella patens, using isopentenyladenine." Planta **165**: 354-358.
Reski, R., Faust, M., Wang, X. H., Wehe, M. and Abel, W. O. (1994). "Genome analysis of the moss *Physcomitrella patens* (Hedw.) B.S.G." Molecular & General Genetics **244**(4): 352-359.
Reski, R., Wehe, M., Hadeler, B., Marienfeld, J. R. and Abel, W. O. (1991). "Cytokinin and Light Quality Interact at the Molecular Level in the Chloroplast-Mutant PC22 of the Moss Physcomitrella." Journal of Plant Physiology **138**(2): 236-243.
Reutter, K., Atzorn, R., Hadeler, B., Schmülling, T. and Reski, R. (1998). "Expression of the bacterial ipt gene in *Physcomitrella* rescues mutations in budding and in plastid division." Planta **206**(2): 196-203.
Reyes-Prieto, A., Hackett, J. D., Soares, M. B., Bonaldo, M. F. and Bhattacharya, D. (2006). "Cyanobacterial contribution to algal nuclear genomes is primarily limited to plastid functions." Current biology **16**(23): 2320-2325.
Richardt, S., Lang, D., Reski, R., Frank, W. and Rensing, S. A. (2007). "PlanTAPDB, a phylogeny-based resource of plant transcription-associated proteins." Plant Physiology **143**(4): 1452-1466.
Richmond, A. E. and Lang, A. (1957). "Effect of kinetin on protein content and survival of detached *Xanthium* leaves." Science **125**: 650-651.
Riefler, M., Novak, O., Strnad, M. and Schmülling, T. (2006). "*Arabidopsis* cytokinin receptor mutants reveal functions in shoot growth, leaf senescence, seed size, germination, root development, and cytokinin metabolism." The Plant Cell **18**(1): 40-54.
Romanov, G. A. and Lomin, S. N. (2009). "Hormone-binding assay using living bacteria expressing eukaryotic receptors." Methods in Molecular Biology **495**: 111-120.
Romanov, G. A., Lomin, S. N. and Schmülling, T. (2006). "Biochemical characteristics and ligand-binding properties of *Arabidopsis* cytokinin receptor AHK3 compared to CRE1/AHK4 as revealed by a direct binding assay." Journal of Experimental Botany **57**(15): 4051-4058.
Romanov, G. A., Spichal, L., Lomin, S. N., Strnad, M. and Schmülling, T. (2005). "A live cell hormone-binding assay on transgenic bacteria expressing a eukaryotic receptor protein." Analytical Biochemistry **347**(1): 129-134.
Sakai, H., Honma, T., Aoyama, T., Sato, S., Kato, T., Tabata, S. and Oka, A. (2001). "ARR1, a transcription factor for genes immediately responsive to cytokinins." Science **294**(5546): 1519-1521.
Sakakibara, H., Takei, K. and Hirose, N. (2006). "Interactions between nitrogen and cytokinin in the regulation of metabolism and development." Trends in Plant Science **11**(9): 440-448.
Sakakibara, K., Nishiyama, T., Sumikawa, N., Kofuji, R., Murata, T. and Hasebe, M. (2003). "Involvement of auxin and a homeodomain-leucine zipper I gene in rhizoid development of the moss *Physcomitrella patens*." Development **130**(20): 4835-4846.
Salinas, J. and Sanchez-Serrano, J. J. (2006). "Arabidopsis - Laboratory manuals", Totown: Humana Press Inc.
Sambrook, J. and Russell, D. W. (2001). "Molecular cloning a laboratory manual". Cold Spring Harbor, NY, Cold Spring Harbor Laboratory Press.
Satbhai, S. B., Yamashino, T., Okada, R., Nomoto, Y., Mizuno, T., Tezuka, Y., Itoh, T., Tomita, M., Otsuki, S. and Aoki, S. (2011). "Pseudo-response regulator (PRR) homologues of the moss *Physcomitrella patens*: insights into the evolution of the PRR family in land plants." DNA Research **18**(1): 39-52.
Saunders, M. J. (1994). Cytokinin and signal transduction. Cytokinins: Chemistry, Activity and Function. D. W. S. Mok and M. C. Mok. Boca Raton, FL, CRC Press**:** 155-166.

Saunders, M. J. and Hepler, P. K. (1983). "Calcium antagonists and calmodulin inhibitors block cytokinin-induced bud formation in *Funaria*." Developmental Biology **99**(1): 41-49.
Schaefer, D. G. (2002). "A new moss genetics: targeted mutagenesis in *Physcomitrella patens*." Annual Reviews of Plant Biology **53**: 477-501.
Schaller, G. E., Mathews, D. E., Gribskov, M. and Walker, J. C. (2002). Two-component signaling elements and histidyl-aspartyl phosphorelays. The Arabidopsis book / American Society of Plant Biologists. **1:** e0071.
Schaller, G. E., Shiu, S. H. and Armitage, J. P. (2011). "Two-component systems and their co-option for eukaryotic signal transduction." Current Biology **21**(9): R320-R330.
Schmülling, T., Werner, T., Riefler, M., Krupková, E. and Bartrina y Manns, I. (2003). "Structure and function of cytokinin oxidase/dehydrogenase genes of maize, rice, *Arabidopsis* and other species." Journal of Plant Research **116**(3): 241-252.
Schneider, C. A., Rasband, W. S. and Eliceiri, K. W. (2012). "NIH Image to ImageJ: 25 years of image analysis." Nature methods **9**(7): 671-675.
Schnell, J. (1978). "On the transfer and expression of bacterial plasmid DNA in higher plants [proceedings]." Archives Internationales de Physiologie (Liege) **86**(4): 901-902.
Schrimpf, G. (2002). "Gentechnische Methoden: Eine Sammlung von Arbeitsanleitungen für das molekularbiologische Labor", Spektrum Akademischer Verlag Heidelberg.
Schulz, P., Reski, R., Maldiney, R., Laloue, M. and Schwartzenberg, K. (2000). "Kinetics of cyokinin production and bud formation in *Physcomitrella*: analysis of wild type, a developmental mutant and two of its ipt transgenics." Journal of Plant Physiology **156**: 768-774.
Schumaker, K. S. and Dietrich, M. A. (1998). "Hormone-induced signaling during moss development." Annual Review of Plant Physiology and Plant Molecular Biology **49**: 501-523.
Schween, G., Gorr, G., Hohe, A. and Reski, R. (2003). "Unique Tissue-Specific Cell Cycle in *Physcomitrella*." Plant Biology **5**(1): 50-58.
Seyer, P., Marty, D., Lescure, A. M. and Péaud-Lenoel, C. (1975). "Effect of cytokinin on chloroplast cyclic differentiation in cultured tobacco cells." Cell Differentiation **4**(3): 187-197.
Shenoy, A. R. (2000). "His kinase or mine? histidine kinases through evolution." Journal of Biosciene **25**(4): 317-322.
Simon, A., Glockner, G., Felder, M., Melkonian, M. and Becker, B. (2006). "EST analysis of the scaly green flagellate *Mesostigma viride* (Streptophyta): implications for the evolution of green plants (Viridiplantae)." BMC Plant Biology **6**: 2.
Skerker, J. M., Perchuk, B. S., Siryaporn, A., Lubin, E. A., Ashenberg, O., Goulian, M. and Laub, M. T. (2008). "Rewiring the specificity of two-component signal transduction systems." Cell **133**(6): 1043-1054.
Slootweg, E., Roosien, J., Spiridon, L. N., Petrescu, A.-J., Tameling, W., Joosten, M., Pomp, R., van Schaik, C., Dees, R., Borst, J. W., Smant, G., Schots, A., Bakker, J. and Goverse, A. (2010). "Nucleocytoplasmic distribution is required for activation of resistance by the potato NB-LRR receptor Rx1 and is balanced by its functional domains." The Plant Cell **22**(12): 4195-4215.
Soyer, O. S. and Bonhoeffer, S. (2006). "Evolution of complexity in signaling pathways." Proceedings of the National Academy of Science U S A **103**(44): 16337-16342.
Soyer, O. S., Salathe, M. and Bonhoeffer, S. (2006). "Signal transduction networks: topology, response and biochemical processes." Journal of Theoretical Biology **238**(2): 416-425.
Sparkes, I., Runions, J., Hawes, C. and Griffing, L. (2009). "Movement and remodeling of the endoplasmic reticulum in nondividing cells of tobacco leaves." The Plant Cell **21**(12): 3937-3949.
Sparkes, I. A., Runions, J., Kearns, A. and Hawes, C. (2006). "Rapid, transient expression of fluorescent fusion proteins in tobacco plants and generation of stably transformed plants." Nature Protocols **1**(4): 2019-2025.
Spichal, L. (2012). "Cytokinins - recent news and views of evolutionally old molecules." Functional Plant Biology **39**(4): 267-284.

Spichal, L., Rakova, N. Y., Riefler, M., Mizuno, T., Romanov, G. A., Strnad, M. and Schmülling, T. (2004). "Two cytokinin receptors of *Arabidopsis thaliana*, CRE1/AHK4 and AHK3, differ in their ligand specificity in a bacterial assay." Plant and Cell Physiology **45**(9): 1299-1305.
Spinner, L., Pastuglia, M., Belcram, K., Pegoraro, M., Goussot, M., Bouchez, D. and Schaefer, D. G. (2010). "The function of TONNEAU1 in moss reveals ancient mechanisms of division plane specification and cell elongation in land plants." Development **137**(16): 2733-2742.
Stamatakis, A. (2006). "RAxML-VI-HPC: maximum likelihood-based phylogenetic analyses with thousands of taxa and mixed models." Bioinformatics **22**(21): 2688-2690.
Stephenson, K. and Hoch, J. A. (2002). "Evolution of signalling in the sporulation phosphorelay." Molecular Microbiology **46**(2): 297-304.
Stirk, W. A., Novak, O., Strnad, M. and van Staden, J. (2003). "Cytokinins in macroalgae." Plant Growth Regulation **41**: 13-24.
Stirk, W. A., Ördög, V. and van Staden, J. (1999). "Identification of the cytokinin isopentenyladenin in a strain of *Arthronema africanum* (cyanobacteria)." Journal of Phycology **35**(1): 89-92.
Stock, A. M., Robinson, V. L. and Goudreau, P. N. (2000). "Two-component signal transduction." Annual Reviews of Biochemistry **69**: 183-215.
Stolz, A., Riefler, M., Lomin, S. N., Achazi, K., Romanov, G. A. and Schmülling, T. (2011). "The specificity of cytokinin signalling in *Arabidopsis thaliana* is mediated by differing ligand affinities and expression profiles of the receptors." The Plant Journal **67**(1): 157-168.
Strepp, R., Scholz, S., Kruse, S., Speth, V. and Reski, R. (1998). "Plant nuclear gene knockout reveals a role in plastid division for the homolog of the bacterial cell division protein FtsZ, an ancestral tubulin." Proceedings of the National Academy of Science U S A **95**(8): 4368-4373.
Suppanz, I., Sarnighausen, E. and Reski, R. (2007). "An integrated physiological and genetic approach to the dynamics of FtsZ targeting and organisation in a moss, *Physcomitrella patens*." Protoplasma **232**(1-2): 1-9.
Suzuki, T., Imamura, A., Ueguchi, C. and Mizuno, T. (1998). "Histidine-containing phosphotransfer (HPt) signal transducers implicated in His-to-Asp phosphorelay in *Arabidopsis*." Plant Cell and Physiology **39**(12): 1258-1268.
Suzuki, T., Miwa, K., Ishikawa, K., Yamada, H., Aiba, H. and Mizuno, T. (2001a). "The *Arabidopsis* sensor His-kinase, AHK4, can respond to cytokinins." Plant and Cell Physiology **42**(2): 107-113.
Suzuki, T., Sakurai, K., Ueguchi, C. and Mizuno, T. (2001b). "Two types of putative nuclear factors that physically interact with histidine-containing phosphotransfer (HPt) domains, signaling mediators in His-to-Asp phosphorelay, in *Arabidopsis thaliana*." Plant and Cell Physiology **42**(1): 37-45.
Sweere, U., Eichenberg, K., Lohrmann, J., Mira-Rodado, V., Baurle, I., Kudla, J., Nagy, F., Schafer, E. and Harter, K. (2001). "Interaction of the response regulator ARR4 with phytochrome B in modulating red light signaling." Science **294**(5544): 1108-1111.
Takei, K., Sakakibara, H. and Sugiyama, T. (2001). "Identification of genes encoding adenylate isopentenyltransferase, a cytokinin biosynthesis enzyme, in *Arabidopsis thaliana*." Journal of Biological Chemistry **276**(28): 26405-26410.
Takei, K., Takahashi, T., Sugiyama, T., Yamaya, T. and Sakakibara, H. (2002). "Multiple routes communicating nitrogen availability from roots to shoots: a signal transduction pathway mediated by cytokinin." Botany **53**(370): 971-977.
Takei, K., Ueda, N., Aoki, K., Kuromori, T., Hirayama, T., Shinozaki, K., Yamaya, T. and Sakakibara, H. (2004). "AtIPT3 is a key determinant of nitrate-dependent cytokinin biosynthesis in *Arabidopsis*." Plant and Cell Physiology **45**(8): 1053-1062.
Tanaka, Y., Suzuki, T., Yamashino, T. and Mizuno, T. (2004). "Comparative studies of the AHP histidine-containing phosphotransmitters implicated in His-to-Asp phosphorelay in *Arabidopsis thaliana*." Bioscience, Biotechnology and Biochemistry **68**(2): 462-465.
Taniguchi, M., Sasaki, N., Tsuge, T., Aoyama, T. and Oka, A. (2007). "ARR1 directly activates cytokinin response genes that encode proteins with diverse regulatory functions." Plant and Cell Physiology **48**(2): 263-277.

Taya, Y., Tanaka, Y. and Nishimura, S. (1978). "5'-AMP is a direct precursor of cytokinin in *Dictyostelium discoideum*." Nature **271**(5645): 545-547.
Taylor, T. N., Kerp, H. and Hass, H. (2005). "Life history biology of early land plants: deciphering the gametophyte phase." Proceedings of the National Academy of Science U S A **102**(16): 5892-5897.
Thelander, M., Olsson, T. and Ronne, H. (2005). "Effect of the energy supply on filamentous growth and development in *Physcomitrella patens*." Journal of Experimental Botany **56**(412): 653-662.
Thompson, J. D., Higgins, D. G. and Gibson, T. J. (1994). "CLUSTAL W: improving the sensitivity of progressive multiple sequence alignment through sequence weighting, position-specific gap penalties and weight matrix choice." Nucleic Acids Research **22**(22): 4673-4680.
Timme, R. E., Bachvaroff, T. R. and Delwiche, C. F. (2012). "Broad phylogenomic sampling and the sister lineage of land plants." PLoS ONE **7**(1): e29696.
Timme, R. E. and Delwiche, C. F. (2010). "Uncovering the evolutionary origin of plant molecular processes: comparison of *Coleochaete* (Coleochaetales) and *Spirogyra* (Zygnematales) transcriptomes." BMC Plant Biology **10**: 96.
To, J. P., Haberer, G., Ferreira, F. J., Deruere, J., Mason, M. G., Schaller, G. E., Alonso, J. M., Ecker, J. R. and Kieber, J. J. (2004). "Type-A *Arabidopsis* response regulators are partially redundant negative regulators of cytokinin signaling." The Plant Cell **16**(3): 658-671.
To, J. P. C., Deruere, J., Maxwell, B. B., Morris, V. F., Hutchison, C. E., Ferreira, F. J., Schaller, G. E. and Kieber, J. J. (2007). "Cytokinin regulates type-A *Arabidopsis* response regulator activity and protein stability via two-component phosphorelay." The Plant Cell **19**(12): 3901-3914.
Towbin, H., Staehelin, T. and Gordon, J. (1979). "Electrophoretic transfer of proteins from polyacrylamide gels to nitrocellulose sheets: procedure and some applications." Proceedings of the National Academy of Science U S A **76**(9): 4350-4354.
Tran, L. S., Shinozaki, K. and Yamaguchi-Shinozaki, K. (2010). "Role of cytokinin responsive two-component system in ABA and osmotic stress signalings." Plant Signaling & Behavior **5**(2): 148-150.
Tran, L. S., Urao, T., Qin, F., Maruyama, K., Kakimoto, T., Shinozaki, K. and Yamaguchi-Shinozaki, K. (2007). "Functional analysis of AHK1/ATHK1 and cytokinin receptor histidine kinases in response to abscisic acid, drought, and salt stress in *Arabidopsis*." Proceedings of the National Academy of Science U S A **104**(51): 20623-20628.
Triant, D. A. and Whitehead, A. (2009). "Simultaneous extraction of high-quality RNA and DNA from small tissue samples." Journal of Heredity **100**(2): 246-250.
Tsai, Y. C., Weir, N. R., Hill, K., Zhang, W., Kim, H. J., Shiu, S. H., Schaller, G. E. and Kieber, J. J. (2012). "Characterization of genes involved in cytokinin signaling and metabolism from rice." Plant Physiology **158**(4): 1666-1684.
Tsujimoto, R., Yamazaki, H., Maeda, S. and Omata, T. (2007). "Distinct roles of nitrate and nitrite in regulation of expression of the nitrate transport genes in the moss *Physcomitrella patens*." Plant and Cell Physiology **48**(3): 484-497.
Ueguchi, C., Koizumi, H., Suzuki, T. and Mituno, T. (2001a). "Novel family of sensor histidine kinase genes in *Arabidopsis thaliana*." Plant and Cell Physiology **42**: 231-235.
Ueguchi, C., Sato, S., Kato, T. and Tabata, S. (2001b). "The AHK4 gene involved in the cytokinin-signaling pathway as a direct receptor molecule in *Arabidopsis thaliana*." Plant and Cell Physiology **42**(7): 751-755.
Utsumi, R., Brissette, R. E., Rampersaud, A., Forst, S. A., Oosawa, K. and Inouye, M. (1989). "Activation of bacterial porin gene expression by a chimeric signal transducer in response to aspartate." Science **245**(4923): 1246-1249.
van Dam, T. J., Rehmann, H., Bos, J. L. and Snel, B. (2009). "Phylogeny of the CDC25 homology domain reveals rapid differentiation of Ras pathways between early animals and fungi." Cellular Signalling **21**(11): 1579-1585.
Vervliet, G., Holsters, M., Teuchy, H., Van Montagu, M. and Schell, J. (1975). "Characterization of different plaque-forming and defective temperate phages in *Agrobacterium*." Journal of General Virology **26**(1): 33-48.

Vogel, C., Bashton, M., Kerrison, N. D., Chothia, C. and Teichmann, S. A. (2004a). "Structure, function and evolution of multidomain proteins." Current Opinion in Structural Biology **14**(2): 208-216.
Vogel, C., Berzuini, C., Bashton, M., Gough, J. and Teichmann, S. A. (2004b). "Supra-domains: evolutionary units larger than single protein domains." Journal of Molecular Biology **336**(3): 809-823.
von Schwartzenberg, K. (2006). "Moss Biology and Phytohormones – Cytokinins in *Physcomitrella*." Plant Biology (Stuttgart, Germany) **8**(3): 382-388.
von Schwartzenberg, K. (2009). Hormonal Regulation of Development by Auxin and Cytokinin in Moss. The Moss *Physcomitrella patens*. C. D. Knight, P. F. Perroud and D. Cove. Chichester, John Wiley & Sons. **36:** 246-297.
von Schwartzenberg, K., Gruhn, N., Lindner, A. C., Landschulze, I., Wegner, N., Gelhaar, F., Novak, O., Strnad, M., Gonneau, M., Nogue, F. and Heyl, A. (in preparation). "Cytokinin receptors play a crucial role in triggering developmental transition on protonema of *Physcomitrella patens*."
von Schwartzenberg, K., Nunez, M. F., Blaschke, H., Dobrev, P. I., Novak, O., Motyka, V. and Strnad, M. (2007). "Cytokinins in the bryophyte *Physcomitrella patens*: analyses of activity, distribution, and cytokinin oxidase/dehydrogenase overexpression reveal the role of extracellular cytokinins." Plant Physiology **145**(3): 786-800.
von Schwartzenberg, K., Pethe, C. and M., L. (2003). "Cytokinin metabolism in Physcomitrella patens – differences and similarities to higher plants." Plant Growth Regulation **39**(2): 99-106.
Wagner, S., Baars, L., Ytterberg, A. J., Klussmeier, A., Wagner, C. S., Nord, O., Nygren, P.-A., van Wijk, K. J. and de Gier, J.-W. (2007). "Consequences of membrane protein overexpression in *Escherichia coli*." Molecular & Cellular Proteomics **9**(1535-9476).
Waller, R. F., Patron, N. J. and Keeling, P. J. (2006). "Phylogenetic history of plastid-targeted proteins in the peridinin-containing dinoflagellate *Heterocapsa triquetra*." International Journal of Systematic and Evolutionary Microbiology **56**(Pt 6): 1439-1447.
Wang, J., Ma, X. M., Kojima, M., Sakakibara, H. and Hou, B. K. (2011). "N-glucosyltransferase UGT76C2 is involved in cytokinin homeostasis and cytokinin response in *Arabidopsis thaliana*." Plant and Cell Physiology **52**(12): 2200-2213.
Wang, N., Soderbom, F., Anjard, C., Shaulsky, G. and Loomis, W. F. (1999). "SDF-2 induction of terminal differentiation in Dictyostelium discoideum is mediated by the membrane-spanning sensor kinase DhkA." Molecular and Cellular Biology **19**(7): 4750-4756.
Wang, T. L., Beutelmann, P. and Cove, D. J. (1981a). "Cytokinin Biosynthesis in Mutants of the Moss *Physcomitrella* patens." Plant Physiology **68**(3): 739-744.
Wang, T. L., Horgan, R. and Cove, D. (1981b). "Cytokinins from the Moss *Physcomitrella patens*." Plant Physiology **68**(3): 735-738.
Wang, Y., Secco, D. and Poirier, Y. (2008). "Characterization of the PHO1 gene family and the responses to phosphate deficiency of *Physcomitrella patens*." Plant Physiology **146**(2): 646-656.
Waterhouse, R. M., Kriventseva, E. V., Meister, S., Xi, Z., Alvarez, K. S., Bartholomay, L. C., Barillas-Mury, C., Bian, G., Blandin, S., Christensen, B. M., Dong, Y., Jiang, H., Kanost, M. R., Koutsos, A. C., Levashina, E. A., Li, J., Ligoxygakis, P., Maccallum, R. M., Mayhew, G. F., Mendes, A., Michel, K., Osta, M. A., Paskewitz, S., Shin, S. W., Vlachou, D., Wang, L., Wei, W., Zheng, L., Zou, Z., Severson, D. W., Raikhel, A. S., Kafatos, F. C., Dimopoulos, G., Zdobnov, E. M. and Christophides, G. K. (2007). "Evolutionary dynamics of immune-related genes and pathways in disease-vector mosquitoes." Science **316**(5832): 1738-1743.
Waters, E. R. (2003). "Molecular adaptation and the origin of land plants." Molecular Phylogenetics and Evolution **29**(3): 456-463.
Weng, G., Bhalla, U. S. and Iyengar, R. (1999). "Complexity in biological signaling systems." Science **284**(5411): 92-96.
Werner, T., Holst, K., Pors, Y., Guivarch, A., Mustroph, A., Chriqui, D., Grimm, B. and Schmülling, T. (2008). "Cytokinin deficiency causes distinct changes of sink and source parameters in tobacco shoots and roots." Journal of Experimental Botany **59**(10): 2659-2672.

Werner, T., Motyka, V., Laucou, V., Smets, R., van Onckelen, H. and Schmülling, T. (2003). "Cytokinin-deficient transgenic *Arabidopsis* plants show multiple developmental alterations indicating opposite functions of cytokinins in the regulation of shoot and root meristem activity." The Plant Cell **15**(11): 2532-2550.
Werner, T., Motyka, V., Strnad, M. and Schmülling, T. (2001). "Regulation of plant growth by cytokinin." Proceedings of the National Academy of Sciences U S A **98**(18): 10487-10492.
Werner, T. and Schmülling, T. (2009). "Cytokinin action in plant development." Current Opinion in Plant Biology **12**(5): 527-538.
Wernersson, R. (2006). "Virtual Ribosome--a comprehensive DNA translation tool with support for integration of sequence feature annotation." Nucleic Acids Research **34**(Web Server issue): W385-388.
West, A. H. and Stock, A. M. (2001). "Histidine kinases and response regulator proteins in two-component signaling systems." Trends in Biochemical Sciences **26**(6): 369-376.
Wodniok, S., Brinkmann, H., Glockner, G., Heidel, A. J., Philippe, H., Melkonian, M. and Becker, B. (2011). "Origin of land plants: do conjugating green algae hold the key?" BMC Evolutionary Biology **11**: 104.
Worden, A. Z., Lee, J. H., Mock, T., Rouze, P., Simmons, M. P., Aerts, A. L., Allen, A. E., Cuvelier, M. L., Derelle, E., Everett, M. V., Foulon, E., Grimwood, J., Gundlach, H., Henrissat, B., Napoli, C., McDonald, S. M., Parker, M. S., Rombauts, S., Salamov, A., Von Dassow, P., Badger, J. H., Coutinho, P. M., Demir, E., Dubchak, I., Gentemann, C., Eikrem, W., Gready, J. E., John, U., Lanier, W., Lindquist, E. A., Lucas, S., Mayer, K. F., Moreau, H., Not, F., Otillar, R., Panaud, O., Pangilinan, J., Paulsen, I., Piegu, B., Poliakov, A., Robbens, S., Schmutz, J., Toulza, E., Wyss, T., Zelensky, A., Zhou, K., Armbrust, E. V., Bhattacharya, D., Goodenough, U. W., Van de Peer, Y. and Grigoriev, I. V. (2009). "Green evolution and dynamic adaptations revealed by genomes of the marine picoeukaryotes *Micromonas*." Science **324**(5924): 268-272.
Wu, S. Z., Ritchie, J. A., Pan, A. H., Quatrano, R. S. and Bezanilla, M. (2011). "Myosin VIII regulates protonemal patterning and developmental timing in the moss *Physcomitrella patens*." Molecular Plant **4**(5): 909-921.
Wuchty, S., Barabasi, A. L. and Ferdig, M. T. (2006). "Stable evolutionary signal in a yeast protein interaction network." BMC Evolutionary Biology **6**: 8.
Wulfetange, K. (2010) Strukturelle und funktionelle Characterisierung des Cytokininrezeptors AHK4/CRE1 aus *Arabidopsis thaliana*. Freie Universität Berlin Institut für Biologie - Angewandte Genetik
Wulfetange, K., Lomin, S. N., Romanov, G. A., Stolz, A., Heyl, A. and Schmülling, T. (2011a). "The Cytokinin Receptors of *Arabidopsis thaliana* are Locating Mainly to the Endoplasmic Reticulum." Plant Physiology **156**: 1808-1818.
Wulfetange, K., Saenger, W., Schmülling, T. and Heyl, A. (2011b). "*E. coli*-based cell-free expression, purification and characterization of the membrane-bound ligand-binding CHASE-TM domain of the cytokinin receptor CRE1/AHK4 of *Arabidopsis thaliana*." Molecular Biotechnology **47**(3): 211-219.
Xu, S., Guerra, D., Lee, U. and Vierling, E. (2013). "S-nitrosoglutathione reductases are low-copy number, cysteine-rich proteins in plants that control multiple developmental and defense responses in *Arabidopsis*." Frontiers in Plant Science **4**.
Yamada, H., Suzuki, T., Terada, K., Takei, K., Ishikawa, K., Miwa, K., Yamashino, T. and Mizuno, T. (2001). "The *Arabidopsis* AHK4 histidine kinase is a cytokinin-binding receptor that transduces cytokinin signals across the membrane." Plant and Cell Physiology **42**(9): 1017-1023.
Yamato, K. T., Ishizaki, K., Fujisawa, M., Okada, S., Nakayama, S., Fujishita, M., Bando, H., Yodoya, K., Hayashi, K., Bando, T., Hasumi, A., Nishio, T., Sakata, R., Yamamoto, M., Yamaki, A., Kajikawa, M., Yamano, T., Nishide, T., Choi, S.-H., Shimizu-Ueda, Y., Hanajiri, T., Sakaida, M., Kono, K., Takenaka, M., Yamaoka, S., Kuriyama, C., Kohzu, Y., Nishida, H., Brennicke, A., Shin-i, T., Kohara, Y., Kohchi, T., Fukuzawa, H. and Ohyama, K. (2007). "Gene organization of the liverwort Y chromosome

reveals distinct sex chromosome evolution in a haploid system." Proceedings of the National Academy of Sciences **104**(15): 6472-6477.
Yasumura, Y., Crumpton-Taylor, M., Fuentes, S. and Harberd, N. P. (2007). "Step-by-step acquisition of the gibberellin-DELLA growth-regulatory mechanism during land-plant evolution." Current Biology **17**(14): 1225-1230.
Yasumura, Y., Pierik, R., Fricker, M. D., Voesenek, L. A. C. J. and Harberd, N. P. (2012). "Studies of *Physcomitrella patens* reveal that ethylene-mediated submergence responses arose relatively early in land-plant evolution." The Plant Journal **72**(6): 947-959.
Yeh, K. C. and Lagarias, J. C. (1998). "Eukaryotic phytochromes: light-regulated serine/threonine protein kinases with histidine kinase ancestry." Proceedings of the National Academy of Science U S A **95**(23): 13976-13981.
Yevdakova, N., Motyka, V., Malbeck, J., Travnikova, A., Novak, O., Strnad, M. and Schwartzenberg, K. (2008). "Evidence for importance of tRNA-dependent cytokinin biosynthetic pathway in the moss *Physcomitrella patens*." Journal of Plant Growth Regulation **27**(3): 271-281.
Yevdakova, N. A. and von Schwartzenberg, K. (2007). "Characterisation of a prokaryote-type tRNA-isopentenyltransferase gene from the moss *Physcomitrella patens*." Planta **226**(3): 683-695.
Yogeeswaran, K., Frary, A., York, T. L., Amenta, A., Lesser, A. H., Nasrallah, J. B., Tanksley, S. D. and Nasrallah, M. E. (2005). "Comparative genome analyses of *Arabidopsis spp.*: Inferring chromosomal rearrangement events in the evolutionary history of *A. thaliana*." Genome Research **15**(4): 505-515.
Yokoyama, A., Yamashino, T., Amano, Y., Tajima, Y., Imamura, A., Sakakibara, H. and Mizuno, T. (2007). "Type-B ARR Transcription Factors, ARR10 and ARR12, are Implicated in Cytokinin-Mediated Regulation of Protoxylem Differentiation in Roots of *Arabidopsis thaliana*." Plant and Cell Physiology **48**(1): 84-96.
Yonekura-Sakakibara, K., Kojima, M., Yamaya, T. and Sakakibara, H. (2004). "Molecular characterization of cytokinin-responsive histidine kinases in maize. Differential ligand preferences and response to *cis*-zeatin." Plant Physiology **134**(4): 1654-1661.
Zimmer, A., Lang, D., Richardt, S., Frank, W., Reski, R. and Rensing, S. A. (2007). "Dating the early evolution of plants: detection and molecular clock analyses of orthologs." Molecular Genetics & Genomics **278**(4): 393-402.
Zimmer, A. D., Lang, D., Buchta, K., Rombauts, S., Nishiyama, T., Hasebe, M., Van de Peer, Y., Rensing, S. A. and Reski, R. (2013). "Reannotation and extended community resources for the genome of the non-seed plant *Physcomitrella patens* provide insights into the evolution of plant gene structures and functions." BMC Genomics **14**: 498.
Zubo, Y. O., Yamburenko, M. V., Selivankina, S. Y., Shakirova, F. M., Avalbaev, A. M., Kudryakova, N. V., Zubkova, N. K., Liere, K., Kulaeva, O. N., Kusnetsov, V. V. and Borner, T. (2008). "Cytokinin stimulates chloroplast transcription in detached barley leaves." Plant Physiology **148**(2): 1082-1093.

Eidesstattliche Erklärung

Hiermit versichere ich, dass ich die vorliegende Dissertation in allen Teilen selbstständig verfasst und keine anderen als die von mir angegebenen Quellen verwendet habe.

Berlin, den

_____

Nijuscha Gruhn